The Mortar Boundary Element Method

A Thesis submitted for the degree of Doctor of Philosophy

by Martin Healey

School of Information Systems, Computing and Mathematics

Brunel University

March 2010

Abstract

This thesis is primarily concerned with the mortar boundary element method (mortar BEM). The mortar finite element method (mortar FEM) is a well established numerical scheme for the solution of partial differential equations. In simple terms the technique involves the splitting up of the domain of definition into separate parts. The problem may now be solved independently on these separate parts, however there must be some sort of matching condition between the separate parts. Our aim is to develop and analyse this technique to the boundary element method (BEM).

The first step in our journey towards the mortar BEM is to investigate the BEM with Lagrangian multipliers. When approximating the solution of Neumann problems on open surfaces by the Galerkin BEM the appropriate boundary condition (along the boundary curve of the surface) can easily be included in the definition of the spaces used. However, we introduce a boundary element Galerkin BEM where we use a Lagrangian multiplier to incorporate the appropriate boundary condition in a weak sense. This is the first step in enabling us to understand the necessary matching conditions for a mortar type decomposition.

We next formulate the mortar BEM for hypersingular integral equations representing the elliptic boundary value problem of the Laplace equation in three dimensions (with Neumann boundary condition). We prove almost quasi-optimal convergence of the scheme in broken Sobolev norms of order 1/2. Sub-domain decompositions can be geometrically non-conforming and meshes must be quasi-uniform only on sub-domains.

We present numerical results which confirm and underline the theory presented concerning the BEM with Lagrangian multipliers and the mortar BEM. Finally we discuss the application of the mortaring technique to the hypersingular integral equation representing the equations of linear elasticity. Based on the assumption of ellipticity of the appearing bilinear form on a constrained space we prove the almost quasi-optimal convergence of the scheme.

Contents

List of Figures

List of Tables

Acknowledgements

I would like to thank the many people who have helped me during the preparation of this thesis.

The first words of thanks must go to my supervisor Prof. Norbert Heuer, without whom this thesis would never have been possible. Prof. Heuer has been a constant source of useful advice and encouragement, and it has been a privilege to work with him. I am especially grateful for our correspondence over the last year which has taken place over quite a considerable distance.

I would also like to thank Prof. G Gatica for his assistance with Chapter 3, particularly with the proof of Lemma 3.4. I must also thank Dr. M Maischak for his program MaiProgs which was used as the basis for the programs used in Chapter 5.

I am also very grateful to my wife, Hazel, whose support has been invaluable. I would also like to thank the rest of my family for their support.

I would like to thank the staff at Brunel University who have made my time at the university enjoyable and stimulating.

Chapter 1

Introduction

In this chapter we first present a brief overview of the thesis, indicating what is contained in each of the following chapters. We then present a brief discussion on the boundary element method (BEM) and related topics which are central to the thesis.

1.1 Overview of Thesis

In this chapter we present the motivation behind the research. We briefly discuss the advantages (and disadvantages) of using techniques such as the BEM, non-conforming methods, and domain decomposition methods. This discussion is intended to give a flavour of what follows and indicate the motivation behind the thesis.

Chapter 2 is split into two parts. In the first part we present the relevant background information on the BEM, the finite element method (FEM) and some extensions to the basic finite element method. Eventually we briefly present the mortar finite element method (mortar FEM). We describe the formulation of the numerical scheme and discuss some of the theoretical results associated with the method. We also discuss some of the problems which shall need to be overcome when translating the mortar FEM over to the boundary element situation. In the second part of the chapter we present a selection of technical results which are required for use in the later chapters. This section is intended as a common point of reference for what follows.

In Chapter 3 we present the boundary element method with Lagrangian multiplier. We introduce the model problem and an integration by parts formula which we shall use to get the boundary terms required to introduce the Lagrangian multipliers. We then present the discrete variational formulation of the scheme (there is no continuous formulation), where we define the bilinear forms that we shall use and the necessary discrete spaces. We then present technical results which are steps on the way to proving our main theorem for this chapter, the quasi-optimal convergence of the scheme.

In Chapter 4 we present the mortar boundary element method (mortar BEM). We proceed in a similar fashion to the previous chapter. Of particular interest we clearly define the sub-domain decomposition that will be used. It is this ability to decompose the domain into sub-domains that is the primary advantage of the mortar BEM over standard BEM schemes. We may mesh each sub-domain independently giving us great freedom in our choice of mesh. As noted we proceed in a similar fashion to the previous chapter, however now in a more complicated situation. We again show several technical results which are required to prove our main theorem. Finally we present the main result of the chapter, the almost quasi-optimal convergence of the scheme in broken Sobolev norms.

In Chapter 5 we present numerical results for both the BEM with Lagrangian multiplier and for the mortar BEM. These results are presented in graphical form in Chapter 5 and also in numerical form in Appendix B. These numerical results confirm the theory and present some interesting points in their own right. For example it is interesting to note the effect of choice of Lagrangian multiplier side on the accuracy of the approximation.

In Chapter 6 we present some technical results for the mortar BEM applied to the equations of linear elasticity. This chapter is an extension of the previous work, showing how the results obtained in previous chapters can be used in different situations. In this chapter we have had to include a conjecture related to the ellipticity of one of the appearing bilinear forms, since we were unable to prove this property. We explain why there are difficulties and present some ideas about how the problem may be overcome.

1.2 Background Information

1.2.1 The Boundary Element Method

The analysis of finite elements for the discretisation of boundary integral equations of the first kind goes bank to Nédélec and Planchard [44], and Hsiao and Wendland [31]. Stephan [53] studied boundary elements for singular problems on open surfaces. Stephan examined the Laplace equations with Neumann boundary condition and reexpressed the problem in terms of a hypersingular integral operator defined over the boundary. The principle advantage of the BEM over other numerical methods like the FEM is that only the boundary of the domain needs to be discretised. However, there is a disadvantage which is that the matrices which appear in the BEM are full unlike in the FEM where they are sparse and banded (and hence can be solved very efficiently). More information on the BEM (and the related integral equations) can, for example, be found in [32, 41] or [51].

1.2.2 Lagrangian Multipliers

Lagrangian multipliers where first analysed for the FEM by Babuška in [1]. The aim was to be able to avoid difficulty in implementing essential boundary conditions. The basic idea is that through the inclusion of a second bilinear form we may use simpler spaces. As always there is however a trade off, although the spaces are simpler the associated linear system is larger and therefore more difficult to solve. A recent approach to the use of Lagrangian multipliers in terms of mixed finite elements is analysed in [2]. Lagrangian multipliers are well known as a classical technique from variational methods.

While there is extensive use of Lagrangian multipliers in the FEM literature, there is no theory on the use of Lagrangian multipliers in the boundary element Galerkin method. There are several reasons why there is no such theory for the BEM:

- In the context of the FEM it has been shown that Lagrangian multiplier methods are particularly useful for boundary value problems with nonhomogeneous Dirichlet boundary conditions. By the inclusion of a second bilinear form we are able to simplify the finite element spaces required to approximate a solution at the expense of making the corresponding linear system larger. However, there are no boundary value problems with representation by boundary integral equations where nonhomogeneous boundary conditions (for the solution of the integral equations) appear. When examining the application of hypersingular operators on open surfaces boundary element function of a conforming method need to vanish at the boundary of the surface [52]. As in the finite element case this homogeneous condition can be easily incorporated into the method without the use of Lagrangian multipliers.

- In the finite element situation the analysis of Dirichlet boundary conditions is well understood since there is a well defined trace operator for restricting functions over the domain to the appropriate part of the boundary. When examining the application of hypersingular operators the analysis of essential boundary conditions is much more difficult due to the fact that there is no well defined trace operator in $H^{1/2}$ (the critical space for hypersingular operators).

The existence of a weak treatment of boundary conditions for the FEM has led to many useful applications, such as non-conforming or discontinuous approximations. The weak treatment of boundary conditions clearly shows us how to deal with interface conditions (either between elements or between sub-domains). In Chapter 3 we present a weak treatment of boundary conditions for the BEM (previously such a weak treatment of the boundary conditions was unknown), which will open the door to new methods that are currently unknown for hypersingular integral operators. Some of these methods include nonconforming or discontinuous domain decomposition methods. The ideas also allow examination of nonconforming or discontinuous elements,for example Crouzeix-Raviart

type (see [30]) or primal hybrid formulations. An extension of this analysis to mortar-type decompositions is shown in Chapter 4.

Essential properties of the analysis of the BEM of boundary integral equations of the first kind on open surfaces [52] include fractional order Sobolev spaces consisting of functions which can be continuously extended by zero onto a larger surface. We note that for certain order Sobolev spaces this is not the same condition as enforcing a homogeneous boundary condition on the space. We aim to take this analysis to the next stage by analysing and implementing this extendibility condition through the use of Lagrangian multipliers. We thus shall provide the analysis for weak interface conditions in $H^{1/2}$ and show that they can be incorporated into discrete subspaces of $H^{1/2}$ in an almost quasi-optimal way. A *quasi-optimal* error estimate is one that gives the convergence order of the best approximation error (Céa's Lemma). "Quasi" comes from a factor in Céas estimate which may be larger than one. We use the term "almost quasi-optimal" for error estimates which are quasi-optimal up to a logarithmically growing factor. In Chapter 3 we consider the model situation of homogeneous boundary conditions for the hypersingular operator (of the Laplacian) on an open surface.

1.2.3 Mortar Methods

The mortar method is a nonconforming Galerkin approximation scheme that can be classified as a non-overlapping domain decomposition method. Domain decomposition techniques are well established for the FEM see [46] and [54] for an overview. We however wish to study the specific domain decomposition technique known as the mortar FEM. The mortar FEM is an extension of the Primal Hybrid FEM introduced in [47], where the constraint of inter-element continuity has been removed at the expense of introducing a Lagrangian multiplier. This allows a more general and less restrictive approach to the construction of finite element approximations. The mortar FEM was first introduced in the early nineties in [5] and [6]. Although originally introduced with the aim of combining spectral methods having different polynomial degrees, or the spectral method with the FEM it can however, as stated, be used as a domain decomposition technique for the finite element method. The original paper has been followed by work by the original and other authors in many areas and extensions to the original ideas such as problems in three dimensions, preconditioning and a posteriori error estimates, see e.g. [3, 11, 12, 35, 36, 57] and [58] to cite a few. In particular, the *hp*-version and graded meshes have been studied in [20] and [50]. Recent advances include the mortar method being applied to parabolic problems [45].

The main attraction of the mortar method is to allow for different discretisations in different parts of the domain of the underlying problem. Different discretisations can result from the use of either different meshes and/or different types of basis functions on

different parts of the domain. In the mortar method the compatibility of discretisations across interfaces of sub-domains is ensured only in a weak sense by some integral matching condition. This means that instead of having a continuous approximation over the whole region we will have discontinuities across interfaces in the approximating function. These discontinuities will add to the error of the method, however this should be balanced by the ability to get more accurate approximations in certain areas of the region. Alternatively it may be a computational pay off: for example we may only require that the solution be accurate in a certain part of the region and not in others so we can concentrate more on that part by using a finer mesh.

Typical applications are in large scale simulations where substructures can be discretised separately. One example of this is in the modelling of an aeroplane where the main body and wings can be discretised separately. The advantages of this approach are that we can optimize our approximation for substructures, that we can solve different parts of the problem separately (e.g. on a parallel computer), and that the meshing of complicated structures can be made simpler by breaking the structure up into smaller parts which can then be meshed more simply. This means that the mortar method allows us to tackle complicated large scale problems by decomposing the large problem into a collection of smaller, easier to solve sub-problems. In this way we can find approximations to problems which may not be possible or practical for standard approximations.

The mortar FEM generalizes to three dimensions, see for example [4, 10] or [35]. It is particularly useful in three dimensions as a complex geometry can often be decomposed into sub-geometries that are more easily meshed independently. The interfaces between sub-domains in the three dimensional case are now two dimensional surfaces, compared to the two dimensional mortar FEM where interfaces where simply one dimensional pieces. This means that unlike in the two dimensional case where we simply had non-conformity across edges, in the three dimensional case we now have non-conformity across surfaces. This, obviously, makes things more complicated computationally in the three-dimensional case. We note that the continuity at cross points constraint that was originally imposed in the two dimensional case now becomes the constraint of continuity along whole edges of the interface in the three dimensional case. This is a severe constraint which would eliminate some of the advantage of the mortar FEM. However as shown in [4] this condition, as in the two dimensional case, can be relaxed to allow a less restrictive method.

Mortar boundary element method

Instead of the standard (conforming) boundary element formulation we shall study the domain decomposition method known as the mortar method. We shall split the domain up into N non-overlapping sub-domains and require a weak compatibility condition on the interfaces between sub-domains. We shall require a compatibility condition across

the interface between two sub-domains. This compatibility condition shall be expressed as an integral over the interface, and in order to produce this integral we require an integration by parts formula. The weak compatibility condition will be incorporated by a Lagrangian multiplier, which means that we require an appropriate integration by parts formula. The weak compatibility condition means that, unlike the standard BEM, our approximate solution may not be continuous across the whole domain (although it is continuous on each sub-domain).

To be precise, we apply the mortar technique directly to the boundary element discretisation, not as a coupling procedure between boundary and finite elements as in [17]. We follow the analysis presented in [3] (and briefly outlined in Section 2.2.6) for the mortar FEM, where projection and extension operators are used to bound the error in the kernel space (of functions satisfying the Lagrangian multiplier condition). Note that there is a shorter presentation by Braess, Dahmen and Wiener [11] where the simpler argument [9, Remark III.4.6] is used to bound this error by a standard approximation error (in un-restricted spaces). Nevertheless, in our case the Strang-type error estimate has a more complicated structure and it is not straightforward to follow the argument [9, Remark III.4.6]. In particular our more complicated structure arises from the lack of a continuous formulation of the mortar scheme.

1.3 Notations

Notations. The symbols "$\lesssim$" and "$\gtrsim$" will be used in the usual sense. In short, $a_h(v) \lesssim b_h(v)$ when there exists a constant $C > 0$ independent of the discretisation parameter h such that $a_h(v) \leq C b_h(v)$. The double inequality $a_h(v) \lesssim b_h(v) \lesssim a_h(v)$ is simplified to $a_h(v) \simeq b_h(v)$. In our case the generic constant C is also independent of the fractional Sobolev index $\epsilon > 0$.

In Chapters 2-5 we will also use the notation v_j for the restriction of a function v to the sub-domain Γ_j. Chapter 6 uses a slightly different notation which is discussed on page 99.

Chapter 2

Mathematical Background

This chapter is split into three distinct parts. In Section 2.1 we begin by briefly presenting the BEM for the Laplace equation. The next step is to discuss the existence and uniqueness of the solution to the proposed scheme and finally to present an error estimate for the scheme.

In Section 2.2 we shall briefly introduce and discuss the non-conforming FEM, the mixed formulation of the FEM and the mortar FEM. We shall pay particular attention to the areas where there are problems in the translation of the method from the finite element situation to the boundary element situation. We also present some well known results which are required for the existence and uniqueness of the solution to the methods which we propose.

In Section 2.3 we shall show some results which are needed for the application of the mortar method to the boundary element situation. We first introduce an integration by parts formula for the problem, followed by some results relating to the surface differential operators used in the integration by parts formula and finally we present some other results which shall be required for the following chapters. This section is intended as a point of common reference for the following chapters.

2.1 The Boundary Element Method

Before presenting the BEM we briefly present some of the spaces and norms which will be required.

Sobolev spaces

In the following we let $\Omega \subset \mathbf{R}^n$ be a domain (or surface when $n = 2$) with Lipschitz boundary $\partial\Omega$. We first define the following spaces:

$C(\Omega)$	space of continuous functions in Ω,
$C^k(\Omega)$	space of k times continuously differentiable functions in Ω,
$C^\infty(\Omega)$	space on infinitely many times continuously differentiable functions in Ω,
$C_0^\infty(\Omega)$	space of functions from $C^\infty(\Omega)$ with compact support.

We now briefly define the needed Sobolev spaces. Let (the Lebesgue integral) of a (suitably smooth and well defined) function v be defined by

$$\|v\|_{L^2(\Omega)} := \left(\int_\Omega |v(x)|^2 \, dx \right)^{1/2}.$$

We then define the Lebesgue space

$$L^2(\Omega) := \left\{ v : \|v\|_{L^2(\Omega)} < \infty \right\},$$

and the product space

$$(L^2(\Omega))^2 := L^2(\Omega) \times L^2(\Omega).$$

For positive integer k we define the norm in $H^k(\Omega)$ as

$$\|u\|_{H^k(\Omega)} := \left(\int_\Omega \sum_{|\alpha| \le k} |D^\alpha u(x)|^2 \, dx \right)^{1/2}.$$

Where we have used the multi-index $\alpha := (\alpha_1, \ldots, \alpha_n)$ (in n dimensions), that $|\alpha| := \sum_{i=1}^n \alpha_i$ and that $D^\alpha := (\frac{\partial}{\partial x_1}) \cdots (\frac{\partial}{\partial x_n})$. We may then define the space $H^k(\Omega)$ as:

$$H^k(\Omega) \quad \text{closure of } C^\infty(\Omega) \text{ under the norm } \|u\|_{H^k(\Omega)}.$$

We also define the space

$$H^1_{\text{loc}}(\Omega) := \{u \text{ a distribution in } \Omega : u \in H^1(\Omega \cap B^R) \, \forall R > 0\},$$

where B^R is the open ball with centre the origin and radius R, and a distribution is a generalised function which allows us to differentiate functions whose derivatives do not exist in a classical sense. We now define the space

$$H_0^1(\Omega) := \{v \in L^2(\Omega);\, \nabla v \in (L^2(\Omega))^2,\, v = 0 \text{ on } \partial\Omega\}.$$

Where ∇v is the gradient of v defined by (in n dimensions)

$$\nabla v = \operatorname{grad} v = \left(\frac{\partial u}{\partial x_i} \right)_{i=1}^n \quad \text{in } \Omega.$$

We may also define $H_0^1(\Omega)$ as

$$H_0^1(\Omega) \quad \text{closure of } C_0^\infty(\Omega) \text{ under the norm } \|u\|_{H^1(\Omega)}.$$

We consider standard Sobolev spaces where the following norms are used: For $0 < s < 1$ we define

$$\|u\|^2_{H^s(\Omega)} := \|u\|^2_{L^2(\Omega)} + |u|^2_{H^s(\Omega)} \tag{2.1}$$

with semi-norm

$$|u|_{H^s(\Omega)} := \Big(\int_\Omega \int_\Omega \frac{|u(x) - u(y)|^2}{|x-y|^{2s+n}}\, dx\, dy\Big)^{1/2}. \tag{2.2}$$

We then define the space

$$H^s(\Omega) \quad \text{completion of } C^\infty(\Omega) \text{ under the norm } \|u\|_{H^s(\Omega)}.$$

For a Lipschitz domain Ω and $0 < s < 1$ we have the norm

$$\|u\|_{\tilde{H}^s(\Omega)} := \Big(|u|^2_{H^s(\Omega)} + \int_\Omega \frac{u(x)^2}{(\operatorname{dist}(x, \partial\Omega))^{2s}}\, dx\Big)^{1/2}. \tag{2.3}$$

We then define the space

$$\tilde{H}^s(\Omega) \quad \text{completion of } C^\infty(\Omega) \text{ under the norm } \|u\|_{\tilde{H}^s(\Omega)}.$$

For $s \in (0, 1/2)$, $\|\cdot\|_{\tilde{H}^s(\Omega)}$ and $\|\cdot\|_{H^s(\Omega)}$ are equivalent norms whereas for $s \in (1/2, 1)$ there holds $\tilde{H}^s(\Omega) = H_0^s(\Omega)$, the latter space being the completion of $C_0^\infty(\Omega)$ with norm in $H^s(\Omega)$. Also we note that functions from $\tilde{H}^s(\Omega)$ are continuously extendable by zero onto a larger domain. For all these results we refer to [26, 38]. For $s > 0$ the spaces $H^{-s}(\Omega)$ and $\tilde{H}^{-s}(\Omega)$ are the dual spaces of $\tilde{H}^s(\Omega)$ and $H^s(\Omega)$, respectively. Fractional order Sobolev spaces can be equivalently defined by interpolation, details on the real K-method may be found in [41, Appendix B].

2.1.1 The Boundary Element Method

The hypersingular integral equation

We consider the problem of the screen surface Γ. For a given function g on Γ we wish to find u in $\Omega := \mathbf{R}^3 \setminus \bar{\Gamma}$ satisfying

$$-\Delta u = 0 \qquad \text{in } \Omega \tag{2.4}$$

$$\frac{\partial u}{\partial n} = g \qquad \text{on } \Gamma \text{ and} \tag{2.5}$$

$$u = o(r^{-1}) \quad \text{as } r := |x| \to \infty. \tag{2.6}$$

Where Δ is the Laplace operator given by

$$\Delta u = \frac{\partial^2 u}{\partial x_1^2} + \frac{\partial^2 u}{\partial x_2^2} + \frac{\partial^2 u}{\partial x_3^2},$$

where $x = (x_1, x_2, x_3) \in \mathbf{R}^3$ are Cartesian coordinates. We also require the normal derivative of a function w defined by

$$\frac{\partial w}{\partial \boldsymbol{n}} = \boldsymbol{n} \cdot \nabla w = \frac{\partial w}{\partial x_1} n_1 + \frac{\partial w}{\partial x_2} n_2 + \frac{\partial w}{\partial x_3} n_3 \quad \text{on } \partial\Omega.$$

Here, $\boldsymbol{n} = (n_1, n_2, n_3)$ denotes the exterior unit normal vector along $\partial\Omega$.

Further we assume that Γ is a bounded, simply connected, orientable, smooth, open surface in $\mathbf{R}^3$ with a smooth boundary curve γ which does not intersect itself. Our solution procedure is to derive boundary integral equations of the first kind on Γ for the jump of the field $[u]$ across Γ. This is expressed in the following theorem.

Theorem 2.1. *[53, Theorem 2.6] $u \in H^1_{\mathrm{loc}}(\Omega)$ is the solution of the screen Neumann problem (2.4) - (2.6) if and only if the jump $[u]|_\Gamma \in \tilde{H}^{1/2}(\Gamma)$ is the solution of the hypersingular integral equation*

$$-\frac{1}{4\pi} \int_\Gamma [u](y) \frac{\partial^2}{\partial \boldsymbol{n}_x \partial \boldsymbol{n}_y} \frac{1}{|x-y|} dS_y = g(x)$$

for $x \in \Gamma$ and given $g \in H^{-1/2}(\Gamma)$.

Model problem

For simplicity let Γ be the plane open surface with polygonal boundary, and we shall denote its boundary by $\partial\Gamma$. We shall identify the surface Γ with a subset of $\mathbf{R}^2$, thus referring to Γ as a domain rather than a surface and also referring to sub-domains of Γ rather than sub-surfaces. Now our model problem is: *For a given $f \in H^{-1/2}(\Gamma)$ find $\phi \in \tilde{H}^{\frac{1}{2}}(\Gamma)$ such that*

$$W\phi(x) := -\frac{1}{4\pi} \frac{\partial}{\partial \mathbf{n}_x} \int_\Gamma \phi(y) \frac{\partial}{\partial \mathbf{n}_y} \frac{1}{|x-y|} \, dS_y = f(x), \quad x \in \Gamma. \tag{2.7}$$

Here, $\mathbf{n}$ is a normal unit vector on Γ, e.g. $\mathbf{n} = (0, 0, 1)^T$. We note that the hypersingular operator W maps $\tilde{H}^{1/2}(\Gamma)$ continuously onto $H^{-1/2}(\Gamma)$ (see [19], [53]).

We have the following weak (variational) formulation of (2.7). *Find $\phi \in \tilde{H}^{\frac{1}{2}}(\Gamma)$ such that*

$$a(\phi, \psi) := \langle W\phi, \psi \rangle_\Gamma = \langle f, \psi \rangle_\Gamma =: F(\psi) \qquad \forall \psi \in \tilde{H}^{1/2}(\Gamma). \tag{2.8}$$

Here, $\langle \cdot, \cdot \rangle_\Gamma$ denotes the $L^2(\Gamma)$ inner product and is also used for its generic extension by duality (e.g. between $H^{-1/2}(\Gamma)$ and $\tilde{H}^{1/2}(\Gamma)$). Later we will indicate just the support where the duality is taken (e.g. Γ or its boundary γ). Here also, $a(\cdot, \cdot)$ is a bilinear form and $F(\cdot)$ is a linear form.

To define the boundary element space we consider a triangulation $\mathcal{T}_h = \{K_j : j = 1, \ldots, m\}$ of Γ into polygons (or elements) K_j, which are typically triangles or rectangles, i.e.

$$\bar{\Gamma} = \bigcup_{K \in \mathcal{T}_h} K.$$

Here we assume that any two polygons are disjoint or intersect at a single vertex or an entire edge. The triangulation $\mathcal{T}_h$ is also called a *mesh* on Γ. Our boundary element space is then

$$\tilde{X}_h := \{\psi_h \in C^0(\bar{\Gamma}) : \psi_h|_K \in \boldsymbol{P}_r(K) \forall K \in \mathcal{T}_h, \psi_h|_{\partial\Gamma} = 0\},\ r \geq 1$$

where $\bar{\Gamma}$ is the closure of Γ, $\boldsymbol{P}_r(K)$ denotes the set of polynomials defined in K and of degree less than or equal to r, $\psi_h|_K$ denotes the restriction of v_h to the element K, and similarly $\psi_h|_{\partial\Gamma}$ denotes the restriction of ψ_h to $\partial\Gamma$. In two dimensions the maximum diameter of the element K is denoted by h and is known as the mesh size parameter.

A standard Galerkin BEM for the approximate solution of (2.8), is to select a piecewise polynomial subspace $\tilde{X}_h \subset \tilde{H}^{\frac{1}{2}}(\Gamma)$ and define an approximant $\tilde{\phi}_h \in \tilde{X}_h$ by

$$a(\tilde{\phi}_h, \psi) := \langle W\tilde{\phi}_h, \psi \rangle_\Gamma = \langle f, \psi \rangle_\Gamma =: F(\psi) \qquad \forall \psi \in \tilde{X}_h.$$

We note that to arrive at the weak formulation we simply multiply by a test function and integrate over the boundary. This is different to the FEM where we require an integration by parts formula (see Section 2.2.1 later) to arrive at the weak formulation which in turn provides us with the necessary boundary integrals to be able to incorporate a Lagrangian multiplier and thus develop the mortar FEM. No such integration by parts formula is used to generate the weak form of the BEM as the restriction to the boundary (of the boundary) of the functions in the test space for the BEM is not well defined (see the trace theorem later Lemma 2.22). This means that there is no immediately obvious term to use as a Lagrangian multiplier and hence generate a mortar BEM. We thus have to find a different way of representing the formulation so that we can incorporate a Lagrangian multiplier.

Existence and uniqueness of solution

We now consider the existence and uniqueness of the solution to the following more general problem

$$\text{Find } u \in V \text{ such that} \quad a(u, v) = F(v) \quad \forall v \in V. \tag{2.9}$$

Where V is a Hilbert space with the associated norm $\|\cdot\|_V$. With the approximation

$$\text{Find } u_h \in V_h \text{ such that} \quad a(u_h, v) = F(v) \quad \forall v \in V_h. \tag{2.10}$$

Where V_h is an appropriately chosen discrete space.

Definition 2.2. We have the following:

- The linear form $F(\cdot) : V \to \mathbf{R}$ is called continuous (or bounded) if

$$\exists C > 0 \, : \, |F(v)| \leq C\|v\|_V \quad \forall v \in V.$$

- The bilinear form $a(\cdot, \cdot) \, : \, V \times V \to \mathbf{R}$ is called continuous (or bounded) if

$$\exists C_\alpha > 0 \, : \, |a(v, w)| \leq C_\alpha \|v\|_V \|w\|_V \quad \forall v, w \in V.$$

- The bilinear form $a(\cdot, \cdot) \, : \, V \times V \to \mathbf{R}$ is called V-elliptic (or simply elliptic or coercive) if

$$\exists \alpha > 0 \, : \, |a(v, v)| \geq \alpha \|v\|_V^2 \quad \forall v \in V.$$

We now state the well known Lax-Milgram Theorem which guarantees existence and uniqueness of the solution. For a proof of the Theorem see e.g. [14, Section 2.7].

Theorem 2.3. ***(Lax-Milgram)*** *Let V be a Hilbert space, $a(\cdot, \cdot)$ a continuous V-elliptic bilinear form and $F(\cdot)$ a continuous linear form on V. Then (2.9) has a unique solution $v \in V$.*

We now state the following result on the error of the approximation of the problem. For a proof of the Theorem see e.g. [14, Section 2.8].

Theorem 2.4. ***(Céa)*** *Let $a(\cdot, \cdot)$ be a continuous V-elliptic bilinear form and $F(\cdot) \in V'$ (V' is the dual space of V). Then, for $V_h \subset V$ the solution $u \in V$ of (2.9) and $u_h \in V_h$ of (2.10) satisfy*

$$\|u - u_h\|_V \leq \frac{C_\alpha}{\alpha} \|u - v\|_V \quad \forall v \in V, \tag{2.11}$$

where C_α is the continuity constant and α is the ellipticity constant of $a(\cdot, \cdot)$ on V.

Error estimate

Now returning to our weak formulation (2.8) we see that $V = \tilde{H}^{1/2}(\Gamma)$ is a Hilbert space, and that the bilinear form $a(\cdot,\cdot)$ is both continuous (on V) and V-elliptic, and that $F(\cdot)$ is a continuous linear form on V. We thus have, by the Lax-Milgram theorem (Theorem 2.3), the existence and uniqueness of a solution to this formulation. We now consider the discrete approximation (2.11) and note that since $V_h \subset V$ the necessary assumptions on the bilinear and linear forms immediately follow. Again, the Lax-Milgram theorem (Theorem 2.3) gives us the existence and uniqueness of a solution to this formulation. This analysis now implies the necessary conditions for the application of Céa's lemma (Theorem 2.4), which gives us a suitable bound on the error of our approximation, through the use of standard approximation theory.

The solution ϕ of (2.8) has strong corner and corner-edge singularities such that $\phi \notin H^1(\Gamma)$ in general, see [56]. A refined error analysis for the conforming BEM yields for quasi-uniform meshes an optimal error estimate

$$\|\phi - \phi_h\|_{\tilde{H}^{1/2}(\Gamma)} \leq C\, h^{1/2},$$

see [8] or [33]. Such an error analysis makes use of an explicit knowledge of the appearing singularities. When using only the Sobolev regularity $\phi \in \tilde{H}^{1-\epsilon}(\Gamma)$ with $\epsilon > 0$, standard approximation theory proves

$$\|\phi - \phi_h\|_{\tilde{H}^{1/2}(\Gamma)} \leq C\, h^{1/2-\epsilon} \|\phi\|_{\tilde{H}^{1-\epsilon}(\Gamma)}.$$

2.2 Mixed Finite Element Methods

In this section we briefly introduce the FEM for the Poisson equation. We then discuss some alternative formulations such as nonconforming formulations, the FEM with Lagrangian multiplier and the mortar FEM. We also introduce some of the theory which will be required to prove existence and uniqueness to the solutions of these formulations as well as provide us with an error estimate for them.

2.2.1 The Finite Element Method

In this section we will give a brief presentation of the derivation of the FEM for the Poisson equation with homogeneous Dirichlet boundary condition. For more details we refer to [9, 14, 18, 22] and [34]. We shall examine the *Poisson equation* with homogeneous Dirichlet boundary condition on a bounded Lipschitz domain $\Omega \subset \mathbf{R}^2$:

$$-\Delta u = f \quad \text{in } \Omega,$$

$$u = 0 \quad \text{on } \partial\Omega. \tag{2.12}$$

Where f is a given function, $\partial\Omega$ denotes the boundary of Ω. The Laplace operator can be rewritten in the following form

$$\Delta u = \operatorname{div} \nabla u,$$

and div is the divergence defined for a vector valued function $\boldsymbol{A} = (A_1, A_2)$ by (in two dimensions)

$$\operatorname{div} \boldsymbol{A} = \frac{\partial A_1}{\partial x_1} + \frac{\partial A_2}{\partial x_2} \quad \text{in } \Omega.$$

Let us now recall the following integration by parts formula.

Lemma 2.5 (First Green formula)**.** *For sufficiently smooth functions v and $\boldsymbol{A} = (A_1, A_2)$ there holds*

$$\int_\Omega \nabla v \cdot \boldsymbol{A}\, dx = \int_{\partial\Omega} v\, \boldsymbol{n} \cdot \boldsymbol{A}\, ds - \int_\Omega v \cdot \operatorname{div} \boldsymbol{A}\, dx$$

The first integral on the right-hand side denotes integration with respect to arc length s along $\partial\Omega$.

Now multiplying the Poisson equation by a sufficiently smooth function v, integrating over Ω and using the first Greens formula we get

$$\int_\Omega f v\, dx = \int_\Omega -\Delta u\, v\, dx = \int_\Omega \nabla u \cdot \nabla v\, dx - \int_{\partial\Omega} \frac{\partial u}{\partial \boldsymbol{n}} v\, ds. \tag{2.13}$$

Now, selecting the space $V := H_0^1(\Omega)$ we see that the boundary term in (2.13) (the integral over $\partial\Omega$) is equal to zero for $v \in V_h$. This leads to the following weak formulation of the Laplace equation

$$\text{Find } u \in V \text{ such that} \quad a(u, v) = F(v) \quad \forall v \in V \tag{2.14}$$

with

$$a(u, v) := \langle \nabla u, \nabla v \rangle_\Omega \text{ and } F(v) := \langle f, v \rangle_\Omega. \tag{2.15}$$

The **finite element method (FEM)** for the solution of (2.12) consists of solving (2.14) with a finite dimensional subspace V_h of V. This finite element space is constructed by piecewise polynomial functions, as we did in the BEM. We may choose the following space:

$$V_h := \{v_h \in C^0(\bar{\Omega}) : v_h|_K \in \boldsymbol{P}_r(K) \forall K \in \mathcal{T}_h, v_h|_{\partial\Omega} = 0\},\ r \geq 1.$$

The FEM for (2.12) then reads

$$\text{Find } u_h \in V_h \text{ such that } a(u_h, v_h) = F(v) \quad \forall v_h \in V_h. \tag{2.16}$$

Appropriate ellipticity and continuity properties may be shown for the forms above. Thus existence and uniqueness of solution follows from Theorem 2.3, and an error estimate can be obtained using Theorem 2.4 and standard approximation theory.

2.2.2 Nonconforming Formulation

We shall now consider the situation when our discrete space is not a subset of our continuous space. By this we mean that

$$V_h \not\subset V.$$

One example of such a discrete space being chosen is where we choose a finite dimensional space that does not satisfy the specified boundary conditions. In (2.14) and (2.16) we had $V_h \subset V = H_0^1(\Omega)$. This means that our discrete functions satisfy the homogeneous boundary condition by the choice of the discrete space. If instead of this we choose $V_h \subset H^1(\Omega) \not\subset V$ i.e. our discrete functions do not satisfy the homogeneous boundary condition we find that we can still apply the Lax-Milgram Theorem (Theorem 2.3) to get existence and uniqueness of the solution but we can no longer appeal to Céa's Theorem (Theorem 2.4) for our error estimate. Instead we must appeal to the Second Strang Lemma. For a proof of the Lemma see e.g. [14, Section 10.1].

Lemma 2.6. *(Strang) Let V and V_h be subspaces of a Hilbert space H. Assume that $a(\cdot,\cdot)$ is a continuous bilinear form defined on H which is V_h-elliptic, with respective continuity and ellipticity constants C_α and α. Let $u \in V$ solve*

$$a(u, v) = F(v) \quad \forall v \in V,$$

where $F \in H'$. Let $u_h \in V_h$ solve

$$a(u_h, v) = F(v) \quad \forall v \in V_h.$$

Then

$$\|u - u_h\|_H \leq \left(1 + \frac{C_\alpha}{\alpha}\right) \inf_{v \in V_h} \|u - v\|_H + \frac{1}{\alpha} \sup_{w \in V_h \setminus \{0\}} \frac{|a(u - u_h, w)|}{\|w\|_H}. \tag{2.17}$$

The second term on the right-hand side of (2.17) would be zero if $V_h \subset V$. Therefore this term measures the degree of nonconformity in the approximation.

2.2.3 Finite Element Method with Lagrangian Multiplier

Lagrangian multipliers are a convenient method for the inclusion of nonhomogeneous essential boundary conditions into the FEM. They allow us to drop the constraint on the space at the expense of including a second bilinear form. The early work on applying this method to the FEM is presented in [1], and a more recent examination is shown in [2]. The approximation of the boundary conditions through the use of a Lagrangian multiplier may be considered as the simplest formulation of the mortar FEM, where we only have one sub-domain.

We shall now examine the Poisson equation with nonhomogeneous Dirichlet (essential) boundary condition on a bounded Lipschitz domain $\Omega \subset \mathbf{R}^2$:

$$\begin{aligned} -\Delta u &= f \quad \text{in } \Omega, \\ u &= g \quad \text{on } \partial\Omega. \end{aligned} \tag{2.18}$$

Where g is a given function. As before we multiply by a suitable function v, integrate over Ω and apply the first Greens formula to get (2.13). Now, selecting the space X as

$$X := H^1(\Omega)$$

we see that by choosing $u, v \in X$ in (2.13) we do not have the situation where the boundary term disappears (we do not have the homogeneous boundary condition included in the definition of our space). We may now define the bilinear form $a(\cdot,\cdot)$ and the linear form $F(\cdot)$ as in (2.15). We also define the bilinear form $b(\cdot,\cdot)$ and the linear form $G(\cdot)$ as

$$\begin{aligned} b(v,\lambda) &= \int_{\partial\Omega} \lambda v \, ds \\ G(v) &= \int_{\partial\Omega} g v \, ds. \end{aligned}$$

In the bilinear form $b(\cdot,\cdot)$ above we have $\lambda = \frac{\partial u}{\partial \boldsymbol{n}}$, this is our Lagrangian multiplier term. We now define the space M (the dual space of the trace space of X) as

$$M := (H^{1/2}(\partial\Omega))' = H^{-1/2}(\partial\Omega).$$

The above spaces lead to the following weak formulation with Lagrangian multiplier of the Laplace equation with nonhomogeneous Dirichlet boundary condition. *Find* $(u,\lambda) \in X \times M$ *such that*

$$a(u,v) + b(\lambda,v) = F(v) \quad \forall v \in X$$

$$b(u,\psi) \;=\; G(\psi) \quad \forall \psi \in M. \tag{2.19}$$

Where $G(\psi)$ is a linear form mapping M onto $\mathbf{R}$. We see that when compared to the weak formulation of the Laplace equation with nonhomogeneous boundary conditions we have used simpler spaces $X = H^1(\Omega)$ rather than $V^g = \{v \in H^1(\Omega);\, v = g \text{ on } \partial\Omega\}$. However this comes at the expense of the introduction of a second bilinear form $b(\cdot,\cdot)$ and the introduction of a second space M. The bilinear form $b(\cdot,\cdot)$ imposes the nonhomogeneous boundary condition in a weak sense. By this we mean that we only require that our solution u satisfies an integral matching condition rather than explicitly stating in the definition of the space that $u = g$ on $\partial\Omega$. The space M is referred to as the Lagrangian multiplier space and its members are referred to as Lagrangian multipliers.

To arrive at this continuous formulation required two items of particular interest when translating to the boundary element situation. Firstly, we required an integration by parts formula which defined a suitable boundary term that can be used as an interface matching condition. Secondly we require the use of the Trace Theorem for the restriction of functions from the domain to the boundary. These are two central issues for the translation from the FEM to the BEM situation.

The **finite element method with Lagrangian multiplier** for the solution of (2.19) is *Find* $(u_h, \lambda_k) \in X_h \times M_k$ *such that*

$$\begin{aligned} a(u_h, v) + b(\lambda_k, v) &= F(v) \quad \forall v \in X_h \\ b(u_h, \psi) &= G(\psi) \quad \forall \psi \in M_k. \end{aligned} \tag{2.20}$$

Where X_h and M_k are finite dimensional subspaces of X and M respectively.

Of particular interest to us shall be a situation similar to the homogeneous Dirichlet boundary condition case. We see that in this case (i.e. $g = 0$) we would have the following formulation: *Find* $(u, \lambda) \in X \times M$ *such that*

$$\begin{aligned} a(u, v) + b(\lambda, v) &= F(v) \quad \forall v \in X \\ b(u, \psi) &= 0 \quad \forall \psi \in M. \end{aligned} \tag{2.21}$$

If we now introduce the space

$$V := \{v \in X : b(v, \psi) = 0 \quad \forall \psi \in M\}. \tag{2.22}$$

We arrive at the equivalent formulation: *Find* $u \in V$ *such that*

$$a(u, v) \;=\; F(v) \quad \forall v \in V. \tag{2.23}$$

Existence and uniqueness results for the finite element method with Lagrangian multiplier follow from the Babuska-Brezzi Theory which shall be detailed below. An error estimate for the method can be obtained through an extension of the Strang-type estimate, which shall also be detailed below.

As explained before, when examining the application of hypersingular operators on open surfaces boundary element functions of a conforming method need to vanish at the boundary of the surface. This homogeneous condition can be easily incorporated into the method through the definition of the space, and the use of simple approximating functions. However, for our mortar method we do not want the approximating functions to vanish at the interface between sub-domains (since the function being approximated does not). This theory gives us an indication of the direction in which to head for an error estimate for our method.

2.2.4 Babuška-Brezzi Theory

We have the following Theorem for the continuous problem defined in (2.19). For a proof see e.g. [48, Theorem 10.1].

Theorem 2.7. *Let the bilinear form $a(\cdot,\cdot)$ be continuous on $X \times X$ and V-elliptic, i.e.*

$$\inf_{v\in V:\|v\|_V=1} a(v,v) > 0. \tag{2.24}$$

Also, let the bilinear form $b(\cdot,\cdot)$ is continuous on $M \times V$ and that it satisfies

$$\inf_{v\in X:\|v\|_X=1} \sup_{\psi\in M:\|\psi\|_M=1} b(\psi,v) > 0. \tag{2.25}$$

Then for each pair of continuous linear forms $F(\cdot)$ on X and $G(\cdot)$ on M, problem (2.19) has a unique solution.

Remark 2.8. Condition (2.25) is often referred to as the inf-sup condition. It is also referred to as the Brezzi-condition, the Babuška-Brezzi condition, or the LBB condition (where the L refers to Ladyzhenskaya). See [49] for an interesting discussion on the naming of this condition.

We also have the following Theorem for the discrete situation. For a proof see e.g. [48, Theorem 10.1].

Theorem 2.9. *Let the bilinear form $a(\cdot,\cdot)$ be V_h-elliptic, let the bilinear form $b(\cdot,\cdot)$ satisfy*

$$\inf_{v_h\in X_h:\|v_h\|_X=1} \sup_{\psi_h\in M_h:\|\psi_h\|_M=1} b(\psi_h,v_h) > 0. \tag{2.26}$$

Then for each pair of linear forms $F(\cdot)$ on X_h and $G(\cdot)$ on M_h, problem (2.20) has a unique solution.

Remark 2.10. Condition (2.26) is called the discrete inf-sup condition or the discrete LBB condition. It says that the choice of the subspaces X_h of X and M_h of M cannot be made independently of one another, and that there is a compatibility condition between the two subspaces.

The Babuška-Brezzi theory can be viewed as a generalisation of the Lax-Milgram theory to the mixed formulation. Condition (2.26) can be equivalently expressed as

$$\exists \beta > 0 : \quad \inf_{\mu \in M_h} \sup_{v \in X_h} \frac{b(v, \mu)}{\|\mu\|_M \|v\|_X} \geq \beta.$$

or

$$\exists \beta > 0 : \quad \sup_{v \in X_h} \frac{b(v, \mu)}{\|v\|_X} \geq \beta \|\mu\|_M \quad \forall \mu \in M_h.$$

Here the constant β is known as the inf-sup constant.

In order to apply this Babuška-Brezzi theory to our proposed methods we need to show the necessary properties of the bilinear forms. For a continuous formulation we would have to show that the bilinear form $a(\cdot, \cdot)$ is continuous on $X \times X$ and V-elliptic and that the bilinear form $b(\cdot, \cdot)$ is continuous on $M \times V$. While some of the properties would directly cross over to the discrete case for the bilinear form $a(\cdot, \cdot)$ it is worth noting that since in general $V_h \not\subset V$ such properties related to these spaces would not directly transfer.

2.2.5 Extension of Strang Type Estimate

We shall now examine the mixed formulation (2.21). We shall seek an approximate solution to (2.21) using the following discrete formulation: *Find* $(u_h, \lambda_h) \in X_h \times M_h$ *such that*

$$\begin{aligned} a(u_h, v_h) + b(\lambda_h, v_h) &= F(v_h) \quad \forall v_h \in X_h \\ b(u_h, \psi_h) &= 0 \quad \forall \psi_h \in M_h. \end{aligned} \tag{2.27}$$

We now define the space

$$V_h = \{v_h \in X_h : b(v_h, \psi_h) = 0 \quad \forall \psi_h \in M_h\}. \tag{2.28}$$

Now we have the equivalent formulation (to (2.27)): *Find* $u_h \in V_h$ *such that*

$$a(u_h, v_h) = F(v_h) \quad \forall v_h \in V_h. \tag{2.29}$$

We recall the Strang type estimate (Lemma 2.6) where the second term on the right hand side of (2.17) is a measure of the non-conformity of the method. We shall now examine this second term, which is

$$\frac{1}{\alpha} \sup_{w \in V_h \setminus \{0\}} \frac{|a(u - u_h, w)|}{\|w\|_M}.$$

For $w \in V_h$,

$$\begin{aligned} a(u - u_h, w) &= a(u, w) - a(u_h, w) \\ &= a(u, w) - F(w) \\ &= -b(w, \lambda) \\ &= -b(w, \lambda - \psi) \quad \forall \psi \in M_h. \end{aligned} \tag{2.30}$$

We note that this requires the existence of a continuous formulation to hold, specifically we require that

$$a(u, w) + b(w, \lambda) = F(w),$$

where $u \in X$ is our continuous solution and since $w \in V_h \subset X_h \subset X$. Now if the bilinear form $b(\cdot, \cdot)$ is continuous we have that

$$|b(w, \lambda - \psi)| \leq \|w\|_X \|\lambda - \psi\|_M. \tag{2.31}$$

Combining (2.30) and (2.31) gives us that

$$|a(u - u_h, w)| \leq \|w\|_X \|\lambda - \psi\|_M.$$

We now have the following bound on the error, for a proof see e.g. [14, Theorem 12.3.7].

Theorem 2.11. *Let $X_h \subset X$ and $M_h \subset M$, and define V_h and V by (2.22) and (2.28) respectively. Assume that the bilinear form $a(\cdot, \cdot)$ is both V and V_h-elliptic. Assume that the bilinear form $b(\cdot, \cdot)$ is continuous on $X \times M$ with constant C. Let u and λ be defined by (2.21), and let u_h be defined by (2.27)(or equivalently (2.29)). Then*

$$\|u - u_h\|_X \leq \left(1 + \frac{C_\alpha}{\alpha}\right) \inf_{v \in V_h} \|u - v\|_X + \frac{C}{\alpha} \inf_{\psi \in M_h \setminus \{0\}} \|\lambda - \psi\|_M. \tag{2.32}$$

As in Lemma 2.6 we have two parts to our error estimate. The second term represents the degree of nonconformity in the method as before only this time it is clear that the contribution stems from the Lagrangian multipliers.

In order to apply this Strang-type theory to our proposed methods we would require both a continuous and a discrete formulation. Not having a continuous formulation would complicate matters, although would not need to be an obstacle.

2.2.6 The Mortar Finite Element Method

We shall follow the procedure as described in [3] for the presentation of the mortar FEM. The conforming sub-domain decomposition will be shown for ease of presentation. We shall discuss the two dimensional case as this has the most relevance to our boundary element case.

We break up the initial domain $\Omega \subset \mathbf{R}^2$ into N non-overlapping sub-domains Ω_i, $1 \leq i \leq N$, which are assumed to be polygonally shaped. They are arranged such that any two sub-domains are disjoint or intersect at a single vertex or an entire edge. This is known as a geometrical conforming decomposition. A geometrical non-conforming decomposition occurs where two sub-domains intersect along part of an edge, but not necessarily the whole edge. The mortar FEM can be extended to the non-conforming case (of sub-domain decomposition), but we shall deal with the conforming case here for the sake of simplicity. We thus have that

$$\bar{\Omega} = \bigcup_{i=1}^{N} \bar{\Omega}_i, \; \Omega_i \cap \Omega_j = \emptyset \text{ for } i \neq j$$

Whenever two sub-domains Ω_i and Ω_j, $i < j$, are adjacent, Γ_{ij} is the common interface,

$$\Gamma_{ij} = \bar{\Omega}_i \cap \bar{\Omega}_j.$$

For simplicity let $\underline{i}$ denote the set of all indices j so that ij exists and $\bar{i}$ is the class of all indices $j \in \underline{i}$ with $j > i$. We denote by $\boldsymbol{n}_{ij}$ the unit normal orientated from Ω_i towards Ω_j and we set $\boldsymbol{n}_{ij} = -\boldsymbol{n}_{ji}$. We also have that the Γ_{ij} form a skeleton, S

$$S := \bigcup_{i=1}^{N} \bigcup_{j \in \bar{i}} \Gamma_{ij}$$

Continuous formulation

We need the following space:

$$X := \left\{ v \in L^2(\Omega) : v|_{\Omega_i} \in H^1(\Omega_i), i = 1, \ldots, N, v|_{\partial\Omega} = 0 \right\},$$

endowed with the norm

$$\|v\|_X := \left(\sum_{i=1}^{N} \|v\|^2_{H^1(\Omega_i)} \right)^{1/2}.$$

Having split the original domain up into sub-domains we now apply our integration by parts formula, Lemma 2.5, on each sub-domain individually to get the following for

$u, v \in X$

$$\int_{\Omega_i} \nabla u \cdot \nabla v \, dx = \int_{\Omega_i} f v \, dx + \int_{\partial\Omega_i} \frac{\partial u}{\partial \boldsymbol{n}} v \, ds.$$

Now summing over all sub-domains, recalling the homogeneous boundary condition on the original domain (which has been included in the space X), we have the following weak mixed continuous formulation: *Find* $(u, \lambda) \in X \times M$ *such that for* $f \in L^2(\Omega)$

$$\begin{aligned} a(u, v) + b(v, \lambda) &= F(v) \qquad \forall v \in X \\ b(u, \mu) &= 0 \qquad \forall \mu \in M \end{aligned} \tag{2.33}$$

where

$$a(u, v) = \sum_{i=1}^{N} \int_{\Omega_i} \nabla u \cdot \nabla v \, dx = \sum_{i=1}^{N} \langle \nabla u, \nabla v \rangle_{\Omega_i} \tag{2.34}$$

$$b(v, \mu) = \sum_{\Gamma_{ij} \subset S} \int_{\Gamma_{ij}} \mu [v] \, dS_x = \sum_{\Gamma_{ij} \subset S} \langle \mu, [v] \rangle_{\Gamma_{ij}} \tag{2.35}$$

$$F(v) = \langle f, v \rangle_{\Omega} \tag{2.36}$$

where $[v]$ is the jump of $v \in X$, it is defined on the skeleton S by $[v] := v|_{\Omega_k} - v|_{\Omega_l}$ on Γ_{kl}. Note that each interface Γ_{kl} appears only once in the sum over S. We note that the normal derivative is a mapping $H^1(\Omega_i) \to H^{-1/2}(\partial\Omega_i)$.

We can thus define the Lagrangian multiplier space M as

$$M := \prod_{\Gamma_{ij} \subset S} H^{-1/2}(\Gamma_{ij}),$$

with the associated norm

$$\|\psi\|_M := \left(\sum_{i=1}^{N} \sum_{j \in \bar{i}} \|\psi\|^2_{H^{-1/2}(\Gamma_{ij})} \right)^{1/2}.$$

We note that for each Γ_{ij} the indexing order is important, for Γ_{ij}, Ω_i is the non-mortar side. This fact, the distinction between mortar and non-mortar side, is very important when considering a non-conforming sub-domain decomposition. Analysis of the continuous problem leads to the jump over Γ_{ij} being $[v] \in \tilde{H}^{1/2}(\Gamma_{ij})$ (the dual space of $H^{-1/2}(\Gamma_{ij})$). This means that in particular we require that the jump vanishes at the end points of the interface.

We place the matching conditions into the definition of our space in the following way

$$V := \{v \in X : b(v, \mu) = 0 \, \forall \mu \in M\} .$$

We thus arrive at the following equivalent formulation of the weak continuous problem: *Find* $u \in V$ *such that*

$$a(u, v) = F(v) \qquad \forall v \in V. \tag{2.37}$$

Discrete formulation

We can now mesh each sub-domain individually, which is the primary advantage of the mortar FEM over the FEM. Each sub-domain can be given a completely different mesh and different finite element approximation spaces can be used on each sub-domain i.e. different piecewise polynomials can be used on different sub-domains. An example of a domain split up into sub-domains with individually meshed sub-domains is shown in Figure 2.1.

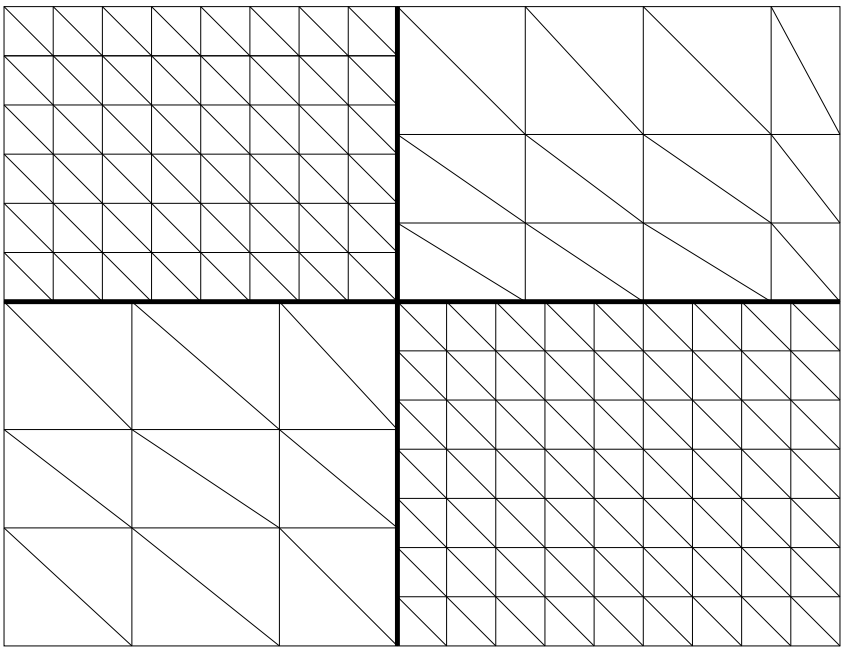

Figure 2.1: An example of a domain decomposed into sub-domains

In order to determine the discrete spaces, we first need to introduce a triangulation

$\mathcal{T}_{h_i}$ of each sub-domain Ω_i, $1 \leq i \leq N$, so that:

$$\bar{\Omega}_i = \bigcup_{\kappa \in \mathcal{T}_{h_i}} \bar{\kappa},$$

where κ represents an element of the triangulation. For simplicity we may assume that the elements are triangles, although the results hold for other types of elements. Let us now define the finite dimensional space:

$$X_{h,i} := \{v_{h,i} \in \boldsymbol{C}(\bar{\Omega}_i),\ \forall \kappa \in \mathcal{T}_{h_i},\ v_{h,i} \in \boldsymbol{P}_r(\kappa),\ v_{h,i}|_{\partial\Omega \cap \partial\Omega_i} = 0\}.$$

We now consider the product space:

$$X_h := \prod_{i=1}^{N} X_{h,i} \qquad X_h \subset X.$$

We now consider the restriction of the triangulation $\mathcal{T}_{h_i}$ over Γ_{ij}, $1 \leq i \leq N$, $j \in \bar{i}$, with vertices $\nu_{1,ij}$ and $\nu_{2,ij}$, results in a regular triangulation denoted by t_{ij}. Note that in general t_{ij} differs from t_{ji}. The trace space of functions from $X_{h,i}$ for the interface Γ_{ij} is given by:

$$W_{h,ij} := \{\chi_{h,ij} \in \boldsymbol{C}(\Gamma_{ij}),\ \forall t \in t_{ij}, \chi_{h,ij}|_t \in \boldsymbol{P}_r(t)\}.$$

The local approximation of the Lagrange multipliers is taken locally in (a subspace of $W_{h,ij}$ of co-dimension two)

$$M_{h,ij} := \{\psi_{h,ij} \in W_{h,ij},\ \forall t \in t_{ij}, \psi_{h,ij}|_t \in \boldsymbol{P}_{r-1}(t) \text{ if } \nu_{1,ij} \text{ or } \nu_{2,ij} \in t\},$$

and we define the global discrete Lagrangian multiplier space to be:

$$M_h := \prod_{i=1}^{N} \prod_{j \in \bar{i}} M_{h,ij} \qquad M_h \subset M.$$

We thus have the following discrete mixed formulation. *Find* $(u_h, \lambda_h) \in X_h \times M_h$ *such that*

$$\begin{aligned} a(u_h, v_h) + b(v_h, \lambda_h) &= F(v) \qquad \forall v_h \in X_h \\ b(u_h, \mu_h) &= 0 \qquad \forall \mu_h \in M_h. \end{aligned} \tag{2.38}$$

The finite element functions that satisfy mortaring conditions form the space $V_h \subset X_h$

$$V_h := \{v_h \in X_h : b(v_h, \mu_h) = 0 \quad \forall \mu_h \in M_h\}. \tag{2.39}$$

This leads to the alternative discrete formulation: *Find* $u_h \in V_h$ *such that*

$$a(u_h, v_h) = \langle f, v_h \rangle_\Omega \qquad \forall v_h \in V_h. \tag{2.40}$$

Existence, uniqueness and error estimate

We shall now consider what is necessary for the existence and uniqueness of the solution to the mortar FEM, and what is required to produce an error estimate. The following ensure the stability of the discrete formulation. Firstly we need the continuity of the bilinear forms $a(.,.)$ and $b(.,.)$ defined in (2.34) and (2.35) respectively with respect to the appropriate norms:

$$|a(u_h, v_h)| \leq c\|u_h\|_X\|v_h\|_X, \quad \forall u_h, v_h \in X_h,$$

and

$$|b(v_h, \mu_h)| \leq c\|v_h\|_X\|\mu_h\|_M \quad \forall u_h \in X_h, \forall \mu_h \in M_h.$$

Next we require the ellipticity of $a(.,.)$ on the space V_h (defined in (2.39)) for the following bound

$$a(v_h, v_h) \geq \alpha\|v_h\|_X^2.$$

Now we need that the bilinear form $b(\cdot,\cdot)$ satisfies the the (discrete) LBB-condition (also known as the inf-sup condition)

$$\inf_{\mu_h \in M_h} \sup_{v_h \in X_h} \frac{b(v_h, \mu_h)}{\|v_h\|_X\|\mu_h\|_M} \geq \beta.$$

The existence and uniqueness of the solution $(u_h, \mu_h) \in X_h \times M_h$ follows from the Babuska-Brezzi theory (See Theorem 2.9). This requires that the bilinear form $a(\cdot,\cdot)$ is continuous on X_h and V_h-elliptic. It also requires that the bilinear form $b(\cdot,\cdot)$ satisfies a discrete inf-sup condition and is continuous on $X_h \times M_h$.

These results lead to the following error estimate, from the Strang-type estimate (Theorem 2.6).

Lemma 2.12. *[3, Lemma 2.4] The discrete solution u_h of (2.38) (or equivalently (2.40)) and the exact solution u of (2.33) (or equivalently (2.37)) satisfy (where $\mu = \frac{\partial u}{\partial \boldsymbol{n}}$)*

$$\|u - u_h\|_X \leq c\left(\inf_{v_h \in V_h} \|u - v_h\|_X + \sup_{v_h \in V_h} \frac{b(v_h, \mu)}{\|v_h\|_X}\right)$$

The first term on the right hand side is the approximation error; the second is the consistency error. The consistency error results from the non-conformity of the method. Bounding the consistency error is relatively straightforward by the continuity of $b(\cdot,\cdot)$, however estimating the approximation error is not. The main difficulty involved is that we are taking the infimum over the constrained space V_h but we are approximating by functions in the unconstrained space X_h. This means that we need to construct a function

v_h such that it satisfies the mortaring conditions if we wish to apply standard approximation theory. This process involves the use of interpolation operators (and projection operators) and as such requires the assumption that the solution to the problem has at least $H^1(\Omega_i)$ regularity. These projection and extension operators allow us to bound the approximation error, see [6, Lemma 4.3 and Theorem 4.4].

We define the following mortar projection operator:

$$\pi_{ij} \,:\, \tilde{H}^{1/2}(\Gamma_{ij}) \rightarrow W_{h,ij} \cap \tilde{H}^{1/2}(\Gamma_{ij})$$

as follows: $\forall \psi \in M_{h,ij}$

$$\int_{\Gamma_{ij}} (\chi - \pi_{ij}\chi)\psi \, ds = 0.$$

Note that the function $\pi_{ij}\chi \in \tilde{H}^{1/2}(\Gamma_{ij})$ is equivalent to the fact that it is vanishing at the extreme points points of Γ_{ij}. This projection operators projects functions from the mortar side onto the Lagrangian multiplier (or non-mortar) side. We require the following property of this projection operator.

Lemma 2.13. *[3, Lemma 2.2] The projector π_{ij} is continuous: $\forall \chi \in \tilde{H}^{1/2}(\Gamma_{ij})$,*

$$\|\pi_{ij}\chi\|_{\tilde{H}^{1/2}(\Gamma_{ij})} \leq C\|\chi\|_{\tilde{H}^{1/2}(\Gamma_{ij})}.$$

We next need the existence and stability of an extension operator for the traces of our discrete functions from the boundary of a sub-domain over the whole sub-domain.

Lemma 2.14. *[3, Lemma 2.3] There exists an extension operator*

$$E_i \,:\, \boldsymbol{C}(\partial\Omega_i) \cap \prod_{j \in \underline{i}} W_{h,ij} \rightarrow X_{h,i},$$

satisfying the stability

$$\|E_i\chi\|_{H^1(\Omega_i)} \leq C\|\chi\|_{H^{1/2}(\partial\Omega_i)},$$

where C is a constant independent of h_i.

We now arrive at the main error estimate.

Lemma 2.15. *[3, Lemma 2.5] Assume the exact solution u of problem (2.33) (or equivalently (2.37)) is in $H_0^1(\Omega)$ is so that for any i, $1 \leq i \leq N$, $u_i = u|_{\Omega_i} \in H^{\lambda_i+1}(\Omega_i)$, $0 \leq \lambda_i \leq r$ and for the discrete solution u_h of (2.38) (or equivalently (2.40)) Then we have*

$$\|u - u_h\|_X \leq C \sum_{i=1}^{N} h_i^{\lambda_i} \|u\|^2_{H^{\lambda_i+1}(\Omega_i)}$$

where h_i is the maximum mesh size on Ω_i.

Finally we note that in [3] the analysis does not stop at this point. An error estimate on the Lagrange multiplier is also examined and the results are extended to the geometrical nonconforming case. However as this is only a brief outline we shall not proceed any further.

When translating from the finite element to the boundary element situation there are several key issues that are going to have to be dealt with. Firstly we require a suitable integration by parts formula which can be used to provide the boundary integral required for the matching condition and the Lagrangian multipliers. A key issue here is the lack of a suitable trace theorem for the restriction of functions to the boundary in the boundary element situation. Once an integration by parts formula has been derived we can then define the required bilinear forms. The appropriate properties of these bilinear forms must then be shown in order to use the theory already described. We shall also need to define suitable extension and projection operators for our functions in order to get an error estimate. Another issue to be overcome is that in general the solution to the BEM has less regularity than that of the FEM, this will have an implication when examining the error estimate of the scheme.

2.3 Technical Details

In this section we shall present some technical details on surface differential operators, transformation to a reference sub-domain and some other results. The surface differential operators are required for the integration by parts formula which will be used to provide us with the required interface matching conditions. The transformation to a reference sub-domain is included as it shows the dependence on the size of the sub-domain of our results. Other results that are used in later chapters are also included here in one common place for ease of reference.

2.3.1 Surface Differential Operators

We shall first define and discuss some surface differential operators which are required to generate an integration by parts formula for the hypersingular integral equation. We recall that for simplicity we let Γ be the plane open surface $(0,1) \times (0,1) \times \{0\}$, and we identify it with the square $(0,1)^2 \subset \mathbf{R}^2$.

We associate with any function φ on a generic surface piece $S \subset \Gamma$, a function $\tilde{\varphi}$ defined in $S \times (-1,1)$ by $\tilde{\varphi}(x_1, x_2, x_3) = \varphi(x_1, x_2)$. We shall also denote by $\mathbf{n}$ the unit normal on S, e.g. $\mathbf{n} = (0,0,1)^T$. Then we define on S for a smooth function φ

$$\operatorname{grad}_{\mathrm{S}} \varphi := (\operatorname{grad} \tilde{\varphi})|_S, \qquad \mathbf{curl}_{\mathrm{S}} \varphi := \operatorname{grad}_{\mathrm{S}} \varphi \times \mathbf{n}.$$

Accordingly, we define for any sufficiently smooth tangential vector field $\boldsymbol{\varphi}$ on S

$$\operatorname{curl}_{\mathrm{S}} \boldsymbol{\varphi} := \mathbf{n} \cdot (\operatorname{curl} \tilde{\boldsymbol{\varphi}})|_S.$$

Here, $\tilde{\boldsymbol{\varphi}}$ is defined component-wise. The definitions of $\operatorname{grad}_{\mathrm{S}}$, $\mathbf{curl}_{\mathrm{S}}$ and $\operatorname{curl}_{\mathrm{S}}$ are appropriate for a non-flat smooth surface (using a coordinate direction normal to S instead of x_3 to define the extensions φ and $\boldsymbol{\varphi}$) whereas, in our case of the flat surface S, they obviously reduce to

$$\operatorname{grad}_{\mathrm{S}} \varphi = \big(\partial_{x_1}\varphi, \partial_{x_2}\varphi, 0\big), \quad \mathbf{curl}_{\mathrm{S}} \varphi = \big(\partial_{x_2}\varphi, -\partial_{x_1}\varphi, 0\big),$$
$$\operatorname{curl}_{\mathrm{S}}(\varphi_1, \varphi_2, 0) = \partial_{x_1}\varphi_2 - \partial_{x_2}\varphi_1.$$

In the following we extend the open surface S to a closed surface $\tilde{S}$. To distinguish between operators on different surfaces we add the notation of the corresponding surface as an index to the operator. We note that the following results also hold true on polyhedral surfaces. In such cases, surface differential operators and corresponding trace spaces need to be dealt with as in [15].

In the following, $\tilde{S}$ always denotes a closed, smooth surface extending the open surface S. Following [16], $\operatorname{curl}_{\tilde{\mathrm{S}}}$ can be extended to a continuous linear mapping from $H^{1/2}(\tilde{S})$ onto $\boldsymbol{H}_t^{-1/2}(\tilde{S})$ where $\boldsymbol{H}_t^{-1/2}(\tilde{S})$ is the closure in $(H^{-1/2}(\tilde{S}))^3$ of

$$\boldsymbol{L}_t^2(\tilde{S}) := \{\boldsymbol{\psi} \in \big(L^2(\tilde{S})\big)^3;\ \boldsymbol{\psi} \cdot \mathbf{n} = 0\}.$$

(Accordingly we will use the space $\boldsymbol{L}_t^2(S)$ below.) We use this extension to $H^{1/2}(\tilde{S})$ to define $\mathbf{curl}_{\mathrm{S}}$ on $H^{1/2}(S)$: Here we have that

$$\mathbf{curl}_{\mathrm{S}} : \begin{cases} H^{1/2}(S) & \to \quad \boldsymbol{H}_t^{-1/2}(S) := \{\boldsymbol{\varphi} \in \big(H^{-1/2}(S)\big)^3;\ \boldsymbol{\varphi} \cdot \mathbf{n} = 0\} \\ v & \mapsto \quad \Big(\mathbf{curl}_{\tilde{\mathrm{S}}}\, \tilde{v}\Big)|_S \end{cases} \tag{2.41}$$

where $\tilde{v} \in H^{1/2}(\tilde{S})$ is an extension of v. The well-posedness of this definition will be proved in Lemma 2.16 below. To be precise, the definition of $\boldsymbol{H}_t^{-1/2}(S)$ in (2.41) is to be understood as the trace of $\boldsymbol{H}_t^{-1/2}(\tilde{S})$ onto S.

Lemma 2.16. *([25, Lemma 2.1]) The operator* $\mathbf{curl}_{\mathrm{S}} : H^{1/2}(S) \to \boldsymbol{H}_t^{-1/2}(S)$ *defined by (2.41) is continuous.*

Proof. The continuity of $\mathbf{curl}_{\mathrm{S}}$ holds by the existence of an extension operator $H^{1/2}(S) \to H^{1/2}(\tilde{S})$, the continuity of $\mathbf{curl}_{\tilde{\mathrm{S}}} : H^{1/2}(\tilde{S}) \to \boldsymbol{H}_t^{-1/2}(\tilde{S})$ (see [16]) and the continuity of the restriction $\boldsymbol{H}_t^{-1/2}(\tilde{S}) \to \boldsymbol{H}_t^{-1/2}(S)$. The definition of $\mathbf{curl}_{\mathrm{S}}$ on $H^{1/2}(S)$ is independent

of the particular extension since, for given $\varphi \in H^{1/2}(S)$ and two extensions $\tilde{\varphi}_1$, $\tilde{\varphi}_2 \in H^{1/2}(\tilde{S})$, there holds (with $\boldsymbol{\psi}^0$ denoting the extension by zero onto $\tilde{S}$ of $\boldsymbol{\psi}$ defined on S)

$$\langle \mathbf{curl}_{\tilde{\mathrm{S}}}(\tilde{\varphi}_1 - \tilde{\varphi}_2), \boldsymbol{\psi}^0 \rangle_{\tilde{S}} = \langle \tilde{\varphi}_1 - \tilde{\varphi}_2, \mathrm{curl}_{\tilde{\mathrm{S}}}\, \boldsymbol{\psi}^0 \rangle_{\tilde{S}} = \langle \tilde{\varphi}_1 - \tilde{\varphi}_2, \mathrm{curl}_{\mathrm{S}}\, \boldsymbol{\psi} \rangle_S = 0 \quad \forall \boldsymbol{\psi} \in \boldsymbol{C}^\infty_{0,t}(S)$$

where

$$\boldsymbol{C}^\infty_{0,t}(S) := \{\boldsymbol{\psi} \in \big(C^\infty_0(S)\big)^3;\ \boldsymbol{\psi} \cdot \mathbf{n} = 0\}$$

is dense in the dual space $(\boldsymbol{H}_t^{-1/2}(S))' = \tilde{\boldsymbol{H}}_t^{1/2}(S)$. □

Lemma 2.17. *([25, Lemma 2.2]) The restriction* $\mathbf{curl}_{\mathrm{S}}\,|_{\tilde{H}^{1/2}(S)}$ *is continuous as a mapping* $\tilde{H}^{1/2}(S) \to \tilde{\boldsymbol{H}}_t^{-1/2}(S)$ *where*

$$\tilde{\boldsymbol{H}}_t^{-1/2}(S) := \{\boldsymbol{\psi} \in \big(\tilde{H}^{-1/2}(S)\big)^3;\ \boldsymbol{\psi} \cdot \mathbf{n} = 0\}.$$

Proof. We introduce the space

$$\boldsymbol{H}_t^{1/2}(S) := \{\boldsymbol{\psi} \in \big(H^{1/2}(S)\big)^3;\ \boldsymbol{\psi} \cdot \mathbf{n} = 0\}$$

and for a function $\boldsymbol{\psi}$ on S let $\boldsymbol{\psi}^0$ denote its extension onto $\tilde{S}$ by 0. For $\varphi \in C^\infty_0(S)$ there holds $\big(\mathrm{curl}_{\mathrm{S}}\, \varphi\big)^0 = \mathrm{curl}_{\tilde{\mathrm{S}}}\, \varphi^0$. Therefore, using the continuity of $\mathbf{curl}_{\tilde{\mathrm{S}}} : H^{1/2}(\tilde{S}) \to \boldsymbol{H}_t^{-1/2}(\tilde{S})$, we obtain

$$\begin{aligned} \|\,\mathbf{curl}_{\mathrm{S}}\, \varphi\|_{\tilde{\boldsymbol{H}}_t^{-1/2}(S)} &= \sup_{\mathbf{0} \neq \boldsymbol{\psi} \in \boldsymbol{H}_t^{1/2}(S)} \frac{\langle \mathbf{curl}_{\mathrm{S}}\, \varphi, \boldsymbol{\psi} \rangle_S}{\|\boldsymbol{\psi}\|_{\boldsymbol{H}_t^{1/2}(S)}} \simeq \sup_{\mathbf{0} \neq \tilde{\boldsymbol{\psi}} \in \boldsymbol{H}_t^{1/2}(\tilde{S})} \frac{\langle \big(\mathbf{curl}_{\mathrm{S}}\, \varphi\big)^0, \tilde{\boldsymbol{\psi}} \rangle_{\tilde{S}}}{\|\tilde{\boldsymbol{\psi}}\|_{\boldsymbol{H}_t^{1/2}(\tilde{S})}} \\ &= \|\,\mathbf{curl}_{\tilde{\mathrm{S}}}\, \varphi^0\|_{\boldsymbol{H}_t^{-1/2}(\tilde{S})} \leq C\, \|\varphi^0\|_{H^{1/2}(\tilde{S})} \simeq \|\varphi\|_{\tilde{H}^{1/2}(S)} \quad \forall \varphi \in C^\infty_0(S). \end{aligned}$$

Here $\simeq$ denotes the equivalence of norms. The assertion follows by the density of $C^\infty_0(S)$ in $\tilde{H}^{1/2}(S)$. □

Lemma 2.18. *([28, Lemma 3.4]) The operator* $\mathbf{curl}_{\mathrm{S}} : H^{\frac{1}{2}+s}(S) \to \boldsymbol{H}_t^{-\frac{1}{2}+s}(S)$ *is continuous for* $s \in [0, 1/2]$.

Proof. By Lemma 2.16 $\mathbf{curl}_{\mathrm{S}} : H^{\frac{1}{2}}(S) \to \boldsymbol{H}_t^{-\frac{1}{2}}(S)$ is continuous, and $\mathbf{curl}_{\mathrm{S}} : H^1(S) \to \boldsymbol{L}^2_t(S) = \boldsymbol{H}^0_t(S)$ is continuous as well (see e.g. [15, Proposition 3.3]). The result follows by interpolation. □

Lemma 2.19. *([25, Lemma 4.1]) There exists a positive constant* C *such that*

$$|\varphi|_{H^{1/2}(S)} \leq C\, \|\,\mathbf{curl}_{\mathrm{S}}\, \varphi\|_{\boldsymbol{H}_t^{-1/2}(S)} \quad \forall \varphi \in H^{1/2}(S).$$

Proof. By Lemma 2.16, $\mathbf{curl}_{\mathrm{S}} : H^{1/2}(S) \to \boldsymbol{H}_t^{-1/2}(S)$ is continuous. We also have that the range of $\mathbf{curl}_{\mathrm{S}}$ is closed in $\boldsymbol{H}_t^{-1/2}(S)$. This follows from the closedness of the range of $\mathbf{curl}_{\tilde{\mathrm{S}}} : H^{1/2}(\tilde{S}) \to \boldsymbol{H}_t^{-1/2}(\tilde{S})$ (see [16]) where $\tilde{S}$ is, as before, a smooth, closed surface containing S. Since the range of $\mathbf{curl}_{\mathrm{S}} : H^{1/2}(S) \to \boldsymbol{H}_t^{-1/2}(S)$ is the restriction onto S of the range of $\mathbf{curl}_{\tilde{\mathrm{S}}} : H^{1/2}(\tilde{S}) \to \boldsymbol{H}_t^{-1/2}(\tilde{S})$, the closedness of the range of $\mathbf{curl}_{\mathrm{S}}$ follows, see e.g. [41, pp. 76f.]. Next we see that the kernel of $\mathbf{curl}_{\mathrm{S}}$ in $H^{1/2}(S)$ consists of constant functions. This follows by noting that any $\varphi \in H^{1/2}(S)$ with $\mathbf{curl}_{\mathrm{S}}\,\varphi = 0$ satisfies $\varphi \in H^1(S)$ such that $\mathbf{curl}_{\mathrm{S}}\,\varphi$ is defined in the usual weak sense. The kernel of $\mathbf{curl}_{\mathrm{S}}\,|_{H^1(S)}$ is given by the constant functions. Therefore, an application of the closed graph theorem yields the estimate

$$\inf_{c\in\mathbb{R}} \|\varphi - c\|_{H^{1/2}(S)} \leq C \,\|\,\mathbf{curl}_{\mathrm{S}}\,\varphi\|_{\boldsymbol{H}_t^{-1/2}(S)} \quad \forall \varphi \in H^{1/2}(S),$$

and the assertion follows by the Poincaré-Friedrichs inequality. □

2.3.2 Integration By Parts Formula

We now turn our attention to an integration-by-parts formula. We require an integration by parts formula to create the boundary terms which shall be used as our integral matching condition in the mortar BEM. Before presenting an integration by parts formula we shall reexpress the hypersingular operator in terms of surface differential operators. An integration by parts formula may then be applied to this alternative formulation.

In the following we need the single layer potential operator V. It is defined by

$$V\boldsymbol{\varphi}(x) := \frac{1}{4\pi}\int_\Gamma \frac{\boldsymbol{\varphi}(y)}{|x-y|}\,dS_y, \quad \boldsymbol{\varphi} \in (\tilde{H}^{-1/2}(\Gamma))^3,\ x \in \Gamma. \tag{2.42}$$

It is well-known, and widely used in the boundary element literature, that the single layer potential operator V can be used to represent the hypersingular operator W, and that their bilinear forms relate like an integration-by-parts formula. This goes back to Nédélec [43] who studied the case of a closed smooth surface. Other equations than the Laplace equation have been examined to show how their representations by hypersingular integral operators can be reexpressed in terms of weakly singular operators, see [40, 43] for Helmholtz and Maxwell equations in three dimensions and [27, 43] for the Lamé system in three dimensions. All the authors mentioned above considered closed smooth systems. Since we did not find a reference for open surfaces we recall this situation in the next lemma.

Lemma 2.20. *(e.g. [25, Lemma 2.3]) There holds*

$$W = \mathrm{curl}_\Gamma\, V\, \mathbf{curl}_\Gamma \quad \textit{in} \quad \mathcal{L}(\tilde{H}^{1/2}(\Gamma), H^{-1/2}(\Gamma)). \tag{2.43}$$

Moreover

$$\langle W\phi, \psi\rangle_\Gamma = \langle V\,\mathbf{curl}_\Gamma\,\psi, \mathbf{curl}_\Gamma\,\phi\rangle_\Gamma \quad \forall \phi, \psi \in \tilde{H}^{1/2}(\Gamma). \tag{2.44}$$

Proof. Using the surface differential operators introduced before, there holds in the distributional sense $W\phi = \mathrm{curl}_\Gamma\, V\,\mathbf{curl}_\Gamma\,\phi$, see [40, 43]. This formula extends from $C_0^\infty(\Gamma)$ to $\phi \in \tilde{H}^{1/2}(\Gamma)$ since $\mathbf{curl}_\Gamma : \tilde{H}^{1/2}(\Gamma) \to \tilde{\boldsymbol{H}}_t^{-1/2}(\Gamma)$ by Lemma 2.17, $V : \tilde{\boldsymbol{H}}_t^{-1/2}(\Gamma) \to \boldsymbol{H}_t^{1/2}(\Gamma)$ by [19], and $\mathrm{curl}_\Gamma : \boldsymbol{H}_t^{1/2}(\Gamma) \to H^{-1/2}(\Gamma)$ since it is the adjoint operator of $\mathbf{curl}_\Gamma$, cf. [15]. The relation (2.44) follows by integration by parts. □

Towards integration by parts

We now present an integration by parts formula.

Lemma 2.21. *(See e.g. [51, Lemma 6.16]) For a smooth scalar function v and a smooth tangential vector field $\boldsymbol{\varphi}$, integration by parts gives*

$$\langle \mathbf{curl}_\Gamma\, v, \boldsymbol{\varphi}\rangle_\Gamma = -\langle v, \mathrm{curl}_\Gamma\,\boldsymbol{\varphi}\rangle_\Gamma + \langle v, \boldsymbol{\varphi}\cdot\mathbf{t}\rangle_\gamma. \tag{2.45}$$

Proof. Using the product rule

$$\nabla \times [v\boldsymbol{\varphi}] = \nabla v \times \boldsymbol{\varphi} + v[\nabla \times \boldsymbol{\varphi}]$$

we obtain

$$\begin{aligned}
\int_\Gamma \mathbf{curl}_\Gamma\, v \cdot \boldsymbol{\varphi} &= \int_\Gamma [\nabla v \times \boldsymbol{n}] \cdot \boldsymbol{\varphi} \\
&= -\int_\Gamma [\boldsymbol{n} \times \nabla v] \cdot \boldsymbol{\varphi} \\
&= -\int_\Gamma [\nabla v \times \boldsymbol{\varphi}] \cdot \boldsymbol{n} \\
&= -\int_\Gamma [\nabla \times [v\boldsymbol{\varphi}] - v[\nabla \times \boldsymbol{\varphi}]] \cdot \boldsymbol{n} \\
&= \int_\Gamma v\,\mathrm{curl}_\Gamma\,\boldsymbol{\varphi} - \int_\gamma v\boldsymbol{\varphi}\mathbf{t}
\end{aligned}$$

by applying the integral theorem of Stokes. □

For a smooth scalar function v and a smooth tangential vector field $\boldsymbol{\varphi}$, integration by parts gives

$$\langle \mathbf{curl}_\Gamma\, v, \boldsymbol{\varphi}\rangle_\Gamma = \langle v, \mathrm{curl}_\Gamma\,\boldsymbol{\varphi}\rangle_\Gamma - \langle v, \boldsymbol{\varphi}\cdot\mathbf{t}\rangle_\gamma. \tag{2.46}$$

Here, $\mathbf{t}$ is the unit tangential vector on γ (oriented mathematically positive when identifying Γ with $(0,1)^2$). We note that if we choose functions v such that they vanish at the boundary e.g. $v \in \tilde{H}^{1/2}(\Gamma)$ then the integral over γ disappears and we are left with

$$\langle \mathbf{curl}_\Gamma\, v, \boldsymbol{\varphi}\rangle_\Gamma = \langle v, \mathrm{curl}_\Gamma\,\boldsymbol{\varphi}\rangle_\Gamma.$$

The Trace Theorem

We now present the following result on the trace operator to show why the integration by parts formula (2.46) does not hold for continuous discrete functions in $H^{1/2}(\Gamma)$ which do not vanish on γ (the boundary of Γ).

Lemma 2.22. *([25, Lemma 4.3]) There exists $C > 0$ such that, for any $\epsilon \in (0, 1/2)$, there holds*

$$\|v\|_{L^2(\gamma)} \leq \frac{C}{\epsilon^{1/2}} \|v\|_{H^{1/2+\epsilon}(\Gamma)} \quad \forall v \in H^{1/2+\epsilon}(\Gamma).$$

Proof. The trace theorem is usually proved by applying local mappings onto the half-space case where the Fourier transformation is used. This yields the estimate

$$\|v\|^2_{L^2(\gamma)} \leq C\, M_s\, \|v\|^2_{H^s(\Gamma)} \quad \forall v \in H^s(\Gamma),\ 1/2 < s \leq 1,$$

with C depending only on Γ and with

$$M_s = \int_{\mathbb{R}} (1 + t^2)^{-s}\, dt,$$

see, e.g., [41, Lemma 3.35, Theorem 3.37]. We note that the norms in $H^s(\Gamma)$ defined by (2.1) and by Fourier transformation are uniformly equivalent for $s \in J$ and any closed interval $J \subset (0, 1)$ (see the proof of Lemma 4.1 in [24]). Therefore, the statement is proved for small $\epsilon > 0$ (bounded away from $1/2$) by noting that $M_{1/2+\epsilon} = O(\epsilon^{-1})$. For larger ϵ the result follows by the continuous injection of higher order Sobolev spaces in lower order spaces. □

Specifically Lemma 2.22 is defined for ϵ on the (open) interval $(0, 1/2)$. Thus for a simple translation from the finite element to the boundary element situation we would replace $v \in \tilde{H}^{1/2}(\Gamma)$ by $v \in H^{1/2}(\Gamma)$. If we apply the integration by parts formula (2.46) to a function in $H^{1/2}(\Gamma)$ we see that the boundary term requires the restriction of this function to the boundary and Lemma 2.22 shows that this is not possible.

2.3.3 Transformation To a Reference Sub-Domain

The following two Lemmas describe the behaviour of Sobolev norms on regions of different sizes.

Lemma 2.23. *[29, Lemma 2] Let $I^n = (0, 1)^n$, $I^n_h = (0, h)^n$ and let*

$$T^n_h : I^n_h \to I^n,\ n = 1, 2, 3,$$

be an affine transformation. For functions u, $\hat{u}$ such that $u = \hat{u} \circ T_h^n$ on I_h^n there holds for $n = 1, 2, 3$

$$\|u\|^2_{\tilde{H}^s(I_h^n)} \simeq h^{n-2s} \|\hat{u}\|^2_{\tilde{H}^s(I^n)} \quad (0 \le s \le 1),$$

and

$$\|u\|^2_{H^s(I_h^n)} \simeq h^{n-2s} \|\hat{u}\|^2_{H^s(I^n)} \quad (-1 \le s \le 0).$$

Lemma 2.24. *[29, Lemma 3] We use the same notation as in Lemma 2.23. For a function u with integral mean zero on I_h^n there holds for $n = 1, 2, 3$*

$$\|u\|^2_{H^s(I_h^n)} \simeq h^{n-2s} \|\hat{u}\|^2_{H^s(I^n)} \quad (0 \le s \le 1),$$

and

$$\|u\|^2_{\tilde{H}^s(I_h^n)} \simeq h^{n-2s} \|\hat{u}\|^2_{\tilde{H}^s(I^n)} \quad (-1 \le s \le 0),$$

provided one of the respective norms is finite.

For a given $S \subset \Gamma$ we denote by T_S an affine bijective transformation from the reference domain $\hat{S}$ onto S. The reference domain in the case of a triangular mesh of the (sub-) domain S is $\hat{S} = \{(x_1, x_2); 0 \le x_1, x_2 \le 1, x_1 + x_2 \le 1\}$ and in the case of a rectangular mesh is $\hat{S} = \{(x_1, x_2); 0 \le x_1, x_2 \le 1\}$. Also, given $v : S \to \mathbf{R}$ we write $\hat{v} := v \circ T_S$. We shall also use the notation $\widehat{\mathbf{curl}_S} := \mathbf{curl}_{\hat{S}}$.

For $S \subset \Gamma$ of (maximum) diameter D_S with (maximum) mesh size h_S, we have the following equivalence of semi-norms when transforming to (and from) a reference domain

$$|v|^2_{H^r(S)} \cong D_S^{2-2r} |\hat{v}|^2_{H^r(\hat{S})} \quad 0 \le r \le 1. \tag{2.47}$$

We also note that the mesh size on the reference domain is now

$$\frac{h_S}{D_S}.$$

This is important as in later chapters we are going to transform to a reference sub-domain and then apply results which have a dependence upon the mesh size on the sub-domain.

In the following we shall not be using functions with integral mean zero, so we cannot apply the results of Lemma 2.24. However, we shall need to know the effect of the diameter of the domain when transforming the norms used in Lemma 2.24.

Lemma 2.25. *For $0 \le r \le 1$ and $0 < D_S \le 1$, we have*

$$\|v\|^2_{H^r(S)} \gtrsim D_S^2 \|\hat{v}\|^2_{H^r(\hat{S})} \text{ and } \|\hat{v}\|^2_{H^r(\hat{S})} \lesssim D_S^{-2} \|v\|^2_{H^r(S)} \tag{2.48}$$

and

$$\|v\|^2_{H^r(S)} \lesssim D_S^{2-2r} \|\hat{v}\|^2_{H^r(\hat{S})} \text{ and } \|\hat{v}\|^2_{H^r(\hat{S})} \gtrsim D_S^{2r-2} \|v\|^2_{H^r(S)}. \tag{2.49}$$

Proof. For $0 \leq r \leq 1$ we have by (2.47)

$$\begin{aligned} \|v\|^2_{H^r(S)} &= \|v\|^2_{L^2(S)} + |v|^2_{H^r(S)} \\ &\cong D_S^2 \|\hat{v}\|^2_{L^2(\widehat{S})} + D_S^{2-2r} |\hat{v}|^2_{H^r(\widehat{S})}. \end{aligned}$$

Now noting that for $0 < D_S \leq 1$ we have $D_S^2 \leq D_S^{2-2r}$ we get (2.48) and (2.49). □

Similarly for the one dimensional situation we have the interval κ of length K_κ is transformed to the interval $\hat{\kappa}$ of unit length.We now have

$$|v|^2_{H^r(\kappa)} \cong K_\kappa^{1-2r} |\hat{v}|^2_{H^r(\widehat{\kappa})} \quad 0 \leq r \leq 1. \tag{2.50}$$

Lemma 2.26. *For $0 \leq r \leq 1/2$ and $0 < K_\kappa \leq 1$, we have*

$$\|v\|^2_{H^r(\kappa)} \gtrsim K_\kappa \|\hat{v}\|^2_{H^r(\widehat{\kappa})} \text{ and } \|\hat{v}\|^2_{H^r(\widehat{\kappa})} \lesssim K_\kappa^{-1} \|v\|^2_{H^r(\kappa)} \tag{2.51}$$

and

$$\|v\|^2_{H^r(\kappa)} \lesssim K_\kappa^{1-2r} \|\hat{v}\|^2_{H^r(\widehat{\kappa})} \text{ and } \|\hat{v}\|^2_{H^r(\widehat{\kappa})} \gtrsim K_\kappa^{2r-1} \|v\|^2_{H^r(\kappa)}. \tag{2.52}$$

Proof. For $0 \leq r \leq 1/2$ we have by (2.50)

$$\begin{aligned} \|v\|^2_{H^r(\kappa)} &= \|v\|^2_{L^2(\kappa)} + |v|^2_{H^r(\kappa)} \\ &\cong K_\kappa \|\hat{v}\|^2_{L^2(\widehat{\kappa})} + K_\kappa^{1-2r} |\hat{v}|^2_{H^r(\widehat{\kappa})}. \end{aligned}$$

Now noting that for $0 < K_\kappa \leq 1$ we have $K_\kappa \leq K_\kappa^{1-2r}$ we get (2.51) and (2.52). □

We next examine the effect of our surface differential operator $\mathbf{curl}_{\mathrm{S}}$ on the scaling properties of certain norms.

Lemma 2.27. *For $0 \leq r \leq 1$ we have for $0 < D_S \leq 1$ we have*

$$\|\,\mathbf{curl}_{\mathrm{S}}\, v\|^2_{\boldsymbol{H}_t^{-r}(S)} \cong D_S^{2r} \|\,\mathbf{curl}_{\widehat{\mathrm{S}}}\, \hat{v}\|^2_{\boldsymbol{H}_t^{-r}(\widehat{S})}.$$

Proof. For $0 \leq r \leq 1$ and $0 < D_S \leq 1$ we have, noting that $\mathbf{curl}_{\mathrm{S}}$ scales like D_S^{-1} (on a two dimensional domain)

$$\|\,\mathbf{curl}_{\mathrm{S}}\, v\|^2_{\boldsymbol{H}_t^{-r}(S)} \cong D_S^{2+2r} D_S^{-2} \|\,\mathbf{curl}_{\widehat{\mathrm{S}}}\, \hat{v}\|^2_{\boldsymbol{H}_t^{-r}(\widehat{S})}.$$

The stated result now follows immediately. □

Lemma 2.28. *For $0 \leq r \leq 1$ we have for $0 < D_S \leq 1$ we have*

$$\|\operatorname{\mathbf{curl}}_{\mathrm{S}} v\|^2_{\tilde{\boldsymbol{H}}_t^{-r}(S)} \gtrsim D_S^{2r} \|\operatorname{\mathbf{curl}}_{\widehat{\mathrm{S}}} \hat{v}\|^2_{\tilde{\boldsymbol{H}}_t^{-r}(\widehat{S})}. \tag{2.53}$$

and

$$\|\operatorname{\mathbf{curl}}_{\mathrm{S}} v\|^2_{\boldsymbol{H}_t^{-r}(S)} \lesssim \|\operatorname{\mathbf{curl}}_{\widehat{\mathrm{S}}} \hat{v}\|^2_{\boldsymbol{H}_t^{-r}(\widehat{S})}. \tag{2.54}$$

Proof. For $0 \leq r \leq 1$ and $0 < D_S \leq 1$ we have

$$\begin{aligned}
\|\operatorname{\mathbf{curl}}_{\mathrm{S}} v\|_{\tilde{\boldsymbol{H}}_t^{-r}(\boldsymbol{S})} &= \sup_{\varphi \in \boldsymbol{H}_t^r(S)} \frac{\langle \varphi, \operatorname{\mathbf{curl}}_{\mathrm{S}} v\rangle_S}{\|\varphi\|_{\boldsymbol{H}_t^r(S)}} \\
&= \sup_{\varphi \in \boldsymbol{H}^r(S)} \frac{\langle \varphi, \operatorname{\mathbf{curl}}_{\mathrm{S}} v\rangle_S}{\left(\|\varphi\|^2_{\boldsymbol{L}_t^2(S)} + |\varphi|^2_{\boldsymbol{H}_t^r(S)}\right)^{1/2}} \\
&\cong \sup_{\hat{\varphi} \in \boldsymbol{H}_t^r(\widehat{S})} \frac{D_S \langle \hat{\varphi}, \operatorname{\mathbf{curl}}_{\widehat{\mathrm{S}}} \hat{v}\rangle_{\widehat{S}}}{\left(D_S^2 \|\hat{\varphi}\|^2_{\boldsymbol{L}_t^2(\widehat{S})} + D_S^{2-2r} |\hat{\varphi}|^2_{\boldsymbol{H}_t^r(\widehat{S})}\right)^{1/2}}
\end{aligned}$$

Using this we can now get the following bounds:

$$\begin{aligned}
\|\operatorname{\mathbf{curl}}_{\mathrm{S}} v\|_{\tilde{\boldsymbol{H}}_t^{-r}(S)} &\gtrsim \sup_{\hat{\varphi} \in \boldsymbol{H}_t^r(\widehat{S})} \frac{D_S \langle \hat{\varphi}, \operatorname{\mathbf{curl}}_{\widehat{\mathrm{S}}} \hat{v}\rangle_{\widehat{S}}}{D_S^{1-r} \|\hat{\varphi}\|_{\boldsymbol{H}_t^r(\widehat{S})}} \\
&\cong D_S^r \|\operatorname{\mathbf{curl}}_{\widehat{\mathrm{S}}} \hat{v}\|_{\tilde{\boldsymbol{H}}_t^{-r}(\widehat{S})},
\end{aligned}$$

which gives us (2.53). For the other bound

$$\begin{aligned}
\|\operatorname{\mathbf{curl}}_{\mathrm{S}} v\|_{\boldsymbol{H}_t^{-r}(S)} &\lesssim \sup_{\hat{\varphi} \in \tilde{\boldsymbol{H}}_t^r(\widehat{S})} \frac{D_S \langle \hat{\varphi}, \operatorname{\mathbf{curl}}_{\widehat{\mathrm{S}}} \hat{v}\rangle_{\widehat{S}}}{D_S \|\hat{\varphi}\|_{\tilde{\boldsymbol{H}}_t^r(\widehat{S})}} \\
&\cong \|\operatorname{\mathbf{curl}}_{\widehat{\mathrm{S}}} \hat{v}\|_{\boldsymbol{H}_t^{-r}(\widehat{S})},
\end{aligned}$$

which gives us (2.54). □

2.3.4 Other Required Results

The following is a result that allows us to bound the tilde norm of a function by the non-tilde norm.

Lemma 2.29. *[29, Lemma 5] Let $R \subset \mathrm{R}^2$ be a Lipschitz domain. There exists $C > 0$ such that for any $s \in (-1/2, 1/2)$ and any $v \in H^s(R)$ there holds*

$$\|v\|_{\tilde{H}^s(R)} \leq \frac{C}{1/2 - |s|} \|v\|_{H^s(R)}.$$

Lemma 2.30. *([28, Lemma 3.2]) Let $v \in \tilde{H}^{-1/2}(R)$, $R \subset \mathbf{R}^2$ a Lipschitz domain, be a piecewise linear function defined on a quasi-uniform mesh on R with mesh size $h < 1$. There exists a constant $C > 0$ which is independent of h (but may depend on the diameter of R) such that there holds*

$$\|v\|_{\tilde{H}^{-1/2}(R)} \leq C|\log(h)|\|v\|_{H^{-1/2}(R)}.$$

Proof. By [29, Lemma 6] there holds for a piecewise polynomial of degree p the estimate

$$\|v\|_{\tilde{H}^{-1/2}(R)} \leq C\log(\frac{p+1}{h})\|v\|_{H^{-1/2}(R)} \qquad p \geq 0, h < 1.$$

Fixing p gives the claimed bound. The proof of [29, Lemma 6] gives full details for rectangular meshes. For triangular meshes the proof applies as well by making use of Schmidt's inequality for triangles, cf. [21, Lemma 5.1]. Nevertheless, we are considering only polynomials of low degrees where Schmidt's inequality is not needed. □

The next Lemma shows the relationships between Sobolev norms over the whole domain and the respective Sobolev norms over sub-domains.

Lemma 2.31. *[29, Lemma 1] Let Γ be a Lipschitz domain in $\mathbf{R}^2$ and let $\{\Gamma_j; j = 1, \ldots, J\}$ be a decomposition of Γ into J Lipschitz domains, i.e.*

$$\bigcup_{j=1}^{J} \bar{\Gamma}_j = \bar{\Gamma} \text{ and } \Gamma_i \cap \Gamma_j = \emptyset \text{ if } i \neq j.$$

Moreover we assume that

1. *for each of the domain Γ_j, $j = 1, \ldots, J$ a finite number (being independent of j and J) of Lipschitz mappings can be used to describe its boundary and that*
2. *the Lipschitz constants of all the boundary mappings are uniformly bounded.*

Then for $s \in [-1, 1]$ and $u \in \tilde{H}^s(\Gamma)$ with $u_j := u|_{\Gamma_j} \in \tilde{H}^s(\Gamma_j)$, $j = 1, \ldots, J$, there exists a constant $c > 0$ which is independent of s, u, and J such that

$$\|u\|^2_{\tilde{H}^s(\Gamma)} \leq c\sum_{j=1}^{J} \|u_j\|^2_{\tilde{H}^s(\Gamma_j)}.$$

Further, for arbitrary $u \in H^s(\Gamma)$,

$$\sum_{j=1}^{J} \|u_j\|^2_{H^s(\Gamma_j)} \leq c\|u\|^2_{H^s(\Gamma)}$$

for a constant c that is independent of s, u, and J.

The next lemma deals with the inverse property of piecewise polynomials.

Lemma 2.32. *[29, Lemma 4] Let Γ be a polygonal domain and let $\{\Gamma_j : j = 1, \ldots, J\}$ be a rectangular mesh on Γ which is assumed to be quasi-uniform, the lengths of the elements being proportional to h. Further let v be a piecewise polynomial of degree p, i.e. $v|_{\Gamma_j}$ is a polynomial of degree p for $j = 1, \ldots, J$. If $v \in \tilde{H}^r(\Gamma)$ for a real number $r \leq 1$, then for $s \leq r$ there holds*

$$\|v\|_{\tilde{H}^r(\Gamma)} \leq ch^{s-r}p^{2(r-s)}\|v\|_{\tilde{H}^s(\Gamma)}.$$

Accordingly, for $v \in H^r(\Gamma)$, there holds

$$\|v\|_{H^r(\Gamma)} \leq ch^{s-r}p^{2(r-s)}\|v\|_{H^s(\Gamma)}.$$

Here, c is a constant that is independent of h and p and, for given r^*, s^* $(s^* \leq r^*)$, is also independent of r and s for $s^* \leq s \leq r \leq r^*$.

Chapter 3

The BEM with Lagrangian Multiplier

In this chapter we present the formulation of the BEM with Lagrangian multiplier. We intend to present the BEM analogue to the method discussed in Section 2.2.3. We shall consider the model situation of the hypersingular operator for the Laplace operator on a plane open surface. A discrete variational formulation shall be presented and analysed. Particular attention shall be paid to the continuity and ellipticity of appearing bilinear forms. An error estimate shall be obtained and compared to that of the standard (conforming) BEM formulation. Numerical results which underline the theory shall be presented later in Chapter 5. This chapter, along with parts of Section 2.3.1 and Chapter 5 have been published in [25].

3.1 Towards a Discrete Formulation

3.1.1 Introduction and Model Problem

Model problem

Now we introduce the model problem. For simplicity let Γ be the plane open surface $(0,1)\times(0,1)\times\{0\}$. We will identify it with the square $(0,1)^2 \subset \mathbf{R}^2$. Our model problem is: *For given* $f \in \tilde{H}^{-1/2}(\Gamma)$ *find* $\phi \in \tilde{H}^{1/2}(\Gamma)$ *such that*

$$W\phi(x) = f(x), \quad x \in \Gamma. \tag{3.1}$$

See (2.7) for the definition of W and recall that $W : \tilde{H}^{1/2}(\Gamma) \to H^{-1/2}(\Gamma)$ (see [19]). Nevertheless, we require f to be slightly more regular than in the standard boundary element formulation (see (2.7)). We require $f \in \tilde{H}^{-1/2}(\Gamma) \subset H^{-1/2}(\Gamma)$. This will be needed

below when testing f with elements of $H^{1/2}(\Gamma)$, rather than in the standard formulation (see Section 2.1.1) where we tested with elements of $\tilde{H}^{1/2}(\Gamma)$. This requirement of extra regularity when compared to the standard formulation (2.7), which required $f \in H^{-1/2}(\Gamma)$ is not a problem, in particular we note that $\tilde{H}^{1/2}(\Gamma) \subset H^{1/2}(\Gamma)$.

The variational formulation of (3.1) is: *Find* $\phi \in \tilde{H}^{1/2}(\Gamma)$ *such that*

$$\langle W\phi, \psi\rangle_\Gamma = \langle f, \psi\rangle_\Gamma \quad \forall \psi \in \tilde{H}^{1/2}(\Gamma). \tag{3.2}$$

We recall a standard BEM (see (2.8)) for the approximate solution of (3.2) is to select a piecewise polynomial subspace $\tilde{X}_h \subset \tilde{H}^{1/2}(\Gamma)$ and to define an approximant $\tilde{\phi}_h \in \tilde{X}_h$ by

$$\langle W\tilde{\phi}_h, \psi\rangle_\Gamma = \langle f, \psi\rangle_\Gamma \quad \forall \psi \in \tilde{X}_h.$$

The conformity condition $\tilde{X}_h \subset \tilde{H}^{1/2}(\Gamma)$ requires that any $v \in \tilde{X}_h$ vanishes on the boundary γ of Γ. Instead of this formulation we shall examine a non-conforming discretisation of (3.2) by using subspaces X_h whose elements do not necessarily vanish on γ (see Section 2.2.2). Our subspaces will satisfy $X_h \subset H^{1/2}(\Gamma)$ where $X_h \not\subset \tilde{H}^{1/2}(\Gamma)$. We thus have a non-conforming discretisation since our discrete space is not a subset of the continuous space. The boundary condition is incorporated weakly by using a Lagrangian multiplier. This means that we do not directly incorporate the boundary condition into the definition of the space. Instead it is included through the inclusion of an additional boundary integral. Note that the natural domain of definition of the hypersingular operator W is $\tilde{H}^{1/2}(\Gamma)$ and not $H^{1/2}(\Gamma)$. This means that we cannot directly substitute our non-conforming discrete space into the problem since the action of W on elements of this space is not well defined, unlike in the FEM situation (see Section 2.2.3). We therefore need to deal with boundary data for an appropriate definition of W and this requires an integration-by-parts formula. We need a way to rewrite W so that it is well defined for functions in our non-conforming discrete space and also supplies us with a suitable boundary term that can be used to define the Lagrangian multipliers.

First let us consider the situation of the conforming continuous formulation (3.2). After that we will study a non-conforming discrete setting. There will be no non-conforming continuous formulation (i.e. a version of (3.2) with $\tilde{H}^{1/2}(\Gamma)$ replaced by $H^{1/2}(\Gamma)$). This is due to the fact that integration by parts involves the trace operator which is not well defined on $H^{1/2}(\Gamma)$ (see the Trace Theorem, Lemma 2.22). We shall use our integration by parts formula to introduce an appropriate boundary term which can be used to incorporate the boundary condition in a weak sense (through a Lagrangian multiplier), and also to reduce the regularity requirements on our approximating functions relative to the standard BEM formulation (we replace $\tilde{H}^{1/2}(\Gamma)$ by $H^{1/2}(\Gamma)$).

Conforming continuous formulation

An immediate consequence of Lemma 2.20 is that an equivalent variational formulation of (3.1) is: *Find* $\phi \in \tilde{H}^{1/2}(\Gamma)$ *such that*

$$\langle V \, \mathbf{curl}_\Gamma \, \phi, \mathbf{curl}_\Gamma \, \psi \rangle_\Gamma = \langle f, \psi \rangle_\Gamma \quad \forall \psi \in \tilde{H}^{1/2}(\Gamma). \tag{3.3}$$

This weak formulation forms the starting point for the BEM with Lagrangian multiplier. For definitions of the surface differential operators and the weakly singular integral operator see Sections 2.3.1 and 2.3.2. This formulation is well known and widely used in the field of boundary elements. This is because it is computationally easier to implement the weakly singular integral operator than the hypersingular integral operator due to the nature of the appearing singularities.

Note that we will consider discrete subspaces of $H^{1/2}(\Gamma)$ where the hypersingular operator W is not well defined (recall W is well defined for functions in $\tilde{H}^{1/2}(\Gamma)$). The formulation (3.3) does make sense for continuous discrete functions which do not vanish on γ (the boundary of Γ), whereas the formulation (3.2) does not. Nevertheless, for the error analysis of our scheme we must relate a discrete version of (3.3) with the original problem (3.1), i.e. with (3.2). This requires an integration-by-parts formula that corresponds to (2.44) but is valid for functions which do not vanish on γ.

3.1.2 Integration By Parts

Applying the integration by parts formula (2.46) to (2.43) we obtain, for sufficiently smooth ϕ and ψ,

$$\langle \mathbf{t} \cdot V \, \mathbf{curl}_\Gamma \, \phi, \psi \rangle_\gamma = \langle W\phi, \psi \rangle_\Gamma - \langle V \, \mathbf{curl}_\Gamma \, \phi, \mathbf{curl}_\Gamma \, \psi \rangle_\Gamma. \tag{3.4}$$

This formula does not extend to $\psi \in H^{1/2}(\Gamma)$ since the trace of such a ψ onto γ is not well defined (by the Trace Theorem, Lemma 2.22). We now have an alternative formulation of W in terms of V and $\mathbf{curl}_\Gamma$ that can be used to define a Lagrangian multiplier in the case where we have non-conforming approximating functions that do not vanish at the boundary. We define the Lagrangian multiplier λ as

$$\lambda = \mathbf{t} \cdot V \, \mathbf{curl}_\Gamma \, \phi.$$

The vanishing condition can now be incorporated using the boundary (of the boundary) integral (the integral over γ), however this term also requires the restriction of the function ψ to the boundary to be well defined. This is not the case for $\psi \in H^{1/2}(\Gamma)$ as described earlier, so we will have to assume slightly more regularity for our approximating functions in order for this term to be well defined and thus allow us to include the vanishing

condition in a weak sense. However, we do not require any extra regularity on ϕ since there holds the following lemma which guarantees sufficient regularity of our Lagrangian multiplier term.

Lemma 3.1. *([25, Lemma 4.2]) For $\phi \in \tilde{H}^{1/2}(\Gamma)$ with $W\phi = f \in \tilde{H}^{-1/2}(\Gamma)$, (3.4) defines $\mathbf{t} \cdot V\,\mathbf{curl}_\Gamma\,\phi \in H^{-1/2}(\gamma)$.*

Proof. Extending $\psi \in H^{1/2}(\gamma)$ to an element of $H^1(\Gamma)$ (using the same name) there holds

$$\begin{aligned}|\langle \mathbf{t} \cdot V\,\mathbf{curl}_\Gamma\,\phi, \psi\rangle_\gamma| &= |\langle f, \psi\rangle_\Gamma - \langle V\,\mathbf{curl}_\Gamma\,\phi, \mathbf{curl}_\Gamma\,\psi\rangle_\Gamma| \\ &\le \|f\|_{\tilde{H}^{-1/2}(\Gamma)}\|\psi\|_{H^{1/2}(\Gamma)} + \|V\,\mathbf{curl}_\Gamma\,\phi\|_{\boldsymbol{L}^2_t(\Gamma)}\|\,\mathbf{curl}_\Gamma\,\psi\|_{\boldsymbol{L}^2_t(\Gamma)} \\ &\le (\|f\|_{\tilde{H}^{-1/2}(\Gamma)} + \|V\,\mathbf{curl}_\Gamma\,\phi\|_{\boldsymbol{H}^{1/2}_t(\Gamma)})\|\psi\|_{H^1(\Gamma)}\end{aligned}$$

with

$$L^2_t(\Gamma) := \{\psi \in \big(L^2(\Gamma)\big)^3;\ \psi \cdot \mathbf{n} = 0\}.$$

The result follows by using the continuity of $\mathbf{curl}_\Gamma : \tilde{H}^{1/2}(\Gamma) \to \tilde{\boldsymbol{H}}_t^{-1/2}(\Gamma)$ (see Lemma 2.17) and $V : \tilde{\boldsymbol{H}}_t^{-1/2}(\Gamma) \to \boldsymbol{H}_t^{1/2}(\Gamma)$ (cf. the proof of Lemma 2.20), and by the continuity of the extension of $\psi \in H^{1/2}(\gamma)$ to $\psi \in H^1(\Gamma)$. □

Remark 3.2. Lemma 3.1 easily generalises to $\mathbf{t} \cdot V\,\mathbf{curl}_\Gamma\,\phi \in H^s(\gamma)$ with $s \in (-1, 0)$ (requiring $f \in \tilde{H}^{s-1/2}(\Gamma)$ in general) but breaks down for $s = 0$. The problem in the case $s = 0$ is that the relevant required mapping property $V : \tilde{\boldsymbol{H}}_t^{-1/2}(\Gamma) \to \tilde{\boldsymbol{H}}_t^{1/2}(\Gamma)$ does not hold. But note that there is an extension operator $L^2(\gamma) \to H^{1/2}(\Gamma)$ (see [42, Lemma 2.3]).

Note also that given $f \in H^s(\Gamma)$, there exist non-unique extensions to $f \in \tilde{H}^s(\Gamma)$ for $s \in (-3/2, 1/2)$. Such an extension need not exist for $s = -1/2$ but is unique if it does exist, see [42, Lemma 5].

In the proof of our main result for this chapter (Theorem 3.7) we will need (3.4) only for functions $\psi \in H^{1/2}(\gamma)$, and for uniqueness of f and $\mathbf{t} \cdot V\,\mathbf{curl}_\Gamma\,\phi$ we require $f \in \tilde{H}^{1/2}(\Gamma)$.

3.1.3 Discrete Variational Formulation with Lagrangian Multiplier

In this section we introduce a BEM formulation with Lagrangian multiplier. In order to introduce the discrete scheme let us define a regular, quasi-uniform mesh $\mathcal{T}_h$ of shape regular elements $T \in \mathcal{T}_h$ such that $\bar{\Gamma} = \cup_{T\in\mathcal{T}_h}\bar{T}$. As usual, h denotes the mesh size (being proportional to the diameters of the elements). Throughout we assume that $h < 1$. This is no restriction of generality and is just needed to simplify the writing of logarithmic terms.

Elements can be triangles or quadrilaterals. Using this mesh we define the boundary element space

$$X_h := \{\phi \in C^0(\Gamma);\ \phi|_T \text{ is a polynomial of degree one } \forall T \in \mathcal{T}_h\}.$$

Note that $X_h \subset H^{1/2}(\Gamma)$, but $X_h \not\subset \tilde{H}^{1/2}(\Gamma)$. While $X_h \subset H^{1/2}(\Gamma)$ it is important to note that it is not equal to it. Our integration by parts formula is not well defined for functions in $H^{1/2}(\Gamma)$, however it is well defined for functions in X_h. This is why we have no continuous formulation but do have a discrete formulation.

For the definition of a discrete Lagrangian multiplier space we introduce a quasi-uniform mesh $\mathcal{G}_k$ on $\gamma = \partial\Gamma$ that consists of straight line pieces $J \in \mathcal{G}_k$: $\gamma = \cup_{J\in\mathcal{G}_k} \bar{J}$. The parameter k refers to the mesh size of $\mathcal{G}_k$ (being proportional to the lengths of the elements). The discrete space for the Lagrangian multiplier is

$$M_k := \{q \in L^2(\gamma);\ q|_J \text{ is constant } \forall J \in \mathcal{G}_k\}.$$

We also define the bilinear forms

$$a(\phi,\psi) := \langle V\,\mathbf{curl}_\Gamma\,\phi, \mathbf{curl}_\Gamma\,\psi\rangle_\Gamma,$$
$$b(\phi,q) := \langle \phi, q\rangle_\gamma := \int_\gamma \phi q\,ds,$$

the linear form

$$F(\phi) := \langle f, \phi\rangle_\Gamma,$$

and the space

$$V_h := \{\phi \in X_h;\ b(\phi,q) = 0\ \forall q \in M_k\}.$$

The boundary element scheme with Lagrangian multiplier for the approximate solution of (3.3) then is: *Find* $(\phi_h, \lambda_k) \in X_h \times M_k$ *such that*

$$\begin{array}{lll} a(\phi_h,\psi) + b(\psi,\lambda_k) & = F(\psi) & \forall \psi \in X_h, \\ b(\phi_h, q) & = 0 & \forall q \in M_k. \end{array} \tag{3.5}$$

This scheme is equivalent to

$$\phi_h \in V_h:\ a(\phi_h,\psi) = F(\psi) \quad \forall \psi \in V_h.$$

Scheme (3.5) has the typical saddle point structure of a variational formulation with Lagrangian multiplier. In the finite element case such a scheme is usually analysed by the Babuška-Brezzi theory (Section 2.2.4), see also [1]. Our situation, however, is not standard in the sense that there is no corresponding continuous saddle point formulation (which is required in standard analysis). Also, we do not intend to derive an error estimate for the Lagrangian multiplier since the corresponding continuous unknown is not well defined when $\phi \in \tilde{H}^{1/2}(\Gamma)$ (it is $\mathbf{t} \cdot V\,\mathbf{curl}_\Gamma\,\phi$ with $\mathbf{t}$ being the unit tangential vector along γ in mathematically positive sense, see (3.4)). Also the Lagrangian multiplier does not represent any physical property in our situation like it does in some mixed-formulations.

3.2 Technical Results and Proof of the Main Result

Obviously, continuity and V_h-ellipticity of $a(\cdot,\cdot)$ are critical for the error analysis of (3.5). Lemma 3.3 below shows the continuity and then Lemma 3.5 proves that $a(\cdot,\cdot)$ is almost uniformly V_h-elliptic.

Continuity of $a(\cdot,\cdot)$

Lemma 3.3. *([25, Lemma 4.4]) The bilinear form $a(\cdot,\cdot)$ is almost uniformly continuous on X_h. More precisely there holds the following upper bounds*

$$a(v,w) \lesssim |\log h| \|v\|_{H^{1/2}(\Gamma)} \|\mathbf{curl}_\Gamma\, w\|_{\tilde{\boldsymbol{H}}_t^{-1/2}(\Gamma)} \quad \forall v,w \in X_h,$$

and

$$a(v,w) \lesssim |\log h|^2 \|v\|_{H^{1/2}(\Gamma)} \|w\|_{H^{1/2}(\Gamma)} \quad \forall v,w \in X_h.$$

Proof. By the continuity of $V:\ \tilde{\boldsymbol{H}}_t^{-1/2}(\Gamma) \to \boldsymbol{H}_t^{1/2}(\Gamma)$ there holds

$$a(v,w) \lesssim \|\mathbf{curl}_\Gamma\, v\|_{\tilde{\boldsymbol{H}}_t^{-1/2}(\Gamma)} \|\mathbf{curl}_\Gamma\, w\|_{\tilde{\boldsymbol{H}}_t^{-1/2}(\Gamma)}.$$

By Lemma 2.30 we have that for any piecewise polynomial on a quasi-uniform mesh

$$\|\mathbf{curl}_\Gamma\, v\|_{\tilde{\boldsymbol{H}}_t^{-1/2}(\Gamma)} \lesssim |\log h| \|\mathbf{curl}_\Gamma\, v\|_{\boldsymbol{H}_t^{-1/2}(\Gamma)} \quad \forall v \in V_h. \tag{3.6}$$

Now applying the continuity of $\mathbf{curl}_\Gamma:\ H^{1/2}(\Gamma) \to \boldsymbol{H}_t^{-1/2}(\Gamma)$ proves both assertions. □

Ellipticity of $a(\cdot,\cdot)$

The next result will be required to prove the ellipticity of the bilinear form $a(\cdot,\cdot)$.

Lemma 3.4. *([25, Lemma 4.5]) The exists $C > 0$ such that for any $h \in (0,1)$ and for sufficiently small k there holds*

$$|v|_{H^{1/2}(\Gamma)} \geq C |\log h|^{-1/2} \|v\|_{H^{1/2}(\Gamma)} \qquad \forall v \in V_h.$$

If k is proportional to a positive power of h then k satisfies the assumption if h is sufficiently small.

Proof. We decompose any $v \in V_h$ into $v = v_0 + d$ with $\int_\Gamma v_0(x)\, dS_x = 0$ such that $d = |\Gamma|^{-1} \int_\Gamma v(x)\, dS_x$. In order to estimate d we note that there holds $\|d\|_{\tilde{H}^{-1}(\gamma)} = |d|\, \|1\|_{\tilde{H}^{-1}(\gamma)}$, that is

$$|d| = \|1\|_{\tilde{H}^{-1}(\gamma)}^{-1} \sup_{q \in H^1(\gamma)\setminus\{0\}} \frac{\langle d, q\rangle_\gamma}{\|q\|_{H^1(\gamma)}}. \tag{3.7}$$

Since $v \in V_h$, i.e. $b(v, q_k) = 0$ for any $q_k \in M_k$, we find

$$\begin{aligned}|\langle d, q\rangle_\gamma| &= |\langle v - v_0, q\rangle_\gamma| = |\langle v, q - q_k\rangle_\gamma - \langle v_0, q\rangle_\gamma| \\ &\leq \|v\|_{L^2(\gamma)}\|q - q_k\|_{L^2(\gamma)} + \|v_0\|_{L^2(\gamma)}\|q\|_{L^2(\gamma)} \quad \forall q_k \in M_k.\end{aligned}$$

We bound the $L^2(\gamma)$-norms of v and v_0 using Lemma 2.22 with a small $\epsilon > 0$ and use the error bound

$$\inf_{q_k \in M_k} \|q - q_k\|_{L^2(\gamma)} \leq Ck\|q\|_{H^1(\gamma)}.$$

The previous estimate then yields

$$|\langle d, q\rangle_\gamma| \leq \frac{C}{\epsilon^{1/2}} k\|v\|_{H^{1/2+\epsilon}(\Gamma)}\|q\|_{H^1(\gamma)} + \frac{C}{\epsilon^{1/2}}\|v_0\|_{H^{1/2+\epsilon}(\Gamma)}\|q\|_{H^1(\gamma)}.$$

Applying the inverse property $\|v\|_{H^{1/2+\epsilon}(\Gamma)} \leq Ch^{-\epsilon}\|v\|_{H^{1/2}(\Gamma)}$ (see, e.g., Lemma 2.32)and selecting $\epsilon := 1/|\log h|$ for $h < 1$, we conclude that there holds

$$|\langle d, q\rangle_\gamma| \leq C|\log h|^{1/2}\left(k\|v\|_{H^{1/2}(\Gamma)} + \|v_0\|_{H^{1/2}(\Gamma)}\right)\|q\|_{H^1(\gamma)}.$$

Making use of (3.7) this yields

$$|d| \leq C|\log h|^{1/2}\left(k\|v\|_{H^{1/2}(\Gamma)} + \|v_0\|_{H^{1/2}(\Gamma)}\right). \tag{3.8}$$

Therefore, using the triangle inequality, we estimate

$$\|v\|^2_{H^{1/2}(\Gamma)} \leq C(\|v_0\|^2_{H^{1/2}(\Gamma)} + d^2) \leq C\,|\log h|\|v_0\|^2_{H^{1/2}(\Gamma)} + C\,|\log h|k^2\|v\|^2_{H^{1/2}(\Gamma)},$$

such that

$$\begin{aligned}(1 - C\,k^2|\log h|)\|v\|^2_{H^{1/2}(\Gamma)} &\leq C\,|\log h|\|v_0\|^2_{H^{1/2}(\Gamma)} \\ &= C\,|\log h|\Big(|v_0|^2_{H^{1/2}(\Gamma)} + \inf_{c\in\mathbb{R}}\|v - c\|^2_{L^2(\Gamma)}\Big) \\ &= C\,|\log h||v|^2_{H^{1/2}(\Gamma)}.\end{aligned}$$

In the last step we made use of the Poincaré-Friedrichs inequality. Selecting k small enough such that $1 - C\,k^2|\log h| > 0$ and dividing by $1 - C\,k^2|\log h|$ proves the lemma. □

The next lemma states three variants of ellipticity for the bilinear form $a(\cdot,\cdot)$. Part (i) will be used to establish our computational error bound (5.1) needed for the numerical experiment. Part (ii) is essential for proving the Strang-type error estimate (see Lemma 2.6) of Theorem 3.6. Part (iii) proves the V_h-ellipticity with $H^{1/2}(\Gamma)$-norm needed for the Babuška-Brezzi theory (see Section 2.2.4). We note that part (iii) would be enough to prove a Strang-type estimate and eventually an a priori error bound, but the ellipticity provided by (ii) leads to a sharper bound.

Lemma 3.5. *([25, Lemma 4.6])* (i) *There holds*

$$a(v,v) \gtrsim |v|^2_{H^{1/2}(\Gamma)} \quad \forall v \in \tilde{H}^{1/2}(\Gamma) \cup H^1(\Gamma).$$

(ii) *There holds for any $h \in (0,1)$ and sufficiently small k*

$$a(v,v) \gtrsim |\log h|^{-1/2} \|v\|_{H^{1/2}(\Gamma)} \| \mathbf{curl}_\Gamma\, v\|_{\tilde{\boldsymbol{H}}_t^{-1/2}(\Gamma)} \quad \forall v \in V_h.$$

If k is proportional to a positive power of h then k satisfies the assumption if h is sufficiently small.
(iii) *Under the conditions of part* (ii) *there holds*

$$a(v,v) \gtrsim |\log h|^{-1} \|v\|^2_{H^{1/2}(\Gamma)} \quad \forall v \in V_h.$$

Proof. We first note that $a(v,v)$ is well defined for any $v \in \tilde{H}^{1/2}(\Gamma) \cup H^1(\Gamma)$. This follows from the mapping properties of V and the continuities $\mathbf{curl}_\Gamma : \tilde{H}^{1/2}(\Gamma) \to \tilde{\boldsymbol{H}}_t^{-1/2}(\Gamma)$ by Lemma 2.17 and $\mathbf{curl}_\Gamma : H^1(\Gamma) \to \boldsymbol{L}^2_t(\Gamma)$. (In fact, one can show that the bilinear form is well defined on $H^{1/2+\epsilon}(\Gamma)$ for any $\epsilon > 0$.)

The ellipticity of V and Lemma 2.19 prove that there holds

$$a(v,v) \gtrsim \| \mathbf{curl}_\Gamma\, v\|^2_{\tilde{\boldsymbol{H}}_t^{-1/2}(\Gamma)} \gtrsim \| \mathbf{curl}_\Gamma\, v\|^2_{\boldsymbol{H}_t^{-1/2}(\Gamma)} \gtrsim |v|^2_{H^{1/2}(\Gamma)} \quad \forall v \in \tilde{H}^{1/2}(\Gamma) \cup H^1(\Gamma).$$

This proves part (i). Now to prove part (ii), we have

$$\begin{aligned} a(v,v) &\gtrsim \| \mathbf{curl}_\Gamma\, v\|^2_{\tilde{\boldsymbol{H}}_t^{-1/2}(\Gamma)} \\ &\gtrsim \| \mathbf{curl}_\Gamma\, v\|_{\tilde{\boldsymbol{H}}_t^{-1/2}(\Gamma)} \| \mathbf{curl}_\Gamma\, v\|_{\boldsymbol{H}_t^{-1/2}(\Gamma)} \\ &\gtrsim \| \mathbf{curl}_\Gamma\, v\|_{\tilde{\boldsymbol{H}}_t^{-1/2}(\Gamma)} |v|_{H^{1/2}(\Gamma)} \quad \forall v \in V_h \subset H^1(\Gamma). \end{aligned}$$

Applying Lemma 3.4 finishes the proof of part (ii). The proof of part (iii) follows in a similar fashion. □

Strang-type error estimate

We are now ready to establish the following Strang-type error result (see Lemma 2.6).

Theorem 3.6. *([25, Theorem 4.1]) Let $\mathcal{T}_h|_\gamma$ be a refinement of $\mathcal{G}_k$ (i.e. any node of $\mathcal{G}_k$ is a boundary node of $\mathcal{T}_h$ and any element of $\mathcal{G}_k$ has a node of $\mathcal{T}_h$ in its interior) and let k be sufficiently small. Then system (3.5) is uniquely solvable and there holds*

$$\|\phi - \phi_h\|_{H^{1/2}(\Gamma)} \lesssim |\log h|^{1/2} \left(\inf_{v \in V_h \cap \tilde{H}^{1/2}(\Gamma)} \|\phi - v\|_{\tilde{H}^{1/2}(\Gamma)} + \sup_{v \in V_h \setminus \{0\}} \frac{|a(\phi - \phi_h, v)|}{\| \mathbf{curl}_\Gamma\, v\|_{\tilde{\boldsymbol{H}}^{-1/2}(\Gamma)}} \right).$$

Proof. The existence and uniqueness of $(\phi_h, \lambda_k) \in X_h \times M_k$ follows from the Babuška-Brezzi theory (see Section 2.2.4). The bilinear form $a(\cdot,\cdot)$ is continuous on X_h by Lemma 3.3 and V_h-elliptic by Lemma 3.5(iii). (The continuity and ellipticity numbers depend on h but this does not matter here.) Moreover, the bilinear form $b(\cdot,\cdot)$ satisfies an inf-sup condition (not necessarily uniformly) since there holds the implication

$$\Big(\mu \in M_k : \quad b(\varphi,\mu) = \langle \varphi,\mu\rangle_\gamma = 0 \quad \forall \varphi \in X_h\Big) \qquad \Rightarrow \qquad \mu = 0$$

(for a given interval $J \in \mathcal{G}_k$ select the nodal hat function associated with a node of $\mathcal{T}_h$ interior to J leading to $\mu = 0$ on J). Therefore, there exists a unique solution $(\phi_h, \lambda_k) \in X_h \times M_k$ of (3.5).

To prove the Strang-type error estimate we follow the standard procedure (see, e.g., [14]). Using the triangle inequality and the quasi-uniform V_h-ellipticity of $a(\cdot,\cdot)$ (see Lemma 3.5(ii)) we find that for any $\psi \in V_h$ there holds

$$\begin{aligned}
\|\phi - \phi_h\|_{H^{1/2}(\Gamma)} &\le \|\phi - \psi\|_{H^{1/2}(\Gamma)} + \|\psi - \phi_h\|_{H^{1/2}(\Gamma)} \\
&\le \|\phi - \psi\|_{H^{1/2}(\Gamma)} + C\,|\log h|^{1/2} \sup_{v\in V_h\setminus\{0\}} \frac{|a(\psi-\phi_h, v)|}{\|\mathbf{curl}_\Gamma\, v\|_{\tilde{\boldsymbol{H}}_t^{-1/2}(\Gamma)}} \\
&\le \|\phi - \psi\|_{H^{1/2}(\Gamma)} \\
&\qquad + C\,|\log h|^{1/2} \left(\sup_{v\in V_h\setminus\{0\}} \frac{|a(\psi-\phi, v)|}{\|\mathbf{curl}_\Gamma\, v\|_{\tilde{\boldsymbol{H}}_t^{-1/2}(\Gamma)}} + \sup_{v\in V_h\setminus\{0\}} \frac{|a(\phi-\phi_h, v)|}{\|\mathbf{curl}_\Gamma\, v\|_{\tilde{\boldsymbol{H}}_t^{-1/2}(\Gamma)}} \right). \qquad (3.9)
\end{aligned}$$

Selecting $\psi \in V_h \cap \tilde{H}^{1/2}(\Gamma)$ (i.e. $\psi = 0$ on γ) we can use the boundedness of $\mathbf{curl}_\Gamma : \tilde{H}^{1/2}(\Gamma) \to \tilde{\boldsymbol{H}}_t^{-1/2}(\Gamma)$ (see Lemma 2.17) and obtain (by also using the continuity of V)

$$\begin{aligned}
|a(\psi-\phi, v)| &\lesssim \|\mathbf{curl}_\Gamma(\psi-\phi)\|_{\tilde{\boldsymbol{H}}_t^{-1/2}(\Gamma)} \|\mathbf{curl}_\Gamma\, v\|_{\tilde{\boldsymbol{H}}_t^{-1/2}(\Gamma)} \\
&\lesssim \|\psi-\phi\|_{\tilde{H}^{1/2}(\Gamma)} \|\mathbf{curl}_\Gamma\, v\|_{\tilde{\boldsymbol{H}}_t^{-1/2}(\Gamma)}. \qquad (3.10)
\end{aligned}$$

A combination of (3.9) and (3.10) finishes the proof. □

Main result

Our main result is the following quasi-optimal error estimate for the approximation of $\phi \in \tilde{H}^{1/2}(\Gamma)$ by $\phi_h \in V_h$.

Theorem 3.7. *([25, Theorem 3.1]) Let $\mathcal{T}_h|_\gamma$ be a refinement of $\mathcal{G}_k$ (i.e. any node of $\mathcal{G}_k$ is a boundary node of $\mathcal{T}_h$ and any element of $\mathcal{G}_k$ has a node of $\mathcal{T}_h$ in its interior) and let*

k be sufficiently small. Then system (3.5) is uniquely solvable and there exists a constant C, independent of h, such that for any small $\epsilon > 0$ there holds the error estimate

$$\|\phi - \phi_h\|_{H^{1/2}(\Gamma)} \lesssim \Big(|\log h|^{1/2} h^{1/2-\epsilon} + |\log h|^{3/2} k^{1/2-\epsilon} \Big) \|\phi\|_{\tilde{H}^{1-\epsilon}(\Gamma)}.$$

In particular, selecting k to be proportional to h, there holds for any small $\epsilon > 0$

$$\|\phi - \phi_h\|_{H^{1/2}(\Gamma)} \lesssim |\log h|^{3/2} h^{1/2-\epsilon} \|\phi\|_{\tilde{H}^{1-\epsilon}(\Gamma)}.$$

Proof. We first apply Theorem 3.6. By assumption, the given function f is in $\tilde{H}^{-1/2}(\Gamma)$. Therefore, by Lemma 3.1, (3.4) holds for any $\psi \in H^{1/2}(\gamma)$. In particular, we can apply (3.4) to elements of $X_h \subset H^1(\Gamma)$. This yields for any $q_k \in M_k$ and $v \in V_h$

$$\begin{aligned} |a(\phi - \phi_h, v)| &= |a(\phi, v) - L(v)| = |\langle \mathbf{t} \cdot V \, \mathbf{curl}_\Gamma \, \phi, v \rangle_\gamma| \\ &= |\langle \mathbf{t} \cdot V \, \mathbf{curl}_\Gamma \, \phi - q_k, v \rangle_\gamma| \leq \|\mathbf{t} \cdot V \, \mathbf{curl}_\Gamma \, \phi - q_k\|_{L^2(\gamma)} \|v\|_{L^2(\gamma)}. \end{aligned} \tag{3.11}$$

By Lemma 2.22 and the inverse property (Lemma 2.32) one obtains, as in the proof of Lemma 3.5,

$$\|v\|_{L^2(\gamma)} \lesssim |\log h|^{1/2} \|v\|_{H^{1/2}(\Gamma)}.$$

Assuming that the mesh size k is small enough we thus obtain with Lemma 3.4 and Lemma 2.19 the bound

$$\|v\|_{L^2(\gamma)} \lesssim |\log h|^{1/2} \|v\|_{H^{1/2}(\Gamma)} \lesssim |\log h| \| \mathbf{curl}_\Gamma \, v\|_{\tilde{\boldsymbol{H}}_t^{-1/2}(\Gamma)}. \tag{3.12}$$

Noting that $\phi \in \tilde{H}^{1-\epsilon}(\Gamma)$ for any $\epsilon > 0$ (see [56]) we conclude that $\mathbf{t} \cdot V \, \mathbf{curl}_\Gamma \, \phi \in H^{1/2-\epsilon}(\gamma)$ for any $\epsilon \in (0, 1/2)$. This follows from the continuity of $\mathbf{curl}_\Gamma : \tilde{H}^{1-\epsilon}(\Gamma) \to \tilde{\boldsymbol{H}}_t^{-\epsilon}(\Gamma)$ (see [7, Lemma 3.1]), $V : \tilde{\boldsymbol{H}}_t^{-\epsilon}(\Gamma) \to \boldsymbol{H}_t^{1-\epsilon}(\Gamma)$, and the tangential trace $\boldsymbol{H}_t^{1-\epsilon}(\Gamma) \to H^{1/2-\epsilon}(\gamma)$. Therefore, a standard approximation estimate gives

$$\inf_{q_k \in M_k} \|\mathbf{t} \cdot V \, \mathbf{curl}_\Gamma \, \phi - q_k\|_{L^2(\gamma)} \lesssim k^{1/2-\epsilon} \|\phi\|_{\tilde{H}^{1-\epsilon}(\Gamma)}. \tag{3.13}$$

We conclude from (3.11), by using (3.12) and (3.13), that

$$|a(\phi - \phi_h, v)| \lesssim k^{1/2-\epsilon} |\log h| \|\phi\|_{\tilde{H}^{1-\epsilon}(\Gamma)} \| \mathbf{curl}_\Gamma \, v\|_{\tilde{\boldsymbol{H}}_t^{-1/2}(\Gamma)}$$

which gives us that

$$\sup_{v \in V_h \setminus \{0\}} \frac{|a(\phi - \phi_h, v)|}{\| \mathbf{curl}_\Gamma \, v\|_{\tilde{\boldsymbol{H}}_t^{-1/2}(\Gamma)}} \lesssim k^{1/2-\epsilon} |\log h| \|\phi\|_{\tilde{H}^{1-\epsilon}(\Gamma)} \quad \forall \epsilon \in (0, 1/2).$$

On the other hand, a standard approximation estimate yields

$$\inf_{v \in V_h \cap \tilde{H}^{1/2}(\Gamma)} \|\phi - v\|_{\tilde{H}^{1/2}(\Gamma)} \lesssim h^{1/2-\epsilon} \|\phi\|_{\tilde{H}^{1-\epsilon}(\Gamma)}.$$

Therefore, the theorem is proved by application of Theorem 3.6. □

Remark 3.8. ([25, Remark 3.1]) The solution ϕ of (3.1) has strong corner and corner-edge singularities such that $\phi \notin H^1(\Gamma)$ in general, see [56]. A refined error analysis for the conforming BEM yields for quasi-uniform meshes an optimal error estimate

$$\|\phi - \phi_h\|_{\tilde{H}^{1/2}(\Gamma)} \lesssim h^{1/2},$$

see [8]. Such an error analysis makes use of an explicit knowledge of the appearing singularities. When using only the Sobolev regularity $\phi \in \tilde{H}^{1-\epsilon}(\Gamma)$ with $\epsilon > 0$, standard approximation theory proves

$$\|\phi - \phi_h\|_{\tilde{H}^{1/2}(\Gamma)} \lesssim h^{1/2-\epsilon}\|\phi\|_{\tilde{H}^{1-\epsilon}(\Gamma)}.$$

Our proof of Theorem 3.7 makes use of standard Sobolev regularity and, thus, cannot be optimal. Without taking into account specific knowledge of the solution ϕ, the appearing parameter ϵ perturbing the rates of convergence $O(h^{1/2})$ and $O(k^{1/2})$, respectively, is unavoidable. The logarithmical perturbation in h in the error estimate is due to the non-conformity of the method. In particular, the non-existence of a trace operator $H^{1/2}(\Gamma) \to L^2(\gamma)$ leads to such a perturbation.

Chapter 4

The Mortar Boundary Element Method

In this chapter we are going to present the formulation of the Mortar BEM. We intend to present the BEM analogue to the method discussed in Section 2.2.6. We begin by presenting the model problem, we then examine an integration by parts formula which shall allow us to generate the required integral matching conditions across interfaces between sub-domains. A discrete variational formulation shall be presented and analysed. Particular attention shall be paid to the continuity and ellipticity of appearing bilinear forms. We shall also examine projection and extension operators similar to those used in Lemma 2.13 and Lemma 2.14. An error estimate shall be obtained and compared to that of the standard BEM formulation. Numerical results which underline the theory shall be presented later in Chapter 5. This chapter, along with parts of Section 2.3.1 and Chapter 5 can be found in [28].

4.1 Towards a Discrete Formulation

4.1.1 Model Problem

We shall now present our model problem. For simplicity let Γ be the plane open surface with polygonal boundary, and we shall denote its boundary by $\partial\Gamma$. We shall identify the surface Γ with a subset of R^2, thus referring to Γ as a domain rather than a surface and also referring to sub-domains of Γ rather than sub-surfaces. Now our model problem is: *For a given* $f \in L^2(\Gamma)$ *find* $\phi \in \tilde{H}^{1/2}(\Gamma)$ *such that*

$$W\phi(x) = f(x), \quad x \in \Gamma. \tag{4.1}$$

We notice that as before in Chapter 3 we have a change in regularity of our right hand side function f when compared to the conforming formulation. We require more regularity than in the case of the BEM with Lagrangian multiplier (see (3.1)), which itself required more regularity than the standard (conforming) BEM formulation (2.7). We require the extra regularity on the function f as we are now splitting the problem up over sub-domains.

Similarly to Chapter 3 we have the following weak (variational) formulation of (4.1). *Find* $\phi \in \tilde{H}^{1/2}(\Gamma)$ *such that*

$$\langle W\phi, \psi\rangle_\Gamma = \langle f, \psi\rangle_\Gamma \qquad \forall \psi \in \tilde{H}^{1/2}(\Gamma). \tag{4.2}$$

We briefly recall that a standard boundary element method (BEM) for the approximate solution of (4.2), is to select a piecewise polynomial subspace $\tilde{X}_h \subset \tilde{H}^{1/2}(\Gamma)$ and define an approximant $\tilde{\phi}_h \in \tilde{X}_h$ by

$$\langle W\tilde{\phi}_h, \psi\rangle_\Gamma = \langle f, \psi\rangle_\Gamma \qquad \forall \psi \in \tilde{X}_h.$$

Instead of this formulation, we shall study the mortar method for the model problem (4.1) (see Section 2.2.6 for the mortar FEM). We shall split the domain up into N non-overlapping sub-domains and require a weak compatibility condition on the interfaces between sub-domains. The weak compatibility condition will be incorporated by a Lagrangian multiplier (see Section 2.2.3). This means that our approximate solution may not be continuous across the whole domain (although it is continuous on each sub-domain).

4.1.2 Sub-domain decomposition

Similarly to Section 2.2.6 (for the mortar FEM), we consider a decomposition of the domain Γ into N non-intersecting sub-domains Γ_i, $i = 1, \ldots, N$, satisfying $\Gamma_i \cap \Gamma_j = \emptyset$ for $i \neq j$, giving rise to a mesh of the whole domain

$$\mathcal{T} := \{\Gamma_1, \ldots, \Gamma_N\}.$$

We assume that each sub-domain Γ_i is either a triangle or a quadrilateral, for ease of presentation of the technical results. We note that more general decompositions into more complex polygonal sub-domains can be dealt with by further decomposing these sub-domains into triangles and quadrilaterals and considering conforming interface conditions on additional interfaces.

Definition 4.1. A *geometrical conforming* sub-domain decomposition is where the sub-domains are arranged such that any two sub-domains are disjoint or intersect at a single vertex or an entire edge. See Figure 4.1(a) for an example of a geometrical conforming sub-domain decomposition. A sub-domain decomposition that is not geometrical conforming

is called a geometrical non-conforming sub-domain decomposition. See Figure 4.1(b) for an example of a geometrical non-conforming sub-domain decomposition. The large dot indicates where two sub-domains intersect at a point that is not a single vertex or an entire edge.

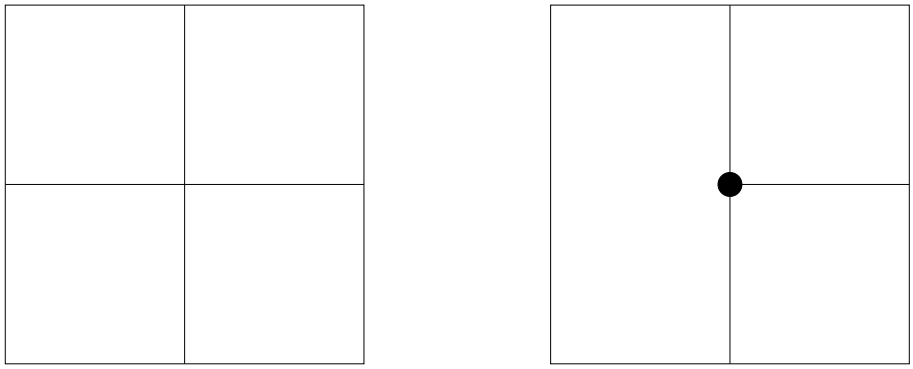

(a) Geometrical conforming sub-domain decomposition

(b) Geometrical non-conforming sub-domain decomposition

Figure 4.1: Sub-domain decomposition examples.

The maximum diameter of a sub-domain Γ_i is denoted by D_i, and we have

$$\underline{D} := \min_{i=1,\ldots,N} D_i, \qquad D := \max_{i=1,\ldots,N} D_i.$$

The *interface* between two neighbouring sub-domains Γ_i, Γ_j, ($i \neq j$, $\bar{\Gamma}_i \cap \bar{\Gamma}_j$ contains more than a point) is denoted by γ_{ij}. The mesh of sub-domains $\mathcal{T}$ can be geometrical non-conforming but must satisfy:

Assumption 4.2. Each interface γ_{ij} consists of an entire edge of sub-domains Γ_i or Γ_j.

Figure 4.2(a) shows a decomposition into sub-domains that satisfies Assumption 4.2, as each interface between two sub-domains is a whole edge of at least one of the sub-domains. Figure 4.2(b) shows a decomposition into sub-domains that does not satisfy Assumption 4.2. In Figure 4.2(b) the interface between the sub-domains Γ_i and Γ_j is not a whole edge of either sub-domain, thus violating Assumption 4.2.

The (relatively) open edges of a sub-domain Γ_i are γ_i^j, $j = 1, \ldots, m$. Here m is a generic number ($m = 3$ if Γ_i is a triangle, $m = 4$ otherwise). Using the symbol $\partial\Gamma$ for the boundary of Γ, and similarly $\partial\Gamma_i$ for the boundary of Γ_i, the skeleton γ of the sub-domain decomposition is defined as

$$\gamma = \bigcup_{i=1}^{N} \partial\Gamma_i \setminus \partial\Gamma.$$

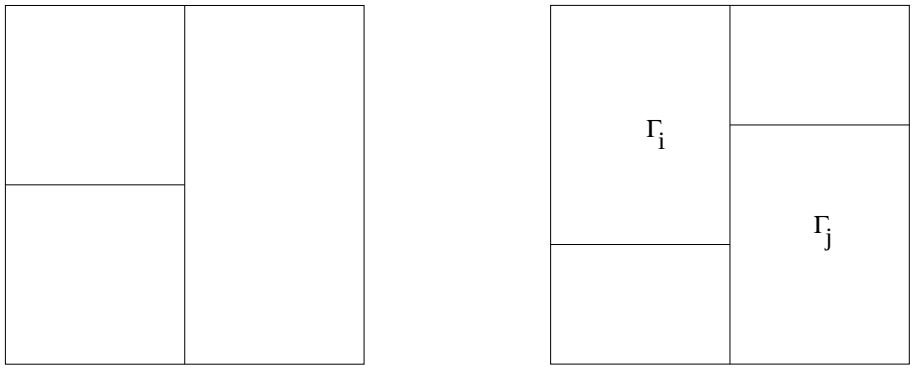

(a) Mesh satisfies Assumption 4.2

(b) Mesh does not satisfy Assumption 4.2

Figure 4.2: Interface examples.

As a result of Assumption 4.2 we are guaranteed that the skeleton is covered by a set of L (L an integer) non-intersecting edges γ_{ij}. By the assumption we have that at least one of Γ_i or Γ_j provides a whole edge to $\gamma_{ij} = \partial\Gamma_i \cap \partial\Gamma_j$. These edges are denoted by $\gamma_1, \ldots, \gamma_L$, giving a decomposition of the skeleton,

$$\bar{\gamma} = \bigcup_{l=1}^{L} \gamma_l,$$

and a mesh on the skeleton denoted by τ,

$$\tau := \{\gamma_1, \ldots, \gamma_L\}.$$

We will refer to these edges as *interface edges*. Each γ_l is the interface between two sub-domains Γ_i and Γ_j, and is an **entire edge** of at least one.

Each interface edge γ_l can be expressed as

$$\gamma_l = \gamma_{l_{\text{lag}}, l_{\text{mor}}} = \partial\Gamma_{l_{\text{lag}}} \cap \partial\Gamma_{l_{\text{mor}}} \tag{4.3}$$

where l_{lag} denotes the *Lagrangian multiplier* side, which is the number of the sub-domain which contributes a whole sub-domain side to the interface γ_l and l_{mor} denotes the *mortar* side, which is the number of the sub-domain which may not contribute a whole side to the interface γ_l. The selection of the index pair $(l_{\text{lag}}, l_{\text{lmor}})$ for $l \in \{1, \ldots, L\}$ is not unique but fixed for a specific sub-domain decomposition of Γ.

In Figure 4.3 we see four examples of the choices of the decomposition of the skeleton and hence the choice of Lagrangian multiplier side. Under Assumption 4.2 these are the

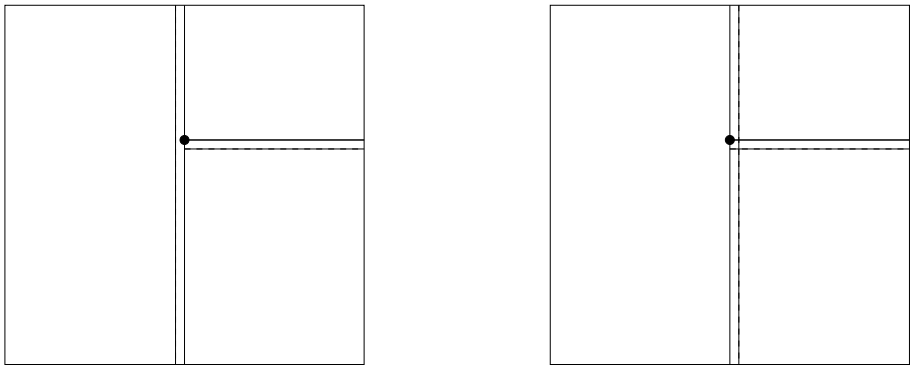

(a) Example i

(b) Example ii

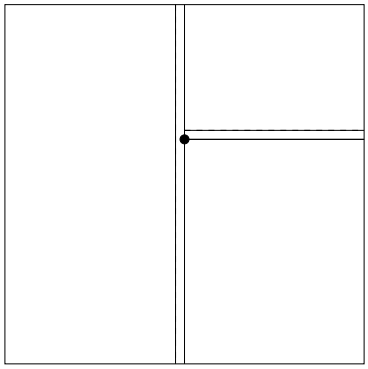

(c) Example iii

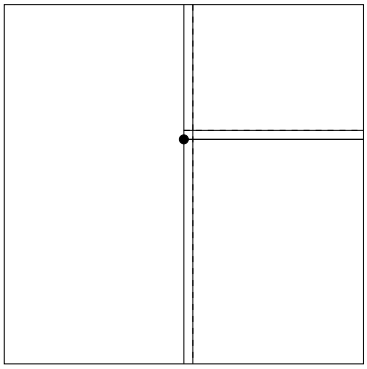

(d) Example iv

Figure 4.3: Lagrangian multiplier side examples.

four choices, since the Lagrangian multiplier side must be a whole edge of the sub-domain over which it is defined.

The length of an interface γ_l is denoted by K_l, and we have

$$\underline{K} := \min_{l=1,\ldots,L} K_l, \qquad K := \max_{l=1,\ldots,L} K_l.$$

We note that as a result of Assumption 4.2 we have that γ_l is a whole edge of $\Gamma_{l_{\text{lag}}}$, this means that K_l is proportional to $D_{l_{\text{lag}}}$. In the mortar method detailed below we shall introduce a Lagrangian multiplier defined over the interfaces and use a mesh on each γ_l which is related to the mesh of $\Gamma_{l_{\text{lag}}}$ restricted to γ_l. The side of γ_l stemming from $\Gamma_{l_{\text{mor}}}$ is usually called the mortar side in the finite element literature and this explains our notation. The side defining the Lagrangian multiplier is often called the non-mortar side.

For the decomposition of Γ we need the product Sobolev space

$$H^s(\mathcal{T}) := \prod_{K\in\mathcal{T}} H^s(K) = \prod_{i=1}^{N} H^s(\Gamma_i)$$

with usual product norm

$$\|\varphi\|^2_{H^s(\mathcal{T})} = \sum_{i=1}^{N} \|\varphi_i\|^2_{H^s(\Gamma_i)}\,.$$

We shall define $\mathbf{curl}_{\mathrm{H}}$ and $\mathrm{curl}_{\mathrm{H}}$ as follows for sufficiently smooth v and $\boldsymbol{\varphi}$:

$$\mathbf{curl}_{\mathrm{H}}\,\varphi = \sum_{i=1}^{N} \left(\mathbf{curl}_{\Gamma_\mathrm{i}}\,\varphi_i\right)^0, \qquad \mathrm{curl}_{\mathrm{H}}\,\boldsymbol{\varphi} = \sum_{i=1}^{N} \left(\mathrm{curl}_{\Gamma_\mathrm{i}}\,\boldsymbol{\varphi}_i\right)^0.$$

Where $\mathbf{curl}_{\Gamma_\mathrm{i}}$, $\mathrm{curl}_{\Gamma_\mathrm{i}}$ are defined as in Chapter 2 and the notation $(\cdot)^0$ indicates extension by zero over the whole of Γ. We shall use the notation

$$\langle\cdot,\cdot\rangle_{\mathcal{T}} := \sum_{i=1}^{N} \langle\cdot,\cdot\rangle_{\Gamma_i}$$
$$\langle\cdot,\cdot\rangle_{\tau} := \sum_{l=1}^{L} \langle\cdot,\cdot\rangle_{\gamma_l}.$$

Here for a domain $S \subset \Gamma$ or an arc S the notation $\langle\cdot,\cdot\rangle_S$ denotes the $L^2(S)$-inner product and its extension by duality. We also use the notations $\langle\cdot,\cdot\rangle_{\mathcal{T}}$ and $\langle\cdot,\cdot\rangle_{\tau}$ for duality pairings of product space corresponding to the given decompositions $\mathcal{T}$ and τ. The notation $[\varphi]$ denotes the jump of the function φ across γ, by this we mean

$$[\varphi]|_{\gamma_l} = \varphi_{l_{\mathrm{lag}}}|_{\gamma_l} - \varphi_{l_{\mathrm{mor}}}|_{\gamma_l},\ l = 1,\ldots,L.$$

4.1.3 Integration by parts

Following Chapter 3 (and [25]) we now examine an integration-by-parts formula for the hypersingular operator. For a smooth scalar function ψ and a smooth tangential vector field $\boldsymbol{\varphi}$, integration by parts applied on a sub-domain using (2.46) gives

$$\langle\mathbf{curl}_{\Gamma_\mathrm{i}}\,\psi,\boldsymbol{\varphi}\rangle_{\Gamma_i} = \langle\psi,\mathrm{curl}_{\Gamma_\mathrm{i}}\,\boldsymbol{\varphi}\rangle_{\Gamma_i} - \langle\psi,\boldsymbol{\varphi}\cdot\mathbf{t}_i\rangle_{\partial\Gamma_i}, \quad i = 1,\ldots,N.$$

Here, $\mathbf{t}_i$ is the unit tangential vector on $\partial\Gamma_i$ (oriented mathematically positive when identifying Γ_i with a subset of $\mathbf{R}^2$ which is compatible with the identification of Γ as a

subset of $\mathbf{R}^2$). Applying this formula to $\boldsymbol{\varphi} = (V\,\mathbf{curl}_\Gamma\,\phi)|_{\Gamma_i}$ (restricted to Γ_i), we obtain for smooth functions ψ and ϕ

$$\langle \mathbf{t}_i \cdot V\,\mathbf{curl}_\Gamma\,\phi, \psi_i\rangle_{\partial\Gamma_i} = \langle \mathrm{curl}_{\Gamma_i} V\,\mathbf{curl}_\Gamma\,\phi, \psi_i\rangle_{\Gamma_i} - \langle V\,\mathbf{curl}_\Gamma\,\phi, \mathbf{curl}_{\Gamma_\mathrm{i}}\,\psi_i\rangle_{\Gamma_i}.$$

Now we sum over i and take into account that $t_i = -t_j$ on γ_{ij}. Further we let $\gamma_0 := \partial\Gamma$, the boundary of the whole domain , use the convention for the jump

$$[\psi]|_{\gamma_0} = \psi|_{\gamma_0},$$

denote by $\mathbf{t}_0$ the unit tangential vector along $\partial\Gamma$ (again mathematically positive oriented) and let $0_{\mathrm{lag}} := 0$ (remember the notation l_{lag} and l_{mor} for the numbers of the Lagrangian multiplier side and mortar side of γ_l, respectively). To put this another way for any sub-domain Γ_i such that $\partial\Gamma \cap \partial\Gamma_i \neq \emptyset$ we define the jump over the interface $\gamma_0|_{\partial\Gamma_i}$ as

$$[\psi]|_{\gamma_0|_{\partial\Gamma_i}} = \psi_{0_{\mathrm{lag}}}|_{\gamma_0|_{\partial\Gamma_i}} - \psi_{0_{\mathrm{mor}}}|_{\gamma_0|_{\partial\Gamma_i}}.$$

We then set $\psi_{0_{\mathrm{lag}}}|_{\gamma_0|_{\partial\Gamma_i}} = \psi_i|_{\gamma_0|_{\partial\Gamma_i}}$ and $\psi_{0_{\mathrm{mor}}}|_{\gamma_0|_{\partial\Gamma_i}} = 0$. This gives us that

$$[\psi]|_{\gamma_0|_{\partial\Gamma_i}} = \psi_i|_{\gamma_0|_{\partial\Gamma_i}}.$$

Now summing over all sub-domains Γ_i such that $\partial\Gamma \cap \partial\Gamma_i \neq \emptyset$ we have that

$$[\psi]|_{\gamma_0} = \psi|_{\gamma_0}.$$

This yields

$$\begin{aligned}\sum_{l=0}^{L}\langle \mathbf{t}_{l_{\mathrm{lag}}} \cdot V\,\mathbf{curl}_\Gamma\,\phi, [\psi]\rangle_{\gamma_l} &= \sum_{i=1}^{N}\langle \mathrm{curl}_{\Gamma_i} V\,\mathbf{curl}_\Gamma\,\phi, \psi_i\rangle_{\Gamma_i} - \sum_{i=1}^{N}\langle V\,\mathbf{curl}_\Gamma\,\phi, \mathbf{curl}_{\Gamma_\mathrm{i}}\,\psi_i\rangle_{\Gamma_i} \\ &= \langle \mathrm{curl}_\Gamma V\,\mathbf{curl}_\Gamma\,\phi, \psi\rangle_{\mathcal{T}} - \langle V\,\mathbf{curl}_\Gamma\,\phi, \mathbf{curl}_{\mathrm{H}}\,\psi\rangle_{\mathcal{T}}\end{aligned}$$

for a piecewise (with respect to $\mathcal{T}$) smooth function ψ on Γ with $\psi_i := \psi|_{\Gamma_i}$, as defined before. Here, more precisely the notation $\mathrm{curl}_{\Gamma_i} V\,\mathbf{curl}_\Gamma\,\phi$ means $\mathrm{curl}_{\Gamma_i}(V\,\mathbf{curl}_\Gamma\,\phi)|_{\Gamma_i}$. Also, in the last step we used the fact that

$$\mathrm{curl}_H\,\varphi = \mathrm{curl}_\Gamma\,\varphi \quad \forall\varphi \in \boldsymbol{H}_{\mathrm{t}}^{1/2}(\Gamma),$$

which holds by a density argument and the continuity of $\mathrm{curl}_\Gamma : \boldsymbol{H}_{\mathrm{t}}^{1/2}(\Gamma) \to H^{-1/2}(\Gamma)$ as the adjoint operator of $\mathbf{curl}_\Gamma : \tilde{H}^{1/2}(\Gamma) \to \tilde{\boldsymbol{H}}_{\mathrm{t}}^{-1/2}(\Gamma)$, cf. Lemma 2.17.

Now we use the relation

$$W\phi = \mathrm{curl}_\Gamma\, V\,\mathbf{curl}_\Gamma\,\phi \quad (\phi \in \tilde{H}^{1/2}(\Gamma)),$$

see [40, 43] and Lemma 2.20. Then choosing a piecewise smooth function ψ with $\psi|_{\partial\Gamma} = 0$ we obtain

$$\langle \lambda, [\psi] \rangle_\tau = \sum_{l=1}^{L} \langle \lambda, [\psi] \rangle_{\gamma_l} = \langle W\phi, \psi \rangle_{\mathcal{T}} - \langle V \, \mathbf{curl}_\Gamma \, \phi, \mathbf{curl}_{\mathrm{H}} \, \psi \rangle_{\mathcal{T}}. \tag{4.4}$$

Here, λ denotes our Lagrangian multiplier on the skeleton γ defined by

$$\lambda|_{\gamma_l} := \mathbf{t}_{l_{\mathrm{lag}}} \cdot (V \, \mathbf{curl}_\Gamma \, \phi)|_{\gamma_l}, \quad l = 1, \ldots, L. \tag{4.5}$$

Relation (4.4) does not extend to $\psi \in H^{1/2}(\mathcal{T})$ since the trace of such a function v onto γ is not well defined (see Lemma 2.22, Trace Theorem). However, there holds the following lemma.

Lemma 4.3. *For $\phi \in \tilde{H}^{1/2}(\Gamma)$ with $W\phi = f \in L^2(\Gamma)$,* (4.4) defines $\lambda \in \prod_{l=1}^{L} H^{-s}(\gamma_l)$ for any $s \in (0, 1/2]$.

Remark 4.4. The above lemma can be extended to values of s larger than $1/2$. Though small values of s represent the interesting cases, the limit $s = 0$ being excluded. Also, the condition on f can be relaxed but excluding the case $f \in H^{-1/2}(\Gamma)$ which is the standard regularity using the mapping properties of the hypersingular operator.

Proof of Lemma 4.3. We must show that λ defined by (4.4) is a bounded linear functional on $\prod_{l=1}^{L} \tilde{H}^s(\gamma_l)$, the dual space of $\prod_{l=1}^{L} H^{-s}(\gamma_l)$.

Let $\psi \in \prod_{l=1}^{L} \tilde{H}^s(\gamma_l)$ be given. We continuously extend ψ to an element $\tilde{\psi} \in H^{s+1/2}(\mathcal{T})$ with $\tilde{\psi} = 0$ on $\partial\Gamma$ such that $[\tilde{\psi}]|_{\gamma_l} = \psi|_{\gamma_l}$. (Simply extend ψ on each interface edge γ_l to a function in $H^{s+1/2}(\Gamma_{l_{\mathrm{lag}}})$ vanishing on $\partial\Gamma_{l_{\mathrm{lag}}} \setminus \gamma_l$ and extend by zero to the rest of Γ. Then sum up with respect to l.) The definition of λ is independent of the particular extension $\tilde{\psi}$, see Lemma 2.16 for details in the case of one sub-domain. Using a duality estimate we obtain from (4.4)

$$\begin{aligned} \sum_{l=0}^{L} \langle \lambda, [\psi] \rangle_{\gamma_l} &= \langle f, \tilde{\psi} \rangle_{\mathcal{T}} - \langle V \, \mathbf{curl}_\Gamma \, \phi, \mathbf{curl}_{\mathrm{H}} \, \tilde{\psi} \rangle_{\mathcal{T}} \\ &\leq \|f\|_{L^2(\Gamma)} \|\tilde{\psi}\|_{L^2(\Gamma)} + \sum_{i=1}^{N} \|V \, \mathbf{curl}_\Gamma \, \phi\|_{\tilde{\boldsymbol{H}}_{\mathrm{t}}^{1/2-s}(\Gamma_i)} \|\mathbf{curl}_{\Gamma_i} \, \tilde{\psi}_i\|_{\boldsymbol{H}_{\mathrm{t}}^{s-1/2}(\Gamma_i)} \end{aligned} \tag{4.6}$$

Now, for $s \in (0, 1/2]$ the norms in $\tilde{\boldsymbol{H}}_{\mathrm{t}}^{1/2-s}(\Gamma_i)$ and $\boldsymbol{H}_{\mathrm{t}}^{1/2-s}(\Gamma_i)$ are equivalent (cf., e.g., [38]) so that together with the mapping property of V [19],

$$V : \; \tilde{\boldsymbol{H}}_{\mathrm{t}}^{-1/2-s}(\Gamma) \to \boldsymbol{H}_{\mathrm{t}}^{1/2-s}(\Gamma),$$

and Lemma 2.17 we obtain

$$\begin{aligned}\sum_{i=1}^{N} \|V\,\mathbf{curl}_\Gamma\,\phi\|^2_{\tilde{\boldsymbol{H}}_{\mathrm{t}}^{1/2-s}(\Gamma_i)} &\lesssim \sum_{i=1}^{N} \|V\,\mathbf{curl}_\Gamma\,\phi\|^2_{\boldsymbol{H}_{\mathrm{t}}^{1/2-s}(\Gamma_i)} \lesssim \|V\,\mathbf{curl}_\Gamma\,\phi\|^2_{\boldsymbol{H}_{\mathrm{t}}^{1/2-s}(\Gamma)} \\ &\lesssim \|\phi\|^2_{\tilde{H}^{1/2}(\Gamma)}.\end{aligned}$$

Here, the appearing constants are independent of ϕ but may depend on s. Also, using Lemma 2.19 we are able to bound (with constant independent of $\tilde{\psi}$)

$$\sum_{i=1}^{N} \|\,\mathbf{curl}_{\Gamma_\mathrm{i}}\,\tilde{\psi}_i\|^2_{\boldsymbol{H}_{\mathrm{t}}^{s-1/2}(\Gamma_i)} \lesssim \sum_{i=1}^{N} \|\tilde{\psi}_i\|^2_{H^{s+1/2}(\Gamma_i)} = \|\tilde{\psi}\|^2_{H^{s+1/2}(\mathcal{T})}.$$

Taking the last two estimates into account, (4.6) proves that

$$\sum_{l=1}^{L} \langle\lambda, [\psi]\rangle_{\gamma_l} \lesssim \left(\|f\|_{L^2(\Gamma)} + \|\phi\|_{\tilde{H}^{1/2}(\Gamma)}\right) \|\tilde{\psi}\|_{H^{s+1/2}(\mathcal{T})}.$$

Using the continuity of the extension (with constant independent of ψ)

$$\|\tilde{\psi}\|^2_{H^{s+1/2}(\mathcal{T})} \lesssim \sum_{l=1}^{L} \|\psi\|^2_{\tilde{H}^s(\gamma_l)}$$

finishes the proof. □

4.2 Discrete Variational Formulation of the Mortar BEM

In this section we first present the meshes and discrete spaces that shall be used to define the mortar BEM. We then present the discrete formulation of the mortar BEM.

4.2.1 Meshes and Discrete Spaces

On each Γ_i ($i \in \{1, \ldots, N\}$) we consider a sequence of regular, quasi-uniform meshes $\mathcal{T}_i$ consisting of shape regular elements which are either triangles or quadrilaterals. This gives us that $\bar{\Gamma}_i = \cup_{T\in\mathcal{T}_i} \bar{T}$, where T is an element of the mesh and $\bar{T}$ is the closure of the element, i.e. we include the boundary. The maximum diameter of elements of $\mathcal{T}_i$ is denoted $h_i < 1$ and we use

$$\underline{h} := \min_{i=1,\ldots,N} h_i, \qquad h := \max_{i=1,\ldots,N} h_i.$$

The assumption that $h_i < 1$ is used throughout the chapter without loss of generality and is needed to make the writing of logarithmic terms easier.

In the case of Γ being a square, Figure 4.4(a) shows a conforming sub-domain decomposition and Figure 4.4(b) shows a nonconforming sub-domain decomposition, each with globally nonconforming (but locally (on each sub-domain) conforming) meshes.

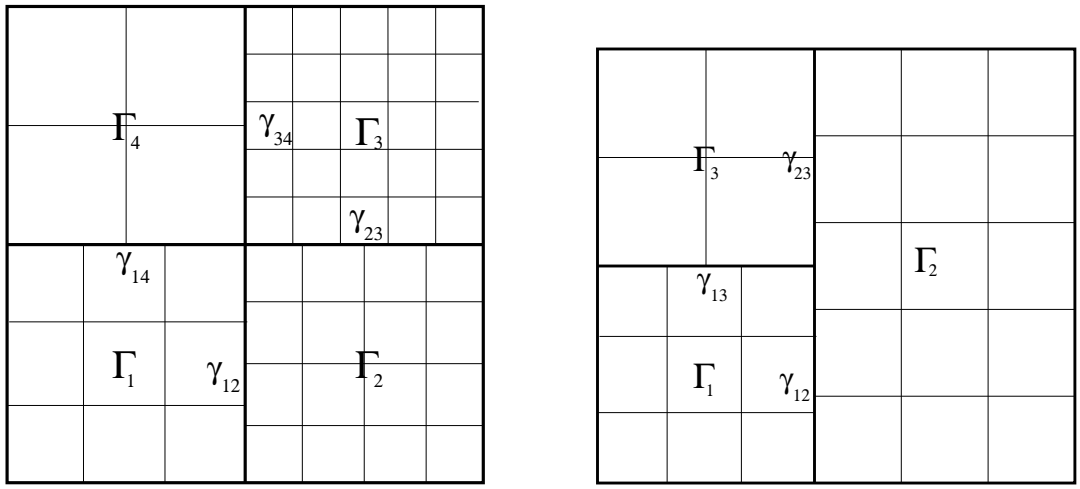

(a) A conforming sub-domain decomposition

(b) A non-conforming sub-domain decomposition

Figure 4.4: Examples of globally nonconforming but locally conforming meshes.

We now introduce the local discrete spaces on sub-domains required for the mortar method consisting of piecewise (bi)linear functions. (Linear if the elements are triangle, bilinear if the elements are rectangles.)

$$X_{h,i} := \{\varphi \in C^0(\Gamma_i);\ \varphi|_T \text{ is a polynomial of degree one}$$

$$\forall T \in \mathcal{T}_i,\ \varphi|_{\partial\Gamma\cap\partial\Gamma_i} = 0\},\ i = 1, \ldots, N. \tag{4.7}$$

The global discrete space on the whole domain Γ is the product space of these spaces over all sub-domains

$$X_h := \prod_{i=1}^{N} X_{h,i}. \tag{4.8}$$

We note that by the definition of the space X_{h_i} functions $v \in X_h$ satisfy the homogeneous boundary condition along the boundary of the whole domain $\partial\Gamma$, but that no conditions of continuity across interfaces are included in the definition of these spaces.

As a result of this these functions are in general discontinuous across sub-domain interfaces, and as such are in general not continuous functions on Γ. Therefore, X_h is not a subspace of the energy space $\tilde{H}^{1/2}(\Gamma)$ (functions in $\tilde{H}^{1/2}(\Gamma)$ are continuous across sub-domain interfaces). As noted before a standard BEM (2.8) chooses as a trial space a subspace of the energy space, which we are not doing here. Instead we shall incorporate the continuity condition across sub-domain interfaces in a weak manner by the inclusion of a Lagrangian multiplier. Functions from different sub-domains will be coupled via a discrete Lagrangian multiplier on the skeleton. This means that our functions will not in general be continuous across sub-domain interfaces but will have this discontinuity constrained in some fashion. This shall cause us to have a non-standard method, and as shall be noted we have an error estimate with two parts (see Lemma 2.6). One part comes from the conforming part of the method and the second part shows the effect of the discontinuities in the approximating function over interfaces on the error.

A mesh on the skeleton γ is needed to define the discrete Lagrangian multiplier space. On each interface edge γ_l we define a trace mesh $\mathcal{T}_{l_{\text{lag}}}|_{\gamma_l}$ being the restriction of the mesh $\mathcal{T}_{l_{\text{lag}}}$ from the sub-domain $\Gamma_{l_{\text{lag}}}$ to the interface γ_l. We recall that by definition γ_l is a whole edge of $\mathcal{T}_{l_{\text{lag}}}$. This inherited trace mesh is quasi-uniform with mesh width $h_{l_{\text{lag}}}$. The mesh used to define the Lagrangian multiplier space $\mathcal{G}_l$ is a coarsening of the trace mesh $\mathcal{T}_{l_{\text{lag}}}|_{\gamma_l}$, such that the following assumption is satisfied.

Assumption 4.5. For any $l \in \{1, \ldots, L\}$ there holds: the mesh $\mathcal{G}_l$ is a strict coarsening of the trace mesh $\mathcal{T}_{l_{\text{lag}}}|_{\gamma_l}$. The mesh $\mathcal{G}_l$ is made up of non-overlapping elements (straight line pieces) that satisfy:

- The elements extreme points are different nodes of $\mathcal{T}_{l_{\text{lag}}}|_{\gamma_l}$, and
- the interior of any element covers at least one interior node of $\mathcal{T}_{l_{\text{lag}}}|_{\gamma_l}$, which is a different node to the extreme nodes of the element.

Figure 4.5 shows how we define our discrete Lagrangian multiplier space. The solid dots represent the restriction to the interface of the mesh of the sub-domain that has been chosen as the Lagrangian multiplier side. The hollow circles represent the choice of nodes for the Lagrangian multiplier space. The dashed lines then represent the Lagrangian multipliers themselves. In Figure 4.5(a) we have an even number of nodes of the mesh of the sub-domain restricted to the interface. We therefore define one of the intervals (the first) of our Lagrangian multiplier space as longer than the others in order to satisfy Assumption 4.5.

The mesh width (length of longest element) of $\mathcal{G}_l$ is denoted by k_l, and

$$\underline{k} := \min_{l=1,\ldots,L} k_l, \qquad k := \max_{l=1,\ldots,L} k_l.$$

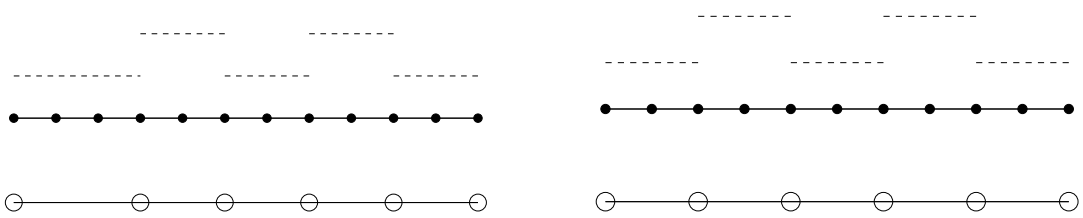

(a) Example i (b) Example ii

Figure 4.5: Definition of discrete Lagrangian multiplier space.

We note that since we have chosen to define our Lagrangian multipliers over a coarsened mesh that we have that k is proportional to h. On each interface edge we define a space of piecewise constant functions,

$$M_{k,l} := \{q \in L^2((\partial\Gamma_l)_k);\ q|_J \text{ is constant } \forall J \in \mathcal{G}_l\}, l = 1, \ldots, L. \tag{4.9}$$

The space for the discrete Lagrangian multiplier is then

$$M_k := \prod_{l=1}^{L} M_{k,l}. \tag{4.10}$$

4.2.2 Setting of the Mortar Boundary Element Method

For the formulation of the mortar boundary element method we define the bilinear forms $a(\cdot,\cdot)$ and $b(\cdot,\cdot)$ by

$$\begin{aligned} a(\varphi,\psi) &:= \langle V\,\mathbf{curl}_{\mathrm{H}}\,\varphi, \mathbf{curl}_{\mathrm{H}}\,\psi\rangle_{\mathcal{T}} := \sum_{i=1}^{N}\langle V\,\mathbf{curl}_{\mathrm{H}}\,\varphi, \mathbf{curl}_{\Gamma_i}\,\psi_i\rangle_{\Gamma_i}, \\ b(\varphi,q) &:= \langle[\varphi], q\rangle_{\tau} := \sum_{l=1}^{L}\langle[\varphi], q\rangle_{\gamma_l}, \end{aligned}$$

and the linear form

$$F(\varphi) = \sum_{i=1}^{n}\langle f_i, \varphi_i\rangle_{\Gamma_i} = \langle f, \varphi\rangle_{\mathcal{T}}.$$

We have for sufficiently smooth functions φ, ψ, and q that there holds

$$a(\varphi,\psi) = \langle V\,\mathbf{curl}_{\mathrm{H}}\,\varphi, \mathbf{curl}_{\mathrm{H}}\,\psi\rangle_{\Gamma}, \quad b(\varphi,q) = \langle[\varphi], q\rangle_{\gamma}.$$

The **mortar boundary element method** for the approximate solution of (4.1) is then: *Find $\phi_h \in X_h$ and $\lambda_k \in M_k$ such that*

$$\begin{aligned} a(\phi_h, \psi) + b(\psi, \lambda_k) &= F(\psi) \qquad \forall \psi \in X_h \\ b(\phi_h, q) &= 0 \qquad \forall q \in M_k. \end{aligned} \tag{4.11}$$

This scheme is equivalent to:
Find $\phi_h \in V_h$ such that

$$a(\phi_h, \psi) = F(\psi) \qquad \forall \psi \in V_h, \tag{4.12}$$

where

$$V_h = \{\psi \in X_h : b(\psi, q) = 0 \quad \forall q \in M_k\}. \tag{4.13}$$

We shall refer to X_h as an *unconstrained space* and V_h as a *constrained space* to indicate the inclusion of the compatibility constraint in the definition of V_h.

4.3 Technical Details and Proof of the Main Result

In this section we present the analysis which leads to our main error result. Continuity and ellipticity of the bilinear form $a(\cdot,\cdot)$ are essential for the error analysis of the problem described in equation (4.11), so we shall now examine these properties of the bilinear form $a(\cdot,\cdot)$. For completeness we show dependence of these results upon sub-domain size. We shall first present the continuity and then the ellipticity.

Continuity of $a(\cdot,\cdot)$

Lemma 4.6. *The bilinear form $a(\cdot,\cdot)$ is almost uniformly continuous on X_h, there holds*

$$|a(v,w)| \lesssim \underline{D}^{-2} |\log(\underline{h}/D)|^2 \, \|v\|_{H^{1/2}(\mathcal{T})} \, \|w\|_{H^{1/2}(\mathcal{T})} \qquad \forall v, w \in X_h.$$

Proof. First we note that for $v, w \in X_h \subset L^2(\Gamma)$ there holds $V \operatorname{\mathbf{curl}}_{\mathrm{H}} v \in \mathbf{L}^2_t(\Gamma)$ so that

$$\langle V \operatorname{\mathbf{curl}}_{\mathrm{H}} v, \operatorname{\mathbf{curl}}_{\mathrm{H}} w \rangle_{\mathcal{T}} = \langle V \operatorname{\mathbf{curl}}_{\mathrm{H}} v, \operatorname{\mathbf{curl}}_{\mathrm{H}} w \rangle_{\Gamma}.$$

Now, using the continuity of $V : \tilde{\boldsymbol{H}}_t^{-1/2}(\Gamma) \to \boldsymbol{H}_t^{1/2}(\Gamma)$ and the estimate for fractional order Sobolev norms $\|\cdot\|_{\tilde{\boldsymbol{H}}_t^{-1/2}(\Gamma)} \lesssim \|\cdot\|_{\tilde{\boldsymbol{H}}_t^{-1/2}(\mathcal{T})}$, we obtain for $v, w \in X_h$

$$\begin{aligned} a(v,w) = \langle V \operatorname{\mathbf{curl}}_{\mathrm{H}} v, \operatorname{\mathbf{curl}}_{\mathrm{H}} w \rangle_{\Gamma} &\lesssim \|\operatorname{\mathbf{curl}}_{\mathrm{H}} v\|_{\tilde{\boldsymbol{H}}_t^{-1/2}(\Gamma)} \|\operatorname{\mathbf{curl}}_{\mathrm{H}} w\|_{\tilde{\boldsymbol{H}}_t^{-1/2}(\Gamma)} \\ &\lesssim \|\operatorname{\mathbf{curl}}_{\mathrm{H}} v\|_{\tilde{\boldsymbol{H}}_t^{-1/2}(\mathcal{T})} \|\operatorname{\mathbf{curl}}_{\mathrm{H}} w\|_{\tilde{\boldsymbol{H}}_t^{-1/2}(\mathcal{T})}. \end{aligned} \tag{4.14}$$

Now examining on each sub-domain and transforming to a reference sub-domain by (2.54), using Lemma 2.18 and Lemma 2.30, then transforming back by (2.48) we see that, for $v \in X_h$

$$\begin{aligned}\|\operatorname{\mathbf{curl}}_{\Gamma_i} v_i\|^2_{\tilde{\boldsymbol{H}}_t^{-1/2}(\Gamma_i)} &\lesssim \|\operatorname{\mathbf{curl}}_{\widehat{\Gamma}_i} \hat{v}_i\|^2_{\tilde{\boldsymbol{H}}_t^{-1/2}(\widehat{\Gamma}_i)} \\ &\lesssim |\log(h_i/D_i)|^2 \|\operatorname{\mathbf{curl}}_{\widehat{\Gamma}_i} \hat{v}_i\|^2_{\boldsymbol{H}_t^{-1/2}(\widehat{\Gamma}_i)} \\ &\lesssim |\log(h_i/D_i)|^2 \|\hat{v}_i\|^2_{H^{1/2}(\widehat{\Gamma}_i)} \\ &\lesssim D_i^{-2} |\log(h_i/D_i)|^2 \|v_i\|^2_{H^{1/2}(\Gamma_i)}.\end{aligned}$$

Giving us that

$$\|\operatorname{\mathbf{curl}}_{\mathrm{H}} v\|_{\tilde{\boldsymbol{H}}_t^{-1/2}(\mathcal{T})} \lesssim \underline{D}^{-1} |\log(\underline{h}/D)| \|v\|_{H^{1/2}(\mathcal{T})} \qquad \forall v \in X_h.$$

Combination with (4.14) proves the statement. □

Lemma 4.6 is not applicable to non-discrete functions. In particular this means we cannot use it when we consider the continuous function that is the solution of our model problem. For the error estimate of the mortar BEM we will require continuity for continuous functions, we therefore need a different continuity estimate for our bilinear form $a(\cdot,\cdot)$, this is given in the following lemma.

Lemma 4.7. *Assume that $u \in \tilde{H}^{1/2+r}(\Gamma)$ $(r > 0)$. Then there holds*

$$a(u - v, w) \lesssim \underline{D}^{-1} s^{-1} \|u - v\|_{H^{1/2+s}(\mathcal{T})} \|\operatorname{\mathbf{curl}}_{\mathrm{H}} w\|_{\tilde{\boldsymbol{H}}_t^{-1/2}(\mathcal{T})} \qquad \forall v, w \in X_h,\ \forall s \in (0, \min\{r, 1/2\}].$$

In particular, the appearing constant is independent of s.

Proof. We note that (4.14) holds for continuous and discrete functions, so that for all $v, w \in X_h$ and $u \in \tilde{H}^{1/2+r}(\Gamma)$ $(r > 0)$ we have

$$a(u - v, w) \lesssim \|\mathbf{curl}_{\mathrm{H}}(u - v)\|_{\tilde{\boldsymbol{H}}_t^{-1/2}(\mathcal{T})} \|\operatorname{\mathbf{curl}}_{\mathrm{H}} w\|_{\tilde{\boldsymbol{H}}_t^{-1/2}(\mathcal{T})}. \tag{4.15}$$

Now using (2.54), the continuous injection $\tilde{\boldsymbol{H}}_t^{-1/2+s}(\Gamma_i) \to \tilde{\boldsymbol{H}}_t^{-1/2}(\Gamma_i)$, Lemma 2.29, the continuity of $\operatorname{\mathbf{curl}}_{\Gamma_i} : H^{1/2+s}(\Gamma_i) \to \boldsymbol{H}_t^{-1/2+s}(\Gamma_i)$ by Lemma 2.18 and (2.48) we can bound for $i \in \{1, \dots, N\}$

$$\begin{aligned}\|\operatorname{\mathbf{curl}}_{\Gamma_i}(u_i - v_i)\|^2_{\tilde{\boldsymbol{H}}_t^{-1/2}(\Gamma_i)} &\lesssim \|\operatorname{\mathbf{curl}}_{\widehat{\Gamma}_i}(\hat{u}_i - \hat{v}_i)\|^2_{\tilde{\boldsymbol{H}}_t^{-1/2}(\widehat{\Gamma}_i)} \\ &\lesssim \|\operatorname{\mathbf{curl}}_{\widehat{\Gamma}_i}(\hat{u}_i - \hat{v}_i)\|^2_{\tilde{\boldsymbol{H}}_t^{-1/2+s}(\widehat{\Gamma}_i)} \\ &\lesssim s^{-2} \|\operatorname{\mathbf{curl}}_{\widehat{\Gamma}_i}(\hat{u}_i - \hat{v}_i)\|^2_{\boldsymbol{H}_t^{-1/2+s}(\widehat{\Gamma}_i)} \\ &\lesssim s^{-2} \|\hat{u}_i - \hat{v}_i\|^2_{H^{1/2+s}(\widehat{\Gamma}_i)} \\ &\lesssim D_i^{-2} s^{-2} \|u_i - v_i\|^2_{H^{1/2+s}(\Gamma_i)}.\end{aligned}$$

Summing over all sub-domains gives us that

$$\|\mathbf{curl}_{\mathrm{H}}(u-v)\|_{\tilde{\boldsymbol{H}}_t^{-1/2}(\mathcal{T})} \lesssim \underline{D}^{-1} s^{-1} \|u-v\|_{H^{1/2+s}(\mathcal{T})}.$$

Combination with (4.15) finishes the proof. □

Before being able to prove V_h ellipticity we require an extension to the following result, which is a generalized version of a discrete Poincaré-Friedrichs inequality in fractional order Sobolev spaces, Theorem 8 in [30].

Proposition 4.8. *There exists a constant $C > 0$, independent of the decomposition $\mathcal{T}$ as long as sub-domains are shape regular, such that for all $\epsilon \in (0, 1/2]$ there holds $\forall v \in H^{1/2+\epsilon}(\mathcal{T})$*

$$\|v\|^2_{L^2(\Gamma)} \leq C \left(\epsilon^{-1} |v|^2_{H^{1/2+\epsilon}(\mathcal{T})} + \sum_{l=1}^{L} K_l^{-1-2\epsilon} \left(\int_{\gamma_l} [v]\, ds \right)^2 \right).$$

Where, K_l is the length of γ_l.

For a proof of Proposition 4.8 see Appendix A. In Lemma 4.9 we adapt the result of Proposition 4.8 to our mortar situation.

Lemma 4.9. *For all $v \in V_h$*

$$\|\,\mathbf{curl}_{\mathrm{H}}\, v\|^2_{\tilde{\boldsymbol{H}}_t^{-1/2}(\Gamma)} \gtrsim \underline{D} |\log(\underline{h}/D)|^{-1} \|v\|^2_{H^{1/2}(\mathcal{T})}.$$

Proof. We first recall that for any $v \in V_h$ we have, by definition (see (4.13)), the interface matching condition $\int_{\gamma_l} [v] \mu \,\mathrm{ds} = 0$ for all $\mu \in M_k$. We thus have that $\int_{\gamma_l} [v] \,\mathrm{ds} = 0$ for any interface edge γ_l since by construction M_k contains a constant function which has the value 1 on γ_l and vanishes on $\gamma \setminus \gamma_l$. Therefore Proposition 4.8 proves that (note the result is independent of sub-domain size)

$$\|v\|^2_{L^2(\Gamma)} \lesssim \epsilon^{-1} \sum_{i=1}^{n} |v_i|^2_{H^{1/2+\epsilon}(\Gamma_i)} \quad \forall v \in V_h. \tag{4.16}$$

Here the appearing constant is independent of $\epsilon \in (0, 1/2]$. Making use of (2.47), the inverse property and again (2.47) we bound

$$\begin{aligned} \sum_{i=1}^{N} |v|^2_{H^{1/2+\epsilon}(\Gamma_i)} &\lesssim \sum_{i=1}^{N} D_i^{1-2\epsilon} |\hat{v}|^2_{H^{1/2+\epsilon}(\hat{\Gamma}_i)} \lesssim \sum_{i=1}^{N} D_i^{1-2\epsilon} (h_i/D_i)^{-2\epsilon} |\hat{v}|^2_{H^{1/2}(\hat{\Gamma}_i)} \\ &\lesssim \sum_{i=1}^{N} D_i^{1-2\epsilon} D_i^{-1} (h_i/D_i)^{-2\epsilon} |v|^2_{H^{1/2}(\Gamma_i)} \quad \forall v \in V_h. \end{aligned} \tag{4.17}$$

Combining (4.16) and (4.17) we have that (recalling $\epsilon \in (0, 1/2]$)

$$\begin{aligned}\|v\|^2_{L^2(\Gamma)} &\lesssim \epsilon^{-1} \sum_{i=1}^{n} D_i^{-2\epsilon} (h_i/D_i)^{-2\epsilon} |v_i|^2_{H^{1/2}(\Gamma_i)} \\ &\lesssim \epsilon^{-1} \sum_{i=1}^{n} D_i^{-1} (h_i/D_i)^{-2\epsilon} |v_i|^2_{H^{1/2}(\Gamma_i)} \quad \forall v \in V_h. \end{aligned} \tag{4.18}$$

Which holds since (assuming $0 < D_i \leq 1$) $D_i^{-2\epsilon} \leq D_i^{-1}$. Now, for any $v \in H^{1/2}(\mathcal{T})$ by (2.53), Lemma 2.19 and (2.47) there holds

$$\begin{aligned}\|\operatorname{\mathbf{curl}}_{\mathrm{H}} v\|^2_{\tilde{\boldsymbol{H}}_t^{-1/2}(\Gamma)} &\gtrsim \|\operatorname{\mathbf{curl}}_{\mathrm{H}} v\|^2_{\boldsymbol{H}_t^{-1/2}(\Gamma)} \\ &\gtrsim \sum_{i=1}^{N} \|\operatorname{\mathbf{curl}}_{\Gamma_\mathrm{i}} v\|^2_{\boldsymbol{H}_t^{-1/2}(\Gamma_i)} \\ &\gtrsim \sum_{i=1}^{N} D_i \|\operatorname{\mathbf{curl}}_{\widehat{\Gamma}_\mathrm{i}} \hat{v}_i\|^2_{\boldsymbol{H}_t^{-1/2}(\widehat{\Gamma}_i)} \\ &\gtrsim \sum_{i=1}^{N} D_i |\hat{v}_i|^2_{H^{1/2}(\widehat{\Gamma}_i)} \\ &\gtrsim \sum_{i=1}^{N} D_i D_i^{-1} |v_i|^2_{H^{1/2}(\Gamma_i)} \\ &\gtrsim \sum_{i=1}^{N} |v_i|^2_{H^{1/2}(\Gamma_i)} = |v|^2_{H^{1/2}(\mathcal{T})}. \end{aligned} \tag{4.19}$$

We recall that

$$\|v\|^2_{H^{1/2}(\mathcal{T})} = \|v\|^2_{L^2(\mathcal{T})} + |v|^2_{H^{1/2}(\mathcal{T})}.$$

Combining (4.18) with (4.19) and selecting $\epsilon = |\log(\underline{h}/D)|^{-1}$ (for $(\underline{h}/D)$ being small enough) proves the statement. □

Ellipticity of $a(\cdot,\cdot)$

We are now ready to prove the V_h-ellipticity of the bilinear form $a(\cdot,\cdot)$.

Lemma 4.10. *The bilinear form $a(\cdot,\cdot)$ is almost uniformly V_h-elliptic, there holds:*

$$a(v,v) \gtrsim \underline{D} |\log(\underline{h}/D)|^{-1} \|v\|^2_{H^{1/2}(\mathcal{T})} \qquad \forall v \in V_h, \tag{4.20}$$

and

$$a(v,v) \gtrsim \underline{D}^{1/2} |\log(\underline{h}/D)|^{-1/2} \|v\|_{H^{1/2}(\mathcal{T})} \|\operatorname{\mathbf{curl}}_{\mathrm{H}} v\|_{\tilde{\mathbf{H}}_t^{-1/2}(\Gamma)} \qquad \forall v \in V_h. \tag{4.21}$$

Proof. As in the proof of Lemma 4.6 we note that for $v \in V_h \subset L^2(\Gamma)$ there holds

$$\langle V \, \mathbf{curl}_{\mathrm{H}} \, v, \mathbf{curl}_{\mathrm{H}} \, v \rangle_{\mathcal{T}} = \langle V \, \mathbf{curl}_{\mathrm{H}} \, v, \mathbf{curl}_{\mathrm{H}} \, v \rangle_{\Gamma}.$$

Now for $v \in V_h$ we have the following using the ellipticity of $V : \tilde{\boldsymbol{H}}_t^{-\frac{1}{2}}(\Gamma) \to \boldsymbol{H}_t^{\frac{1}{2}}(\Gamma)$ and Lemma 4.9

$$\begin{aligned} a(v,v) &= \langle V \, \mathbf{curl}_{\mathrm{H}} \, v, \mathbf{curl}_{\mathrm{H}} \, v \rangle_{\Gamma} \\ &\gtrsim \| \, \mathbf{curl}_{\mathrm{H}} \, v \|^2_{\tilde{\boldsymbol{H}}_t^{-1/2}(\Gamma)} \\ &\gtrsim \underline{D} |\log(\underline{h}/D)|^{-1} \|v\|^2_{H^{1/2}(\mathcal{T})}. \end{aligned}$$

Which gives (4.20). The estimate (4.21) is obtained by bounding $\| \, \mathbf{curl}_{\mathrm{H}} \, v \|_{\tilde{\boldsymbol{H}}_t^{-1/2}(\Gamma)}$ only once with Lemma 4.9. □

In order to achieve a Strang-type error estimate (see Lemma 2.6) we shall need to extend functions from interfaces onto sub-domains (see Lemma 2.14 for the mortar FEM). This shall also be required in the proof of the inf-sup condition. We now define extension operators that extend piecewise linear functions from interface edges to piecewise (bi)linear functions on the corresponding Lagrangian sub-domain.

$$E_l : X_{h,l_{\mathrm{lag}}}|_{\bar{\gamma}_l} \to X_{h,l_{\mathrm{lag}}}, \quad l = 1, \ldots, L. \tag{4.22}$$

Here for $v \in X_{h,l_{\mathrm{lag}}}|_{\bar{\gamma}_l}$, the extension $E_l v$ is the function of $X_{h,l_{\mathrm{lag}}}$ that coincides with v in the nodes on $\bar{\gamma}_l$ from the mesh $\mathcal{T}_{l_{\mathrm{lag}}}$ and is zero in the remaining nodes of $\mathcal{T}_{l_{\mathrm{lag}}}$.

Lemma 4.11. *For all $v \in X_{h,l_{\mathrm{lag}}}|_{\bar{\gamma}_l}$, and for all $s \in [0,1]$, $l = 1, \ldots, L$*

$$\|E_l v\|_{H^s(\Gamma_{l_{\mathrm{lag}}})} \lesssim D_{l_{\mathrm{lag}}}^{1/2} (h_{l_{\mathrm{lag}}}/D_{l_{\mathrm{lag}}})^{1/2-s} \|v\|_{L^2(\gamma_l)}.$$

In particular the appearing constant is independent of s.

Proof. Using the equivalence of norms in finite dimensional spaces and scaling properties of the L^2-norm one obtains, by taking into account the construction of E_l and using (2.47),

$$\begin{aligned} \|E_l v\|^2_{L^2(\Gamma_{l_{\mathrm{lag}}})} &\lesssim D^2_{l_{\mathrm{lag}}} \|\widehat{E_l v}\|^2_{L^2(\hat{\Gamma}_{l_{\mathrm{lag}}})} \\ &\lesssim D^2_{l_{\mathrm{lag}}} (h_{l_{\mathrm{lag}}}/D_{l_{\mathrm{lag}}}) \|\hat{v}\|^2_{L^2(\hat{\gamma}_l)} \\ &\lesssim D^2_{l_{\mathrm{lag}}} (h_{l_{\mathrm{lag}}}/D_{l_{\mathrm{lag}}}) K_l^{-1} \|v\|^2_{L^2(\gamma_l)} \\ &\lesssim D_{l_{\mathrm{lag}}} (h_{l_{\mathrm{lag}}}/D_{l_{\mathrm{lag}}}) \|v\|^2_{L^2(\gamma_l)} \quad \forall v \in X_{h,l_{\mathrm{lag}}}|_{\bar{\gamma}_l}. \end{aligned} \tag{4.23}$$

In the above we have used that the interface γ_l (of length K_l) is a whole edge of the sub-domain $\Gamma_{l_{\mathrm{lag}}}$ and thus has length proportional to $D_{l_{\mathrm{lag}}}$. Analogously we find using (2.47)

$$|E_l v|^2_{H^1(\Gamma_{l_{\mathrm{lag}}})} \lesssim |\widehat{E_l v}|^2_{H^1(\hat{\Gamma}_{l_{\mathrm{lag}}})}$$

$$\begin{aligned} &\lesssim (h_{l_{\text{lag}}}/D_{l_{\text{lag}}})^{-1}|\hat{v}|^2_{H^1(\hat{\gamma}_l)} \\ &\lesssim (h_{l_{\text{lag}}}/D_{l_{\text{lag}}})^{-1}K_l|v|^2_{H^1(\gamma_l)} \\ &\lesssim D_{l_{\text{lag}}}(h_{l_{\text{lag}}}/D_{l_{\text{lag}}})^{-1}|v|^2_{H^1(\gamma_l)} \quad \forall v \in X_{h,l_{\text{lag}}}|_{\bar{\gamma}_l}. \end{aligned} \tag{4.24}$$

We can now show by combining (4.23) and (4.24) that

$$\begin{aligned} \|E_l v\|^2_{H^1(\Gamma_{l_{\text{lag}}})} &= \|E_l v\|^2_{L^2(\Gamma_{l_{\text{lag}}})} + |E_l v|^2_{H^1(\Gamma_{l_{\text{lag}}})} \\ &\lesssim D_{l_{\text{lag}}}\Big((h_{l_{\text{lag}}}/D_{l_{\text{lag}}})\|v\|^2_{L^2(\gamma_l)} + (h_{l_{\text{lag}}}/D_{l_{\text{lag}}})^{-1}|v|^2_{H^1(\gamma_l)}\Big) \\ &\lesssim D_{l_{\text{lag}}}(h_{l_{\text{lag}}}/D_{l_{\text{lag}}})^{-1}\|v\|^2_{H^1(\gamma_l)} \quad \forall v \in X_{h,l_{\text{lag}}}|_{\bar{\gamma}_l}. \end{aligned} \tag{4.25}$$

The result then follows by interpolation between (4.23) and (4.25). □

Inf-sup condition

Lemma 4.12. *The bilinear form $b(\cdot,\cdot)$ satisfies the discrete inf-sup condition:*

$$\exists \beta > 0 : \quad \sup_{v \in X_h} \frac{b(v,\mu)}{\|v\|_{H^{1/2}(\mathcal{T})}} \geq \beta \|\mu\|_{L^2(\gamma)} \quad \forall \mu \in M_k.$$

Proof. Let $\mu \in M_k$ be given. On each interface edge γ_l, μ is a piecewise constant function on $\mathcal{G}_l$, a mesh that is coarser than the trace mesh $\mathcal{T}_{l_{\text{lag}}}|_{\bar{\gamma}_l}$ stemming from the Lagrangian multiplier side $\Gamma_{l_{\text{lag}}}$, cf. Assumption 4.5. On γ_l we construct a piecewise linear function $w_l \in X_{h,l_{\text{lag}}}|_{\gamma_l}$ in the following way. For each element $J \in \mathcal{G}_l$, w_l vanishes at the endpoints of J, coincides with μ at one interior node of J and is linearly interpolated elsewhere on γ_l. See Figure 4.6 for an example where μ is represented by the dashed line and w_l by the solid line. The bullets indicate the nodes of the mesh for the Lagrangian multiplier and the dashes indicate additional nodes of the trace mesh (from the Lagrangian multiplier side).

We then extend w_l to $\tilde{w}_l$ in X_h by first extending to $E_l w_l \in X_{h,l_{\text{lag}}}$ (cf. (4.22)) and then further by zero onto Γ. Eventually we define $v := \sum_{l=1}^{L} \tilde{w}_l$.

Note that $\tilde{w}_l$ vanishes on all interface edges except γ_l. The trace of $\tilde{w}_l$ onto γ_l from $\Gamma_{l_{\text{lag}}}$ equals w_l whereas the trace coming from the other side $\Gamma_{l_{\text{mor}}}$ vanishes. This yields

$$[v] = [\tilde{w}_l] = w_l \quad \text{on} \quad \gamma_l, \qquad l = 1, \ldots, L. \tag{4.26}$$

By the construction of w_l there holds, uniformly for $\mu \in M_k$,

$$\|\mu\|^2_{L^2(\gamma_l)} \simeq \langle w_l, \mu \rangle_{\gamma_l} \simeq \|w_l\|^2_{L^2(\gamma_l)}, \quad l = 1, \ldots, L. \tag{4.27}$$

Also, taking into account that each sub-domain Γ_i has a limited number of (interface) edges, determined by the relation $l \in \{1, \ldots, L\} : \; l_{\text{lag}} = i$, Lemma 4.11 yields

$$\begin{aligned} \|v\|^2_{H^{1/2}(\mathcal{T})} &= \sum_{i=1}^{N} \Big\| \sum_{l\in\{1,\ldots,L\}:\, l_{\text{lag}}=i} E_l w_l \Big\|^2_{H^{1/2}(\Gamma_i)} \\ &\lesssim \sum_{i=1}^{N} \sum_{l\in\{1,\ldots,L\}:\, l_{\text{lag}}=i} \|E_l w_l\|^2_{H^{1/2}(\Gamma_i)} \\ &= \sum_{l=1}^{L} \|E_l w_l\|^2_{H^{1/2}(\Gamma_{l_{\text{lag}}})} \lesssim \sum_{l=1}^{L} \|w_l\|^2_{L^2(\gamma_l)}. \end{aligned} \tag{4.28}$$

Now, using (4.26), (4.27) and (4.28), we finish the proof by bounding

$$b(v,\mu) = \sum_{l=1}^{L} \langle [v], \mu\rangle_{\gamma_l} = \sum_{l=1}^{L} \langle w_l, \mu\rangle_{\gamma_l} \simeq \|\mu\|_{L^2(\gamma)} \Big(\sum_{l=1}^{L} \|w_l\|^2_{L^2(\gamma_l)} \Big)^{1/2} \gtrsim \|\mu\|_{L^2(\gamma)} \|v\|_{H^{1/2}(\mathcal{T})}.$$

□

(a) (b)

Figure 4.6: Construction of w_l in the proof of Lemma 4.12.

Lemma 4.13. *For all $v \in X_h$ there holds*

$$\|[v]\|^2_{L^2(\gamma)} \lesssim \underline{D}^{-1} |\log(\underline{h}/D)| \|v\|^2_{H^{1/2}(\mathcal{T})}.$$

Proof. By the triangle inequality and Lemma 2.22 there holds uniformly for $\epsilon \in (0, 1/2)$

and for any $v \in X_h$, using (2.52) and noting that K_l is proportional to $D_{l_{\text{lag}}}$

$$\begin{aligned}
\|[v]\|^2_{L^2(\gamma)} &\lesssim \sum_{l=1}^{L} K_l \left(\|\hat{v}_{l_{\text{lag}}}\|^2_{L^2(\widehat{\gamma}_l)} + \|\hat{v}_{l_{\text{mor}}}\|^2_{L^2(\widehat{\gamma}_l)} \right) \\
&\lesssim \epsilon^{-1} \sum_{l=1}^{L} K_l \left(\|\hat{v}_{l_{\text{lag}}}\|^2_{H^{1/2+\epsilon}(\widehat{\Gamma}_{l_{\text{lag}}})} + \|\hat{v}_{l_{\text{mor}}}\|^2_{H^{1/2+\epsilon}(\widehat{\Gamma}_{l_{\text{mor}}})} \right) \\
&\lesssim \epsilon^{-1} \sum_{i=1}^{n} D_i \|\hat{v}_i\|^2_{H^{1/2+\epsilon}(\widehat{\Gamma}_i)} \quad \forall v \in X_h.
\end{aligned}$$

The inverse property, applied separately to $v_i = v|_{\Gamma_i}$, yields

$$\begin{aligned}
\sum_{i=1}^{n} \|\hat{v}_i\|^2_{H^{1/2+\epsilon}(\widehat{\Gamma}_i)} &\lesssim \sum_{i=1}^{n} (h_i/D_i)^{-2\epsilon} \|\hat{v}_i\|^2_{H^{1/2}(\widehat{\Gamma}_i)} \\
&\lesssim \underline{D}^{-2} (\underline{h}/D)^{-2\epsilon} \|v\|^2_{H^{1/2}(\mathcal{T})} \quad \forall v \in X_h,
\end{aligned}$$

by an application of (2.48). Selecting $\epsilon = |\log(\underline{h}/D)|^{-1}$ (for $(\underline{h}/D)$ being small enough) finishes the proof. □

Continuity of $b(\cdot,\cdot)$

Lemma 4.14. *The bilinear form $b(\cdot,\cdot)$ is almost uniformly discretely continuous, in the sense that*

$$b(v,\mu) \lesssim \underline{D}^{-1/2} |\log(\underline{h}/D)|^{1/2} \|v\|_{H^{1/2}(\mathcal{T})} \|\mu\|_{L^2(\gamma)} \quad \forall v \in X_h, \forall \mu \in M_k. \tag{4.29}$$

Let $\psi \in L^2(\gamma)$ be given. Then there holds

$$b(v,\psi) \lesssim \underline{D}^{-1} |\log(\underline{h}/D)| \inf_{\mu \in M_k} \|\psi - \mu\|_{L^2(\gamma)} \|\, \mathbf{curl}_{\mathrm{H}}\, v\|_{\tilde{\boldsymbol{H}}_t^{-1/2}(\Gamma)} \quad \forall v \in V_h. \tag{4.30}$$

Proof. There holds

$$b(v,\mu) = \sum_{l=1}^{L} \langle [v], \mu \rangle_{\gamma_l} \leq \|[v]\|_{L^2(\gamma)} \|\mu\|_{L^2(\gamma)} \quad \forall v \in X_h, \forall \mu \in M_k.$$

Estimate (4.29) follows with the help of Lemma 4.13. To prove (4.30) we start as before and note that by definition of V_h there holds $b(v,\mu) = 0\ \forall \mu \in M_k$, $\forall v \in V_h$. Therefore, for any $\mu \in M_k$ and $v \in V_h$, we find that for $\psi \in L^2(\gamma)$

$$b(v,\psi) \leq \|[v]\|_{L^2(\gamma)} \|\psi - \mu\|_{L^2(\gamma)}. \tag{4.31}$$

The proof of (4.30) is finished by noting that combination of Lemmas 4.13 and 4.9 yields

$$\|[v]\|_{L^2(\gamma)} \lesssim \underline{D}^{-1/2} |\log(\underline{h}/D)|^{1/2} \|v\|_{H^{1/2}(\mathcal{T})} \lesssim \underline{D}^{-1} |\log(\underline{h}/D)| \, \|\, \mathbf{curl}_{\mathrm{H}}\, v\|_{\tilde{\boldsymbol{H}}_{\mathrm{t}}^{-1/2}(\Gamma)} \quad \forall v \in V_h.$$

□

Existence and uniqueness

We are now ready to prove the following Strang-type error estimate.

Theorem 4.15. *The system (4.11) is uniquely solvable. For $\phi \in \tilde{H}^{1/2+r}(\Gamma)$, $r \in (0, 1/2]$, being the solution of (4.2), and $\phi_h \in X_h$ being the solution of (4.11) there holds*

$$\|\phi - \phi_h\|_{H^{1/2}(\mathcal{T})} \lesssim \quad \underline{D}^{-2} |\log(\underline{h}/D)|^{1/2} \left(s^{-1} \inf_{v \in V_h} \|\phi - v\|_{H^{1/2+s}(\mathcal{T})} + \sup_{w \in V_h \setminus \{0\}} \frac{|a(\phi - \phi_h, w)|}{\|\mathbf{curl}_{\mathrm{H}}\, w\|_{\tilde{\boldsymbol{H}}_t^{-1/2}(\Gamma)}} \right)$$

uniformly for $s \in (0, r]$.

Proof. The existence and uniqueness of $(\phi_h, \lambda_k) \in X_h \times M_k$ follows from the Babuška-Brezzi theory (see Section 2.2.4). Indeed, the bilinear form $a(\cdot, \cdot)$ is continuous on X_h by Lemma 4.6 and V_h-elliptic by Lemma 4.10, and the bilinear form $b(\cdot, \cdot)$ is continuous on $X_h \times M_k$ by (4.29) and satisfies a discrete inf-sup condition by Lemma 4.12. The continuity and ellipticity bounds depend on h and D but that does not influence the unique solvability of the discrete scheme.

The error estimate (c.f., Lemma 2.6) is obtained by the usual steps. Combining (2.49), the triangle inequality, (2.48), the non-standard ellipticity and continuity properties of $a(\cdot, \cdot)$ (cf. (4.21) and Lemma 4.7) we obtain for any $v \in V_h$

$$\begin{aligned}
\|\phi - \phi_h\|_{H^{1/2}(\mathcal{T})} &\leq \underline{D}^{-1/2} \left\{ \|\phi - v\|_{H^{1/2}(\mathcal{T})} + \|v - \phi_h\|_{H^{1/2}(\mathcal{T})} \right\} \\
&\lesssim \underline{D}^{-1/2} \left\{ \|\phi - v\|_{H^{1/2}(\mathcal{T})} + \underline{D}^{-1/2} |\log(\underline{h}/D)|^{1/2} \sup_{w \in V_h \setminus \{0\}} \frac{a(v - \phi_h, w)}{\|\mathbf{curl}_{\mathrm{H}}\, w\|_{\tilde{\boldsymbol{H}}_{\mathrm{t}}^{-1/2}(\Gamma)}} \right\} \\
&\leq \underline{D}^{-1/2} \left\{ \|\phi - v\|_{H^{1/2}(\mathcal{T})} + \underline{D}^{-1/2} |\log(\underline{h}/D)|^{1/2} \left(\sup_{w \in V_h \setminus \{0\}} \frac{a(v - \phi, w)}{\|\mathbf{curl}_{\mathrm{H}}\, w\|_{\tilde{\boldsymbol{H}}_{\mathrm{t}}^{-1/2}(\Gamma)}} \right. \right. \\
&\qquad \left. \left. + \sup_{w \in V_h \setminus \{0\}} \frac{a(\phi - \phi_h, w)}{\|\mathbf{curl}_{\mathrm{H}}\, w\|_{\tilde{\boldsymbol{H}}_{\mathrm{t}}^{-1/2}(\Gamma)}} \right) \right\} \\
&\lesssim \underline{D}^{-1/2} \left\{ \underline{D}^{-1/2} \|\phi - v\|_{H^{1/2}(\mathcal{T})} + s^{-1} \underline{D}^{-3/2} |\log(\underline{h}/D)|^{1/2} \|\phi - v\|_{H^{1/2+s}(\mathcal{T})} \right. \\
&\qquad \left. + \underline{D}^{-1/2} |\log(\underline{h}/D)|^{1/2} \sup_{w \in V_h \setminus \{0\}} \frac{a(\phi - \phi_h, w)}{\|\mathbf{curl}_{\mathrm{H}}\, w\|_{\tilde{\boldsymbol{H}}_{\mathrm{t}}^{-1/2}(\Gamma)}} \right\}.
\end{aligned}$$

This proves the stated error bound. □

In order to analyse the upper bound provided by Theorem 4.15 we need, in addition to the extension operators E_l defined before (in (4.22)), projection operators which have particular properties (see Lemma 2.13 for the mortar FEM situation). Let us define projection operators π_l acting on $L^2(\gamma_l)$ and mapping onto special continuous, piecewise linear functions on γ_l, $l = 1, \ldots, L$. We recall that on each γ_l we have two meshes: the trace mesh $\mathcal{T}_{l_{\text{lag}}}|_{\gamma_l}$ stemming from the mesh on the sub-domain $\Gamma_{l_{\text{lag}}}$ of the Lagrangian side, and the mesh $\mathcal{G}_l$ for the Lagrangian multiplier. For each element $J \in \mathcal{G}_l$ we consider a hat function $\phi_{l,J}$ that vanishes at the endpoints of J and has the tip at a node of $\mathcal{T}_{l_{\text{lag}}}|_{\gamma_l}$ that is interior to J. This choice is not unique if J contains more than two elements of the trace mesh. In that case we select an arbitrary but fixed node for the definition of $\phi_{l,J}$. Using this notation we define

$$\pi_l : \; L^2(\gamma_l) \to \operatorname{span}\{\phi_{l,J};\; J \in \mathcal{G}_l\} \subset X_{h,l_{\text{lag}}}, \quad l = 1, \ldots, L, \tag{4.32}$$

such that the integral mean zero conditions

$$\langle v - \pi_l v, 1\rangle_J = 0 \quad \forall J \in \mathcal{G}_l,\; l = 1, \ldots, L$$

hold. This operator satisfies the following properties:

Lemma 4.16. *For any $v \in L^2(\gamma_l)$, $\pi_l v$ vanishes at the endpoints of γ_l, $l = 1, \ldots, L$, and there holds*

$$\langle v - \pi_l v, \mu\rangle_{\gamma_l} = 0 \quad \forall v \in L^2(\gamma_l),\; \forall \mu \in M_{k,l}, \quad l = 1, \ldots, L, \tag{4.33}$$

$$\|\pi_l v\|_{L^2(\gamma_l)} \lesssim \|v\|_{L^2(\gamma_l)} \quad \forall v \in L^2(\gamma_l),\; l = 1, \ldots, L. \tag{4.34}$$

Proof. For $l \in \{1, \ldots, L\}$ let $v \in L^2(\gamma_l)$ be given. By definition of π_l, $\pi_l v$ vanishes at the endpoints of γ_l, and the orthogonality (4.33) follows by noting that any $\mu \in M_{k,l}$ is constant on any $J \in \mathcal{G}_l$.

To show (4.34) let $J \in \mathcal{G}_l$ be given. With $\phi_{l,J}$ being the hat function defined previously (with height 1) there holds

$$\pi_l v = \frac{2}{|J|}\Big(\int_J v\, ds\Big)\; \phi_{l,J} \quad \text{on} \quad J$$

so that

$$\|\pi_l v\|^2_{L^2(J)} = \frac{4}{3|J|}\Big(\int_J v\, ds\Big)^2 \le \frac{4}{3}\|v\|^2_{L^2(J)}.$$

Summing over $J \in \mathcal{G}_l$ finishes the proof. □

We are now ready to analyse the first term of the upper bounds provided by Theorem 4.15.

Lemma 4.17. *For $r \in (0, 1/2]$ let $\phi \in H^{1/2+r}(\Gamma)$. There holds*

$$\begin{aligned}\inf_{v\in V_h} \|\phi - v\|^2_{H^{1/2+s}(\mathcal{T})} \;\lesssim\; & \underline{D}^{-1-2s} \Big\{ \|\phi - w\|^2_{H^{1/2+s}(\mathcal{T})} \\ & + \sum_{l=1}^{L} D_{l_{\rm lag}} (h_{l_{\rm lag}}/D_{l_{\rm lag}})^{-2s} \Big(\|\phi - w_{l_{\rm lag}}\|^2_{L^2(\gamma_l)} \\ & + \|\phi - w_{l_{\rm mor}}\|^2_{L^2(\gamma_l)} \Big) \Big\} \quad \forall w \in X_h\end{aligned}$$

uniformly for $s \in (0, r]$.

Proof. Let $w \in X_h$ be given. We adapt w such that the new function satisfies the jump conditions defining V_h, cf. (4.13). We set

$$v := w + \sum_{l=1}^{L} r^l \in X_h$$

with

$$r^l := \begin{cases} E_l \pi_l (w_{l_{\rm lag}}|_{\gamma_l} - w_{l_{\rm mor}}|_{\gamma_l}) & \text{on } \bar\Gamma_{l_{\rm lag}}, \\ 0 & \text{elsewhere.} \end{cases}$$

Here, E_l and π_l are the extension and projection operators specified in (4.22) and (4.32), respectively. Note that, since $\pi_l(w_{l_{\rm lag}}|_{\gamma_l} - w_{l_{\rm mor}}|_{\gamma_l})$ vanishes at the endpoints of γ_l, the extension $E_l\pi_l(w_{l_{\rm lag}}|_{\gamma_l} - w_{l_{\rm mor}}|_{\gamma_l})$ vanishes on $\partial\Gamma_{l_{\rm lag}} \setminus \gamma_l$. Therefore, using (4.33) one immediately obtains

$$\begin{aligned}\langle [v], \mu\rangle_{\gamma_l} &= \langle v_{l_{\rm lag}} - v_{l_{\rm mor}}, \mu\rangle_{\gamma_l} = \langle w_{l_{\rm lag}} + r^l - w_{l_{\rm mor}}, \mu\rangle_{\gamma_l} \\ &= \langle w_{l_{\rm lag}} - w_{l_{\rm mor}} + \pi_l(w_{l_{\rm lag}}|_{\gamma_l} - w_{l_{\rm mor}}|_{\gamma_l}), \mu\rangle_{\gamma_l} = 0 \qquad \forall \mu \in M_{k,l},\ l = 1, \dots, L.\end{aligned}$$

That is, $v \in V_h$. We start bounding the error by using (2.49), the triangle inequality and (2.48)

$$\begin{aligned}\|\phi - v\|^2_{H^{1/2+s}(\mathcal{T})} &= \sum_{i=1}^{N} \Big\| \phi_i - w_i - \sum_{l\in\{1,\dots,L\}:\, l_{\rm lag}=i} r^l \Big\|^2_{H^{1/2+s}(\Gamma_i)} \\ &\lesssim \underline{D}^{-1-2s} \left\{ \sum_{i=1}^{N} \|\phi_i - w_i\|^2_{H^{1/2+s}(\Gamma_i)} + \sum_{l=1}^{L} \|r^l\|^2_{H^{1/2+s}(\Gamma_{l_{\rm lag}})} \right\}. \quad (4.35)\end{aligned}$$

Applying Lemma 4.11, (4.34) and the triangle inequality we find that there holds

$$\|r^l\|_{H^{1/2+s}(\Gamma_{l_{\rm lag}})} \;\lesssim\; D^{1/2}_{l_{\rm lag}} (h_{l_{\rm lag}}/D_{l_{\rm lag}})^{-s} \|\pi_l(w_{l_{\rm lag}}|_{\gamma_l} - w_{l_{\rm mor}}|_{\gamma_l})\|_{L^2(\gamma_l)}$$

$$\begin{aligned} &\lesssim D_{l_{\mathrm{lag}}}^{1/2}(h_{l_{\mathrm{lag}}}/D_{l_{\mathrm{lag}}})^{-s}\|w_{l_{\mathrm{lag}}}-w_{l_{\mathrm{mor}}}\|_{L^2(\gamma_l)} \\ &\lesssim D_{l_{\mathrm{lag}}}^{1/2}(h_{l_{\mathrm{lag}}}/D_{l_{\mathrm{lag}}})^{-s}\Big(\|\phi-w_{l_{\mathrm{lag}}}\|_{L^2(\gamma_l)}+\|\phi-w_{l_{\mathrm{mor}}}\|_{L^2(\gamma_l)}\Big). \quad (4.36)\end{aligned}$$

Combining (4.35) and (4.36) one obtains the assertion. □

Error estimate

The next result proves an a-priori error estimate for the mortar BEM.

Theorem 4.18. *Let ϕ and ϕ_h be the solutions of* (4.2) *and* (4.11)*, respectively. Assuming that $\phi \in \tilde{H}^{1/2+r}(\Gamma)$ ($r \in (0,1/2]$) there holds $\lambda \in \prod_{l=1}^{L} H^r(\gamma_l)$ and we have the a priori error estimate*

$$\begin{aligned}\|\phi-\phi_h\|_{H^{1/2}(\mathcal{T})}^2 \lesssim\ & s^{-2}\underline{D}^{-5-2s}|\log(\underline{h}/D)|\Bigg(\|\phi-v\|_{H^{1/2+s}(\mathcal{T})}^2 \\ &+D(\underline{h}/D)^{-2s}\sum_{l=1}^{L}\Big(\|\phi-v_{l_{\mathrm{lag}}}\|_{L^2(\gamma_l)}^2+\|\phi-v_{l_{\mathrm{mor}}}\|_{L^2(\gamma_l)}^2\Big)\Bigg) \\ &+\underline{D}^{-6}|\log(\underline{h}/D)|^3\,\|\lambda-\mu\|_{L^2(\gamma)}^2 \qquad \forall v\in X_h,\ \forall \mu\in M_k\end{aligned}$$

uniformly for $s \in (0,r]$. Here, λ is the Lagrangian multiplier defined by (4.4) and (4.5)*.*

Proof. Since $\phi \in \tilde{H}^{1/2+r}(\Gamma)$ there holds

$$\lambda|_{\gamma_l} = \mathbf{t}_{l_{\mathrm{lag}}} \cdot (V\,\mathbf{curl}_\Gamma\,\phi)|_{\gamma_l} \in H^r(\gamma_l), \quad l=1,\dots,L.$$

To this end note that $\mathbf{curl}_\Gamma : \tilde{H}^{1/2+r}(\Gamma) \to \tilde{\boldsymbol{H}}_{\mathrm{t}}^{r-1/2}(\Gamma)$ (combine Lemma 2.17 with the continuity $\mathbf{curl}_\Gamma : H_0^1(\Gamma) \to \boldsymbol{L}_{\mathrm{t}}^2(\Gamma)$) and $V : \tilde{\boldsymbol{H}}_{\mathrm{t}}^{r-1/2}(\Gamma) \to \boldsymbol{H}_{\mathrm{t}}^{1/2+r}(\Gamma)$. The trace theorem (Lemma 2.22) concludes the claimed regularity of λ. In particular there holds $\lambda \in L^2(\gamma)$.

By definition of V_h, and making use of Lemma 4.3, we find

$$a(\phi-\phi_h,w) = a(\phi,w) - F(w) = b(w,\lambda) \quad \forall w \in V_h.$$

Application of (4.30) yields

$$a(\phi-\phi_h,w) \lesssim \underline{D}^{-1}|\log(\underline{h}/D)| \inf_{\mu\in M_k}\|\lambda-\mu\|_{L^2(\gamma)}\|\,\mathbf{curl}_{\mathrm{H}}\,w\|_{\tilde{\boldsymbol{H}}_{\mathrm{t}}^{-1/2}(\Gamma)} \quad \forall w\in V_h.$$

Therefore, combining Theorem 4.15 with Lemma 4.17 we obtain

$$\begin{aligned}\|\phi-\phi_h\|^2_{H^{1/2}(\mathcal{T})} \lesssim\ & \underline{D}^{-4}|\log(\underline{h}/D)|\Bigg\{s^{-2}\underline{D}^{-1-2s}\Bigg(\|\phi-v\|^2_{H^{1/2+s}(\mathcal{T})} \\ & +\sum_{l=1}^{L} D_{l_{\mathrm{lag}}}(h_{l_{\mathrm{lag}}}/D_{l_{\mathrm{lag}}})^{-2s}\Big(\|\phi-v_{l_{\mathrm{lag}}}\|^2_{L^2(\gamma_l)}+\|\phi-v_{l_{\mathrm{mor}}}\|^2_{L^2(\gamma_l)}\Big)\Bigg) \\ & +\underline{D}^{-2}|\log(\underline{h}/D)|^2\,\|\lambda-\mu\|^2_{L^2(\gamma)}\Bigg\} \qquad \forall v\in X_h,\ \forall \mu\in M_k.\end{aligned}$$

This proves the statement. □

Main result

The following theorem is the main result concerning the mortar BEM.

Theorem 4.19. *There exists a unique solution (ϕ_h,λ_k) of (4.11). Assume that the solution ϕ of (4.2) satisfies $\phi\in\tilde{H}^{1/2+r}(\Gamma)$ ($r\in(0,1/2]$). Then there holds*

$$\|\phi-\phi_h\|_{H^{1/2}(\mathcal{T})}\lesssim \underline{D}^{-4}(|\log(\underline{h}/D)|^2(h/\underline{D})^r+\underline{D}^{-3}|\log(\underline{h}/D)|^{3/2}(k/\underline{K})^r)\|\phi\|_{\tilde{H}^{1/2+r}(\Gamma)}.$$

For proportional mesh sizes h and k this means that

$$\|\phi-\phi_h\|_{H^{1/2}(\mathcal{T})}\lesssim \underline{D}^{-4}|\log(\underline{h}/D)|^2(h/\underline{D})^r\|\phi\|_{\tilde{H}^{1/2+r}(\Gamma)}.$$

Proof. By Theorem 4.15 the system (4.11) is uniquely solvable. We employ the general a priori estimate by Theorem 4.18 to show the given error bound. By standard approximation theory there exist $v\in X_h$ and $\mu\in M_k$ such that (using (2.49) and (2.48))

$$\begin{aligned}\sum_{i=1}^{n}\|\phi_i-v_i\|^2_{H^{1/2+s}(\Gamma_i)} &\lesssim \sum_{i=1}^{n} D_i^{1-2s}\|\hat{\phi}_i-\hat{v}_i\|^2_{H^{1/2+s}(\widehat{\Gamma}_i)} \\ &\lesssim \sum_{i=1}^{n} D_i^{1-2s}(h_i/D_i)^{2(r-s)}\|\hat{\phi}_i\|^2_{H^{1/2+r}(\widehat{\Gamma}_i)} \\ &\lesssim \sum_{i=1}^{n} D_i^{1-2s}(h_i/D_i)^{2(r-s)}D_i^{-2}\|\phi_i\|^2_{H^{1/2+r}(\Gamma_i)} \\ &\lesssim \underline{D}^{-1-2s}(h/\underline{D})^{2(r-s)}\|\phi\|^2_{\tilde{H}^{1/2+r}(\Gamma)} \\ &\lesssim \underline{D}^{-2}(h/\underline{D})^{2(r-s)}\|\phi\|^2_{\tilde{H}^{1/2+r}(\Gamma)}, \qquad (4.37)\end{aligned}$$

and (using (2.52) and (2.51))

$$\begin{aligned}\|\lambda-\mu\|^2_{L^2(\gamma)} &\lesssim \sum_{l=1}^{L} K_l\|\hat\lambda-\hat\mu\|^2_{L^2(\widehat\gamma_l)}\\ &\lesssim \sum_{l=1}^{L} K_l(k_l/K_l)^{2r}\|\hat\lambda\|^2_{H^r(\widehat\gamma_l)}\\ &\lesssim \sum_{l=1}^{L} K_l(k_l/K_l)^{2r}K_l^{-1}\|\lambda\|^2_{H^r(\gamma_l)}\\ &\lesssim \sum_{l=1}^{L}(k_l/K_l)^{2r}\|\lambda\|^2_{H^r(\gamma_l)}, \end{aligned}\tag{4.38}$$

and as in the proof of Theorem 4.18 we conclude that $\sum_{l=1}^{L}\|\lambda\|^2_{H^r(\gamma_l)}\lesssim\|\phi\|^2_{\tilde H^{1/2+r}(\Gamma)}$. By Lemma 2.22 we bound (recalling that K_l is proportional to $D_{l_{\rm lag}}$)

$$\begin{aligned}\|\phi-v_{l_{\rm lag}}\|_{L^2(\gamma_l)} &\lesssim K_l^{1/2}\|\hat\phi-\hat v_{l_{\rm lag}}\|_{L^2(\widehat\gamma_l)}\\ &\lesssim K_l^{1/2}s^{-1/2}\|\hat\phi-\hat v\|_{H^{1/2+s}(\widehat\Gamma_{l_{\rm lag}})}\\ &\lesssim K_l^{1/2}s^{-1/2}(h_{l_{\rm lag}}/D_{l_{\rm lag}})^{r-s}\|\hat\phi\|_{H^{1/2+r}(\widehat\Gamma_{l_{\rm lag}})}\\ &\lesssim K_l^{1/2}s^{-1/2}(h_{l_{\rm lag}}/D_{l_{\rm lag}})^{r-s}D_{l_{\rm lag}}^{-1}\|\phi\|_{H^{1/2+r}(\Gamma_{l_{\rm lag}})}\\ &\lesssim D_{l_{\rm lag}}^{-1/2}s^{-1/2}(h_{l_{\rm lag}}/D_{l_{\rm lag}})^{r-s}\|\phi\|_{H^{1/2+r}(\Gamma_{l_{\rm lag}})}, \end{aligned}\tag{4.39}$$

and accordingly the mortar part $\|\phi-v_{l_{\rm mor}}\|_{L^2(\gamma_l)}$. Since $\tilde H^{1/2+r}(\Gamma)\subset H^{1/2+r}(\Gamma)$ we have that

$$\sum_{l=1}^{L}\|\phi\|^2_{H^{1/2+r}(\Gamma_{l_{\rm lag}})}\lesssim\|\phi\|^2_{H^{1/2+r}(\mathcal{T})}\lesssim\|\phi\|^2_{\tilde H^{1/2+r}(\Gamma)}.$$

Using these bounds in Theorem 4.18 and selecting $s=|\log(\underline{h}/D)|^{-1}$ we obtain the assertion. □

Remark 4.20. As in Remark 3.8 we note that, in our case of an open surface Γ, the solution ϕ of (4.1) has strong corner and corner-edge singularities which cannot be exactly described by standard Sobolev regularity. It is well-known that $\phi\in\tilde H^r(\Gamma)$ for any $r<1$ (see, e.g., [55]) so that the error estimate by Theorem 4.19 holds for any $r<1/2$. In general $\phi\notin H^1_0(\Gamma)$ but a more specific error analysis for the conforming BEM yields for quasi-uniform meshes the optimal error estimate

$$\|\phi-\phi_h\|_{\tilde H^{1/2}(\Gamma)}\lesssim h^{1/2},$$

see [8]. The logarithmical perturbations in $\underline{h}$ and D of our error estimate are due to the non-conformity of the mortar method. They stem from the non-existence of a trace operator within $H^{1/2}(\Gamma)$ and from non-local properties of the fractional order Sobolev norms (the difference between $\tilde{H}^{1/2}$ and $H^{1/2}$-spaces).

Remark 4.21. The mortar method may be able to be applied to other BEM boundary conditions provided that certain necessary conditions are met. Firstly an appropriate integration by parts formula involving surface differential operators is required to calculate the necessary interface matching conditions. Next the system would have to satisfy appropriate ellipticity and continuity conditions, including the Babuška-Brezzi condition. Finally suitable projection and extension operators acting on appropriate spaces would have to exist.

Chapter 5

Numerical Results

In this chapter we present numerical results for the BEM with Lagrangian multiplier and the mortar BEM. These results agree with the theory and give the expected rates of convergence. In the mortar BEM situation we consider sequences of meshes which are refined on each individual sub-domain. This means that on each sub-domain the mesh size becomes smaller and smaller, however the decomposition of the whole domain into sub-domains remains fixed. Thus the sub-domain size remains the same throughout each experiment and we are only interested in the effect of the mesh size (on the sub-domains) on the convergence rate of the scheme.

5.1 An Error Estimate

We consider the model problems (3.1) and (4.20) (for the BEM with Lagrangian multiplier and the Mortar BEM respectively) with $\Gamma = (0,1) \times (0,1)$ and $f = 1$. The discretisations for the methods shall be discussed later in the relevant sections. Before proceeding to this we must first discuss the error estimate that is to be presented.

Implementing the scheme (3.5) in the Lagrangian multiplier situation (or (4.2) in the mortar BEM situation) we calculate the approximation $\phi_h \in V_h \subset X_h$ to the exact solution ϕ of (3.1) in the Lagrangian multiplier situation (or (4.1) in the mortar BEM situation). Since ϕ is unknown there is no direct way to calculate the error $\|\phi - \phi_h\|_{H^{1/2}(\Gamma)}$ in the Lagrangian multiplier situation (or $\|\phi - \phi_h\|_{H^{1/2}(\mathcal{T})}$ in the mortar BEM situation). Instead, we approximate an upper bound to the semi-norm $|\phi - \phi_h|_{H^{1/2}(\Gamma)}$ in the Lagrangian multiplier situation (or $|\phi - \phi_h|_{H^{1/2}(\mathcal{T})}$in the mortar BEM situation).

In the following we present the results for $\mathcal{T}$ where $\mathcal{T} = \Gamma$ in the situation of the BEM with Lagrangian multiplier and $\mathcal{T} = \mathcal{T}$ in the Mortar BEM situation. By Lemma 3.5(i) for the BEM with Lagrangian multiplier (or the proof of Lemma 4.9 for the mortar BEM)

there holds

$$a(\phi-\phi_h,\phi-\phi_h)\gtrsim|\phi-\phi_h|^2_{H^{1/2}(\mathcal{T})}. \tag{5.1}$$

Moreover, since ϕ solves (3.1) and ϕ_h solves (3.5) for the BEM with Lagrangian multiplier (or (4.1) and (4.2) for the mortar BEM respectively), we find that there holds

$$\begin{aligned}a(\phi-\phi_h,\phi-\phi_h)&=a(\phi,\phi)-2a(\phi,\phi_h)+a(\phi_h,\phi_h)\\&=\langle W\phi,\phi\rangle_\Gamma-2a(\phi,\phi_h)+F(\phi_h)-b(\phi_h,\lambda_k)\\&=\langle W\phi,\phi\rangle_\Gamma+F(\phi_h)-2a(\phi,\phi_h).\end{aligned}$$

Now for the BEM with Lagrangian multiplier situation we set

$$[\phi_h]=\phi_h|_\gamma,$$

and use the standard jump notation for the mortar BEM (see (4.3)). For the BEM with Lagrangian multiplier, as in (3.11) we can apply (3.4) (or by (4.4) for the mortar BEM) and we obtain

$$a(\phi,\phi_h)=F(\phi_h)-\langle[\phi_h],\lambda\rangle_\gamma.$$

Such that, with the previous relation,

$$a(\phi-\phi_h,\phi-\phi_h)=\langle W\phi,\phi\rangle_\Gamma-F(\phi_h)+2\,\langle[\phi_h],\lambda\rangle_\gamma\le\langle W\phi,\phi\rangle_\Gamma-F(\phi_h)+2\,\|[\phi_h]\|_{L^2(\gamma)}\|\lambda\|_{L^2(\gamma)}. \tag{5.2}$$

As in the proof of Theorem 3.7 for the BEM with Lagrangian multiplier (or Theorem 4.18 for the mortar BEM) we establish that $\|\lambda\|_{L^2(\gamma)}$ is bounded by a constant depending on ϕ. Therefore, by (5.1) we find that

$$|\phi-\phi_h|^2_{H^{1/2}(\mathcal{T})}\lesssim|\langle W\phi,\phi\rangle_\Gamma-F(\phi_h)|+\|[\phi_h]\|_{L^2(\gamma)}.$$

The terms $F(\phi_h)$ and $\|[\phi_h]\|_{L^2(\gamma)}$ can be easily calculated and $\langle W\phi,\phi\rangle_\Gamma$ can be approximated by an extrapolated value that we denote by $\|\phi\|^2_{\mathrm{ex}}$ (cf. [23]). Therefore, instead of the relative error $\|\phi-\phi_h\|_{H^{1/2}(\mathcal{T})}/\|\phi\|_{H^{1/2}(\Gamma)}$, we present results for the expression

$$\Big(|\,\|\phi\|^2_{\mathrm{ex}}-F(\phi_h)|+\|[\phi_h]\|_{L^2(\gamma)}\Big)^{1/2}/\|\phi\|_{\mathrm{ex}}, \tag{5.3}$$

which is, up to a constant factor, an upper bound for $|\phi-\phi_h|_{H^{1/2}(\mathcal{T})}/\|\phi\|_{\mathrm{ex}}$. In the figures below we show different error curves, indicated by numbers (n) $(n=1,\dots,4)$ as follows.

(1) $\Big(|\,\|\phi\|^2_{\mathrm{ex}}-F(\phi_h)|+\|[\phi_h]\|_{L^2(\gamma)}\Big)^{1/2}$ "Total approximation error"

(2) $\Big(|\,\|\phi\|^2_{\mathrm{ex}}-F(\phi_h)|\Big)^{1/2}$ "Part 1 of the error"

(3) $\|[\phi_h]\|^{1/2}_{L^2(\gamma)}$ "Part 2 of the error"

(4) $a(\phi-\tilde{\phi}_h,\phi-\tilde{\phi}_h)^{1/2}$ "Conforming BEM".

Here, $\tilde{\phi}_h$ denotes a conforming boundary element solution. Additionally, all curves are normalized by $\|\phi\|_{\text{ex}}$. Therefore, to resume, an error curve (1) represents the upper bound (5.3) for the (normalized) error $|\phi - \phi_h|_{H^{1/2}(\mathcal{T})}$ of our approximation (BEM with Lagrangian multiplier or mortar BEM). Curves (2) and (3) are the two components of (1). Here, (3) controls the non-conformity of the approximant ϕ_h. Curve (4) represents the error of the conforming BEM. In this case it is equivalent to the error in energy norm $\|\phi - \tilde{\phi}_h\|_{\tilde{H}^{1/2}(\Gamma)}$.

All results are plotted on double logarithmic scales versus $1/h$. For our numerical experiments we always use rectangular meshes for the mortar BEM, h_i refers to the diameter of the longest element on Γ_i, and $h := \max_i h_i$ as before. For the BEM with Lagrangian multiplier we set $\Gamma_i = \Gamma$ and so h refers to the diameter of the longest element on Γ.

General remarks

Let us note that the part $\|[\phi_h]\|_\gamma^{1/2}$ of the error expression (5.3) is an overestimation. Indeed, our substitution (5.3) for $|\phi - \phi_h|_{H^{1/2}(\mathcal{T})}/\|\phi\|_{\text{ex}}$ is not precise. On the one hand we replaced the term $2\,\|\lambda\|_{L^2(\gamma)}$ in (5.2) by 1 (and the generic constant in (5.1) by 1).

On the other hand in the BEM with Lagrangian multiplier situation the term $\langle \mathbf{t} \cdot V\,\mathbf{curl}_\Gamma\,\phi, \phi_h\rangle_\gamma$ is of higher order than $\|\phi_h\|_{L^2(\gamma)}$. According to the proof of Theorem 3.7 (see (3.11) and (3.13)) there holds

$$\begin{aligned}|\langle \mathbf{t} \cdot V\,\mathbf{curl}_\Gamma\,\phi, \phi_h\rangle_\gamma| &\le C\,k^{1/2-\epsilon}\|\phi\|_{\tilde{H}^{1-\epsilon}(\Gamma)}\|\phi_h\|_{L^2(\gamma)} \\ &= C\,(2h)^{1/2-\epsilon}\|\phi\|_{\tilde{H}^{1-\epsilon}(\Gamma)}\|\phi_h\|_{L^2(\gamma)} \quad (\epsilon > 0).\end{aligned}$$

Equivalently in the Mortar BEM situation we have that $\langle [\phi_h], \lambda\rangle_\gamma$ is of higher order than $\|[\phi_h]\|_{L^2(\gamma)}$. According to (4.31) and by standard approximation theory there holds for any $r < 1/2$

$$|\langle [\phi_h], \lambda\rangle_\gamma| \lesssim \|[\phi_h]\|_{L^2(\gamma)} \inf_{\psi \in M_k} \|\lambda - \psi\|_{L^2(\gamma)} \lesssim k^r \Big(\sum_{l=1}^{L} |\lambda|^2_{H^r(\gamma_l)}\Big)^{1/2} \|[\phi_h]\|_{L^2(\gamma)}.$$

This shows that $\langle [\phi_h], \lambda\rangle_\gamma$ is of higher order than $\|[\phi_h]\|_{L^2(\gamma)}$. Note that, by the proof of Theorem 4.18 and since $\phi \in H^{1/2+r}(\Gamma)$, we have the regularity $\lambda \in \prod_{l=1}^{L} H^r(\gamma_l) \quad \forall r < 1/2$. Therefore, by the above and (5.2) the term

$$\Big(|\,\|\phi\|_{\text{ex}} - F(\phi_h)|\Big)^{1/2}/\|\phi\|_{\text{ex}} \qquad \text{(curve (2), "Part 1 of error")}$$

is asymptotically equal to

$$a(\phi - \phi_h, \phi - \phi_h)^{1/2}/\|\phi\|_{\text{ex}}.$$

5.2 BEM With Lagrangian Multiplier

In the case of the BEM with Lagrangian multiplier the meshes $\mathcal{T}_h$ are uniform consisting of squares of side-length h and for each $\mathcal{T}_h$ we select the mesh $\mathcal{G}_k$ which is compatible with $\mathcal{T}_h|_\gamma$ (as required by Theorem 3.7) with $k = 2h$ (see Figure 5.1 where the bullets indicate the nodes of $\mathcal{G}_k$).These meshes define the boundary element space X_h and the space M_k for the Lagrangian multiplier.

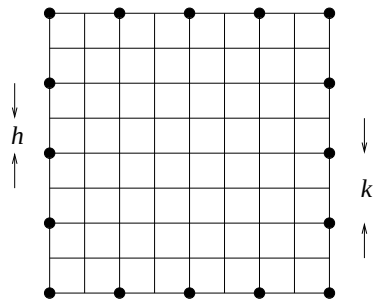

Figure 5.1: Uniform meshes $\mathcal{T}_h$ and $\mathcal{G}_k$.

As can be seen, the curve (1) in Figure 5.2 is parallel to the curve indicated by (4) which gives the errors in $\tilde{H}^{1/2}(\Gamma)$ of the corresponding conforming method (i.e. $V_h \subset \tilde{H}^{1/2}(\Gamma)$ using the same meshes). Actually, for $\phi \in \tilde{H}^{1/2}(\Gamma)$, $\|\phi\|^2_{\tilde{H}^{1/2}(\Gamma)}$ and $a(\phi,\phi)$ are equivalent and the latter expression is used. Both errors, (1) and (4), behave like $O(h^{1/2})$ whose curve is also given. In this way the result of Theorem 3.7 is underlined.

Note, however, that we do not observe an ϵ-perturbation (reduced convergence $O(h^{1/2-\epsilon})$) nor a poly-logarithmic perturbation in $1/h$. The absence of an ϵ-perturbation is expected, cf. Remark 3.8. The absence of a poly-logarithmic perturbation in h in this range of unknowns can be caused by the fact that we did not take the $L^2(\Gamma)$ part of the error in $H^{1/2}(\Gamma)$ into account since our results are, up to constant factors, upper bounds only for the semi-norm $|u - u_h|_{H^{1/2}(\Gamma)}$ (see Lemma 3.5(i)). Also, we do not know whether our bounds including the logarithmic terms are sharp.

Considering the results in Figure 5.2 it appears that the errors of the BEM with Lagrangian multiplier are much larger than those of the conforming method. This is not true for our model problem. This is since, as discussed previously, that the part $\|\phi_h\|^{1/2}_{L^2(\gamma)}$ of the error expression (5.3) is an overestimation. We recall that we have that

$$\Big(|\langle W\phi,\phi\rangle_\Gamma - \langle f,\phi_h\rangle_\Gamma|\Big)^{1/2}/\|\phi\|_{\rm ex} \qquad \text{“Part 1 of error”},$$

is asymptotically equal to

$$a(\phi-\phi_h,\phi-\phi_h)^{1/2}/\|\phi\|_{\rm ex},$$

and this dominates the error. The former numbers are the ones given by curve (2) ("Part 1 of error") and curve (4) ("Conforming BEM") presents the numbers $a(\phi - \tilde{\phi}_h, \phi - \tilde{\phi}_h)^{1/2}/\|\phi\|_{\text{ex}}$ where $\tilde{\phi}_h$ is the conforming BEM-approximation of ϕ. Both curves seem to coincide asymptotically indicating the good performance of the BEM with Lagrangian multiplier. We also include the values of $\|\phi_h\|^{1/2}_{L^2(\gamma)}/\|\phi\|_{\text{ex}}$ (curve (3) "Part 2 of error") to confirm that they dominate our expression (5.3). The behaviour of this curve, indicating $\|\phi_h\|_{L^2(\gamma)} = O(h)$, demonstrates that our non-conforming BEM very efficiently approximates the conformity condition that (conforming) ansatz functions must vanish on γ.

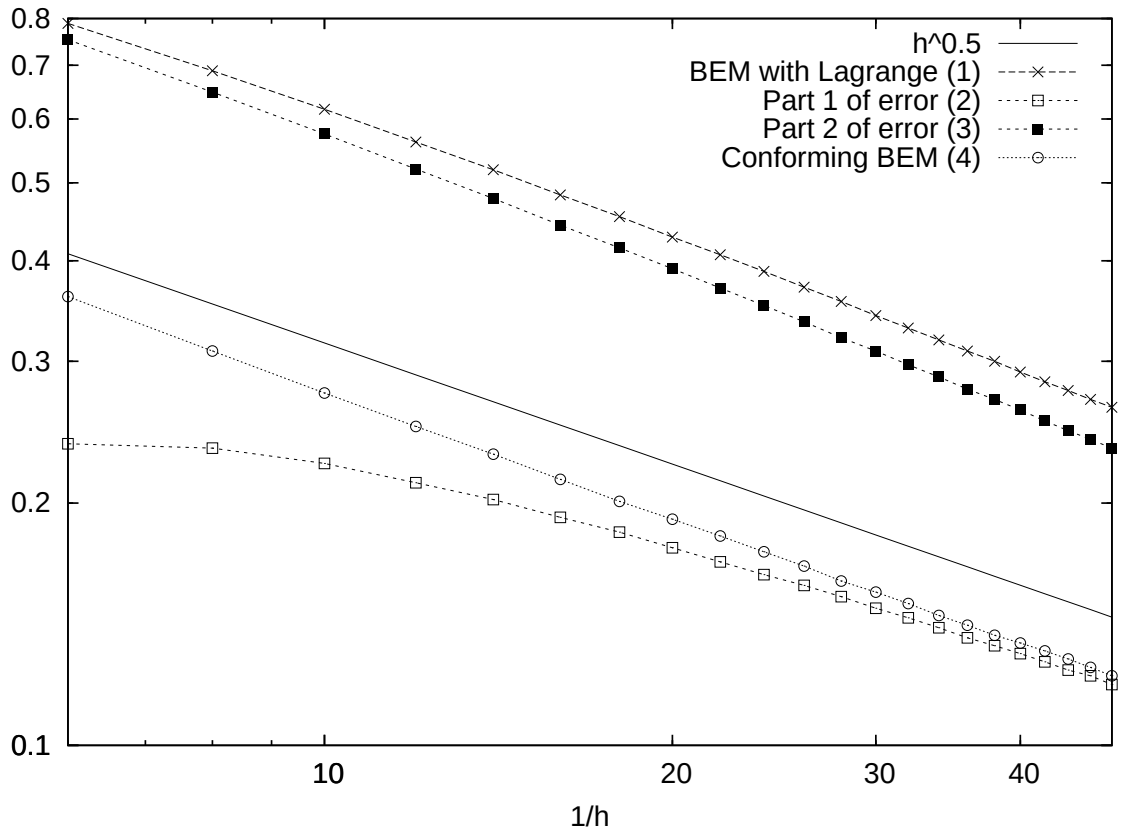

Figure 5.2: Relative error curves for the BEM with Lagrangian multiplier

5.3 Mortar Boundary Element Method

5.3.1 Mortar BEM - Conforming Sub-Domain Decomposition

In the case of our chosen model problem there holds $\phi \in \tilde{H}^{1/2+r}(\Gamma)$ for any $r < 1/2$ (see Remark 4.20) so that by Theorem 4.19 we expect a convergence of the mortar method close to $h^{1/2}$, the convergence of the conforming BEM (cf. Remark 4.20). This assumes that the mesh sizes h (of the sub-domain meshes) and k (of the meshes for the Lagrangian multiplier on the skeleton) are proportional, which will be the case in all our experiments. In fact, the elements of the mesh for the Lagrangian multiplier will always consist of two or three elements of the trace mesh (see Assumption 4.5).

Mortar BEM experiment 1 (Results in Figure 5.5)

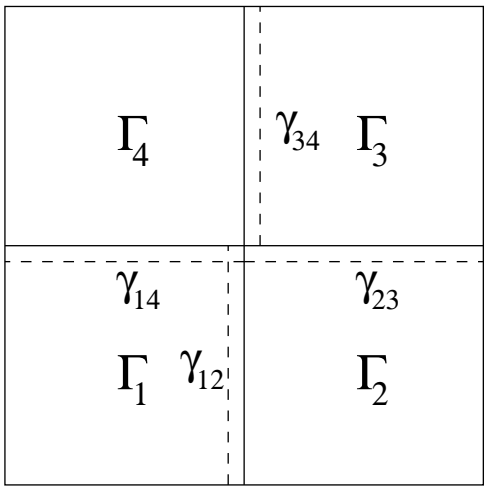

Figure 5.3: Choice of Lagrangian multiplier side for Experiment 1

First let us consider a conforming decomposition of Γ into four sub-domains as indicated in Figure 5.3. We shall choose the Lagrangian multipliers to be defined over the sides as shown in Figure 5.3. Moreover, let us first test the case where the separate meshes on the sub-domains form globally conforming meshes (we take uniform meshes consisting of squares). The corresponding results are shown in Figure 5.5 and Table B.2 shows the corresponding dimensions and mesh sizes. Along with the curves (1), (2), (4) we plot the values of $h^{1/2}$. The numerical results indicate a convergence of the order $O(h^{1/2})$, for the conforming as well as the mortar BEM. According to the discussion above this is the best one can expect. The curves (1) and (2), referring to our upper bound (5.3) and the first

term in (5.3), respectively, are almost identical to each other as well as to the conforming BEM. This means that the second term in (5.3), which in the next plots will be labelled by (3), is negligible in comparison. Indeed, in this symmetric case the jumps $[\phi_h]$ disappear and the numerical results vanish at the order of single precision. Therefore, in this plot, we do not show the curve (3). The results in Figure 5.5 show that the Mortar BEM very effectively approximates the conforming BEM in this situation as expected.

As in Section 5.2, for the BEM with Lagrangian multiplier, we do not observe a logarithmical perturbation of the convergence in this range of number of unknowns. This may be caused by the fact that we have not included the L^2-parts of the error since our results are, up to constant factors, upper bounds for the semi-norm $|\phi - \phi_h|_{H^{1/2}(\mathcal{T})}$. Also, we do not know whether our bounds involving the logarithmic terms are sharp.

Mortar BEM experiment 2 (Results in Figure 5.6)

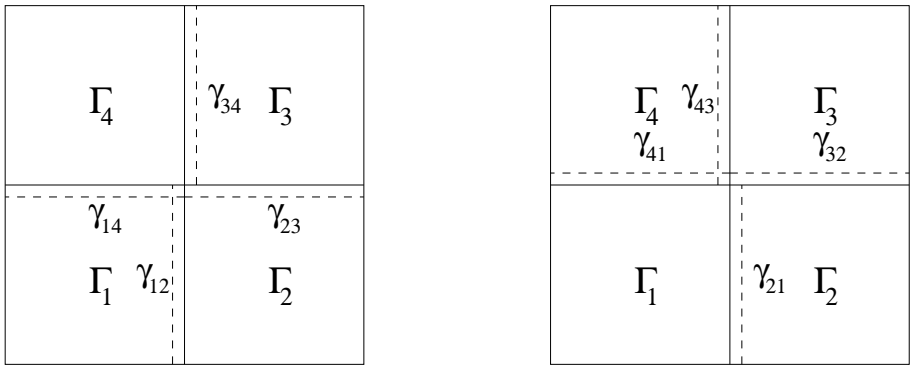

(a) Lagrangian multipliers I (b) Lagrangian multipliers II

Figure 5.4: Different Lagrangian multiplier sides.

Now let us test globally non-conforming meshes. Again we use uniform meshes consisting of squares on each sub-domain. We mesh as in Figure 4.4(a) starting with 2, 3, 4, and 5 "slides" on Γ_1, Γ_2, Γ_3, and Γ_4 respectively, and increase the number of slides in each sub-domain by one in each step of our sequence of meshes. We perform experiments with the Lagrangian multipliers defined in two different ways as shown in Figure 5.4. The corresponding results are shown in Figure 5.6 and the mesh sizes and dimensions are shown in Table B.3. Again, a convergence of the expected order $O(h^{1/2})$ is confirmed. Curve (3) indicates very fast convergence of the jumps $\|[\phi_h]\|_{L^2(\gamma)} \to 0$. In the experiments below, however, we observe a slower convergence. In this particular sequence of meshes, where we increase the slides on the sub-domains by the same amount, the trace meshes from

different sides on a particular interface edge approach each other in a certain sense. We conjecture that this specific situation ("approaching" conforming meshes) causes the fast convergence of the jumps.

Mortar BEM experiment 3 (Results in Figure 5.7)

For the next experiment we start with a mesh of four squares on each sub-domain (the sub-domains are again as in Figure 4.4(a)), and increase the numbers of slides on different sub-domains by different steps (increase by 2, 3, 4, 5 slides on Γ_1, Γ_2, Γ_3, and Γ_4 respectively). The results are shown in Figure 5.7 and the corresponding mesh sizes and dimensions are shown in Table B.4. In this case both error parts, curves (2) and (3), behave like $O(h^{1/2})$, thus confirming the good performance of the mortar BEM.

In Figure 5.7 we clearly see the effect that defining the Lagrangian multiplier in a different way has on the performance of the method. We see that in particular situations this can actually be quite a dramatic change. While, as expected, the choice of Lagrangian multipliers has little effect on "Part 1 of the error" it has a large effect on "Part 2 of the error". This is expected since it is the second part of the error which measures the error contributed by the jumps of the functions over the interfaces. The large differences in the two curves (3) are likely caused by the different choices of Lagrangian multiplier sides. In experiment II we choose the Lagrangian multiplier sides as shown in Figure 5.4(b). Of particular note we choose the Lagrangian multipliers to be defined over the restrictions of Γ_4 to the bounding interfaces. This means that we are choosing the sub-domain with the finest mesh thus making the Lagrangian multipliers as numerous as possible. The differences in the curves (3) appear to be particularly large when we have an even number of slides on all sub-domains. This could be because we are close to a conforming situation.

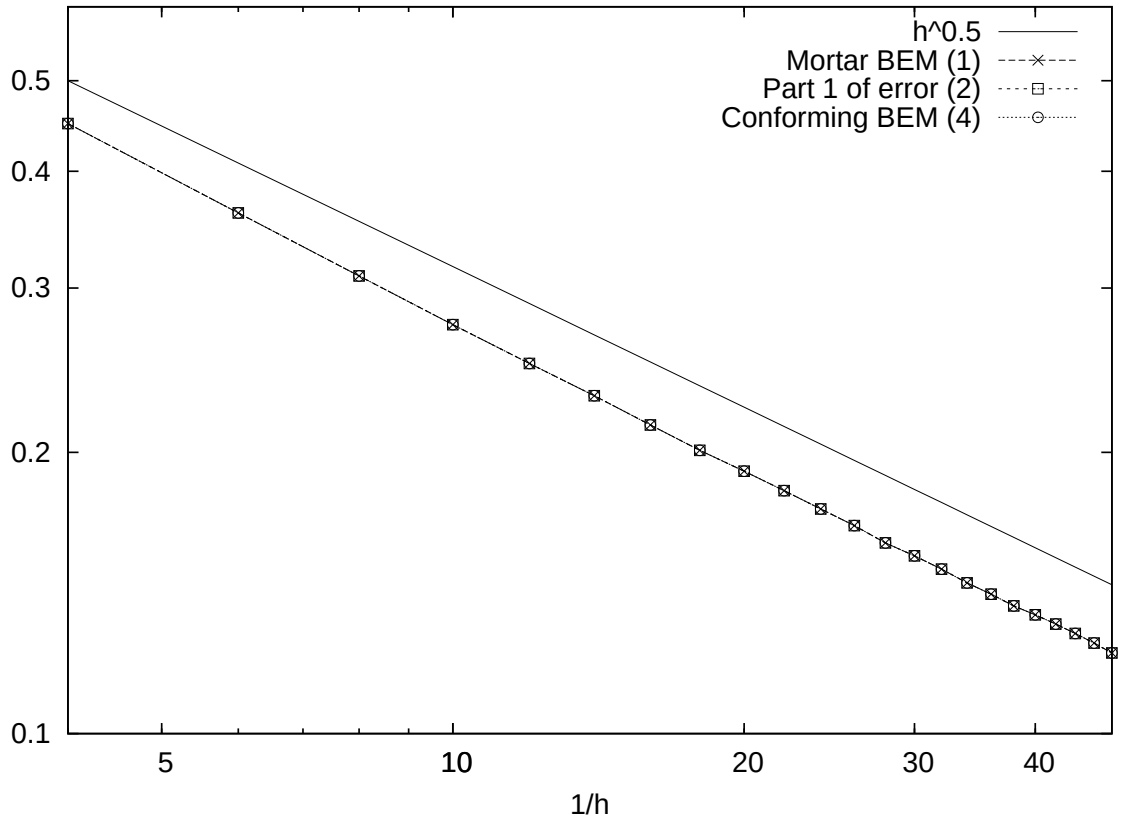

Figure 5.5: Mortar BEM experiment 1 - A conforming mesh of sub-domains as shown in Figure 4.4(a). Each sub-domain has the same mesh.

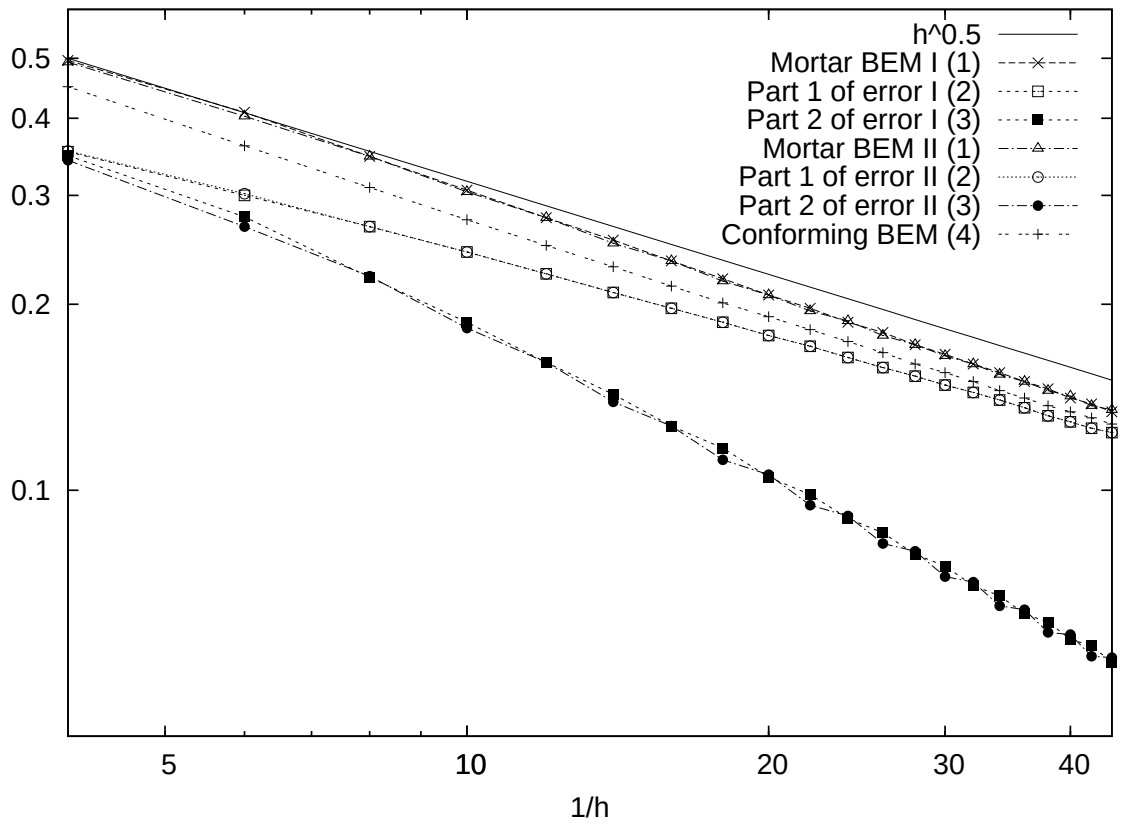

Figure 5.6: Mortar BEM experiment 2 - A conforming mesh of sub-domains as shown in Figure 4.4(a). Each sub-domain has a different mesh and the number of subdivisions on each sub-domain increases by the same amount.

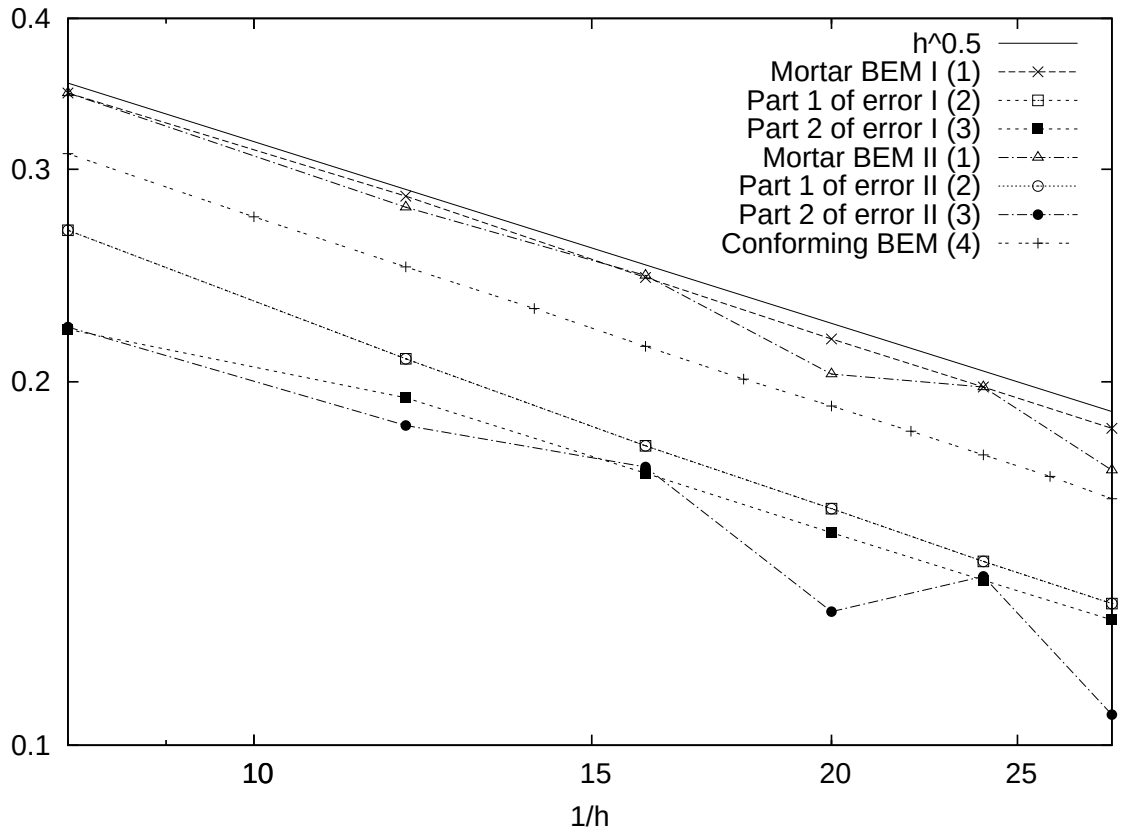

Figure 5.7: Mortar BEM experiment 3 - A conforming mesh of sub-domains as shown in Figure 4.4(a). Each sub-domain has a different mesh and the number of subdivisions on each sub-domain increases by a different amount.

5.3.2 Mortar BEM - Non-Conforming Sub-Domain Decomposition I

We now consider the situation of a non-conforming decomposition of the domain into sub-domains. We use the mesh of sub-domains as shown in Figure 5.8, and we choose the Lagrangian multiplier sides as shown in Figure 5.8.

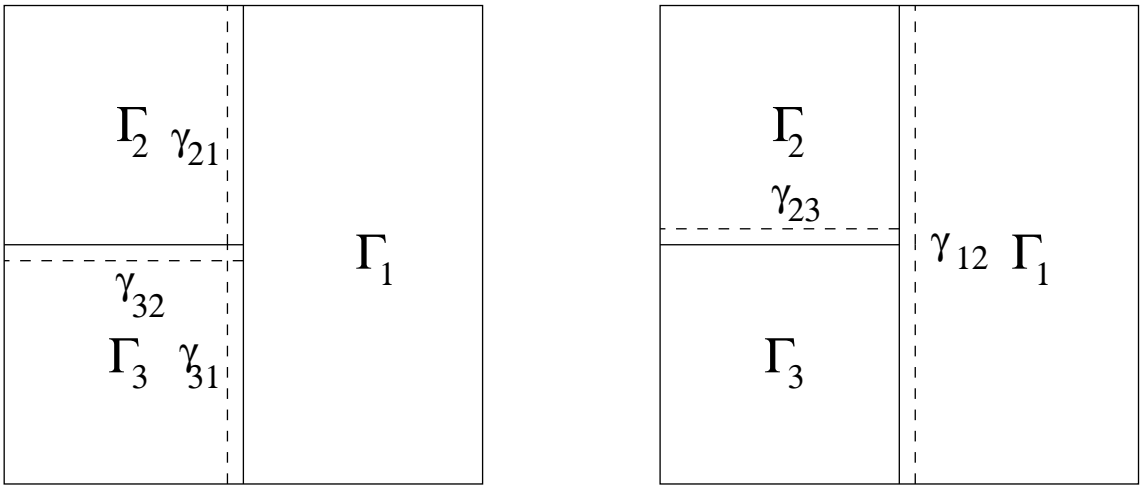

(a) Lagrangian multipliers I (b) Lagrangian multipliers II

Figure 5.8: Different Lagrangian multiplier sides.

Figures 5.10, 5.11, and 5.12 present the results for a nonconforming mesh of sub-domains as shown in Figure 5.8. The curves in the Figures 5.10, 5.11, and 5.12 again demonstrate the expected behaviour of the mortar BEM.

Mortar BEM experiment 4 (Results in Figure 5.10)

Figure 5.10 presents the results when we have the same number of slides on each sub-domain. This means that on one sub-domain we have a larger mesh size, and the elements of this sub-domain are now rectangles and no longer squares. For this experiment we present the mesh sizes and dimensions in Table B.5. We start with two slides on each sub-domain and increase this number by one at each step. This means that we effectively have a conforming mesh across sub-domains Γ_2 and Γ_3.

The irregularities in Figure 5.10 curves (3) and the values of jumps across the interfaces, (and hence curve (1)) are likely caused by the mesh becoming alternately conforming then nonconforming at the interior node where the sub-domains intersect as shown

in Figure 5.9. We thus get a better approximation (lower relative error) when we have a conforming situation at this internal node (as shown in Figures 5.9(a) and 5.9(c)) than when we have a nonconforming situation at the internal node (as shown in Figures 5.9(b) and 5.9(d)). In Figure 5.9 a nonconforming interface node is indicated by a small circle. We note however these irregularities only appear when we have the Lagrangian multiplier sides chosen as in Figure 5.8(a).

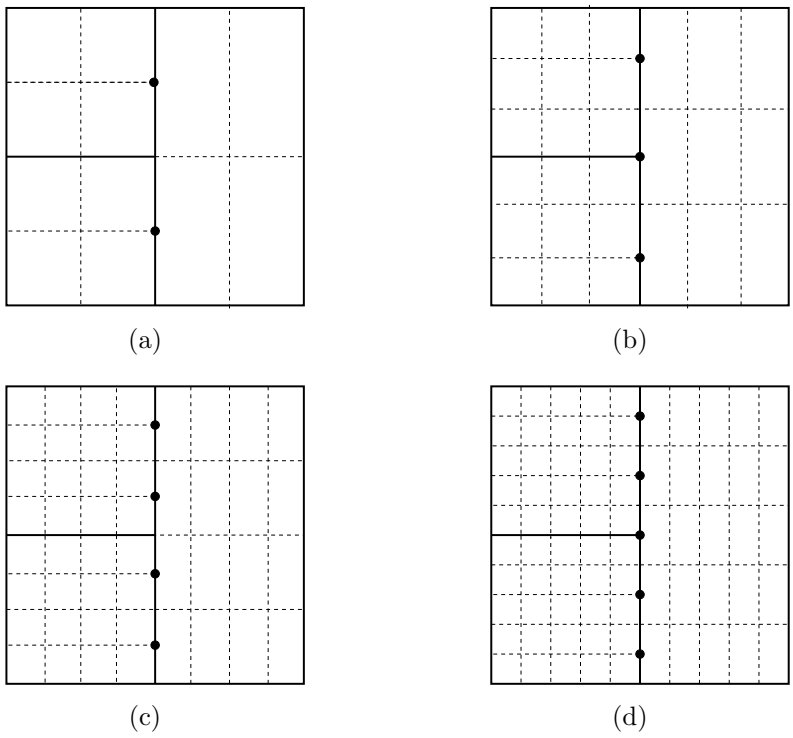

Figure 5.9: Examples of the mesh refinement procedure as used for the results shown in Figure 5.10

Mortar BEM experiment 5 (Results in Figure 5.11)

We now consider the fully non-conforming mortar method, i.e. with non-conforming sub-domain decomposition and non-conforming meshes. However in this experiment the degree of non-conformity (especially between Γ_2 and Γ_3) is not large. Figure 5.11 (and Table B.6) presents the results when we start with 2, 3, and 4 "slides" on Γ_1, Γ_2, and Γ_3 respectively and increase the number of slides in each sub-domain by one in each step

of our sequence of meshes. In this experiment we see little difference in the choice of Lagrangian multiplier sides.

Mortar BEM experiment 6 (Results in Figure 5.12)

We consider again the fully non-conforming mortar method, i.e. with non-conforming sub-domain decomposition and non-conforming meshes. In this experiment through our choice of the size of increase in the number of slides we have a high degree of non-conformity. We decompose Γ into three sub-domains as in Figure 5.9 and use the initial meshes given there. Next slides on sub-domains are increased in each direction by 2, 3, 4 on Γ_1, Γ_2, Γ_3, respectively in each step. The numerical results are shown in Figure 5.12 and again confirm the expected convergence of the mortar BEM. The corresponding numbers of unknowns for the steps are listed in Table B.7.

In this experiment we see a large difference in the choice of Lagrangian multiplier sides. As expected when the Lagrangian multipliers are defined over the finer meshes (Γ_2 and Γ_3) we see improved results.

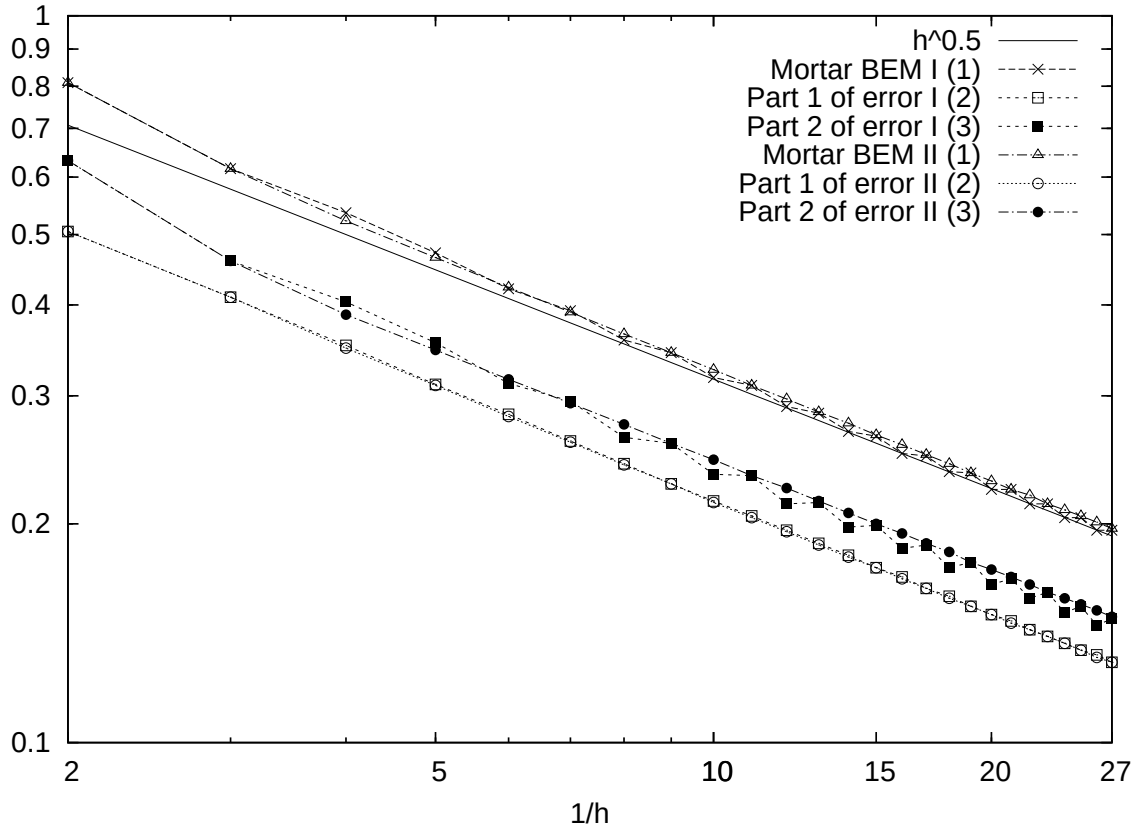

Figure 5.10: Mortar BEM experiment 4 - A nonconforming mesh of sub-domains as shown in Figure 4.4(b). Each sub-domain has the same number of subdivisions.

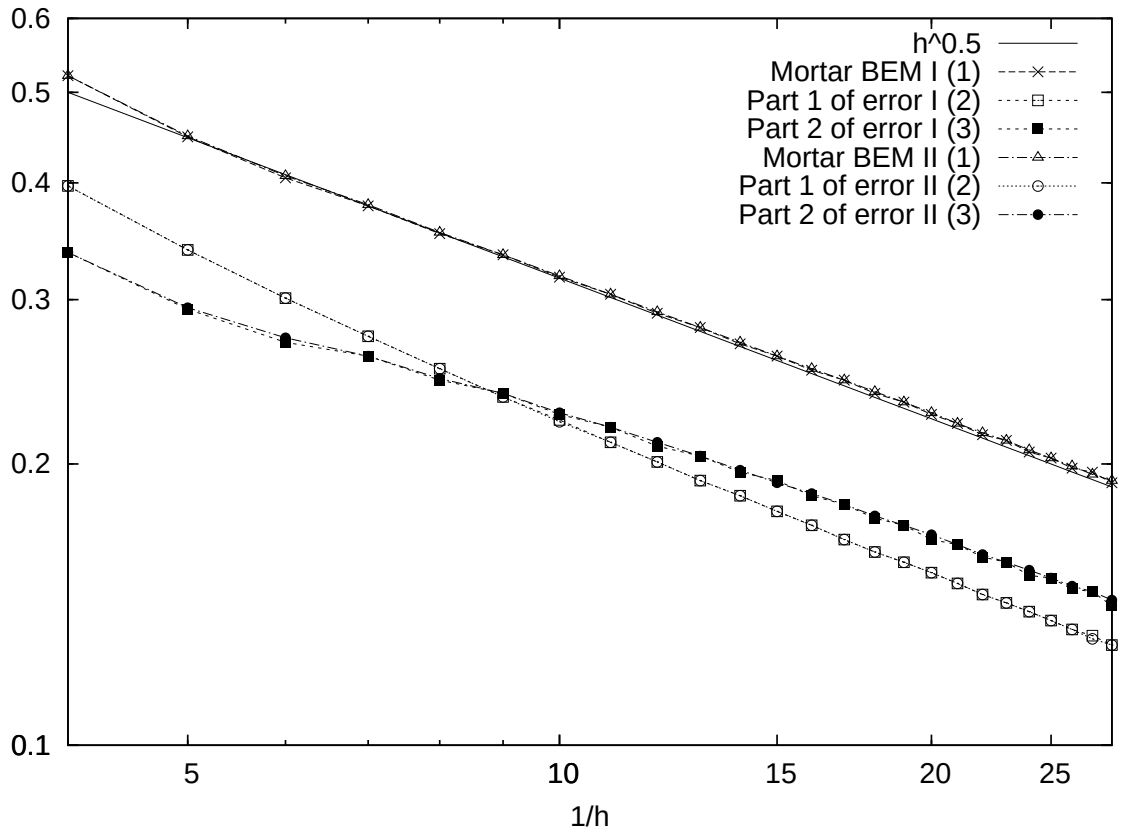

Figure 5.11: Mortar BEM experiment 5 - A nonconforming mesh of sub-domains as shown in Figure 4.4(b). Each sub-domain has a different mesh and the number of subdivisions on each sub-domain increases by the same amount.

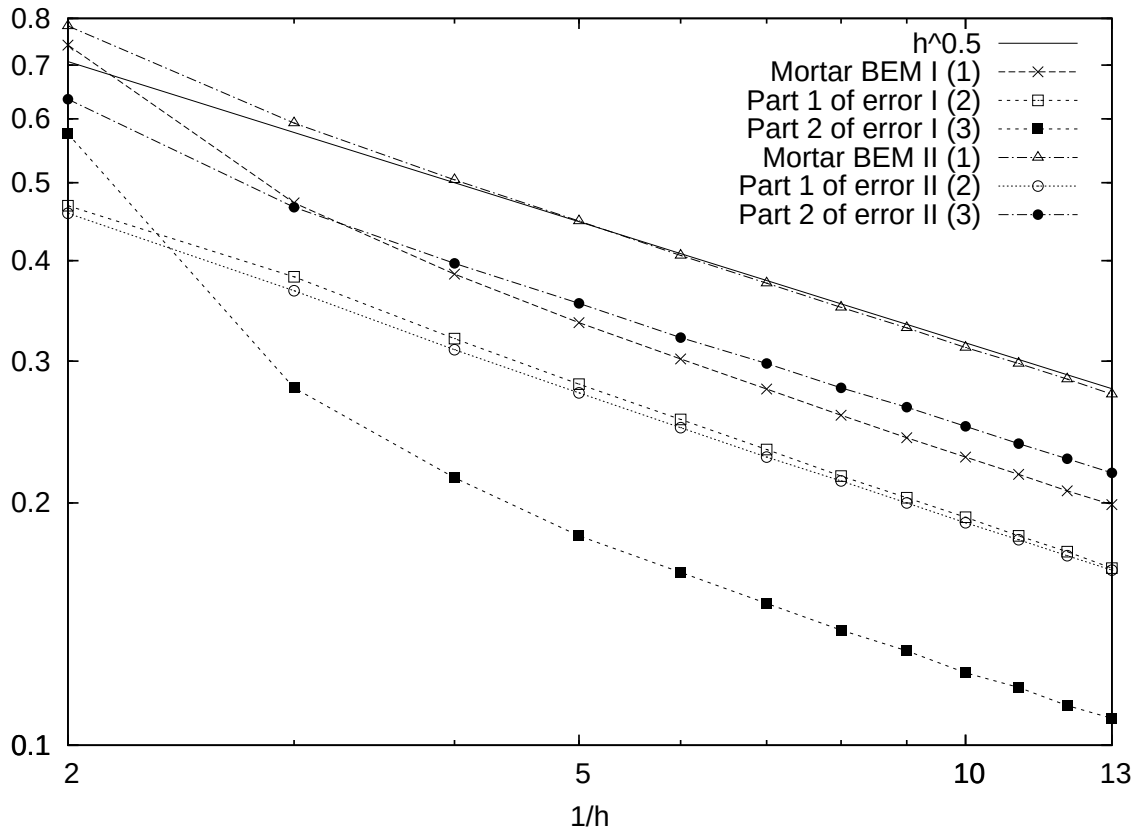

Figure 5.12: Mortar BEM experiment 6 - A nonconforming mesh of sub-domains as shown in Figure 4.4(b). Each sub-domain has a different mesh and the number of subdivisions on each sub-domain increases by a different amount.

5.3.3 Mortar BEM - Non-Conforming Sub-Domain Decomposition II

We now consider a second nonconforming situation as shown in Figure 5.13. This mesh does not satisfy Assumption 4.2. This is because the interface between sub-domains Γ_2 and Γ_4 is not a whole edge of either of them. This is why we have used a different numbering system for the Lagrangian multipliers.

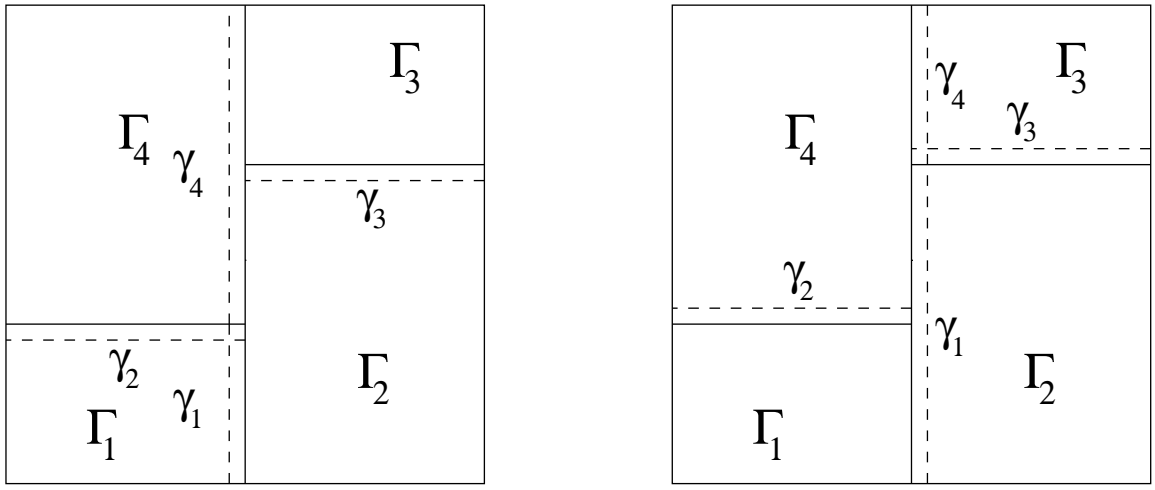

(a) Lagrangian multipliers I

(b) Lagrangian multipliers II

Figure 5.13: Different Lagrangian multiplier sides for a second nonconforming decomposition

Figures 5.15, 5.16, and 5.17 present the results for a nonconforming mesh of sub-domains as shown in Figure 5.13. The curves in the Figures 5.15, 5.16, and 5.17 again demonstrate the expected behaviour of the mortar BEM.

Mortar BEM experiment 7 (Results in Figure 5.15)

Figure 5.15 presents the results when we have the same number of slides on each sub-domain (mesh sizes and dimensions are given in Table B.8). This means that on two sub-domains we have a larger mesh size, and the elements of all sub-domains are now rectangles. Figure 5.14 indicates the mesh refinement when we have the same number of slides on each sub-domain.

This initially appears to simply be a symmetrical variation of the two meshes and choice of Lagrangian multiplier sides. However this is not the case. The definition of the Lagrangian multipliers when there is an odd number of slides on the mesh over which

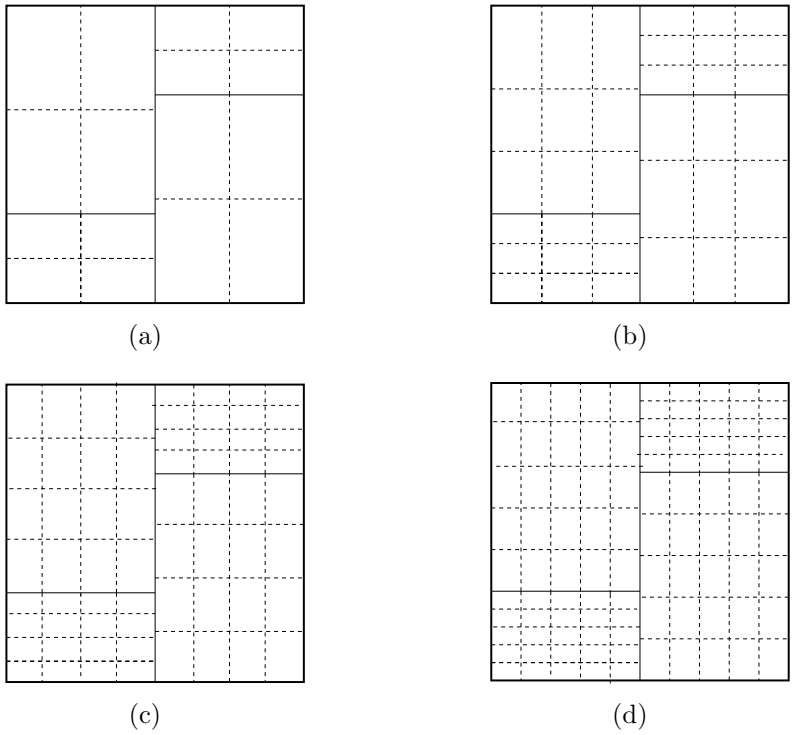

Figure 5.14: Examples of the mesh refinement procedure as used for the results shown in Figure 5.15

they are defined requires that the first Lagrangian multiplier is defined over three slides. This first Lagrangian multiplier is defined in a non-symmetric fashion in the two choices of Lagrangian multiplier side. It is likely the positioning of this first Lagrangian multiplier that causes a difference. We define the longest interval at the "start" of each edge over which the Lagrangian multiplier is defined. As each interface is a straight line we associate the standard directional conventions, increasing from left to right, or down to up. Therefore each interface is deemed to start with either its lowest or its leftmost point. This means that in Figure 5.13(a) the interface γ_4 starts at the lower right corner in sub-domain Γ_4. So for a sufficiently small mesh size the longest Lagrangian multiplier is defined over the interface between the two largest sub-domains Γ_2 and Γ_4. However in Figure 5.13(b) the interface γ_1 (symmetrically the same interface) starts at the lower left corner of sub-domain Γ_2. So for a sufficiently small mesh size the longest Lagrangian multiplier is defined over the interface between the a large sub-domain Γ_2 and a small sub-domain Γ_1. We believe it is this which causes the differences in the results in the situation when the Lagrangian multiplier is defined over an odd number of slides. We

note that when there is an even number of slides we simply have a symmetric variation in the definition of the Lagrangian multiplier space.

Mortar BEM experiment 8 (Results in Figure 5.16)

Figure 5.16 presents the result when we start with a different number of slides on each sub-domain and the increase the number of slides on each sub-domain by one at each iteration (mesh sizes and dimensions are given in Table B.9). We again see the jumps in the curves (3) having a large impact on the total error. The differences in the two curves (3) is likely caused by our choice of Lagrangian multiplier side.

Mortar BEM Experiment 9 (Results in Figure 5.17)

Figure 5.17 presents the results when we start with a different number of slides on each sub-domain and then increase the number of slides on each sub-domain by a different number on each sub-domain (mesh sizes and dimensions are given in Table B.10). If we examine the sizes of the Lagrangian multiplier spaces in experiment I and experiment II (M_kI and M_kII in Table B.10 respectively) we see that the choice of Lagrangian multipliers shown in Figure 5.13(a) gives a larger (dimension-wise) Lagrangian multiplier space than the choice shown in Figure 5.13(b). This is most likely the cause of the differences between the curves (3) in Figure 5.17.

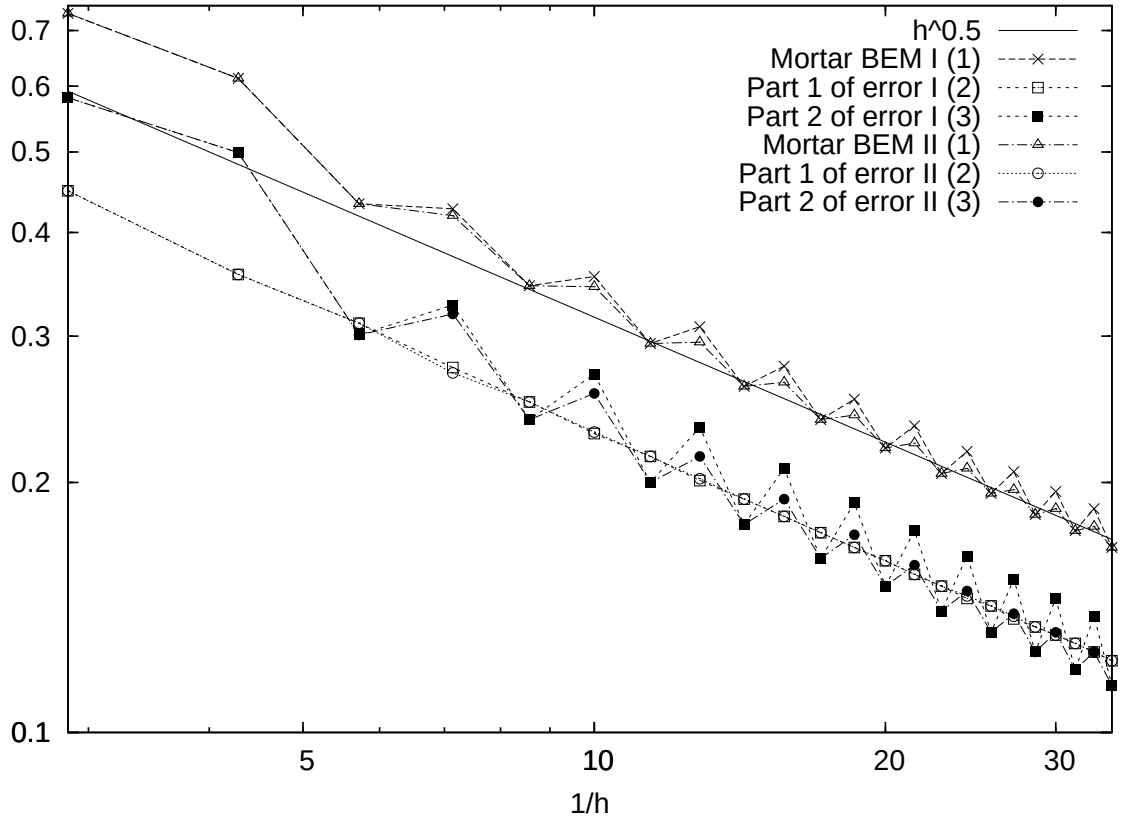

Figure 5.15: Mortar BEM experiment 7 - A nonconforming mesh of sub-domains as shown in Figure 5.13. Each sub-domain has the same number of subdivisions.

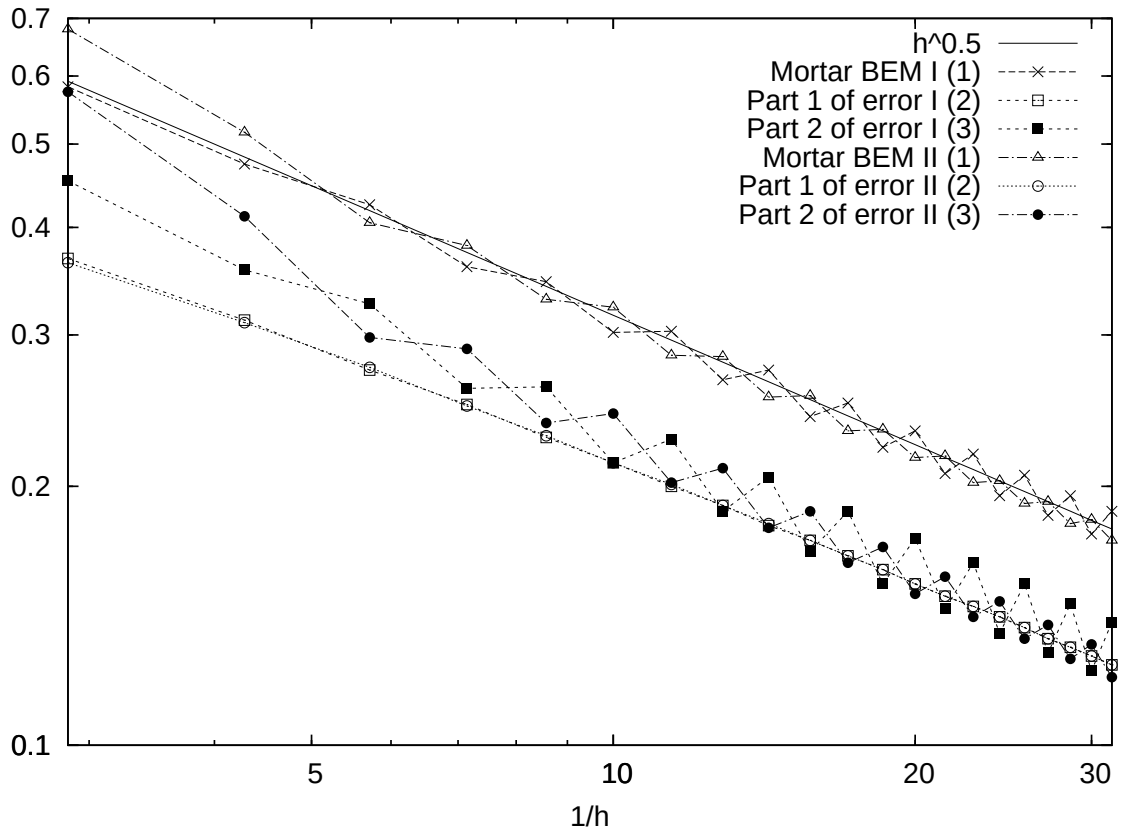

Figure 5.16: Mortar BEM experiment 8 - A nonconforming mesh of sub-domains as shown in Figure 5.13. Each sub-domain has a different mesh and the number of subdivisions on each sub-domain increases by the same amount.

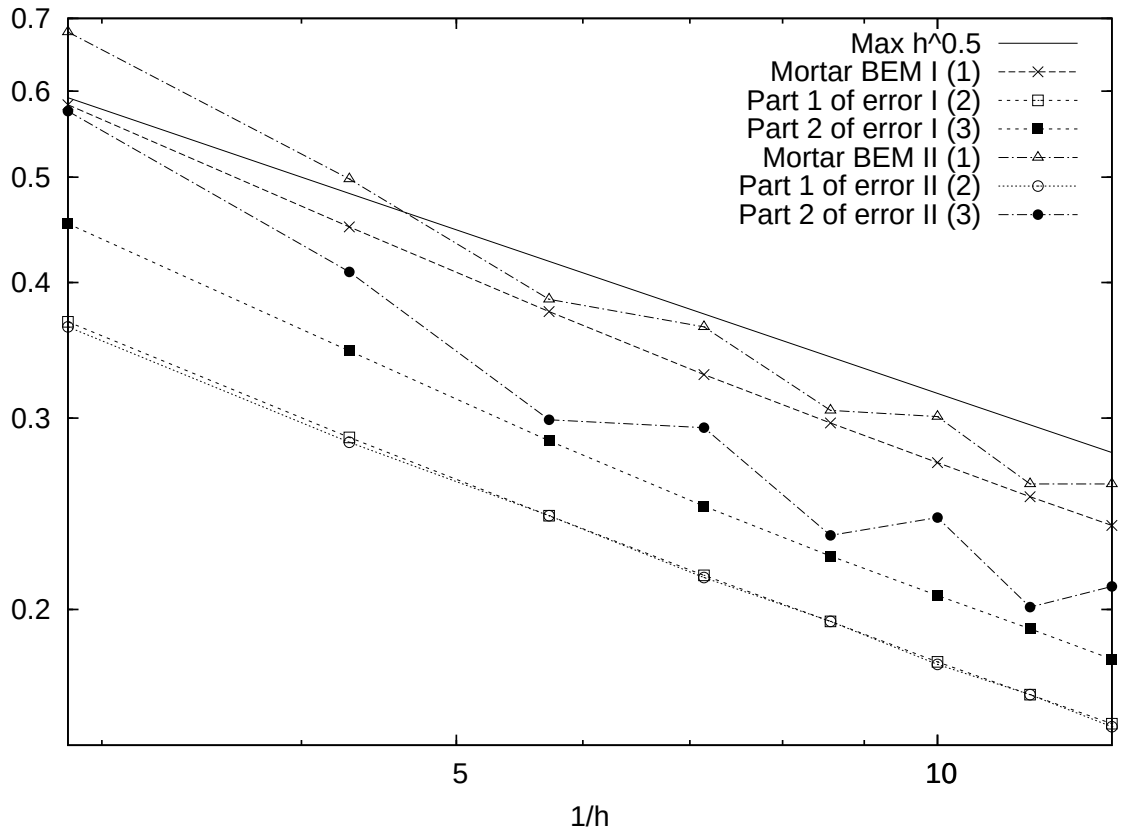

Figure 5.17: Mortar BEM experiment 9 - A nonconforming mesh of sub-domains as shown in Figure 5.13. Each sub-domain has a different mesh and the number of subdivisions on each sub-domain increases by a different amount.

Chapter 6

Mortar BEM for Linear Elasticity

In this chapter we shall extend the results of the mortar BEM from the case of the Laplacian to linear elasticity (the Lamé system). We first examine the background and setting of the three dimensional Neumann problem in linear elasticity. We then examine the model problem and discuss the derivation of the model problem. As in the previous chapters we require an integration by parts formula to switch from the hypersingular integral equation to an alternative formulation involving weakly singular integrals and present us with the relevant boundary terms which can be used to define a Lagrangian multiplier. Once we have specified the formulation of the mortar method for linear elasticity we move onto the analysis. We examine results on the existence and uniqueness of the solution to the proposed scheme and we examine an error estimate.

Notations

In this section we shall use different notation to that used previously. We are going to be dealing with functions which are vectors, e.g. $\boldsymbol{\phi} = (\phi_1, \phi_2, \phi_3)$, where the subscript indicates the component of the vector and not the restriction to a sub-domain as previously used. We shall use the notation $\phi_i|_{\Gamma_j}$ to indicate the restriction of the i^{th} component of the vector $\boldsymbol{\phi}$ to the sub-domain Γ_j.

6.1 Background

6.1.1 Linear Elasticity

We consider the three dimensional Neumann crack problem in linear elasticity. First we recall some notions of linear elasticity from [27] and [37]. We follow the formulation of the problem as described in [52]. Let the crack surface be denoted by Γ (a plane open surface

with polygonal boundary). The problem under consideration is for the displacement field $\boldsymbol{u}$ of a homogeneous, isotropic elastic material $\Omega := \mathbf{R}^3 \setminus \bar{\Gamma}$.

We let $\boldsymbol{u}(x) = (u_1(x), u_2(x), u_3(x))^T$ be the displacement vector for $x \in \mathbf{R}^3$ where $x = (x_1, x_2, x_3)^T$ and $\sigma_{ij}(\boldsymbol{u})$ be the *stress field* corresponding to the *displacement vector* $\boldsymbol{u}$. The stress-displacement relationships for an isotropic elastic material are

$$\sigma_{ij}(\boldsymbol{u}) = \lambda \delta_{ij} \operatorname{div} \boldsymbol{u} + 2\mu\epsilon_{ij}, \quad 1 \le i, j \le 3, \tag{6.1}$$

where λ and μ are the *Lamé* constants and δ_{ij} is the *Kronecker delta*. We assume that $\mu > 0$ and $\lambda > \frac{2}{3}\mu$. The *strain tensor* ϵ_{ij} in terms of displacements in (6.1) is given by

$$\epsilon_{ij}(\boldsymbol{u}) = \frac{1}{2}\left(\frac{\partial u_i}{\partial x_j} + \frac{\partial u_j}{\partial x_i}\right), \quad 1 \le i, j \le 3.$$

For $x \in \mathbf{R}^3$ and an arbitrary unit vector $\boldsymbol{n}(x) = (n_1(x), n_2(x), n_3(x))^T$ the matrix differential operator $\boldsymbol{T}(\partial_x, \boldsymbol{n}(x))$ is called the *stress operator* and is defined by

$$\boldsymbol{T}(\partial_x, \boldsymbol{n}(x)) = (T_{ij}(\partial_x, \boldsymbol{n}(x)))_{3\times 3}, \tag{6.2}$$

with

$$T_{ij}(\partial_x, \boldsymbol{n}(x)) = \lambda n_i(x)\frac{\partial}{\partial x_j} + \mu n_j(x)\frac{\partial}{\partial x_i} + \mu\delta_{ij}\frac{\partial}{\partial \boldsymbol{n}(x)}, \quad 1 \le i, j \le 3. \tag{6.3}$$

$\boldsymbol{T}(\partial_x, \boldsymbol{n}(x))$ denotes the stress at the point x along the direction $\boldsymbol{n}(x)$ in terms of the displacement $\boldsymbol{u}(x)$.

The equilibrium equations without boundary force in elastostatics are

$$\sum_{j=1}^{3} \frac{\partial \sigma_{ij}(\boldsymbol{u})}{\partial x_j} = 0, \qquad i = 1, 2, 3,$$

or

$$\mu\Delta\boldsymbol{u} + (\lambda + \mu) \operatorname{grad} \operatorname{div} \boldsymbol{u} = \mathbf{0}, \tag{6.4}$$

in terms of displacements.

We consider the Neumann problem:

$$\begin{aligned} \mu\Delta\boldsymbol{u} + (\lambda + \mu) \operatorname{grad} \operatorname{div} \boldsymbol{u} &= \mathbf{0}, \text{ in } \Omega \\ \boldsymbol{T}(\partial_x, \boldsymbol{n}(x))\boldsymbol{u} &= \boldsymbol{g}, \text{ on } \partial\Omega = \Gamma, \end{aligned} \tag{6.5}$$

where $\boldsymbol{n}(x)$ denotes the outward unit normal on Γ and $\boldsymbol{g} = (g_1(x), g_2(x), g_3(x))^T$ is a vector valued function on the crack surface Γ satisfying

$$\int_\Gamma \boldsymbol{g}(x)\, dS = 0 \text{ and } \int_\Gamma x \times \boldsymbol{g}(x)\, dS = 0.$$

Under this condition the Neumann problem has a unique solution up to rigid body motions. The *rigid body motions* are the functions $\boldsymbol{\chi} \in \mathcal{R}$ where

$$\mathcal{R} = \text{span}\left\{ \begin{pmatrix} 1 \\ 0 \\ 0 \end{pmatrix}, \begin{pmatrix} 0 \\ 1 \\ 0 \end{pmatrix}, \begin{pmatrix} 0 \\ 0 \\ 1 \end{pmatrix}, \begin{pmatrix} -x_2 \\ x_1 \\ 0 \end{pmatrix}, \begin{pmatrix} 0 \\ -x_3 \\ x_2 \end{pmatrix}, \begin{pmatrix} x_3 \\ 0 \\ -x_1 \end{pmatrix} \right\}. \tag{6.6}$$

The rigid body motions can be equivalently defined as the span of the six functions $\boldsymbol{\chi}_j : \Gamma \to \mathbf{R}^3$ $(1 \leq j \leq 6)$ defined by

$$\boldsymbol{\chi}_l = \boldsymbol{e}_l \text{ and } \boldsymbol{\chi}_{l+3} = \boldsymbol{e}_l \times \boldsymbol{x} \text{ for } \boldsymbol{x} \in \Gamma \text{ and } 1 \leq l \leq 3,$$

where $\boldsymbol{e}_l$ is the l^{th} column of the 3×3 identity matrix. For our crack problems we need (as in (2.6)) some additional conditions to guarantee the uniqueness of our integral formulation. We require the radiation conditions:

$$\boldsymbol{u}(x) = o(1) \text{ and } \frac{\partial}{\partial x_j}\boldsymbol{u}(x) = o\left(\frac{1}{|x|}\right) \text{ as } |x| \to \infty.$$

We note that the boundary condition in (6.5)

$$\boldsymbol{T}(\partial_x, \boldsymbol{n}(x))\boldsymbol{u} = \boldsymbol{g}, \text{ on } \partial\Omega = \Gamma,$$

can be equivalently expressed in terms of vectors as

$$\boldsymbol{T}(\partial_x, \boldsymbol{n}(x))(\boldsymbol{u}) := \lambda \operatorname{div} \boldsymbol{u}\boldsymbol{n} + 2\mu\frac{\partial \boldsymbol{u}}{\partial \boldsymbol{n}} + \mu\boldsymbol{n} \times \operatorname{curl} \boldsymbol{u} = \boldsymbol{g}, \text{ on } \partial\Omega = \Gamma.$$

This is the notation used in [52].

6.1.2 Model problem

Let $\boldsymbol{U}^*(x-y)$ denote the fundamental solution matrix of the Navier system (6.4). We then have that

$$\boldsymbol{U}^*(x-y) \equiv (U^{*,1}(x-y), U^{*,2}(x-y), U^{*,3}(x-y)) \equiv (U^*_{ij}(x-y))_{3\times 3}, \tag{6.7}$$

with

$$U^*_{ij} = \frac{1}{8\pi\mu(\lambda+2\mu)}\left\{(\lambda+3\mu)\frac{\delta_{ij}}{|x-y|} + (\lambda+\mu)\frac{(x_i-y_i)(x_j-y_j)}{|x-y|^3}\right\}. \tag{6.8}$$

The matrix $\boldsymbol{U}^*(x)$ is symmetric and every column and row of $\boldsymbol{U}^*(x)$ satisfy the Navier system (6.4) at every point $x \in \mathbf{R}^3$, except the origin.

We now consider the double-layer potential (for linear elasticity)

$$\boldsymbol{u}(x) = \int_\Gamma (\boldsymbol{T}(\partial_y, \boldsymbol{n}(y))\boldsymbol{U}^*(x-y))^T \boldsymbol{\phi}(y)\, dS_y, \tag{6.9}$$

where $\boldsymbol{n}(y)$ denotes the unit outward normal vector at $y \in \Gamma$ and $\boldsymbol{\phi}$ is a vector valued function on Γ to be determined. As in Theorem 2.1 $\boldsymbol{\phi}$ represents $[\boldsymbol{u}]$, the jump of $\boldsymbol{u}$ over the crack surface. In (6.9) for a suitable given $\boldsymbol{\phi}$ we have that $\boldsymbol{u}(x)$ is a solution of (6.4). The double-layer potential (6.9) can be used to reduce the Neumann problem (6.5) to the *hypersingular boundary integral equation* (see [52, Theorem 3.1]) for a given function $\boldsymbol{g} \in \boldsymbol{H}^{1/2}(\Gamma)$

$$\begin{aligned} W_{le}\boldsymbol{\phi}(x) \;:=\; & \int_\Gamma \boldsymbol{T}(\partial_x, \boldsymbol{n}(x))(\boldsymbol{T}(\partial_y, \boldsymbol{n}(y))\boldsymbol{U}^*(x-y))^T \boldsymbol{\phi}(y)\, dS_y = \boldsymbol{g}(x), \\ & x \in \Gamma,\ \boldsymbol{\phi}(x) \in \tilde{\boldsymbol{H}}^{1/2}(\Gamma). \end{aligned} \tag{6.10}$$

Where we use the notation

$$\boldsymbol{H}^s(\Gamma) := (H^s(\Gamma))^3 \text{ and } \tilde{\boldsymbol{H}}^s(\Gamma) := (\tilde{H}^s(\Gamma))^3.$$

The integral equation (6.10) is quite difficult to approximate because of the hypersingular kernel (as it was in the case of the Laplacian in previous chapters). To this end a formulation of the hypersingular equation (6.10) using weakly singular integrals was given by Nédélec in the following theorem.

Theorem 6.1. *[43, Theorem 3]. We have, for Γ a closed surface*

$$\langle W_{le}\boldsymbol{\phi}, \boldsymbol{\psi}\rangle_\Gamma = \sum_{i,j=1}^{3} \int_\Gamma \int_\Gamma G_{ij..}(x-y)\, \mathbf{curl}_\Gamma\, \phi_i(x) \cdot \mathbf{curl}_\Gamma\, \psi_j(y)\, dS_x dS_y$$

where $G_{ij..}$ is a tensor of order 4 given by

$$G_{ij..} = -\mathbf{curl}_{\mathrm{x}}\mathbf{curl}_{\mathrm{y}}\mathrm{A}_{\mathrm{i,j.}}(\mathrm{x}-\mathrm{y}),$$

A being a tensor of order 4 given by

$$\begin{aligned} A_{ijkl}(x) =& \frac{4\mu(\lambda+\mu)}{2\mu+\lambda}\cdot\frac{\partial^4}{\partial x_i\partial x_j\partial x_k\partial x_l}\left(\frac{|x|^5}{2880\pi}\right) \\ &+\frac{2\lambda\mu}{\mu+\lambda}\left(\frac{\partial^2}{\partial x_i\partial x_j}\left(\frac{|x|^3}{96\pi}\right)\delta_{kl}+\frac{\partial^2}{\partial x_l\partial x_k}\left(\frac{|x|^3}{96\pi}\right)\delta_{ij}\right) \\ &+\mu\left(\frac{\partial^2}{\partial x_i\partial x_k}\left(\frac{|x|^3}{96\pi}\right)\delta_{lj}+\frac{\partial^2}{\partial x_j\partial x_k}\left(\frac{|x|^3}{96\pi}\right)\delta_{li}\right. \\ &\left.+\frac{\partial^2}{\partial x_j\partial x_l}\left(\frac{|x|^3}{96\pi}\right)\delta_{ki}\frac{\partial^2}{\partial x_i\partial x_l}\left(\frac{|x|^3}{96\pi}\right)\delta_{kj}\right) \\ &+\mu\frac{|x|}{8\pi}\left(\delta_{ki}\delta_{lj}+\delta_{li}\delta_{jk}\right)+\frac{2\mu\lambda}{2\mu+\lambda}\left(\frac{|x|}{8\pi}\right)\delta_{ij}\delta_{kl}. \end{aligned}$$

The given bilinear form is symmetric and elliptic on the space $(H^{1/2}(\Gamma))^3/_{\mathcal{R}}$.

However this formula is extremely complicated, so we shall use an alternative representation proposed by Han in [27]. As in our earlier situation this is the starting point for our integration by parts formula, and enables us to split the problem up over sub-domains. We have the following mapping property of W_{le} (from [19]) for an open surface Γ

$$W_{le} : \tilde{\boldsymbol{H}}^{1/2}(\Gamma) \to \boldsymbol{H}^{-1/2}(\Gamma).$$

As in the mortar BEM situation of Chapter 4 we need to assume more regularity of the given function $\boldsymbol{g}$ than in a standard formulation. In (6.10) we had $\boldsymbol{g} \in \boldsymbol{H}^{1/2}(\Gamma)$, however for our mortar method we shall require $\boldsymbol{g} \in \boldsymbol{L}^2(\Gamma)$, as was the case in Chapter 4. A standard boundary element formulation would be to multiply the hypersingular integral equation (6.10) by an appropriate test function and integrate over the boundary to get: *Find* $\boldsymbol{\phi}(x) \in \tilde{\boldsymbol{H}}^{1/2}(\Gamma)$ *such that*

$$\langle W_{le}\boldsymbol{\phi}(x), \boldsymbol{\psi}(x)\rangle_\Gamma = \langle \boldsymbol{g}(x), \boldsymbol{\psi}(x)\rangle_\Gamma \qquad \forall \boldsymbol{\psi}(x) \in \tilde{\boldsymbol{H}}^{1/2}(\Gamma). \tag{6.11}$$

Sub-domain decomposition, meshes and discrete spaces

The same notation and conventions that have been used previously to describe the sub-domain decomposition, meshes and discrete spaces shall be used in this chapter. For details see Chapter 4, in particular for details on sub-domain decomposition see Section 4.1.2 and for details on meshes and discrete spaces see Section 4.2.1. We shall introduce two new discrete spaces which are simply product spaces of already defined spaces from Chapter 4:

$$\boldsymbol{X}_h = (X_h)^3 \text{ and } \boldsymbol{M}_k = (M_k)^3.$$

The space X_h was defined in (4.7) and (4.8), and the space M_k was defined in (4.9) and (4.10).

6.1.3 Integration By Parts Formula

As in Chapter 4 we wish to reformulate our hypersingular integral equation in terms of weakly singular integrals and appropriate derivatives. As before we require an integration by parts formula for this and importantly we require knowledge of the boundary term which this integration by parts introduces for our interface matching condition.

To begin, let us define the differential operator (as in [27]), which are the Günter derivatives (see e.g. [32]) in matrix form for $x \in \Gamma$

$$\boldsymbol{\mathcal{M}}^{\Gamma}(\partial_x, \boldsymbol{n}(x)) = (\mathcal{M}^{\Gamma}_{ij}(\partial_x, \boldsymbol{n}(x)))_{3\times 3}. \tag{6.12}$$

The superscript shows restriction of function to the domain and shall be useful later when defining functions over sub-domains (in the same way that we used a subscript in Section 2.3.1). In (6.12) we have the Günter derivatives

$$\mathcal{M}^{\Gamma}_{ij}(\partial_x, \boldsymbol{n}(x)) = n_j(x)\frac{\partial}{\partial x_i} - n_i(x)\frac{\partial}{\partial x_j}. \tag{6.13}$$

We can now write the following operators

$$\begin{aligned}
\mathcal{M}^{\Gamma}_{11}(\partial_x, \boldsymbol{n}(x)) &= \mathcal{M}^{\Gamma}_{22}(\partial_x, \boldsymbol{n}(x)) = \mathcal{M}^{\Gamma}_{33}(\partial_x, \boldsymbol{n}(x)) = 0 \\
\mathcal{M}^{\Gamma}_{32}(\partial_x, \boldsymbol{n}(x)) &= -\mathcal{M}^{\Gamma}_{23}(\partial_x, \boldsymbol{n}(x)) = \frac{\partial}{\partial \boldsymbol{S}^{\Gamma}_1(x)} \\
\mathcal{M}^{\Gamma}_{13}(\partial_x, \boldsymbol{n}(x)) &= -\mathcal{M}^{\Gamma}_{31}(\partial_x, \boldsymbol{n}(x)) = \frac{\partial}{\partial \boldsymbol{S}^{\Gamma}_2(x)} \\
\mathcal{M}^{\Gamma}_{21}(\partial_x, \boldsymbol{n}(x)) &= -\mathcal{M}^{\Gamma}_{12}(\partial_x, \boldsymbol{n}(x)) = \frac{\partial}{\partial \boldsymbol{S}^{\Gamma}_3(x)}.
\end{aligned}$$

Where

$$\begin{aligned}
\boldsymbol{S}^{\Gamma}_1(x) &= (0, -n_3(x), n_2(x))^T \qquad x \in \Gamma \\
\boldsymbol{S}^{\Gamma}_2(x) &= (n_3(x), 0, -n_1(x))^T \qquad x \in \Gamma \\
\boldsymbol{S}^{\Gamma}_3(x) &= (-n_2(x), n_1(x), 0)^T \qquad x \in \Gamma.
\end{aligned}$$

We note that $\boldsymbol{\mathcal{M}}^{\Gamma}(\partial_x, \boldsymbol{n}(x))$ can be expressed in matrix form as

$$\begin{pmatrix} 0 & -\frac{\partial}{\partial \boldsymbol{S}_3^{\Gamma}} & \frac{\partial}{\partial \boldsymbol{S}_2^{\Gamma}} \\ \frac{\partial}{\partial \boldsymbol{S}_3^{\Gamma}} & 0 & -\frac{\partial}{\partial \boldsymbol{S}_1^{\Gamma}} \\ -\frac{\partial}{\partial \boldsymbol{S}_2^{\Gamma}} & \frac{\partial}{\partial \boldsymbol{S}_1^{\Gamma}} & 0 \end{pmatrix}. \tag{6.14}$$

Following Han [27] we let $\boldsymbol{\phi}(x) = (\phi_1(x), \phi_2(x), \phi_3(x))^T$ and $\boldsymbol{\psi}(x) = (\psi_1(x), \psi_2(x), \psi_3(x))^T$ be the traces of $\boldsymbol{u}(x) = (u_1(x), u_2(x), u_3(x))^T$ and $\boldsymbol{v}(x) = (v_1(x), v_2(x), v_3(x))^T$ respectively. We present the following lemma as the proof gives us an indication as to where our boundary term in the integration by parts formula will come from.

Lemma 6.2. *[27, equation (3.12)] For a closed surface Γ and functions $\boldsymbol{\phi}, \boldsymbol{\psi} \in \boldsymbol{H}^{1/2}(\Gamma)/_{\mathcal{R}}$, we have the following identity*

$$\begin{aligned} \langle W_{le}\boldsymbol{\phi}, \boldsymbol{\psi}\rangle_{\Gamma} = & \int_{\Gamma}\int_{\Gamma} \frac{\mu}{4\pi}\frac{1}{|x-y|}\left(\sum_{k=1}^{3}\frac{\partial \boldsymbol{\psi}(x)}{\partial \boldsymbol{S}_k^{\Gamma}(x)}\cdot\frac{\partial \boldsymbol{\phi}(y)}{\partial \boldsymbol{S}_k^{\Gamma}(y)}\right) dS_y dS_x \\ & + \int_{\Gamma}\int_{\Gamma} (\boldsymbol{\mathcal{M}}^{\Gamma}(\partial_x, \boldsymbol{n}(x))\boldsymbol{\psi}(x))^T \left(\frac{\mu}{2\pi} I \frac{1}{|x-y|}\right. \\ & \qquad \left. -4\mu^2 \boldsymbol{U}^*(x-y)\right) \boldsymbol{\mathcal{M}}^{\Gamma}(\partial_y, \boldsymbol{n}(y))\boldsymbol{\phi}(y)\, dS_y dS_x \\ & + \int_{\Gamma}\int_{\Gamma} \frac{\mu}{4\pi}\sum_{i,j,k=1}^{3} (\mathcal{M}_{kj}^{\Gamma}(\partial_x, \boldsymbol{n}(x))\psi_i(x))\frac{1}{|x-y|}(\mathcal{M}_{ki}^{\Gamma}(\partial_y, \boldsymbol{n}(y))\phi_j(y))\, dS_y dS_x. \end{aligned} \tag{6.15}$$

Proof. We now refer back to the model problem (6.11) and see that this can be expressed as

$$\langle W_{le}\boldsymbol{\phi}, \boldsymbol{\psi}\rangle_{\Gamma} = -\int_{\Gamma} (\boldsymbol{T}(\partial_x, \boldsymbol{n}(x))\boldsymbol{u}(x)) \cdot \boldsymbol{\psi}(x) dS_x. \tag{6.16}$$

In the above $\boldsymbol{u}$ can be replaced by the double-layer potential defined in (6.9). The stress operator defined in (6.2) and (6.3) can be re-expressed as [27, equation (2.12)]

$$\begin{aligned} \boldsymbol{T}(\partial_x, \boldsymbol{n}(x))\boldsymbol{u}(x) &= \sum_{k=1}^{3}\frac{\partial}{\partial \boldsymbol{S}_k^{\Gamma}(x)}\int_{\Gamma}\frac{\mu}{4\pi}\frac{1}{|x-y|}\frac{\partial \boldsymbol{\phi}(y)}{\partial \boldsymbol{S}_k^{\Gamma}(y)} dS_y \\ &+ \boldsymbol{\mathcal{M}}^{\Gamma}(\partial_x, \boldsymbol{n}(x))\int_{\Gamma}\left(4\mu^2 \boldsymbol{U}^*(x-y)\right. \\ &\qquad \left. -\frac{\mu}{2\pi} I \frac{1}{|x-y|}\right)\boldsymbol{\mathcal{M}}^{\Gamma}(\partial_y, \boldsymbol{n}(y))\boldsymbol{\phi}(y) dS_y \\ &- \frac{\mu}{4\pi}\int_{\Gamma}\left[\boldsymbol{\mathcal{M}}^{\Gamma}(\partial_x, \boldsymbol{n}(x))\frac{1}{|x-y|}\boldsymbol{\mathcal{M}}^{\Gamma}(\partial_y, \boldsymbol{n}(y))\right]^T \boldsymbol{\phi}(y) dS_y. \end{aligned} \tag{6.17}$$

We recall that $\boldsymbol{U}^*(x-y)$ is the fundamental solution matrix of the Navier system as defined in (6.7) and (6.8). Now substituting (6.16) into (6.17) we get the following representation

$$\langle W_{le}\boldsymbol{\phi},\boldsymbol{\psi}\rangle_\Gamma =$$

$$-\int_\Gamma \left(\sum_{k=1}^{3}\frac{\partial}{\partial \boldsymbol{S}_k^\Gamma(x)}\int_\Gamma \frac{\mu}{4\pi}\frac{1}{|x-y|}\frac{\partial\boldsymbol{\phi}(y)}{\partial \boldsymbol{S}_k^\Gamma(y)}\,dS_y\right)\cdot\boldsymbol{\psi}(x)\,dS_x \tag{6.18}$$

$$-\int_\Gamma \boldsymbol{\mathcal{M}}^\Gamma(\partial_x,\boldsymbol{n}(x))\int_\Gamma \big(4\mu^2\boldsymbol{U}^*(x-y) \tag{6.19}$$

$$-\frac{\mu}{2\pi}I\frac{1}{|x-y|}\Big)\boldsymbol{\mathcal{M}}^\Gamma(\partial_y,\boldsymbol{n}(y))\boldsymbol{\phi}(y)\,dS_y\cdot\boldsymbol{\psi}(x)\,dS_x \tag{6.20}$$

$$+\int_\Gamma\frac{\mu}{4\pi}\int_\Gamma\left[\boldsymbol{\mathcal{M}}^\Gamma(\partial_x,\boldsymbol{n}(x))\frac{1}{|x-y|}\boldsymbol{\mathcal{M}}^\Gamma(\partial_y,\boldsymbol{n}(y))\right]^T\boldsymbol{\phi}(y)\,dS_y\cdot\boldsymbol{\psi}(x)\,dS_x. \tag{6.21}$$

Finally integrating by parts (using Stokes Theorem, see [32, Lemma 2.2.3] for details) we get the stated result [27, equation (3.12)]. □

We now need to define this integration by parts and discern the relevant boundary terms, it is obvious that when we apply Stokes Theorem the required boundary term will appear (given suitable boundary conditions and suitable continuity of the functions). We also clearly see that the integration by parts is applied term by term, so we can examine each of the three terms in order once we have defined the integration by parts formula.

Now from [39] we have that for a scalar function $\psi_i(x)$ (surface differential operators as defined in Section 2.3.1)

$$\frac{\partial\psi_i(x)}{\partial\boldsymbol{S}_k^\Gamma(x)} = (\boldsymbol{n}(x)\times\operatorname{grad}_\Gamma\psi_i(x))_k = (\mathbf{curl}_\Gamma\,\psi_i(x))_k. \tag{6.22}$$

We can now use this to get an integration by parts formula.

Lemma 6.3. *For an open surface Γ, scalars a, b and the normal (to the boundary $\partial\Gamma$) vector $\boldsymbol{n}$ we have*

$$-\int_\Gamma\frac{\partial a}{\partial\boldsymbol{S}_k^\Gamma}b = \int_\Gamma\frac{\partial b}{\partial\boldsymbol{S}_k^\Gamma}a + \int_{\partial\Gamma}abn_k. \tag{6.23}$$

Proof. For scalars a, b and the normal vector $\boldsymbol{n}$ we have

$$\begin{aligned}\operatorname{grad}\times(ab\boldsymbol{n}) &= \operatorname{grad}ab\times\boldsymbol{n} + ab\operatorname{grad}\times\boldsymbol{n}\\ &= \operatorname{grad}ab\times\boldsymbol{n}\end{aligned}$$

$$
\begin{aligned}
&= (a \operatorname{grad} b + b \operatorname{grad} a) \times \boldsymbol{n} \\
&= a \operatorname{grad} b \times \boldsymbol{n} + b \operatorname{grad} a \times \boldsymbol{n} \\
&= -(\boldsymbol{n} \times \operatorname{grad} b)a - (\boldsymbol{n} \times \operatorname{grad} a)b. \qquad (6.24)
\end{aligned}
$$

Now by Stokes Theorem, which states for a vector valued function $\boldsymbol{F}$

$$\int_\Gamma \operatorname{grad} \times \boldsymbol{F} = \int_{\partial\Gamma} \boldsymbol{F}. \qquad (6.25)$$

We have combining (6.24) and (6.25) that

$$\int_\Gamma -(\boldsymbol{n} \times \operatorname{grad} b)a - (\boldsymbol{n} \times \operatorname{grad} a)b = \int_\Gamma \operatorname{grad} \times (ab\boldsymbol{n}) = \int_{\partial\Gamma} ab\boldsymbol{n}. \qquad (6.26)$$

Now examining the k^{th} component of (6.26) we get the following integration by parts formula

$$\int_\Gamma -(\boldsymbol{n} \times \operatorname{grad} b)_k a - (\boldsymbol{n} \times \operatorname{grad} a)_k b = \int_{\partial\Gamma} ab n_k. \qquad (6.27)$$

We can alternatively express (6.27) as an integration by parts formula of the form claimed by an application of (6.22). □

Lemma 6.4. *Let Γ be an open surface and $\boldsymbol{\phi}, \boldsymbol{\psi}$ sufficiently smooth. For our integration by parts formula applied to (6.18) we have:*

$$
\begin{aligned}
&-\int_\Gamma \left(\sum_{k=1}^{3} \frac{\partial}{\partial \boldsymbol{S}_k^\Gamma(x)} \int_\Gamma \frac{\mu}{4\pi} \frac{1}{|x-y|} \frac{\partial \boldsymbol{\phi}(y)}{\partial \boldsymbol{S}_k^\Gamma(y)} \, dS_y \right) \cdot \boldsymbol{\psi}(x) \, dS_x \\
&\qquad = \int_\Gamma \int_\Gamma \frac{\mu}{4\pi} \frac{1}{|x-y|} \left(\sum_{k=1}^{3} \frac{\partial \boldsymbol{\psi}(x)}{\partial \boldsymbol{S}_k^\Gamma(x)} \cdot \frac{\partial \boldsymbol{\phi}(y)}{\partial \boldsymbol{S}_k^\Gamma(y)} \right) dS_y dS_x \\
&\qquad\qquad + \sum_{k=1}^{3} \int_{\partial\Gamma} \mu V \left(\frac{\partial \boldsymbol{\phi}(x)}{\partial \boldsymbol{S}_k^\Gamma(x)} \right) \boldsymbol{\psi}(x) n_k(x) \, ds. \qquad (6.28)
\end{aligned}
$$

Proof. We let a and b in (6.23) be defined by

$$a = \int_\Gamma \frac{\mu}{4\pi} \frac{1}{|x-y|} \frac{\partial \phi_i(y)}{\partial \boldsymbol{S}_k^\Gamma(y)} \, dS_y \text{ and } b = \psi_i(x).$$

We thus get from our integration by parts formula (6.23) applied to (6.18) that

$$-\int_\Gamma \frac{\partial}{\partial \boldsymbol{S}_k^\Gamma(x)} \int_\Gamma \frac{\mu}{4\pi} \frac{1}{|x-y|} \frac{\partial \phi_i(y)}{\partial \boldsymbol{S}_k^\Gamma(y)} \, dS_y \psi_i(x) \, dS_x$$

$$= \int_\Gamma \int_\Gamma \frac{\mu}{4\pi} \frac{1}{|x-y|} \frac{\partial \psi_i(x)}{\partial \boldsymbol{S}_k^\Gamma(x)} \frac{\partial \phi_i(y)}{\partial \boldsymbol{S}_k^\Gamma(y)} \, dS_y dS_x + \int_{\partial\Gamma} \int_\Gamma \frac{\mu}{4\pi} \frac{1}{|x-y|} \frac{\partial \phi_i(y)}{\partial \boldsymbol{S}_k^\Gamma(y)} \, dS_y . \psi_i(x) n_k(x) \, ds.$$

We can now sum over i and k to gives the stated result. □

Let us define the following matrix:

$$\boldsymbol{N} = \begin{pmatrix} 0 & -n_3 & n_2 \\ n_3 & 0 & -n_1 \\ -n_2 & n_1 & 0 \end{pmatrix}. \tag{6.29}$$

We note the similarity of the above matrix (6.29) to the matrix $\boldsymbol{\mathcal{M}}^\Gamma$ defined in (6.14).

Lemma 6.5. *Let Γ be an open surface and $\boldsymbol{\phi}, \boldsymbol{\psi}$ sufficiently smooth. For our integration by parts formula applied to (6.20) we have*

$$\begin{aligned} -\int_\Gamma \boldsymbol{\mathcal{M}}^\Gamma(\partial_x, \boldsymbol{n}(x)) \int_\Gamma \big(& 4\mu^2 \boldsymbol{U}^*(x-y) \\ & - \frac{\mu}{2\pi} I \frac{1}{|x-y|} \Big) \boldsymbol{\mathcal{M}}^\Gamma(\partial_y, \boldsymbol{n}(y)) \boldsymbol{\phi}(y) \, dS_y \cdot \boldsymbol{\psi}(x) \, dS_x \\ = \int_\Gamma \int_\Gamma & (\boldsymbol{\mathcal{M}}^\Gamma(\partial_x, \boldsymbol{n}(x)) \boldsymbol{\psi}(x))^T \left(\frac{\mu}{2\pi} \boldsymbol{I} \frac{1}{|x-y|} \right. \\ & \left. - 4\mu^2 \boldsymbol{U}^*(x-y) \big) \boldsymbol{\mathcal{M}}^\Gamma(\partial_y, \boldsymbol{n}(y)) \boldsymbol{\phi}(y) \, dS_y dS_x \right. \\ + \int_{\partial\Gamma} & (\boldsymbol{N} \boldsymbol{\psi}(x))^T \left(\int_\Gamma \big(4\mu^2 \boldsymbol{U}^*(x-y) \right. \\ & \left. - \frac{\mu}{2\pi} \boldsymbol{I} \frac{1}{|x-y|} \Big) \boldsymbol{\mathcal{M}}^\Gamma(\partial_y, \boldsymbol{n}(y)) \boldsymbol{\phi}(y) \, dS_y \right) ds. \end{aligned} \tag{6.30}$$

Proof. For vectors $\boldsymbol{A} = (A_1, A_2, A_3)^T$ and $\boldsymbol{\psi} = (\psi_1, \psi_2, \psi_3)^T$ where $\boldsymbol{A}$ is given by

$$\boldsymbol{A} = \int_\Gamma \left(4\mu^2 \boldsymbol{U}^*(x-y) - \frac{\mu}{2\pi} I \frac{1}{|x-y|} \right) \boldsymbol{\mathcal{M}}(\partial_y, \boldsymbol{n}(y)) \boldsymbol{\phi}(y) \, dS_y. \tag{6.31}$$

We have with the use of our integration by parts formula (6.23) and the definition of the matrix $\boldsymbol{\mathcal{M}}^\Gamma(\partial_x, \boldsymbol{n}(x))$ (see (6.14)) the following

$$-\int_\Gamma \boldsymbol{\mathcal{M}}^\Gamma(\partial_x, \boldsymbol{n}(x)) \boldsymbol{A} \cdot \boldsymbol{\psi} \, dS_x = -\int_\Gamma \begin{pmatrix} 0 & -\frac{\partial}{\partial \boldsymbol{S}_3^\Gamma} & \frac{\partial}{\partial \boldsymbol{S}_2^\Gamma} \\ \frac{\partial}{\partial \boldsymbol{S}_3^\Gamma} & 0 & -\frac{\partial}{\partial \boldsymbol{S}_1^\Gamma} \\ -\frac{\partial}{\partial \boldsymbol{S}_2^\Gamma} & \frac{\partial}{\partial \boldsymbol{S}_1^\Gamma} & 0 \end{pmatrix} \begin{pmatrix} A_1 \\ A_2 \\ A_3 \end{pmatrix} \cdot \begin{pmatrix} \psi_1 \\ \psi_2 \\ \psi_3 \end{pmatrix} dS_x$$

$$
\begin{aligned}
&= -\int_\Gamma \begin{pmatrix} -\frac{\partial A_2}{\partial \boldsymbol{S}_3^\Gamma} + \frac{\partial A_3}{\partial \boldsymbol{S}_2^\Gamma} \\ \frac{\partial A_1}{\partial \boldsymbol{S}_3^\Gamma} - \frac{\partial A_3}{\partial \boldsymbol{S}_1^\Gamma} \\ -\frac{\partial A_1}{\partial \boldsymbol{S}_2^\Gamma} + \frac{\partial A_2}{\partial \boldsymbol{S}_1^\Gamma} \end{pmatrix} \cdot \begin{pmatrix} \psi_1 \\ \psi_2 \\ \psi_3 \end{pmatrix} dS_x \\
&= -\int_\Gamma \left(-\frac{\partial A_2}{\partial \boldsymbol{S}_3^\Gamma} + \frac{\partial A_3}{\partial \boldsymbol{S}_2^\Gamma}\right)\psi_1 + \left(\frac{\partial A_1}{\partial \boldsymbol{S}_3^\Gamma} - \frac{\partial A_3}{\partial \boldsymbol{S}_1^\Gamma}\right)\psi_2 + \left(-\frac{\partial A_1}{\partial \boldsymbol{S}_2^\Gamma} + \frac{\partial A_2}{\partial \boldsymbol{S}_1^\Gamma}\right)\psi_3 \, dS_x \\
&= \int_\Gamma \frac{\partial A_2}{\partial \boldsymbol{S}_3^\Gamma}\psi_1 - \frac{\partial A_3}{\partial \boldsymbol{S}_2^\Gamma}\psi_1 - \frac{\partial A_1}{\partial \boldsymbol{S}_3^\Gamma}\psi_2 + \frac{\partial A_3}{\partial \boldsymbol{S}_1^\Gamma}\psi_2 + \frac{\partial A_1}{\partial \boldsymbol{S}_2^\Gamma}\psi_3 - \frac{\partial A_2}{\partial \boldsymbol{S}_1^\Gamma}\psi_3 \, dS_x \\
&= \int_\Gamma -\frac{\partial \psi_1}{\partial \boldsymbol{S}_3^\Gamma}A_2 + \frac{\partial \psi_1}{\partial \boldsymbol{S}_2^\Gamma}A_3 + \frac{\partial \psi_2}{\partial \boldsymbol{S}_3^\Gamma}A_1 - \frac{\partial \psi_2}{\partial \boldsymbol{S}_1^\Gamma}A_3 - \frac{\partial \psi_3}{\partial \boldsymbol{S}_2^\Gamma}A_1 + \frac{\partial \psi_3}{\partial \boldsymbol{S}_1^\Gamma}A_2 \, dS_x \\
&+ \int_{\partial\Gamma} -\psi_1 A_2 \boldsymbol{n}_3 + \psi_1 A_3 \boldsymbol{n}_2 + \psi_2 A_1 \boldsymbol{n}_3 - \psi_2 A_3 \boldsymbol{n}_1 - \psi_3 A_1 \boldsymbol{n}_2 + \psi_3 A_2 \boldsymbol{n}_1 \, ds \\
&= -\int_\Gamma \begin{pmatrix} -\frac{\partial \psi_2}{\partial \boldsymbol{S}_3^\Gamma} + \frac{\partial \psi_3}{\partial \boldsymbol{S}_2^\Gamma} \\ \frac{\partial \psi_1}{\partial \boldsymbol{S}_3^\Gamma} - \frac{\partial \psi_3}{\partial \boldsymbol{S}_1^\Gamma} \\ -\frac{\partial \psi_1}{\partial \boldsymbol{S}_2^\Gamma} + \frac{\partial \psi_2}{\partial \boldsymbol{S}_1^\Gamma} \end{pmatrix} \cdot \begin{pmatrix} A_1 \\ A_2 \\ A_3 \end{pmatrix} dS_x + \int_{\partial\Gamma} (\boldsymbol{N}\psi(x))^T \boldsymbol{A} \, ds \\
&= \int_\Gamma (\boldsymbol{\mathcal{M}}^\Gamma(\partial_x, \boldsymbol{n}(x))\boldsymbol{\psi}(x))^T \cdot \boldsymbol{A} \, dS_x + \int_{\partial\Gamma} (\boldsymbol{N}\boldsymbol{\psi}(x))^T \boldsymbol{A} \, ds.
\end{aligned}
$$

Which gives the stated result. □

Lemma 6.6. *Let Γ be an open surface and $\boldsymbol{\phi}, \boldsymbol{\psi}$ sufficiently smooth. For our integration by parts formula applied to (6.21) we have*

$$
\begin{aligned}
&\int_\Gamma \frac{\mu}{4\pi} \int_\Gamma \left[\boldsymbol{\mathcal{M}}^\Gamma(\partial_x, \boldsymbol{n}(x)) \frac{1}{|x-y|} \boldsymbol{\mathcal{M}}^\Gamma(\partial_y, \boldsymbol{n}(y))\right]^T \boldsymbol{\phi}(y) \, dS_y \cdot \boldsymbol{\psi}(x) \, dS_x \\
&\quad = \int_\Gamma \int_\Gamma \frac{\mu}{4\pi} \sum_{i,j,k=1}^{3} (\mathcal{M}_{kj}^\Gamma(\partial_x, \boldsymbol{n}(x))\psi_i(x)) \frac{1}{|x-y|} (\mathcal{M}_{ki}^\Gamma(\partial_y, \boldsymbol{n}(y))\phi_j(y)) \, dS_y dS_x \\
&\qquad + \int_{\partial\Gamma} \sum_{i,j,k=1}^{3} \psi_i(x) \left(\int_\Gamma \frac{\mu}{4\pi} \frac{1}{|x-y|} (\mathcal{M}_{ki}^\Gamma(\partial_y, \boldsymbol{n}(y))\phi_j(y)) \, dS_y\right) \boldsymbol{N}_{ij} \, ds. \quad (6.32)
\end{aligned}
$$

Proof. Similar expansions to those used in the examination of the second term before give us the stated result. □

Integration by parts formula

We now introduce our integration by parts formula for the open surface Γ.

Lemma 6.7. *Let Γ be an open surface and $\boldsymbol{\phi}, \boldsymbol{\psi}$ sufficiently smooth functions. We have the following integration by parts formula*

$$
\begin{aligned}
&-\int_\Gamma \left(\sum_{k=1}^{3} \frac{\partial}{\partial \boldsymbol{S}_k^\Gamma(x)} \int_\Gamma \frac{\mu}{4\pi} \frac{1}{|x-y|} \frac{\partial \boldsymbol{\phi}(y)}{\partial \boldsymbol{S}_k^\Gamma(y)} \, dS_y \right) \cdot \boldsymbol{\psi}(x) \, dS_x \\
&\quad - \int_\Gamma \boldsymbol{\mathcal{M}}^\Gamma(\partial_x, \boldsymbol{n}(x)) \int_\Gamma \Big(4\mu^2 \boldsymbol{U}^*(x-y) \\
&\qquad - \frac{\mu}{2\pi} \boldsymbol{I} \frac{1}{|x-y|} \Big) \boldsymbol{\mathcal{M}}^\Gamma(\partial_y, \boldsymbol{n}(y)) \boldsymbol{\phi}(y) \, dS_y \cdot \boldsymbol{\psi}(x) \, dS_x \\
&\quad + \int_\Gamma \frac{\mu}{4\pi} \int_\Gamma \left[\boldsymbol{\mathcal{M}}^\Gamma(\partial_x, \boldsymbol{n}(x)) \frac{1}{|x-y|} \boldsymbol{\mathcal{M}}^\Gamma(\partial_y, \boldsymbol{n}(y)) \right]^T \boldsymbol{\phi}(y) \, dS_y \cdot \boldsymbol{\psi}(x) \, dS_x \\
&= \int_\Gamma \int_\Gamma \frac{\mu}{4\pi} \frac{1}{|x-y|} \left(\sum_{k=1}^{3} \frac{\partial \boldsymbol{\psi}(x)}{\partial \boldsymbol{S}_k^\Gamma(x)} \cdot \frac{\partial \boldsymbol{\phi}(y)}{\partial \boldsymbol{S}_k^\Gamma(y)} \right) dS_y dS_x \\
&\quad + \int_\Gamma \int_\Gamma (\boldsymbol{\mathcal{M}}^\Gamma(\partial_x, \boldsymbol{n}(x)) \boldsymbol{\psi}(x))^T \left(\frac{\mu}{2\pi} I \frac{1}{|x-y|} \right. \\
&\qquad \left. - 4\mu^2 \Gamma(x-y) \right) \boldsymbol{\mathcal{M}}^\Gamma(\partial_y, \boldsymbol{n}(y)) \boldsymbol{\phi}(y) \, dS_y dS_x \\
&\quad + \int_\Gamma \int_\Gamma \frac{\mu}{4\pi} \sum_{i,j,k=1}^{3} (\mathcal{M}_{kj}^\Gamma(\partial_x, \boldsymbol{n}(x)) \psi_i(x)) \frac{1}{|x-y|} (\mathcal{M}_{ki}^\Gamma(\partial_y, \boldsymbol{n}(y)) \phi_j(y)) \, dS_y dS_x \\
&\qquad + \sum_{k=1}^{3} \int_{\partial\Gamma} \mu V \left(\frac{\partial \boldsymbol{\phi}(y)}{\partial \boldsymbol{S}_k^\Gamma(y)} \right) \boldsymbol{\psi}(x) n_k(x) \, dS_y ds \\
&\qquad + \int_{\partial\Gamma} (\boldsymbol{N}\boldsymbol{\psi}(x))^T \left(\int_\Gamma \left(4\mu^2 \boldsymbol{U}^*(x-y) - \frac{\mu}{2\pi} \boldsymbol{I} \frac{1}{|x-y|} \right) \boldsymbol{\mathcal{M}}^\Gamma(\partial_y, \boldsymbol{n}(y)) \boldsymbol{\phi}(y) \, dS_y \right) ds \\
&\qquad + \int_{\partial\Gamma} \sum_{i,j,k=1}^{3} \psi_i(x) \left(\int_\Gamma \frac{\mu}{4\pi} \frac{1}{|x-y|} (\mathcal{M}_{ki}^\Gamma(\partial_y, \boldsymbol{n}(y)) \phi_j(y)) \, dS_y \right) \boldsymbol{N}_{ij} \, ds.
\end{aligned}
$$

Proof. Bringing the three parts (6.28), (6.30), and (6.32) together we get the stated representation of the bilinear form defined in (6.16). This is exactly an integration by parts formula which can be used to transform (6.18-6.21) into (6.15) with an appropriate boundary term (subject to appropriate boundary conditions and continuity of the functions). □

If we now apply this integration by parts formula (6.23) on sub-domains instead of over the whole domain, and take into account the jump of the function across an interface as before in the case of the Laplacian (see (4.3)) we now arrive at our bilinear forms $a(\cdot,\cdot)$ and $b(\cdot,\cdot)$.

We now have the following, which is defined over the decomposition of all the subdomains, for sufficiently smooth $\boldsymbol{\psi}$ and $\boldsymbol{\phi}$

$$\begin{aligned}
\langle W_{le}\boldsymbol{\phi},\boldsymbol{\psi}\rangle_\Gamma &= \int_{\mathcal{T}}\int_\Gamma \frac{\mu}{4\pi}\frac{1}{|x-y|}\left(\sum_{k=1}^{3}\frac{\partial\boldsymbol{\psi}(x)}{\partial\boldsymbol{S}_k^H(x)}\cdot\frac{\partial\boldsymbol{\phi}(y)}{\partial\boldsymbol{S}_k^\Gamma(y)}\right)dS_y dS_x && (6.33)\\
&+\int_{\mathcal{T}}\int_\Gamma(\boldsymbol{\mathcal{M}}^H(\partial_x,\boldsymbol{n}(x)\boldsymbol{\psi}(x)))^T\left(\frac{\mu}{2\pi}\boldsymbol{I}\frac{1}{|x-y|}\right.\\
&\qquad\left.-4\mu^2\boldsymbol{U}^*(x-y)\right)\boldsymbol{\mathcal{M}}^\Gamma(\partial_y,\boldsymbol{n}(y))\boldsymbol{\phi}(y)\,dS_y dS_x && (6.34)\\
&+\int_{\mathcal{T}}\int_\Gamma\frac{\mu}{4\pi}\sum_{i,j,k=1}^{3}(\mathcal{M}_{kj}^H(\partial_x,\boldsymbol{n}(x))\psi_i(x))\\
&\qquad\frac{1}{|x-y|}(\mathcal{M}_{ki}^\Gamma(\partial_y,\boldsymbol{n}(y))\phi_j(y))\,dS_y dS_x && (6.35)\\
&\sum_{k=1}^{3}\int_\tau\frac{\mu}{4\pi}\int_\Gamma\frac{1}{|x-y|}\left(\frac{\partial\boldsymbol{\phi}(y)}{\partial\boldsymbol{S}_k^\Gamma(y)}\right)[\boldsymbol{\psi}(x)]n_k(x)\,dS_y ds && (6.36)\\
&+\int_\tau(\boldsymbol{N}[\boldsymbol{\psi}(x)])^T\left(\int_\Gamma\left(4\mu^2\boldsymbol{U}^*(x-y)\right.\right.\\
&\qquad\left.\left.-\frac{\mu}{2\pi}\boldsymbol{I}\frac{1}{|x-y|}\right)\boldsymbol{\mathcal{M}}^\Gamma(\partial_y,\boldsymbol{n}(y))\boldsymbol{\phi}(y)\,dS_y\right)ds && (6.37)\\
&+\int_\tau\sum_{i,j,k=1}^{3}[\psi_i(x)]\left(\int_\Gamma\frac{\mu}{4\pi}\frac{1}{|x-y|}(\mathcal{M}_{ki}^\Gamma(\partial_y,\boldsymbol{n}(y))\phi_j(y))\,dS_y\right)\boldsymbol{N}_{ij}\,ds. && (6.38)
\end{aligned}$$

We shall now re-express this in terms more appropriate for analysis to take place. We use the following notation

$$\frac{\partial\phi_j}{\partial\boldsymbol{S}_k^H}=\sum_{i=1}^{N}\left(\frac{\partial\phi_j|_{\Gamma_i}}{\partial\boldsymbol{S}_k^{\Gamma_i}}\right)^0=\sum_{i=1}^{N}(\mathbf{curl}_{\Gamma_i}\,\phi_j|_{\Gamma_i})_k^0=(\mathbf{curl}_{\mathrm{H}}\,\phi_j)_k.$$

To start we examine (6.33). We recall that $\boldsymbol{\psi}(x)=(\psi_1(x),\psi_2(x),\psi_3(x))^T$ so we have that

$$\frac{\partial\boldsymbol{\psi}(x)}{\partial\boldsymbol{S}_k^H(x)}=\left(\frac{\partial\psi_1(x)}{\partial\boldsymbol{S}_k^H(x)},\frac{\partial\psi_2(x)}{\partial\boldsymbol{S}_k^H(x)},\frac{\partial\psi_3(x)}{\partial\boldsymbol{S}_k^H(x)}\right)^T.$$

We also note that using a result from [39, Section 6.2] we get the following:

$$\sum_{k=1}^{3}\frac{\partial\boldsymbol{\psi}}{\partial\boldsymbol{S}_k^H}\cdot\frac{\partial\boldsymbol{\phi}}{\partial\boldsymbol{S}_k^H}=\sum_{k=1}^{3}(\mathbf{curl}_{\mathrm{H}}\,\boldsymbol{\psi})_k\cdot(\mathbf{curl}_{\mathrm{H}}\,\boldsymbol{\phi})_k$$

$$
\begin{aligned}
&= \sum_{k=1}^{3} \begin{pmatrix} (\mathbf{curl}_{\mathrm{H}}\,\psi_1)_k \\ (\mathbf{curl}_{\mathrm{H}}\,\psi_2)_k \\ (\mathbf{curl}_{\mathrm{H}}\,\psi_3)_k \end{pmatrix} \cdot \begin{pmatrix} (\mathbf{curl}_{\mathrm{H}}\,\phi_1)_k \\ (\mathbf{curl}_{\mathrm{H}}\,\phi_2)_k \\ (\mathbf{curl}_{\mathrm{H}}\,\phi_3)_k \end{pmatrix} \\
&= \sum_{i=1}^{3} (\mathbf{curl}_{\mathrm{H}}\,\psi_i) \cdot (\mathbf{curl}_{\mathrm{H}}\,\phi_i). \qquad (6.39)
\end{aligned}
$$

We now have that

$$
\int_{\mathcal{T}} \int_{\Gamma} \frac{\mu}{4\pi} \frac{1}{|x-y|} \left(\sum_{k=1}^{3} \frac{\partial \boldsymbol{\psi}(x)}{\partial \boldsymbol{S}_k^H(x)} \cdot \frac{\partial \boldsymbol{\phi}(y)}{\partial \boldsymbol{S}_k^{\Gamma}(y)} \right) dS_y dS_x = \mu \sum_{i=1}^{3} \langle V\,\mathbf{curl}_{\Gamma}\,\phi_i, \mathbf{curl}_{\mathrm{H}}\,\psi_i \rangle_{\mathcal{T}}. \qquad (6.40)
$$

Where the single layer potential operator for the Laplace equation V was defined in (2.42). This completes our examination of the first term. We now examine the second part of $a(\cdot,\cdot)$ defined by (6.34),

$$
\begin{aligned}
\int_{\mathcal{T}} \int_{\Gamma} (\boldsymbol{\mathcal{M}}^H(\partial_x, \boldsymbol{n}(x))\boldsymbol{\psi}(x))^T \Big(& \frac{\mu}{2\pi} \boldsymbol{I} \frac{1}{|x-y|} \\
& -4\mu^2 \boldsymbol{U}^*(x-y) \Big) \boldsymbol{\mathcal{M}}^{\Gamma}(\partial_y, \boldsymbol{n}(y))\boldsymbol{\phi}(y)\, dS_y dS_x,
\end{aligned}
$$

and we see that this term must be further split into two parts for analysis to take place. We first examine

$$
\int_{\mathcal{T}} \int_{\Gamma} (\boldsymbol{\mathcal{M}}^H(\partial_x, \boldsymbol{n}(x))\boldsymbol{\psi}(x))^T \left(\frac{\mu}{2\pi} \boldsymbol{I} \frac{1}{|x-y|} \right) \boldsymbol{\mathcal{M}}^{\Gamma}(\partial_y, \boldsymbol{n}(y))\boldsymbol{\phi}(y)\, dS_y dS_x. \qquad (6.41)
$$

We use again a result from [39, Section 6.2] that

$$
\begin{aligned}
&(\boldsymbol{\mathcal{M}}^H(\partial_x, \boldsymbol{n}(x))\boldsymbol{\psi}(x))^T \boldsymbol{\mathcal{M}}^H(\partial_y, \boldsymbol{n}(y))\boldsymbol{\phi}(y) \\
&= \sum_{i,j=1}^{3} (\mathbf{curl}_{\mathrm{H}}\,\psi_i(x))_j (\mathbf{curl}_{\mathrm{H}}\,\phi_i(y))_j - (\mathbf{curl}_{\mathrm{H}}\,\psi_i(x))_j (\mathbf{curl}_{\mathrm{H}}\,\phi_j(y))_i. \qquad (6.42)
\end{aligned}
$$

Combining (6.41) and (6.42) gives us for the first part of the second term in (6.34),

$$
\begin{aligned}
&\int_{\mathcal{T}} \int_{\Gamma} (\boldsymbol{\mathcal{M}}^H(\partial_x, \boldsymbol{n}(x))\boldsymbol{\psi}(x))^T \left(\frac{\mu}{2\pi} \boldsymbol{I} \frac{1}{|x-y|} \right) \boldsymbol{\mathcal{M}}^{\Gamma}(\partial_y, \boldsymbol{n}(y))\boldsymbol{\phi}(y)\, dS_x dS_y \\
&= 2\mu \left(\sum_{i=1}^{3} \langle V\,\mathbf{curl}_{\Gamma}\,\phi_i, \mathbf{curl}_{\mathrm{H}}\,\psi_i \rangle_{\mathcal{T}} - \sum_{i=1}^{3} \langle V\,((\mathbf{curl}_{\Gamma}\,\phi_j)_i)_{j=1}^{3}, \mathbf{curl}_{\mathrm{H}}\,\psi_i \rangle_{\mathcal{T}} \right). \qquad (6.43)
\end{aligned}
$$

We now examine the second part of (6.34). We have

$$\int_{\mathcal{T}}\int_{\Gamma}(\boldsymbol{\mathcal{M}}^{H}(\partial_x,\boldsymbol{n}(x)\boldsymbol{\psi}(x)))^{T}\left(-4\mu^2\boldsymbol{U}^{*}(x-y)\right)\boldsymbol{\mathcal{M}}^{\Gamma}(\partial_y,\boldsymbol{n}(y))\boldsymbol{\phi}(y)\,dS_y dS_x$$

$$=-4\mu^2\langle\boldsymbol{V}_{le}(\boldsymbol{\mathcal{M}}^{\Gamma}(\partial_x,\boldsymbol{n}(x))\boldsymbol{\phi}(x))\boldsymbol{\mathcal{M}}^{H}(\partial_x,\boldsymbol{n}(x))\boldsymbol{\psi}(x)\rangle_{\mathcal{T}}. \tag{6.44}$$

Where $\boldsymbol{V}_{le}$ is the single layer potential operator for linear elasticity. The single layer potential operator for linear elasticity $\boldsymbol{V}_{le}$ is defined as:

$$\boldsymbol{V}_{le}\boldsymbol{\varphi}(x):=\int_{\Gamma}\boldsymbol{U}^{*}(x-y)\boldsymbol{\varphi}(y)\,dS_y.$$

Finally we examine (6.35). We again have from [39, Section 6.2] that

$$\begin{aligned}&\int_{\mathcal{T}}\int_{\Gamma}\frac{\mu}{4\pi}\sum_{i,j,k=1}^{3}(\mathcal{M}^{H}_{kj}(\partial_x,\boldsymbol{n}(x)\psi_i(x)))\frac{1}{|x-y|}(\mathcal{M}^{\Gamma}_{ki}(\partial_y,\boldsymbol{n}(y)\phi_j(y)))\,dS_y dS_x\\&=\mu\left(\sum_{i=1}^{3}\langle V\,\mathbf{curl}_{\Gamma}\,\phi_i,\mathbf{curl}_{\mathrm{H}}\,\psi_i\rangle_{\mathcal{T}}-\sum_{i=1}^{3}\langle V\left((\mathbf{curl}_{\Gamma}\,\phi_j)_j\right)_{j=1}^{3},\left((\mathbf{curl}_{\mathrm{H}}\,\psi_i)_i\right)_{k=1}^{3}\rangle_{\mathcal{T}}\right).\end{aligned} \tag{6.45}$$

We now define our bilinear form $a(\cdot,\cdot)$ by summing together (6.40), (6.43), (6.44), and (6.45) as

$$a(\boldsymbol{\psi},\boldsymbol{\phi})=\sum_{i=1}^{3}\mu\langle V\,\mathbf{curl}_{\mathrm{H}}\,\phi_i,\mathbf{curl}_{\mathrm{H}}\,\psi_i\rangle_{\mathcal{T}} \tag{6.46}$$

$$-\sum_{i=1}^{3}2\mu\langle V\left((\mathbf{curl}_{\mathrm{H}}\,\phi_k)_i\right)_{k=1}^{3},\mathbf{curl}_{\mathrm{H}}\,\psi_i\rangle_{\mathcal{T}} \tag{6.47}$$

$$-4\mu^2\langle\boldsymbol{V}_{le}\boldsymbol{\mathcal{M}}^{H}(\partial_x,\boldsymbol{n}(x))\boldsymbol{\phi},\boldsymbol{\mathcal{M}}^{H}(\partial_x,\boldsymbol{n}(x))\boldsymbol{\psi}\rangle_{\mathcal{T}} \tag{6.48}$$

$$-\mu\sum_{i=1}^{3}\langle V\left((\mathbf{curl}_{\mathrm{H}}\,\phi_j)_j\right)_{j=1}^{3},\left((\mathbf{curl}_{\mathrm{H}}\,\psi_i)_i\right)_{k=1}^{3}\rangle_{\mathcal{T}}. \tag{6.49}$$

We shall now re-express the boundary term (6.36)-(6.38) in the form $b\langle[\boldsymbol{\psi}],\boldsymbol{\xi}\rangle_{\tau}$. We examine the three parts separately, so as to determine our Lagrangian multiplier $\boldsymbol{\xi}$. Starting with (6.36) we set

$$\sum_{k=1}^{3}\int_{\tau}\frac{\mu}{4\pi}\int_{\Gamma}\frac{1}{|x-y|}\left(\frac{\partial\boldsymbol{\phi}(y)}{\partial\boldsymbol{S}^{\Gamma}_{k}(y)}\right)[\boldsymbol{\psi}(x)]n_k(x)\,dS_y ds=\langle[\boldsymbol{\psi}],\boldsymbol{\xi}_1\rangle_{\tau}.$$

This gives us that

$$\boldsymbol{\xi}_1|_{\gamma_l} = \sum_{k=1}^{3} \mu \left(V \left(\frac{\partial \boldsymbol{\phi}(y)}{\partial \boldsymbol{S}_k^{\Gamma}(y)} \right) \right) \Big|_{\gamma_l} n_k(x). \tag{6.50}$$

Alternatively we can express $\boldsymbol{\xi}_1$ as $\boldsymbol{\xi}_1 = (\boldsymbol{n}(x) \cdot (V\, \mathbf{curl}_{\Gamma}\, \boldsymbol{\phi}_i)|_{\gamma_l})_{i=1}^{3}$. We now examine the second part (6.37) of the boundary term

$$\int_{\tau} (\boldsymbol{N}[\boldsymbol{\psi}(x)])^T \left(\int_{\Gamma} \big(4\mu^2 \boldsymbol{U}^*(x-y) \right.$$
$$\left. - \frac{\mu}{2\pi} \boldsymbol{I} \frac{1}{|x-y|} \right) \boldsymbol{\mathcal{M}}^{\Gamma}(\partial_y, \boldsymbol{n}(y)) \boldsymbol{\phi}(y)\, dS_y \Bigg)\, ds = \langle [\boldsymbol{\psi}], \boldsymbol{\xi}_2 \rangle_{\tau}.$$

Now since $(\boldsymbol{N}[\boldsymbol{\psi}(x)])^T = ([\boldsymbol{\psi}(x)])^T \boldsymbol{N}^T$, we have that

$$\boldsymbol{\xi}_2|_{\gamma_l} = \boldsymbol{N}^T \left(\left(4\mu^2 V_{le} - 2\mu V \right) \boldsymbol{\mathcal{M}}^{\Gamma}(\partial_y, \boldsymbol{n}(y)) \boldsymbol{\phi}(y) \right) |_{\gamma_l}. \tag{6.51}$$

Finally we examine the third part (6.38) of the bilinear form $b(\cdot, \cdot)$

$$\int_{\tau} \sum_{i,j,k=1}^{3} [\psi_i(x)] \left(\int_{\Gamma} \frac{\mu}{4\pi} \frac{1}{|x-y|} (\mathcal{M}_{ki}^{\Gamma}(\partial_y, \boldsymbol{n}(y)) \phi_j(y))\, dS_y \right) \boldsymbol{N}_{ij}\, ds = \langle [\boldsymbol{\psi}], \boldsymbol{\xi}_3 \rangle_{\tau}.$$

This gives us

$$\boldsymbol{\xi}_3|_{\gamma_l} = \left(\sum_{k=1}^{3} \mu \left(\left(V(\mathcal{M}_{ki}^{\Gamma}(\partial_y, \boldsymbol{n}(y)) \phi_j(y)) \big|_{\gamma_l} \right)_{j=1}^{3} \cdot (\boldsymbol{N}_{ij})_{j=1}^{3} \right)_{i=1}^{3} \right)_{i=1}^{3}. \tag{6.52}$$

We thus have by (6.50), (6.51), and (6.52) our boundary term $b(\cdot, \cdot)$ associated with (6.33) to (6.35) is given by

$$b(\boldsymbol{\psi}, \boldsymbol{\xi}) = \langle [\boldsymbol{\psi}], \boldsymbol{\xi} \rangle_{\tau} = \sum_{l=1}^{L} \langle [\boldsymbol{\psi}], \boldsymbol{\xi} \rangle_{\gamma_l} \text{ where } \boldsymbol{\xi} = \sum_{i=1}^{3} \boldsymbol{\xi}_i. \tag{6.53}$$

We now have our standard mixed formulation as in the previous situations, we can thus proceed as before to prove existence and uniqueness of a solution and an error estimate. Our mixed formulation of the Mortar BEM for linear elasticity is thus: *Find* $\boldsymbol{\phi}_h \in \boldsymbol{X}_h$ *and* $\boldsymbol{\xi}_k \in \boldsymbol{M}_k$ *such that*

$$\begin{aligned} a(\boldsymbol{\phi}_h, \boldsymbol{\psi}) + b(\boldsymbol{\psi}, \boldsymbol{\xi}_k) &= F(\boldsymbol{\psi}) \qquad && \forall \boldsymbol{\psi} \in \boldsymbol{X}_h \\ b(\boldsymbol{\phi}_h, \boldsymbol{\eta}) &= 0 && \forall \boldsymbol{\eta} \in \boldsymbol{M}_k. \end{aligned} \tag{6.54}$$

For the bilinear forms $a(\cdot,\cdot)$ defined in (6.49)-(6.49) and $b(\cdot,\cdot)$ defined in (6.53) . As in the previous chapters we have that this scheme is equivalent to: *Find* $\boldsymbol{\phi}_h \in \boldsymbol{V}_h$ *such that*

$$a(\boldsymbol{\phi}_h, \boldsymbol{\psi}) = F(\boldsymbol{\psi}) \qquad \forall \boldsymbol{\psi} \in \boldsymbol{V}_h. \tag{6.55}$$

Where the constrained space $\boldsymbol{V}_h$ is defined as

$$\boldsymbol{V}_h = \{\boldsymbol{\psi} \in \boldsymbol{X}_h : b(\boldsymbol{\psi}, \boldsymbol{\eta}) = 0 \quad \forall \boldsymbol{\eta} \in \boldsymbol{M}_k\}. \tag{6.56}$$

6.2 Technical Results and Proof of the Main Result

In this section we present the analysis which leads to our main error result. As in the previous chapters continuity and ellipticity of the bilinear form $a(\cdot,\cdot)$ are essential for the error analysis of the problem described in (6.54). We first present some results relating to the continuity of $a(\cdot,\cdot)$ which shall be used to show that associated with a function that satisfies our model problem is a Lagrangian multiplier that is well defined despite the absence of an appropriate trace theorem.

Preliminary remarks

We first examine some bounds for our bilinear form $a(\cdot,\cdot)$ defined in (6.46)-(6.49).

Lemma 6.8. *For the first part (6.46) of the bilinear form* $a(\cdot,\cdot)$ *we have*

$$\begin{aligned}
&\mu \sum_{i=1}^{3} \langle V \operatorname{\mathbf{curl}}_{\mathrm{H}} \phi_i, \operatorname{\mathbf{curl}}_{\mathrm{H}} \psi_i \rangle_{\mathcal{T}} \\
&\qquad \lesssim \mu \left(\sum_{i=1}^{3} \| \operatorname{\mathbf{curl}}_{\mathrm{H}} \phi_i \|_{\tilde{\boldsymbol{H}}_t^{-1/2}(\mathcal{T})} \right) \left(\sum_{i=1}^{3} \| \operatorname{\mathbf{curl}}_{\mathrm{H}} \psi_i \|_{\tilde{\boldsymbol{H}}_t^{-1/2}(\mathcal{T})} \right).
\end{aligned} \tag{6.57}$$

Proof. As in the case of the Laplacian we have by the continuity of $V : \tilde{\boldsymbol{H}}_t^{-1/2}(\Gamma) \to \boldsymbol{H}_t^{1/2}(\Gamma)$ (by [19]) we have

$$\begin{aligned}
&\mu \sum_{i=1}^{3} \langle V \operatorname{\mathbf{curl}}_{\mathrm{H}} \phi_i, \operatorname{\mathbf{curl}}_{\mathrm{H}} \psi_i \rangle_{\mathcal{T}} \\
&\qquad \lesssim \mu \sum_{i=1}^{3} \| \operatorname{\mathbf{curl}}_{\mathrm{H}} \psi_i \|_{\tilde{\boldsymbol{H}}_t^{-1/2}(\mathcal{T})} \| \operatorname{\mathbf{curl}}_{\mathrm{H}} \phi_i \|_{\tilde{\boldsymbol{H}}_t^{-1/2}(\mathcal{T})} \\
&\qquad \lesssim \mu \left(\sum_{i=1}^{3} \| \operatorname{\mathbf{curl}}_{\mathrm{H}} \phi_i \|_{\tilde{\boldsymbol{H}}_t^{-1/2}(\mathcal{T})} \right) \left(\sum_{i=1}^{3} \| \operatorname{\mathbf{curl}}_{\mathrm{H}} \psi_i \|_{\tilde{\boldsymbol{H}}_t^{-1/2}(\mathcal{T})} \right).
\end{aligned}$$

Which is the stated result. □

Lemma 6.9. *For the second part (6.47) of the bilinear form $a(\cdot,\cdot)$ we have*

$$\begin{aligned}
&|\sum_{i=1}^{3} 2\mu\langle V\left((\mathbf{curl}_{\mathrm{H}}\,\phi_j)_i\right)_{j=1}^{3}, \mathbf{curl}_{\mathrm{H}}\,\psi_i\rangle_{\mathcal{T}}| \\
&\qquad \lesssim 2\mu\left(\sum_{i=1}^{3}\|\,\mathbf{curl}_{\mathrm{H}}\,\phi_i\|_{\tilde{\boldsymbol{H}}_t^{-1/2}(\mathcal{T})}\right)\left(\sum_{i=1}^{3}\|\,\mathbf{curl}_{\mathrm{H}}\,\psi_i\|_{\tilde{\boldsymbol{H}}_t^{-1/2}(\mathcal{T})}\right). \qquad (6.58)
\end{aligned}$$

Proof. Now by the continuity of $V : \tilde{\boldsymbol{H}}_t^{-1/2}(\Gamma) \to \boldsymbol{H}_t^{1/2}(\Gamma)$ (by [19]) we have

$$\begin{aligned}
&|\sum_{i=1}^{3} 2\mu\langle V\left((\mathbf{curl}_{\mathrm{H}}\,\phi_j)_i\right)_{j=1}^{3}, \mathbf{curl}_{\mathrm{H}}\,\psi_i\rangle_{\mathcal{T}}| \\
&\qquad \lesssim 2\mu\sum_{i=1}^{3}\|\left((\mathbf{curl}_{\mathrm{H}}\,\phi_j)_i\right)_{j=1}^{3}\|_{\tilde{\boldsymbol{H}}_t^{-1/2}(\mathcal{T})}\|\,\mathbf{curl}_{\mathrm{H}}\,\psi_i\|_{\tilde{\boldsymbol{H}}_t^{-1/2}(\mathcal{T})} \\
&\qquad \lesssim 2\mu\left(\sum_{i=1}^{3}\|\left((\mathbf{curl}_{\mathrm{H}}\,\phi_j)_i\right)_{j=1}^{3}\|_{\tilde{\boldsymbol{H}}_t^{-1/2}(\mathcal{T})}\right)\left(\sum_{i=1}^{3}\|\,\mathbf{curl}_{\mathrm{H}}\,\psi_i\|_{\tilde{\boldsymbol{H}}_t^{-1/2}(\mathcal{T})}\right) \\
&\qquad \lesssim 2\mu\left(\sum_{i=1}^{3}\|\,\mathbf{curl}_{\mathrm{H}}\,\phi_i\|_{\tilde{\boldsymbol{H}}_t^{-1/2}(\mathcal{T})}\right)\left(\sum_{i=1}^{3}\|\,\mathbf{curl}_{\mathrm{H}}\,\psi_i\|_{\tilde{\boldsymbol{H}}_t^{-1/2}(\mathcal{T})},\right) \qquad (6.59)
\end{aligned}$$

by a simple rearrangement of terms. The stated result then follows immediately. □

Lemma 6.10. *For the third part (6.48) of the bilinear form $a(\cdot,\cdot)$ we have*

$$\begin{aligned}
&|4\mu^2\langle \boldsymbol{V}_{le}(\boldsymbol{\mathcal{M}}^H(\partial_x,\boldsymbol{n}(x))\boldsymbol{\phi}(x))\boldsymbol{\mathcal{M}}^H(\partial_x,\boldsymbol{n}(x))\boldsymbol{\psi}(x)\rangle_{\mathcal{T}}| \\
&\qquad \lesssim 4\mu^2\left(\sum_{i=1}^{3}\|\,\mathbf{curl}_{\mathrm{H}}\,\phi_i\|_{\tilde{\boldsymbol{H}}_t^{-1/2}(\mathcal{T})}\right)\left(\sum_{i=1}^{3}\|\,\mathbf{curl}_{\mathrm{H}}\,\psi_i\|_{\tilde{\boldsymbol{H}}_t^{-1/2}(\mathcal{T})}\right). \qquad (6.60)
\end{aligned}$$

Proof. From [19] we have the continuity of $V_{le} : \tilde{\boldsymbol{H}}^{-1/2}(\Gamma) \to \boldsymbol{H}^{1/2}(\Gamma)$ which gives us that

$$\begin{aligned}
&|4\mu^2\langle \boldsymbol{V}_{le}(\boldsymbol{\mathcal{M}}^H(\partial_x,\boldsymbol{n}(x))\boldsymbol{\phi}(x))\boldsymbol{\mathcal{M}}^H(\partial_x,\boldsymbol{n}(x)\boldsymbol{\psi}(x))\rangle_{\mathcal{T}}| \\
&\qquad \lesssim 4\mu^2\|\boldsymbol{\mathcal{M}}^H(\partial_x,\boldsymbol{n}(x))\boldsymbol{\phi}(x)\|^2_{\tilde{\boldsymbol{H}}^{-1/2}(\mathcal{T})}\|\boldsymbol{\mathcal{M}}^H(\partial_x,\boldsymbol{n}(x))\boldsymbol{\phi}(x)\|^2_{\tilde{\boldsymbol{H}}^{-1/2}(\mathcal{T})}. \qquad (6.61)
\end{aligned}$$

The norm in (6.61) can be expressed as

$$\begin{aligned}\|\boldsymbol{\mathcal{M}}^H(\partial_x,\boldsymbol{n}(x))\boldsymbol{\phi}(x)\|^2_{\tilde{\boldsymbol{H}}^{-1/2}(\mathcal{T})} = \\ \|-(\mathbf{curl}_{\mathrm{H}}\,\phi_2)_3+(\mathbf{curl}_{\mathrm{H}}\,\phi_3)_2\|^2_{\tilde{H}^{-1/2}(\mathcal{T})} \\ +\|(\mathbf{curl}_{\mathrm{H}}\,\phi_1)_3-(\mathbf{curl}_{\mathrm{H}}\,\phi_3)_1\|^2_{\tilde{H}^{-1/2}(\mathcal{T})} \\ +\|-(\mathbf{curl}_{\mathrm{H}}\,\phi_1)_2+(\mathbf{curl}_{\mathrm{H}}\,\phi_2)_1\|^2_{\tilde{H}^{-1/2}(\mathcal{T})}. \qquad (6.62)\end{aligned}$$

We can trivially bound (6.62) by the triangle inequality and adding in the extra terms in the following way:

$$\|\boldsymbol{\mathcal{M}}^H(\partial_x,\boldsymbol{n}(x))\boldsymbol{\phi}(x)\|^2_{\tilde{\boldsymbol{H}}^{-1/2}(\mathcal{T})} \lesssim \sum_{i=1}^{3}\|\,\mathbf{curl}_{\mathrm{H}}\,\phi_i\|^2_{\tilde{\boldsymbol{H}}^{-1/2}(\mathcal{T})} \lesssim \sum_{i=1}^{3}\|\,\mathbf{curl}_{\mathrm{H}}\,\phi_i\|^2_{\tilde{\boldsymbol{H}}_t^{-1/2}(\mathcal{T})}.$$

The stated result then follows immediately. □

Lemma 6.11. *For the fourth part of $a(\cdot,\cdot)$ defined by (6.49) we have*

$$\begin{aligned}|\mu\sum_{j=1}^{3}\langle V\left((\mathbf{curl}_{\mathrm{H}}\,\phi_k)_k\right)_{k=1}^3,\left((\mathbf{curl}_{\Gamma}\,\psi_j)_j\right)_{k=1}^3\rangle_{\mathcal{T}}| \\ \lesssim \mu\left(\sum_{i=1}^{3}\|\,\mathbf{curl}_{\mathrm{H}}\,\phi_i\|_{\tilde{\boldsymbol{H}}_t^{-1/2}(\mathcal{T})}\right)\left(\sum_{i=1}^{3}\|\,\mathbf{curl}_{\mathrm{H}}\,\psi_i\|_{\tilde{\boldsymbol{H}}_t^{-1/2}(\mathcal{T})}\right). \qquad (6.63)\end{aligned}$$

Proof. We can bound in a similar fashion to the proof of Lemma 6.9 to give the stated result. □

Integration by parts formula

All the authors mentioned previously considered closed smooth systems. Since we did not find a reference for open surfaces we recall the situation in the next lemma.

Lemma 6.12. *The following holds in $\mathcal{L}(\tilde{\boldsymbol{H}}^{1/2}(\Gamma),\boldsymbol{H}^{-1/2}(\Gamma))$.*

$$\begin{aligned}W_{le} &= -\mu\left(\frac{\partial}{\partial\boldsymbol{S}_k^{\Gamma}(x)}\right)_{k=1}^3 V\left(\frac{\partial}{\partial\boldsymbol{S}_k^{\Gamma}(x)}\right)_{k=1}^3 && (6.64)\\ &\quad -4\mu^2\boldsymbol{\mathcal{M}}^{\Gamma}(\partial_x,\boldsymbol{n}(x))\boldsymbol{V}_{le}\boldsymbol{\mathcal{M}}^{\Gamma}(\partial_x,\boldsymbol{n}(x)) && (6.65)\\ &\quad +2\mu\boldsymbol{\mathcal{M}}^{\Gamma}(\partial_x,\boldsymbol{n}(x))V\boldsymbol{\mathcal{M}}^{\Gamma}(\partial_x,\boldsymbol{n}(x)) && (6.66)\\ &\quad +\mu\left[\boldsymbol{\mathcal{M}}^{\Gamma}(\partial_x,\boldsymbol{n}(x))V\boldsymbol{\mathcal{M}}^{\Gamma}(\partial_x,\boldsymbol{n}(x))\right]^T. && (6.67)\end{aligned}$$

Where V is the single layer potential operator for the Laplacian defined in (2.42), and $\boldsymbol{V}_{le}$ is the single layer potential operator for linear elasticity. Moreover, the equality defined in (6.18) - (6.21) holds for all $\boldsymbol{\phi}, \boldsymbol{\psi} \in \tilde{\boldsymbol{H}}^{1/2}(\Gamma)$.

Proof. We have, by Lemma 2.17 that $\mathbf{curl}_\Gamma : \tilde{H}^{1/2}(\Gamma) \to \tilde{\boldsymbol{H}}_t^{-1/2}(\Gamma)$, and by Lemma 2.18 $\mathbf{curl}_\Gamma : H^{1/2}(\Gamma) \to \tilde{\boldsymbol{H}}_t^{-1/2}(\Gamma)$. We also have (from [19]) that $V : \tilde{\boldsymbol{H}}^{-1/2}(\Gamma) \to \boldsymbol{H}^{1/2}(\Gamma)$, and $\boldsymbol{V}_{le} : \tilde{\boldsymbol{H}}^{-1/2}(\Gamma) \to \boldsymbol{H}^{1/2}(\Gamma)$. Using the result that $\frac{\partial \cdot}{\partial \boldsymbol{S}_k^\Gamma(x)} = (\mathbf{curl}_\Gamma \cdot)_k$, we have that $\frac{\partial \cdot}{\partial \boldsymbol{S}_k^\Gamma(x)} : \tilde{H}^{1/2}(\Gamma) \to \tilde{H}^{-1/2}(\Gamma)$ and $\frac{\partial \cdot}{\partial \boldsymbol{S}_k^\Gamma(x)} : H^{1/2}(\Gamma) \to \tilde{H}^{-1/2}(\Gamma)$. It immediately follows that $\boldsymbol{\mathcal{M}}^\Gamma(\partial_x, \boldsymbol{n}(x)) : \tilde{\boldsymbol{H}}^{1/2}(\Gamma) \to \tilde{\boldsymbol{H}}^{-1/2}(\Gamma)$ and $\boldsymbol{\mathcal{M}}^\Gamma(\partial_x, \boldsymbol{n}(x)) : \boldsymbol{H}^{1/2}(\Gamma) \to \tilde{\boldsymbol{H}}^{-1/2}(\Gamma)$. The results then follow in an analogous fashion to Lemma 2.20. □

We now examine an integration by parts formula for the hypersingular operator for linear elasticity. Similar reasoning to that used in the situation of the Laplacian (see Section 4.1.3) gives us for sufficiently smooth $\boldsymbol{\phi}$ and $\boldsymbol{\psi}$:

$$\begin{aligned}
\langle \boldsymbol{\xi}, [\boldsymbol{\psi}] \rangle_\tau =& \langle W_{le} \boldsymbol{\phi}, \boldsymbol{\psi} \rangle_{\mathcal{T}} && (6.68)\\
&- \Bigg(\sum_{i=1}^{3} \mu \langle V \, \mathbf{curl}_\Gamma \, \phi_i, \mathbf{curl}_{\mathrm{H}} \, \psi_i \rangle_{\mathcal{T}} && (6.69)\\
&\quad - \sum_{i=1}^{3} 2\mu \langle V \left((\mathbf{curl}_\Gamma \, \phi_k)_i \right)_{k=1}^3, \mathbf{curl}_{\mathrm{H}} \, \psi_i \rangle_{\mathcal{T}} && (6.70)\\
&\quad - 4\mu^2 \langle \boldsymbol{V}_{le} \boldsymbol{\mathcal{M}}^\Gamma(\partial_x, \boldsymbol{n}(x)) \boldsymbol{\phi}, \boldsymbol{\mathcal{M}}^H(\partial_x, \boldsymbol{n}(x)) \boldsymbol{\psi} \rangle_{\mathcal{T}} && (6.71)\\
&\quad - \mu \sum_{i=1}^{3} \langle V \left((\mathbf{curl}_\Gamma \, \phi_j)_j \right)_{j=1}^3, \left((\mathbf{curl}_{\mathrm{H}} \, \psi_i)_i \right)_{k=1}^3 \rangle_{\mathcal{T}} \Bigg). && (6.72)
\end{aligned}$$

Here, $\boldsymbol{\xi}$ denotes our Lagrangian multiplier on the skeleton γ defined by

$$\begin{aligned}
\boldsymbol{\xi}|_{\gamma_l} :=& \sum_{k=1}^{3} \mu \left(V \frac{\partial \boldsymbol{\phi}(y)}{\partial \boldsymbol{S}_k^\Gamma(y)} \right) \Big|_{\gamma_l} n_k(x) \\
&+ \boldsymbol{N}^T \left(\left(4\mu^2 V_{le} - 2\mu V \right) \boldsymbol{\mathcal{M}}^\Gamma(\partial_y, \boldsymbol{n}(y)) \boldsymbol{\phi}(y) \right) |_{\gamma_l} \\
&+ \left(\sum_{k=1}^{3} \mu \left(\left(V(\mathcal{M}_{ki}^\Gamma(\partial_y, \boldsymbol{n}(y)) \phi_j(y)) \right) |_{\gamma_l} \right)_{j=1}^3 \cdot (\boldsymbol{N}_{ij})_{j=1}^3 \right)_{i=1}^3 . \qquad (6.73)
\end{aligned}$$

Proceeding in a similar fashion to Lemma 3.1 and Lemma 4.3 we have:

Lemma 6.13. *For $\boldsymbol{\phi} \in \tilde{\boldsymbol{H}}^{1/2}(\Gamma)$ with $W\boldsymbol{\phi} = \boldsymbol{f} \in \boldsymbol{L}^2(\Gamma)$, we have $\boldsymbol{\xi} \in \prod_{l=1}^{L} \boldsymbol{H}^{-s}(\gamma_l)$ for any $s \in (0, 1/2]$.*

Proof. Let $\boldsymbol{\psi} \in \prod_{l=1}^{L} \boldsymbol{H}^s(\gamma_l)$ be given. We continuously extend $\boldsymbol{\psi}$ to an element $\tilde{\boldsymbol{\psi}} \in \boldsymbol{H}^{s+1/2}(\mathcal{T})$ with $\tilde{\boldsymbol{\psi}} = 0$ on $\partial\Gamma$ such that $[\tilde{\boldsymbol{\psi}}]|_{\gamma_l} = \boldsymbol{\psi}|_{\gamma_l}$. The definition of $\boldsymbol{\xi}$ is independent of the particular extension $\tilde{\boldsymbol{\psi}}$ (see Lemma 3.1 and Lemma 4.3). Using a duality estimate we obtain from our integration by parts formula (6.68)-(6.72) that

$$\sum_{l=1}^{L} \langle \boldsymbol{\xi}, [\boldsymbol{\psi}] \rangle_{\gamma_l} = \langle \boldsymbol{f}, \tilde{\boldsymbol{\psi}} \rangle_{\mathcal{T}} - a(\boldsymbol{\phi}, \tilde{\boldsymbol{\psi}}). \tag{6.74}$$

We now have that

$$\langle \boldsymbol{f}, \tilde{\boldsymbol{\psi}} \rangle_{\mathcal{T}} \lesssim \|\boldsymbol{f}\|_{\boldsymbol{L}^2(\Gamma)} \|\tilde{\boldsymbol{\psi}}\|_{\boldsymbol{L}^2(\Gamma)} \lesssim \|\boldsymbol{f}\|_{\boldsymbol{L}^2(\Gamma)} \|\tilde{\boldsymbol{\psi}}\|^2_{\boldsymbol{H}^{s+1/2}(\mathcal{T})}. \tag{6.75}$$

The bilinear form $a(\boldsymbol{\phi}, \tilde{\boldsymbol{\psi}})$ can be bounded in the following way

$$\begin{aligned}
a(\boldsymbol{\phi}, \tilde{\boldsymbol{\psi}}) \lesssim \sum_{i=1}^{N} \Bigg(& \sum_{j=1}^{3} \|V \operatorname{\mathbf{curl}}_\Gamma \phi_j\|_{\tilde{\boldsymbol{H}}_t^{1/2-s}(\Gamma_i)} \|\operatorname{\mathbf{curl}}_{\Gamma_i} \tilde{\psi}_j|_{\Gamma_i}\|_{\boldsymbol{H}_t^{s-1/2}(\Gamma_i)} && (6.76)\\
& + \sum_{j=1}^{3} \|V ((\operatorname{\mathbf{curl}}_\Gamma \phi_k)_j)_{k=1}^3\|_{\tilde{\boldsymbol{H}}_t^{1/2-s}(\Gamma_i)} \|\operatorname{\mathbf{curl}}_{\Gamma_i} \tilde{\psi}_j|_{\Gamma_i}\|_{\boldsymbol{H}_t^{s-1/2}(\Gamma_i)} && (6.77)\\
& + \|\boldsymbol{V}_{le} \boldsymbol{\mathcal{M}}^{\Gamma}(\partial_x, \boldsymbol{n}(x))\boldsymbol{\phi}\|_{(\tilde{\boldsymbol{H}}^{1/2-s}(\Gamma_i))^3} \|\boldsymbol{\mathcal{M}}^{\Gamma_i}(\partial_x, \boldsymbol{n}(x))\tilde{\boldsymbol{\psi}}|_{\Gamma_i}\|_{(\boldsymbol{H}^{s-1/2}(\Gamma_i))^3} && (6.78)\\
& + \sum_{j=1}^{3} \|V ((\operatorname{\mathbf{curl}}_\Gamma \phi_k)_k)_{k=1}^3\|_{\tilde{\boldsymbol{H}}_t^{1/2-s}(\Gamma_i)} \|((\operatorname{\mathbf{curl}}_{\Gamma_i} \tilde{\psi}_j|_{\Gamma_i})_j)_{k=1}^3\|_{\boldsymbol{H}_t^{s-1/2}(\Gamma_i)} \Bigg). && (6.79)
\end{aligned}$$

Now, as in the mortar BEM for the Laplacian situation (see Lemma 4.3), for $s \in (0, 1/2]$ the norms in $\tilde{\boldsymbol{H}}_{\mathrm{t}}^{1/2-s}(\Gamma_i)$ and $\boldsymbol{H}_{\mathrm{t}}^{1/2-s}(\Gamma_i)$ are equivalent (cf., e.g., [38]) so that together with the mapping property of V (from [19]), $V : \tilde{\boldsymbol{H}}_{\mathrm{t}}^{-1/2-s}(\Gamma) \to \boldsymbol{H}_{\mathrm{t}}^{1/2-s}(\Gamma)$, and Lemma 2.17 we obtain

$$\sum_{i=1}^{N} \sum_{j=1}^{3} \|V \operatorname{\mathbf{curl}}_\Gamma \phi_j\|^2_{\tilde{\boldsymbol{H}}_{\mathrm{t}}^{1/2-s}(\Gamma_i)} \lesssim \sum_{j=1}^{3} \|\phi_j\|^2_{\tilde{H}^{1/2}(\Gamma)} = \|\boldsymbol{\phi}\|^2_{\tilde{\boldsymbol{H}}^{1/2}(\Gamma)}.$$

Here, the appearing constants are independent of ϕ_j. Also, using Lemma 2.19 we are able to bound (with constant independent of $\tilde{\boldsymbol{\psi}}$)

$$\sum_{i=1}^{N} \sum_{j=1}^{3} \|\operatorname{\mathbf{curl}}_{\Gamma_i} \tilde{\psi}_j|_{\Gamma_i}\|^2_{\boldsymbol{H}_{\mathrm{t}}^{s-1/2}(\Gamma_i)} \lesssim \sum_{j=1}^{3} \|\tilde{\psi}_j\|^2_{H^{s+1/2}(\mathcal{T})} = \|\tilde{\boldsymbol{\psi}}\|^2_{\boldsymbol{H}^{s+1/2}(\mathcal{T})}.$$

Using these results and the proofs of Lemmas 6.8, 6.9, and 6.11 we may bound (6.76), (6.77) and (6.79). It remains to bound (6.78). We have the mapping property of $\boldsymbol{V}_{le}$ (from [19]), $\boldsymbol{V}_{le} : \tilde{\boldsymbol{H}}^{-1/2-s}(\Gamma) \to \boldsymbol{H}^{1/2-s}(\Gamma)$, which using the proof of Lemma 6.10, gives us

$$\begin{aligned}\sum_{i=1}^{N} \|\boldsymbol{V}_{le}\boldsymbol{\mathcal{M}}^{\Gamma}(\partial_x, \boldsymbol{n}(x))\boldsymbol{\phi}\|^2_{\tilde{\boldsymbol{H}}_t^{1/2-s}(\Gamma_i)} &\lesssim \sum_{i=1}^{N} \|\boldsymbol{\mathcal{M}}^{\Gamma}(\partial_x, \boldsymbol{n}(x))\boldsymbol{\phi}\|^2_{\tilde{\boldsymbol{H}}_t^{-1/2-s}(\Gamma_i)} \\ &\lesssim \sum_{i=1}^{N}\sum_{j=1}^{3} \|\,\mathbf{curl}_{\Gamma}\,\phi_j\|^2_{\tilde{\boldsymbol{H}}_t^{-1/2-s}(\Gamma_i)} \\ &\lesssim \sum_{j=1}^{3} \|\phi_j\|^2_{\tilde{H}^{1/2}(\Gamma)} = \|\boldsymbol{\phi}\|^2_{\tilde{\boldsymbol{H}}^{1/2}(\Gamma)}.\end{aligned}$$

Taking these estimates into account, (6.74) proves that

$$\sum_{l=1}^{L} \langle \boldsymbol{\xi}, [\boldsymbol{\psi}] \rangle_{\gamma_l} \lesssim \left(\|\boldsymbol{f}\|_{\boldsymbol{L}^2(\Gamma)} + \|\boldsymbol{\phi}\|_{\tilde{\boldsymbol{H}}^{1/2}(\Gamma)} \right) \|\tilde{\boldsymbol{\psi}}\|_{\boldsymbol{H}^{s+1/2}(\mathcal{T})}.$$

Finally using the continuity of the extension (with constant independent of $\boldsymbol{\psi}$)

$$\|\tilde{\boldsymbol{\psi}}\|^2_{\boldsymbol{H}^{s+1/2}(\mathcal{T})} \lesssim \sum_{l=1}^{L} \|\boldsymbol{\psi}\|^2_{\tilde{\boldsymbol{H}}^{s}(\gamma_l)}$$

finishes the proof. □

Continuity of the bilinear form $a(\cdot,\cdot)$

As in the previous chapters we need to examine the continuity and ellipticity properties of the bilinear form $a(\cdot,\cdot)$.

Lemma 6.14. *(i) The bilinear form $a(\cdot,\cdot)$ is almost uniformly continuous on $\boldsymbol{X}_h$, there holds*

$$|a(\boldsymbol{\psi}, \boldsymbol{\zeta})| \lesssim \left(\mu + \mu^2\right) \underline{D}^{-2} |\log(\underline{h}/D)|^2 \, \|\boldsymbol{\psi}\|_{\boldsymbol{H}^{1/2}(\mathcal{T})} \, \|\boldsymbol{\zeta}\|_{\boldsymbol{H}^{1/2}(\mathcal{T})} \qquad \forall \boldsymbol{\psi}, \boldsymbol{\zeta} \in \boldsymbol{X}_h.$$

(ii) Assume that $\boldsymbol{\phi} \in \tilde{\boldsymbol{H}}^{1/2+r}(\Gamma)$ $(r > 0)$. Then there holds

$$|a(\boldsymbol{\phi} - \boldsymbol{\psi}, \boldsymbol{\zeta})| \lesssim \left(\mu + \mu^2\right) \underline{D}^{-1} s^{-1} |\log(\underline{h}/D)| \|\boldsymbol{\phi} - \boldsymbol{\psi}\|_{\boldsymbol{H}^{1/2+s}(\mathcal{T})} \|\boldsymbol{\zeta}\|_{\boldsymbol{H}^{\frac{1}{2}}(\mathcal{T})}$$

$$\forall \boldsymbol{\psi}, \boldsymbol{\zeta} \in \boldsymbol{X}_h, \, \forall s \in (0, \max\{r, 1/2\}].$$

In particular the appearing constant is independent of s.

Proof. Combining Lemmas 6.8, 6.9, 6.10, and 6.11 we get

$$a(\boldsymbol{\psi},\boldsymbol{\zeta}) \lesssim \left(\mu+\mu^2\right)\left(\sum_{i=1}^{3}\|\,\mathbf{curl}_{\mathrm{H}}\,\psi_i\|_{\tilde{\boldsymbol{H}}_t^{-1/2}(\mathcal{T})}\right)\left(\sum_{i=1}^{3}\|\,\mathbf{curl}_{\mathrm{H}}\,\zeta_i\|_{\tilde{\boldsymbol{H}}_t^{-1/2}(\mathcal{T})}\right). \tag{6.80}$$

We now apply previous results from Chapter 4 to (6.80). For part (i) of the lemma we have for $\boldsymbol{\psi},\boldsymbol{\zeta}\in\boldsymbol{X}_h$ by the proof of Lemma 4.6 that

$$\begin{aligned} a(\boldsymbol{\psi},\boldsymbol{\zeta}) &\lesssim \left(\mu+\mu^2\right)\underline{D}^{-2}|\log(\underline{h}/D)|^2\left(\sum_{i=1}^{3}\|\psi_i\|_{H^{1/2}(\mathcal{T})}\right)\left(\sum_{i=1}^{3}\|\zeta_i\|_{H^{1/2}(\mathcal{T})}\right)\\ &\lesssim \left(\mu+\mu^2\right)\underline{D}^{-2}|\log(\underline{h}/D)|^2\|\boldsymbol{\psi}\|_{\boldsymbol{H}^{1/2}(\mathcal{T})}\|\boldsymbol{\zeta}\|_{\boldsymbol{H}^{1/2}(\mathcal{T})}. \end{aligned}$$

Similarly for part (ii) of the lemma we have for $\boldsymbol{\phi}\in\tilde{\boldsymbol{H}}^{1/2+r}(\Gamma)$ $(r>0)$ and $\boldsymbol{\psi},\boldsymbol{\zeta}\in\boldsymbol{X}_h$ with $s\in(0,\max\{r,1/2\}]$ by following the proof of Lemma 4.7 the stated result. □

Ellipticity of the bilinear form $a(\cdot,\cdot)$

As we are currently unable to provide a proof of the $\boldsymbol{V}_h$-ellipticity of the bilinear form $a(\cdot,\cdot)$ we instead conjecture the required property. We also introduce the quotient space. We note that the rigid body motions are defined over the whole domain, so we must consider their restriction to the boundary in our situation.

Conjecture 6.15. The bilinear form $a(\cdot,\cdot)$ is $\boldsymbol{V}_h$-elliptic, there holds:

$$a(\boldsymbol{\psi},\boldsymbol{\psi}) \geq C_e(h,D)\|\boldsymbol{\psi}\|^2_{\boldsymbol{H}^{1/2}(\mathcal{T})/\mathcal{R}} \qquad \forall\boldsymbol{\psi}\in\boldsymbol{V}_h.$$

Here $C_e(h,D)$ is the unknown ellipticity constant which may (or may not) depend upon h and D.

Assumption 6.16. Conjecture 6.15 is true.

Remark 6.17. Han [27] and Nedelec [43] both show ellipticity of their formulations on closed surfaces. However translation to our situation of the open surface is not obvious. The minus signs which appear in the definition of the bilinear form $a(\cdot,\cdot)$ ((6.46)-(6.49)) cause problems when trying to give an appropriate bound for ellipticity. For continuity it was a simple step to replace them by their absolute values. However this cannot be done for ellipticity. Thus it is very difficult to examine the components of the bilinear form as we did for continuity (see Lemmas 6.8-6.11). It may be possible to prove the ellipticity by considering an equivalent representation of the bilinear form $a(\cdot,\cdot)$ using different integral operators or different surface differential operators. However, it is not obvious what form of representation would be suitable.

The kernel of the hypersingular operator $\boldsymbol{W}_{le}$ is given by the space of rigid body motions $\mathcal{R}$. We may therefore have a situation where $\boldsymbol{W}_{le}\boldsymbol{\phi} = 0$, $\boldsymbol{\phi} \in \mathcal{R}$ but $\|\boldsymbol{\phi}\|_{\boldsymbol{H}^{1/2}(\mathcal{T})} \neq 0$. This is why we require ellipticity on the quotient space.

Inf-sup condition

We now apply the extension operators defined in (4.22). We apply the previously defined extension operators to the components of the vector.

Lemma 6.18. *The bilinear form $b(\cdot,\cdot)$ satisfies the discrete inf-sup condition:*

$$\exists \beta > 0 : \quad \sup_{\boldsymbol{\psi} \in X_h} \frac{b(\boldsymbol{\psi}, \boldsymbol{\xi})}{\|\boldsymbol{\psi}\|_{\boldsymbol{H}^{1/2}(\mathcal{T})}} \geq \beta \|\boldsymbol{\xi}\|_{\boldsymbol{L}^2(\gamma)} \quad \forall \boldsymbol{\xi} \in \boldsymbol{M}_k.$$

Proof. Let $\boldsymbol{\xi} \in \boldsymbol{M}_K$ be given. We construct a function $\boldsymbol{w}$ (as in Lemma 4.12), which on each element J is zero at the end points of the element, coincides with (each component of) $\boldsymbol{\xi}$ at one interior node and is linear interpolated elsewhere. We then extend this function using the extension operators defined in (4.22) on the components of $\boldsymbol{w} \in \boldsymbol{L}^2(\gamma)$ to $\tilde{\boldsymbol{w}} \in \boldsymbol{X}_h$. We now have that

$$\|\boldsymbol{\xi}\|^2_{\boldsymbol{L}^2(\gamma_l)} \simeq \langle \boldsymbol{w}_{\gamma_l}, \boldsymbol{\xi} \rangle_{\gamma_l} \simeq \|\boldsymbol{w}_{\gamma_l}\|^2_{\boldsymbol{L}^2(\gamma_l)}.$$

We may now show that by Lemma 4.11 (as in Lemma 4.12),

$$\|\boldsymbol{\psi}\|^2_{\boldsymbol{H}^{1/2}(\mathcal{T})} \lesssim \sum_{l=1}^{L} \sum_{j=1}^{3} \|E_l(w_j|_{\gamma_l})\|^2_{H^{1/2}(\Gamma_{l_{\text{lag}}})} \lesssim \sum_{l=1}^{L} \|\boldsymbol{w}|_{\gamma_l}\|^2_{\boldsymbol{L}^2(\Gamma_{l_{\text{lag}}})}.$$

We now finish the proof by bounding (again as in Lemma 4.12),

$$\begin{aligned} b(\boldsymbol{\psi}, \boldsymbol{\xi}) &= \sum_{l=1}^{L} \langle [\boldsymbol{\psi}], \boldsymbol{\xi} \rangle_{\gamma_l} = \sum_{l=1}^{L} \langle \boldsymbol{w}_l, \boldsymbol{\xi} \rangle_{\gamma_l} \simeq \|\boldsymbol{\xi}\|_{\boldsymbol{L}^2(\gamma)} \left(\sum_{l=1}^{L} \|\boldsymbol{w}_l\|^2_{\boldsymbol{L}^2(\gamma_l)} \right)^{1/2} \\ &\gtrsim \|\boldsymbol{\xi}\|_{\boldsymbol{L}^2(\gamma)} \|\boldsymbol{\psi}\|_{\boldsymbol{H}^{1/2}(\mathcal{T})}. \end{aligned}$$

□

Discrete continuity

Lemma 6.19. *The bilinear form $b(\cdot,\cdot)$ is almost uniformly discretely continuous, in the sense that*

$$b(\boldsymbol{\psi}, \boldsymbol{\xi}) \lesssim \underline{D}^{-1/2} |\log(\underline{h}/D)|^{1/2} \|\boldsymbol{\psi}\|_{\boldsymbol{H}^{1/2}(\mathcal{T})} \|\boldsymbol{\xi}\|_{\boldsymbol{L}^2(\gamma)} \quad \forall \boldsymbol{\psi} \in \boldsymbol{X}_h, \forall \boldsymbol{\xi} \in \boldsymbol{M}_k.$$

Let $\boldsymbol{\eta} \in L^2(\gamma)^3$ be given. Then there holds

$$b(\boldsymbol{\psi}, \boldsymbol{\eta}) \lesssim \underline{D}^{-1/2} |\log(\underline{h}/D)|^{1/2} \inf_{\boldsymbol{\xi} \in \boldsymbol{M}_k} \|\boldsymbol{\eta} - \boldsymbol{\xi}\|_{\boldsymbol{L}^2(\gamma)} \|\boldsymbol{\psi}\|_{\boldsymbol{H}^{1/2}(\mathcal{T})} \quad \forall \boldsymbol{\psi} \in \boldsymbol{V}_h. \tag{6.81}$$

Proof. As in the case of the Laplacian (Lemma 4.14) we have

$$b(\boldsymbol{\psi}, \boldsymbol{\xi}) = \sum_{l=1}^{L} \langle [\boldsymbol{\psi}], \boldsymbol{\xi} \rangle_{\gamma_l} \leq \|[\boldsymbol{\psi}]\|_{\boldsymbol{L}^2(\gamma)} \|\boldsymbol{\xi}\|_{\boldsymbol{L}^2(\gamma)}. \tag{6.82}$$

The first part of the lemma follows directly from the fact that

$$\|[\boldsymbol{\psi}]\|^2_{\boldsymbol{L}^2(\gamma)} = \sum_{i=1}^{3} \|[\psi_i]\|^2_{L^2(\gamma)}, \tag{6.83}$$

where $\psi_i \in X_h$ and by an application of Lemma 4.14 we have

$$\|[\psi_i]\|^2_{L^2(\gamma)} \lesssim \underline{D}^{-1} |\log(\underline{h}/D)| \|\psi_i\|^2_{H^{1/2}(\mathcal{T})}. \tag{6.84}$$

Combining (6.82), (6.83), and (6.84) gives us that

$$b(\boldsymbol{\psi}, \boldsymbol{\xi}) \lesssim \underline{D}^{-1/2} |\log(\underline{h}/D)|^{1/2} \|\boldsymbol{\psi}\|_{\boldsymbol{H}^{1/2}(\mathcal{T})} \|\boldsymbol{\xi}\|_{\boldsymbol{L}^2(\gamma)}.$$

The second part of the lemma follows by noting that by the definition of $\boldsymbol{V}_h$ (which states that $b(\boldsymbol{\psi}, \boldsymbol{\eta}) = 0 \ \forall \boldsymbol{\psi} \in \boldsymbol{V}_h \ \forall \boldsymbol{\eta} \in \boldsymbol{M}_k$) we have that

$$b(\boldsymbol{\psi}, \boldsymbol{\xi}) \leq \|[\boldsymbol{\psi}]\|_{\boldsymbol{L}^2(\gamma)} \|\boldsymbol{\xi} - \boldsymbol{\eta}\|_{\boldsymbol{L}^2(\gamma)}.$$

We then bound the norm of $[\boldsymbol{\psi}]$ as before in (6.83) and (6.84) to finish the proof. □

Error estimate

For the following Strang-type estimate (see Lemma 2.6) we can no longer use exactly the same technique used in the previous chapters (see Theorems 3.6 and 4.15). The ideas used for a sharper estimate in the previous work (using norm of $\mathbf{curl}_{\Gamma_i}$) cannot be applied here due to our less accurate ellipticity estimate Conjecture 6.15 (see Lemmas 3.5 and 4.10).

Theorem 6.20. *Assume that Assumption 6.16 holds. Then the system (6.54) is uniquely solvable. For $\boldsymbol{\phi} \in \tilde{\boldsymbol{H}}^{1/2+r}(\Gamma)$, $r \in (0, 1/2]$, being the solution of (6.11), and $\boldsymbol{\phi}_h \in \boldsymbol{X}_h$ being the solution of (6.54) there holds*

$$\|\boldsymbol{\phi} - \boldsymbol{\phi}_h\|_{\boldsymbol{H}^{1/2}(\mathcal{T})/\mathcal{R}} \lesssim \quad C_e(h, D) \underline{D}^{-3/2} |\log(\underline{h}/D)| \left(s^{-1} \inf_{\boldsymbol{\psi} \in \boldsymbol{V}_h} \|\boldsymbol{\phi} - \boldsymbol{\psi}\|_{\boldsymbol{H}^{1/2+s}(\mathcal{T})/\mathcal{R}} \right.$$

$$+ \sup_{\boldsymbol{\zeta}\in\boldsymbol{V}_h\setminus\{\boldsymbol{0}\}} \frac{|a(\boldsymbol{\phi}-\boldsymbol{\phi}_h,\boldsymbol{\zeta})|}{\|\boldsymbol{\zeta}\|_{\boldsymbol{H}^{\frac{1}{2}}(\mathcal{T})/\mathcal{R}}}\Bigg)$$

uniformly for $s \in (0, r]$*, assuming that* $\underline{D}^{-1/2} \lesssim C_e(h, D)\underline{D}^{-1}$.

Proof. The existence and uniqueness of $(\boldsymbol{\phi}_h, \boldsymbol{\lambda}_k) \in \boldsymbol{X}_h \times \boldsymbol{M}_k$ follows from the Babuška-Brezzi theory. The bilinear form $a(\cdot,\cdot)$ is continuous on $\boldsymbol{X}_h$ by Lemma 6.14(i) and we conjectured the $\boldsymbol{V}_h$-elliptic by Conjecture 6.15. The bilinear form $b(\cdot,\cdot)$ is continuous on $\boldsymbol{X}_h \times \boldsymbol{M}_k$ by Lemma 6.19 and satisfies a discrete inf-sup condition by Lemma 6.18. The continuity and ellipticity bounds depend on h and D but that does not influence the unique solvability of the discrete scheme.

The error estimate is obtained by the usual steps. Combining the triangle inequality, ellipticity and continuity properties of $a(\cdot,\cdot)$, cf. Conjecture 6.15 and Lemma 6.14(ii), we obtain for any $\boldsymbol{\psi} \in \boldsymbol{V}_h$

$$\begin{aligned}
\|\boldsymbol{\phi}-\boldsymbol{\phi}_h\|_{\boldsymbol{H}^{1/2}(\mathcal{T})/\mathcal{R}} &\le \underline{D}^{-1/2}\left\{\|\boldsymbol{\phi}-\boldsymbol{\psi}\|_{\boldsymbol{H}^{1/2}(\mathcal{T})/\mathcal{R}} + \|\boldsymbol{\psi}-\boldsymbol{\phi}_h\|_{\boldsymbol{H}^{1/2}(\mathcal{T})/\mathcal{R}}\right\}\\
&\lesssim \underline{D}^{-1/2}\left\{\|\boldsymbol{\phi}-\boldsymbol{\psi}\|_{\boldsymbol{H}^{1/2}(\mathcal{T})/\mathcal{R}} + C_e(h,D)\sup_{\boldsymbol{\zeta}\in\boldsymbol{V}_h\setminus\{\boldsymbol{0}\}}\frac{a(\boldsymbol{\psi}-\boldsymbol{\phi}_h,\boldsymbol{\zeta})}{\|\boldsymbol{\zeta}\|_{\boldsymbol{H}^{1/2}(\mathcal{T})/\mathcal{R}}}\right\}\\
&\le \underline{D}^{-1/2}\left\{\|\boldsymbol{\phi}-\boldsymbol{\psi}\|_{\boldsymbol{H}^{1/2}(\mathcal{T})/\mathcal{R}} + C_e(h,D)\left(\sup_{\boldsymbol{\zeta}\in\boldsymbol{V}_h\setminus\{\boldsymbol{0}\}}\frac{a(\boldsymbol{\psi}-\boldsymbol{\phi},\boldsymbol{\zeta})}{\|\boldsymbol{\zeta}\|_{\boldsymbol{H}^{1/2}(\mathcal{T})/\mathcal{R}}}\right.\right.\\
&\qquad\left.\left.+\sup_{\boldsymbol{\zeta}\in\boldsymbol{V}_h\setminus\{\boldsymbol{0}\}}\frac{a(\boldsymbol{\phi}-\boldsymbol{\phi}_h,\boldsymbol{\zeta})}{\|\boldsymbol{\zeta}\|_{\boldsymbol{H}^{1/2}(\mathcal{T})/\mathcal{R}}}\right)\right\}\\
&\lesssim \underline{D}^{-1/2}\left\{\underline{D}^{-1/2}\|\boldsymbol{\phi}-\boldsymbol{\psi}\|_{\boldsymbol{H}^{1/2+s}(\mathcal{T})/\mathcal{R}}\right.\\
&\qquad + C_e(h,D)s^{-1}|\log(\underline{h}/D)|\underline{D}^{-1}\|\boldsymbol{\phi}-\boldsymbol{\psi}\|_{\boldsymbol{H}^{1/2+s}(\mathcal{T})/\mathcal{R}}\\
&\qquad\left. + C_e(h,D)\sup_{\boldsymbol{\zeta}\in\boldsymbol{V}_h\setminus\{\boldsymbol{0}\}}\frac{a(\boldsymbol{\phi}-\boldsymbol{\phi}_h,\boldsymbol{\zeta})}{\|\boldsymbol{\zeta}\|_{\boldsymbol{H}^{1/2}(\mathcal{T})/\mathcal{R}}}\right\}.
\end{aligned}$$

Assuming that $\underline{D}^{-1/2} \lesssim C_e(h, D)\underline{D}^{-1}$ gives the stated error bound. □

As with the extension operators the projection operators used in Chapter 4 shall be used to further our error estimate. Again we apply the extension operators from Lemma 4.16 and the projection operators from Lemma 4.16 to the components of the vectors to get the desired results.

Lemma 6.21. *For $r \in (0,1/2]$ let $\boldsymbol{\phi} \in \tilde{\boldsymbol{H}}^{1/2+r}(\Gamma)$. There holds*

$$\begin{aligned}\inf_{\boldsymbol{\psi}\in\boldsymbol{V}_h} \|\boldsymbol{\phi}-\boldsymbol{\psi}\|_{\boldsymbol{H}^{1/2+s}(\mathcal{T})/\mathcal{R}} \lesssim \underline{D}^{-1-2s}\Big\{&\|\boldsymbol{\phi}-\boldsymbol{\zeta}\|_{\boldsymbol{H}^{1/2+r}(\Gamma)/\mathcal{R}} \\ &+\sum_{l=1}^{L} D_{l_{\mathrm{lag}}}(h_{l_{\mathrm{lag}}}/D_{l_{\mathrm{lag}}})^{-2s}\Big(\|\boldsymbol{\phi}-\boldsymbol{\zeta}|_{\Gamma_{l_{\mathrm{lag}}}}\|^2_{\boldsymbol{L}^2(\gamma_l)/\mathcal{R}} \\ &+\|\boldsymbol{\phi}-\boldsymbol{\zeta}|_{\Gamma_{l_{\mathrm{mor}}}}\|^2_{\boldsymbol{L}^2(\gamma_l)/\mathcal{R}}\Big)\Big\} \quad \forall \boldsymbol{\zeta}\in\boldsymbol{X}_h\end{aligned}$$

uniformly for $s \in (0,r]$.

Proof. We recall the definition of the product norm

$$\|\boldsymbol{\phi}-\boldsymbol{\psi}\|^2_{\boldsymbol{H}^{1/2+s}(\mathcal{T})} = \sum_{i=1}^{3} \|\phi_i-\psi_i\|^2_{H^{1/2+s}(\mathcal{T})}. \tag{6.85}$$

We can now bound as in Chapter 4 by applying Lemma 4.17 to (6.85) we have that for $\boldsymbol{\zeta}\in\boldsymbol{X}_h$

$$\begin{aligned}\|\boldsymbol{\phi}-\boldsymbol{\psi}\|^2_{\boldsymbol{H}^{1/2+s}(\mathcal{T})} \lesssim \underline{D}^{-1-2s}\Bigg(\sum_{i=1}^{3}\Big\{&\|\phi_i-\zeta_i\|^2_{H^{1/2+s}(\mathcal{T})} \\ &+\sum_{l=1}^{L} D_{l_{\mathrm{lag}}}(h_{l_{\mathrm{lag}}}/D_{l_{\mathrm{lag}}})^{-2s}\Big(\|\phi_i-\zeta_i|_{\Gamma_{l_{\mathrm{lag}}}}\|^2_{L^2(\gamma_l)} \\ &+\|\phi_i-\zeta_i|_{\Gamma_{l_{\mathrm{mor}}}}\|^2_{L^2(\gamma_l)}\Big)\Big\}\Bigg).\end{aligned}$$

The result immediately follows for the quotient space. □

Theorem 6.22. *Assume that Assumption 6.16 holds. Then let $\boldsymbol{\phi}$ and $\boldsymbol{\phi}_h$ be the solutions of (6.11) and (6.54) respectively. Assuming that $\boldsymbol{\phi}\in\tilde{\boldsymbol{H}}^{1/2+r}(\Gamma)$, $r\in(0,1/2]$, there holds $\boldsymbol{\xi}\in\prod_{l=1}^{L}\boldsymbol{H}^r(\gamma_l)$ and we have the a priori error estimate*

$$\begin{aligned}\|\boldsymbol{\phi}-\boldsymbol{\phi}_h\|^2_{\boldsymbol{H}^{1/2+s}(\mathcal{T})/\mathcal{R}} \lesssim (C_e(h,D))^2\Big\{&\underline{D}^{-4-2s}|\log(\underline{h}/D)|^2 s^{-2}\Big(\|\boldsymbol{\phi}-\boldsymbol{\zeta}\|^2_{\tilde{\boldsymbol{H}}^{1/2+r}(\Gamma)/\mathcal{R}} \\ &+D(\underline{h}/D)^{-2s}\sum_{l=1}^{L}\Big(\|\boldsymbol{\phi}-\boldsymbol{\zeta}|^2_{\Gamma_{l_{\mathrm{lag}}}}\|^2_{\boldsymbol{L}^2(\gamma_l)/\mathcal{R}} \\ &+\|\boldsymbol{\phi}-\boldsymbol{\zeta}|^2_{\Gamma_{l_{\mathrm{mor}}}}\|^2_{\boldsymbol{L}^2(\gamma_l)/\mathcal{R}}\Big)\Big) \\ &+\underline{D}^{-4}|\log(\underline{h}/D)|^3 \inf_{\boldsymbol{\xi}\in\boldsymbol{M}_k}\|\boldsymbol{\eta}-\boldsymbol{\xi}\|^2_{\boldsymbol{L}^2(\gamma)/\mathcal{R}}\Big\} \\ &\forall\boldsymbol{\zeta}\in\boldsymbol{X}_h,\ \forall\boldsymbol{\xi}\in\boldsymbol{M}_k.\end{aligned}$$

uniformly for $s \in (0, r]$, assuming that $\underline{D}^{-1/2} \lesssim C_e(h, D)\underline{D}^{-1}$. Here, $\boldsymbol{\xi}$ is the Lagrangian multiplier defined by (6.72) and (6.73).

Proof. Since $\boldsymbol{\phi} \in \tilde{\boldsymbol{H}}^{1/2+r}(\Gamma)$ ($r \in (0, 1/2]$) there holds $\boldsymbol{\xi}|_{\gamma_l} \in \boldsymbol{H}^r(\gamma_l)$. By combining (6.36) and (6.39) we have by (6.50)

$$\boldsymbol{\xi}_1 = \sum_{k=1}^{3} \mu V \begin{pmatrix} (\mathbf{curl}_\Gamma\, \phi_1)_k \\ (\mathbf{curl}_\Gamma\, \phi_2)_k \\ (\mathbf{curl}_\Gamma\, \phi_3)_k \end{pmatrix} n_k(x).$$

Now using the continuity of $\mathbf{curl}_\Gamma : \tilde{H}^{1/2+r}(\Gamma) \to \tilde{\boldsymbol{H}}_t^{r-1/2}(\Gamma)$ we have that

$$\frac{\partial \cdot}{\partial \boldsymbol{S}_k^\Gamma(x)} : \tilde{H}^{1/2+r}(\Gamma) \to \tilde{H}^{r-1/2}(\Gamma).$$

We now have that

$$\begin{pmatrix} (\mathbf{curl}_\Gamma\, \phi_1)_k \\ (\mathbf{curl}_\Gamma\, \phi_2)_k \\ (\mathbf{curl}_\Gamma\, \phi_3)_k \end{pmatrix} \in \tilde{\boldsymbol{H}}^{r-1/2}(\Gamma) \not\subset \tilde{\boldsymbol{H}}_t^{r-1/2}(\Gamma).$$

From [19] we have the continuity $V : \tilde{\boldsymbol{H}}^{r-1/2}(\Gamma) \to \boldsymbol{H}^{1/2+r}(\Gamma)$ and an application of the trace theorem (Lemma 2.22) gives us that $\boldsymbol{\xi}|_{\gamma_l} \in \boldsymbol{H}^r(\gamma_l)$. The result follows for ξ_3 (defined by (6.51))and the second part of ξ_2 (defined by (6.52)) by the same reasoning. The first part of ξ_2 (defined by (6.52)) follows by the continuity of $V_{le} : \tilde{\boldsymbol{H}}^{r-1/2}(\Gamma) \to \boldsymbol{H}^{1/2+r}(\Gamma)$ (from [19]). Proceeding as above we arrive at the desired result. In particular there holds $\boldsymbol{\xi} \in \boldsymbol{L}^2(\gamma)$.

As in the proof of Theorem 4.18 we have that, by Lemma 6.13,

$$|a(\boldsymbol{\phi} - \boldsymbol{\phi}_h, \boldsymbol{\zeta})| = |b(\boldsymbol{\phi}, \boldsymbol{\xi})| \qquad \forall \boldsymbol{\zeta} \in \boldsymbol{V}_h.$$

Where $\boldsymbol{\xi}$ is the Lagrangian multiplier associated with with $\boldsymbol{\phi}$. Application of (6.81) yields

$$a(\boldsymbol{\phi} - \boldsymbol{\phi}_h, \boldsymbol{\zeta}) \lesssim \underline{D}^{-1/2} |\log(\underline{h}/D)|^{1/2} \inf_{\boldsymbol{\xi} \in \boldsymbol{M}_k} \|\boldsymbol{\eta} - \boldsymbol{\xi}\|_{\boldsymbol{L}^2(\gamma)} \|\boldsymbol{\zeta}\|_{\boldsymbol{H}^{1/2}(\mathcal{T})} \quad \forall \boldsymbol{\psi} \in \boldsymbol{V}_h.$$

Therefore combining Theorem 6.20 with Lemma 6.21 we obtain

$$\begin{aligned}\|\boldsymbol{\phi}-\boldsymbol{\phi}_h\|^2_{\boldsymbol{H}^{1/2+s}(\mathcal{T})/\mathcal{R}} \lesssim\ & (C_e(h,D))^2\underline{D}^{-3}|\log(\underline{h}/D)|^2\Big\{s^{-2}\underline{D}^{-1-2s}\Big(\|\boldsymbol{\phi}-\boldsymbol{\zeta}\|^2_{\boldsymbol{H}^{1/2+r}(\Gamma)/\mathcal{R}}\\ &+D(\underline{h}/D)^{-2s}\sum_{l=1}^{L}\Big(\|\boldsymbol{\phi}-\boldsymbol{\zeta}|^2_{\Gamma_{l_{\mathrm{lag}}}}\|^2_{\boldsymbol{L}^2(\gamma_l)/\mathcal{R}}\\ &+\|\boldsymbol{\phi}-\boldsymbol{\zeta}|^2_{\Gamma_{l_{\mathrm{mor}}}}\|^2_{\boldsymbol{L}^2(\gamma_l)/\mathcal{R}}\Big)\Big)\\ &+\underline{D}^{-1}|\log(\underline{h}/D)|\inf_{\boldsymbol{\xi}\in\boldsymbol{M}_k}\|\boldsymbol{\eta}-\boldsymbol{\xi}\|^2_{\boldsymbol{L}^2(\gamma)/\mathcal{R}}\Big\}\\ &\forall\boldsymbol{\zeta}\in\boldsymbol{X}_h,\ \forall\boldsymbol{\xi}\in\boldsymbol{M}_k.\end{aligned}$$

The statement then immediately follows. □

Main result

Theorem 6.23. *Assume that Assumption 6.16 holds. Then there exists a unique solution* $(\boldsymbol{\phi}_h,\boldsymbol{\xi}_k)$ *of (6.54). Assume that the solution* $\boldsymbol{\phi}$ *of (6.11) satisfies* $\boldsymbol{\phi}\in\tilde{\boldsymbol{H}}^{1/2+r}(\Gamma)$ *(*$r\in(0,1/2]$*). Then there holds*

$$\begin{aligned}\|\boldsymbol{\phi}-\boldsymbol{\phi}_h\|_{\boldsymbol{H}^{1/2}(\mathcal{T})/\mathcal{R}} \lesssim\ & \Big(\underline{D}^{-9/2}|\log(\underline{h}/D)|^{5/2}(h/\underline{D})^r\\ &+\underline{D}^{-2}|\log(\underline{h}/D)|^{3/2}(k/\underline{K})^r\Big)\|\boldsymbol{\phi}\|_{\tilde{\boldsymbol{H}}^{1/2+r}(\Gamma)}\end{aligned}$$

For proportional mesh sizes h *and* k *this means that*

$$\|\boldsymbol{\phi}-\boldsymbol{\phi}_h\|_{\boldsymbol{H}^{1/2}(\mathcal{T})/\mathcal{R}}\lesssim\Big(\underline{D}^{-9/2}|\log(\underline{h}/D)|^{5/2}(h/\underline{D})^r\Big)\|\boldsymbol{\phi}\|_{\tilde{\boldsymbol{H}}^{1/2+r}(\Gamma)}$$

Assuming that $\underline{D}^{-1/2}\lesssim C_e(h,D)\underline{D}^{-1}$.

Proof. By Theorem 6.20, system (6.54) is uniquely solvable. We use the general a-priori estimate given by Theorem 6.22 to show the given error bound. Similarly to the proof of Theorem 4.19 we have by standard approximation theory that there exist $\boldsymbol{\zeta}\in\boldsymbol{X}_h$ and $\boldsymbol{\xi}\in\boldsymbol{M}_k$ such that (for the components of our vectors) we have by (4.37)

$$\|\phi_i-\zeta_i\|^2_{H^{1/2+s}(\mathcal{T})}\lesssim\underline{D}^{-2}(h/\underline{D})^{2(r-s)}\|\phi_i\|^2_{\tilde{H}^{1/2+r}(\Gamma)},$$

and by (4.38)

$$\|\eta_i-\xi_i\|^2_{L^2(\gamma)}\lesssim(k/\underline{K})^{2r}\sum_{l=1}^{L}\|\eta_i\|^2_{H^r(\gamma_l)}.$$

As in the proof of Theorem 6.22 one concludes that $\sum_{l=1}^{L} \|\eta_i\|^2_{H^r(\gamma_l)} \lesssim \|\phi_i\|^2_{H^{1/2+r}(\Gamma)}$. By Lemma 2.22 one bounds, as in Theorem 4.19 (recalling that K_l is proportional to $D_{l_{\rm lag}}$), by (4.39)

$$\|\phi_i - \zeta_i|_{\Gamma_{l_{\rm lag}}}\|_{L^2(\gamma_l)} \lesssim D_{l_{\rm lag}}^{-1/2} s^{-1/2} (h_{l_{\rm lag}}/D_{l_{\rm lag}})^{r-s} \|\phi_i\|_{H^{1/2+r}(\Gamma_{l_{\rm lag}})},$$

and accordingly the mortar part $\|\boldsymbol{\phi} - \boldsymbol{\zeta}_{l_{\rm mor}}\|_{\boldsymbol{L}^2(\gamma_l)}$. Using these bounds in Theorem 6.22 and selecting $s = |\log(\underline{h}/D)|^{-1}$ one obtains the assertion. □

Chapter 7

Conclusions and Further Research

In this chapter we shall review the main results presented in the thesis and make suggestions for further research.

7.1 Conclusions

In Chapter 3 we presented the formulation of the BEM with Lagrangian multiplier for the Laplacian. This method allowed us to approximate the boundary conditions used in the standard boundary element formulation. While, in itself, the method is not really a viable solution it is the first step in allowing us to formulate a mortar style approximation to the problem. We proved the almost quasi-optimal convergence of the scheme, and compared it to the standard (conforming) BEM (to which it is slightly inferior).

In Chapter 4 we presented the formulation of the mortar BEM. The method allows sub-domain decompositions to be (globally) geometrically non-conforming and meshes to be quasi-uniform only on sub-domains. However we do have the restriction of Assumption 4.2. We were able to prove almost quasi-optimal convergence of the scheme, and its dependence upon sub-domain size. However these results may not be optimal and may be able to be improved upon. The result is not optimal because of the dependence on sub-domain size of some of the estimates. Also when bounding sub-domain size we have not always used optimal bounds, for example we replaced $D_i^{-2\epsilon}$ by D_i^{-1} in (4.18) and $\underline{D}^{-1-2s}$ by $\underline{D}^{-2}$ in (4.37). The slight loss of optimality is caused by the lack of a trace operator for functions in $H^{1/2}$.

In Chapter 5 we presented numerical results for both the boundary element method with Lagrangian multiplier and for the mortar boundary element method. These results underlined the theoretical results of the previous chapters. In particular for the mortar boundary element method we were able to show the effects of defining the Lagrangian multipliers in different ways on the accuracy of the approximation. We were also able to

show results for a decomposition of sub-domains which did not satisfy Assumption 4.2.

In Chapter 6 we presented the formulation of the mortar boundary element method for linear elasticity. These results are an extension of the work in Chapter 4. We were unable to prove the V_h ellipticity of the bilinear form $a(\cdot,\cdot)$. Instead we presented Conjecture 6.15 and discussed some of the problems we encountered in Remark 6.17. Assuming that the conjecture was true we were able to prove a quasi-optimal result similar to that proved in Chapter 4.

7.2 Suggestions for further research

We shall now present suggestions relating to how the work in this thesis can be extended. We also include some unanswered questions which arose during the preparation of this thesis.

In Chapter 3 we presented the formulation of the BEM with Lagrangian multiplier for the Laplacian. We presented an error estimate which showed how the accuracy of the solution depended on the mesh size. The obvious extension to this is to extend this h-version (dependence on sub-domain size) to a p-version (dependence on polynomial degree), and eventually a full hp-version (dependence on both mesh size and polynomial degree). By a p-version we mean a scheme where instead of reducing the mesh size to improve the accuracy of the approximation we increase the polynomial degree on each element to improve the accuracy. A full hp-scheme would be one where we would be able to both decrease the mesh size and increase the polynomial degree to get an improved approximation. Not only would we be able to gain a better approximation through the use of higher degree polynomials defined over the domain (we used piecewise linear functions in Chapter 3) we must use higher degree polynomials for the Lagrangian multiplier space (we used piecewise constant functions over a coarsened mesh in Chapter 3). This would make the analysis and implementation of the method more complicated.

In Chapter 4 we presented the formulation of the mortar boundary element method. As in Chapter 3 we presented an error estimate which showed how the accuracy of the approximation depended upon mesh size (and also upon sub-domain size). Again the obvious extension is to develop a p-version and then a full hp-scheme. The ability to use different mesh sizes and different polynomial degrees on separate sub-domains would be a useful tool. Also, the ability to be able to use polynomials of different degrees on each interface in the definition of the Lagrangian multiplier space would lead to a better approximation. Another extension would be to relax Assumption 4.2, which stated that each interface was a whole edge of at least one of the sub-domains that form the interface. This is a restriction that would be useful to remove, and the numerical results (see Section 5.3.3) appear to suggest that the assumption can be relaxed.

In Chapter 6 we presented the formulation of the mortar BEM for linear elasticity. The first thing to be further examined is Conjecture 6.15 which states the ellipticity of the bilinear form $a(\cdot,\cdot)$ on the constrained space. As discussed in Remark 6.17 the proof of this conjecture has obstacles to be overcome. As in the previous paragraph the results could be extended to a full *hp*-scheme for a more versatile and accurate method. The relaxation of Assumption 4.2 would also have a knock on effect into the results of this chapter.

Further objectives beyond what have been stated above are many and varied. Other operators could be examined, such as the Helmholtz or Maxwell operators which would have new difficulties as they do not possess the same properties as those examined in this thesis (the Helmholtz operator is indefinite, and the Maxwell operator is not elliptic or positive definite). Related problems from numerical linear algebra could also be examined. These may include the analysis of specific solvers and preconditioners for the systems described in this thesis. Related to this point is the the notion of parallel implementations of the mortar BEM to make use of the independence of the sub-domains. By this we mean that different processors could handle different parts (sub-domains) of the problem, improving the speed and efficiency of the scheme.

Appendix A

Proof of Proposition 4.8

This section presents the proof of Proposition 4.8. We note that this result needs only hold for a conforming decomposition of triangles. A decomposition into rectangles can easily be decomposed in to a decomposition of triangles, e.g. by connecting two opposite corners of a rectangle. A non-conforming decomposition can be transformed into a conforming one by the further subdivision of sub-domains, see [13]. We show in Figure A.1 an example of such a transformation of a decomposition.

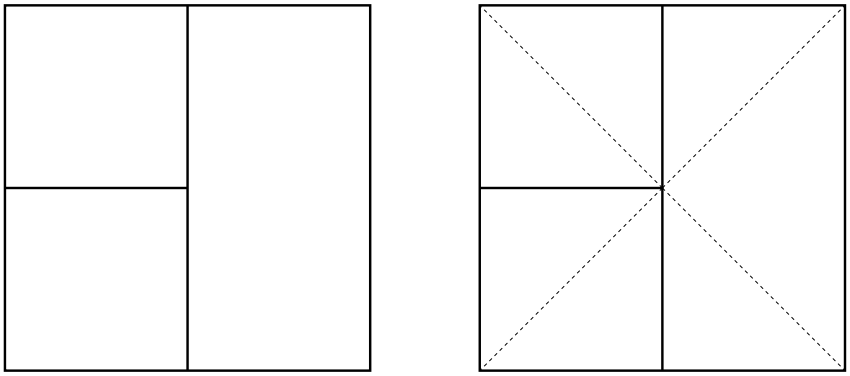

Figure A.1: Mesh example

We shall use the following notation for our decomposition into triangles. We shall denote the set of all triangles in the decomposition by $\mathcal{T}_t$, and we shall use $t \in \mathcal{T}_t$ to denote a generic triangle in the decomposition and use h_t to represent the diameter of a triangle. We shall denote by e an edge of a triangle t, and use h_e to denote the length of an edge e. The set of all edges of the decomposition shall be denoted by $\mathcal{E}_{\mathcal{T}_t}$. $\hat{t}$ is the

reference triangle as described earlier. We shall also use the space

$$V_{T_t} := \{v \in L_2(\Gamma) \ : \ (\mathcal{I}v)|_t \in P_1(t) \text{ for any } t \in \mathcal{T}_t \text{ and } v \text{ is continuous at the common side of any two neighbouring sub-domains and } v|_{\partial\Gamma} = 0\}.$$

Following [13] we define the following interpolation operators,

$$\mathcal{I} : \prod_{t\in\mathcal{T}_t} H^1(t) \to V_{T_t}$$
$$(\mathcal{I}v)(m_e) := \frac{1}{h_e}\int_e \{v\},$$

where m_e is the midpoint of the edge e, and $\{v\}$ is the average of the values of v approaching e from the elements sharing e, and

$$\Pi : \prod_{t\in\mathcal{T}_t} H^1(t) \to \prod_{t\in\mathcal{T}_t} P_1(t)$$
$$(\Pi v)(m_e) := \frac{1}{h_e}\int_e v|_t.$$

Note that there holds, for $[v]$ the jump of v over the edge e,

$$(\mathcal{I}v - \Pi v)|_t(m_e) = \frac{1}{2h_e}\int_e [v].$$

Lemma A.1. *For all $\epsilon \in (0.1/2)$, $v \in H^{1/2+\epsilon}(\mathcal{T}_t)$, and $t \in \mathcal{T}_t$,*

$$\sum_{t\in\mathcal{T}_t} |\mathcal{I}v - \Pi v|^2_{H^{1/2+\epsilon}(t)} \lesssim \sum_{e\in\mathcal{E}(t)\setminus\partial\Gamma} h_e^{-1-2\epsilon} |\int_e [v]|^2 \tag{A.1}$$

$$\sum_{t\in\mathcal{T}_t} |\Pi v|^2_{H^{1/2+\epsilon}(t)} \lesssim \sum_{t\in\mathcal{T}_t} \epsilon^{-1} |v|^2_{H^{1/2+\epsilon}(t)} \tag{A.2}$$

$$\sum_{t\in\mathcal{T}_t} \|v - \Pi v\|^2_{L_2(\Gamma)} \lesssim \sum_{t\in\mathcal{T}_t} \epsilon^{-1} h_t^{1+2\epsilon} |v|^2_{H^{1/2+\epsilon}(t)}. \tag{A.3}$$

Proof. For (A.1) we have from [13] that

$$\sum_{t\in\mathcal{T}_t} |\mathcal{I}v - \Pi v|^2_{H^1(t)} \lesssim \sum_{e\in\mathcal{E}(t)\setminus\partial\Gamma} h_e^{-2} |\int_e [v]|^2,$$

$$\sum_{t\in\mathcal{T}_t} \|\mathcal{I}v - \Pi v\|^2_{L_2(t)} \lesssim \sum_{e\in\mathcal{E}(t)\setminus\partial\Gamma} |\int_e [v]|^2.$$

The result follows by interpolation. For (A.2) and (A.3) we simply follow the proof of [30, Lemma 9]. □

Lemma A.2. *For all $\epsilon \in (0, 1/2)$ and $v \in H^{1/2+\epsilon}(\mathcal{T}_t)$*

$$\sum_{t\in\mathcal{T}_t} |\mathcal{I}v|^2_{H^{1/2+\epsilon}(\mathcal{T}_t)} \lesssim \sum_{t\in\mathcal{T}_t} \epsilon^{-1}|v|^2_{H^{1/2+\epsilon}(t)} + \sum_{e\in\mathcal{E}(t)\setminus\partial\Gamma} h_e^{-1-2\epsilon}|\int_e [v]|^2 \tag{A.4}$$

$$\|v - \mathcal{I}v\|^2_{L_2(\Gamma)} \lesssim \sum_{t\in\mathcal{T}_t} \epsilon^{-1}h_t^{1+2\epsilon}|v|^2_{H^{1/2+\epsilon}(t)} + \sum_{e\in\mathcal{E}(t)\setminus\partial\Gamma} |\int_e [v]|^2. \tag{A.5}$$

Proof. We simply follow the proof of [30, Lemma 10]. □

Let $W_{\mathcal{T}_t}$ be the space of continuous P_2 finite elements on T_t. Let $E_{\mathcal{T}_t} : V_{\mathcal{T}_t} \to W_{\mathcal{T}_t}$ be the interpolation operator that takes values at midpoints of sides and average values at vertices. Let $F_{\mathcal{T}_t} : W_{\mathcal{T}_t} \to V_{\mathcal{T}_t}$ be the interpolation operator that takes values only on the midpoints of the sides. Note that $F_{\mathcal{T}_t}E_{\mathcal{T}_t} = I$ in $V_{\mathcal{T}_t}$, and that in particular $\mathcal{I}v \in V_{\mathcal{T}_t}$ for $v \in H^{1/2+\epsilon}(\mathcal{T}_t)$.

Lemma A.3. *For all $r \in (0, 1)$, and $\forall \xi \in V_{\mathcal{T}_t}$*

$$\|E_{\mathcal{T}_t}\xi - \xi\|^2_{L_2(\Gamma)} \lesssim \sum_{t\in\mathcal{T}_t} h_t^{2r}|\xi|^2_{H^r(t)} \tag{A.6}$$

$$\|E_{\mathcal{T}_t}\xi\|_{L_2(\Gamma)} \approx \|\xi\|_{L_2(\Gamma)} \tag{A.7}$$

$$|E_{\mathcal{T}_t}\xi|^2_{L_2(\Gamma)} \lesssim \sum_{t\in\mathcal{T}_t} |\xi|^2_{H^r(t)}. \tag{A.8}$$

Proof. We simply follow the proof of [30, Lemma 11]. □

Lemma A.4. *For all $r \in (0, 1)$ and for all $\xi \in V_{\mathcal{T}_t}$*

$$\|\xi\|^2_{L_2(\Gamma)} \lesssim \sum_{t\in\mathcal{T}_t} |\xi|^2_{H^r(t)}. \tag{A.9}$$

Proof. Again we follow the proof of [30, Proposition 12]. We note that the term $|\int_\Gamma \xi|$ is not included as a result of our boundary conditions, the constant function 0 is the only admissible constant function due the boundary conditions and the continuity condition across a midpoint of a side imposed on functions in $V_{\mathcal{T}_t}$. □

Proposition A.5. *For $v \in \prod_{i=1}^n H^{1/2+\epsilon}(\mathcal{T}_t)$*

$$\|v\|^2_{L_2(\Gamma)} \lesssim \sum_{t\in\mathcal{T}_t} \epsilon^{-1}|v|^2_{H^{1/2+\epsilon}(t)} + \sum_{e\in\mathcal{E}(t)\setminus\partial\Gamma} h_e^{-1-2\epsilon}|\int_e [v]|^2. \tag{A.10}$$

Proof. For $v \in \prod_{t\in\mathcal{T}_t} H^{1/2+\epsilon}(\mathcal{T}_t)$ by the triangle inequality and Lemma A.4

$$\begin{aligned}\|v\|^2_{L_2(\Gamma)} &= \|v + \mathcal{I}v - \mathcal{I}v\|^2_{L_2(\Gamma)} \\ &\lesssim \|v - \mathcal{I}v\|^2_{L_2(\Gamma)} + \|\mathcal{I}v\|^2_{L_2(\Gamma)} \\ &\lesssim \|v - \mathcal{I}v\|^2_{L_2(\Gamma)} + \sum_{t\in\mathcal{T}_t} |\mathcal{I}v|^2_{H^{1/2+\epsilon}(t)}.\end{aligned}$$

We can now apply (A.4) and (A.5) to get the stated result. □

Proof of Proposition 4.8. It is immediate that the jump across any artificial edges which have been added to the original decomposition into sub-domains ($\Gamma_i, i \in \{1,\ldots,N\}$ see Section 4.1.2) to turn the decomposition into a conforming decomposition of triangles is equal to zero, as in the original decomposition the function is continuous across this edge at all points. We are thus left only with jumps across the original edges. We also note that

$$\prod_{i=1}^{n} H^{1/2+\epsilon}(\Gamma_i) \subset \prod_{t\in\mathcal{T}_t} H^{1/2+\epsilon}(t).$$

The result then follows.

Appendix B

Tables Of Numerical Results

In this appendix we present in tabular form the numerical results presented in the figures in Chapter 5. We present the numerical results at the precision of three significant figures for conciseness.

BEM with Lagrangian multiplier (Results in Figure 5.2)

	Dimension		Part 1	Part 2	BEM	
h	X_h	M_k	of error	of error	Lagrange	BEM
1/6	49	12	0.237	0.753	0.789	0.361
1/8	81	16	0.234	0.648	0.689	0.309
1/10	121	20	0.224	0.575	0.617	0.274
1/12	169	24	0.212	0.520	0.562	0.249
1/14	225	28	0.202	0.478	0.519	0.230
1/16	289	32	0.192	0.443	0.483	0.214
1/18	361	36	0.184	0.415	0.454	0.201
1/20	441	40	0.176	0.391	0.428	0.191
1/22	529	44	0.169	0.370	0.407	0.182
1/24	625	48	0.163	0.352	0.388	0.174
1/26	729	52	0.158	0.336	0.371	0.167
1/28	841	56	0.153	0.321	0.356	0.160
1/30	961	60	0.148	0.309	0.342	0.155
1/32	1089	64	0.144	0.297	0.330	0.150
1/34	1225	68	0.140	0.287	0.319	0.145
1/36	1369	72	0.136	0.277	0.309	0.141
1/38	1521	76	0.133	0.269	0.300	0.137
1/40	1681	80	0.130	0.261	0.291	0.134
1/42	1849	84	0.127	0.253	0.283	0.131
1/44	2025	88	0.124	0.246	0.276	0.128
1/46	2209	92	0.122	0.240	0.269	0.125
1/48	2401	96	0.119	0.234	0.263	0.122

Table B.1: Dimensions and mesh sizes for BEM with Lagrangian multiplier

Mortar BEM experiment 1 (Results in Figure 5.5)

	Dimension		Part 1	Part 2	Mortar	
h	X_h	M_k	of error	of error	BEM	BEM
1/4	16	4	0.450	$0.561 * 10^{-7}$	0.450	0.450
1/6	36	4	0.361	$0.369 * 10^{-6}$	0.361	0.361
1/8	64	8	0.309	$0.132 * 10^{-6}$	0.309	0.309
1/10	100	8	0.274	$0.599 * 10^{-6}$	0.274	0.274
1/12	144	12	0.249	$0.133 * 10^{-5}$	0.249	0.249
1/14	196	12	0.230	$0.161 * 10^{-5}$	0.230	0.230
1/16	256	16	0.214	$0.519 * 10^{-6}$	0.214	0.214
1/18	324	16	0.201	$0.237 * 10^{-5}$	0.201	0.201
1/20	400	20	0.191	$0.439 * 10^{-5}$	0.191	0.191
1/22	484	20	0.182	$0.505 * 10^{-5}$	0.182	0.182
1/24	576	24	0.174	$0.801 * 10^{-5}$	0.174	0.174
1/26	676	24	0.167	$0.737 * 10^{-5}$	0.167	0.167
1/28	784	28	0.160	$0.106 * 10^{-4}$	0.160	0.160
1/30	900	28	0.155	$0.909 * 10^{-5}$	0.155	0.155
1/32	1024	32	0.150	$0.263 * 10^{-5}$	0.150	0.150
1/34	1156	32	0.145	$0.852 * 10^{-5}$	0.145	0.145
1/36	1296	36	0.141	$0.161 * 10^{-4}$	0.141	0.141
1/38	1444	36	0.137	$0.156 * 10^{-4}$	0.137	0.137
1/40	1600	40	0.134	$0.187 * 10^{-4}$	0.134	0.134
1/42	1764	40	0.131	$0.230 * 10^{-4}$	0.131	0.131
1/44	1936	44	0.128	$0.194 * 10^{-4}$	0.128	0.128
1/46	2116	44	0.125	$0.231 * 10^{-4}$	0.125	0.125
1/48	2304	48	0.122	$0.292 * 10^{-4}$	0.122	0.122

Table B.2: Dimensions and mesh sizes for mortar BEM experiment 1

Mortar BEM experiment 2 (Results in Figure 5.6)

max h			min h	Dimension			Part 1 of	Part 2 of	Mortar	Part 1 of	Part 2 of	Mortar
h_1	h_2	h_3	h_4	X_h	M_k I	M_k II	Error I	Error I	BEM I	Error II	Error II	BEM II
1/4	1/6	1/8	1/10	54	5	7	0.353	0.348	0.496	0.354	0.342	0.493
1/6	1/8	1/10	1/12	86	6	10	0.300	0.277	0.409	0.302	0.267	0.403
1/8	1/10	1/12	1/14	126	9	11	0.267	0.221	0.347	0.267	0.222	0.347
1/10	1/12	1/14	1/16	174	10	14	0.243	0.187	0.306	0.243	0.183	0.304
1/12	1/14	1/16	1/18	230	13	15	0.224	0.161	0.276	0.224	0.161	0.276
1/14	1/16	1/18	1/20	294	14	18	0.209	0.143	0.254	0.209	0.139	0.251
1/16	1/18	1/20	1/22	366	17	19	0.197	0.127	0.235	0.197	0.127	0.235
1/18	1/20	1/22	1/24	446	18	22	0.187	0.117	0.220	0.187	0.112	0.218
1/20	1/22	1/24	1/26	534	21	23	0.178	0.105	0.207	0.178	0.106	0.207
1/22	1/24	1/26	1/28	630	22	26	0.171	$0.984 * 10^{-1}$	0.197	0.171	$0.946 * 10^{-1}$	0.195
1/24	1/26	1/28	1/30	734	25	27	0.164	$0.901 * 10^{-1}$	0.187	0.164	$0.909 * 10^{-1}$	0.188
1/26	1/28	1/30	1/32	846	26	30	0.158	$0.853 * 10^{-1}$	0.180	0.158	$0.820 * 10^{-1}$	0.178
1/28	1/30	1/32	1/34	966	29	31	0.153	$0.788 * 10^{-1}$	0.172	0.153	$0.797 * 10^{-1}$	0.172
1/30	1/32	1/34	1/36	1094	30	34	0.148	$0.754 * 10^{-1}$	0.166	0.148	$0.725 * 10^{-1}$	0.165
1/32	1/34	1/36	1/38	1230	33	35	0.144	$0.701 * 10^{-1}$	0.160	0.144	$0.710 * 10^{-1}$	0.160
1/34	1/36	1/38	1/40	1374	34	38	0.140	$0.675 * 10^{-1}$	0.155	0.140	$0.650 * 10^{-1}$	0.154
1/36	1/38	1/40	1/42	1526	37	39	0.136	$0.631 * 10^{-1}$	0.150	0.136	$0.641 * 10^{-1}$	0.150
1/38	1/40	1/42	1/44	1686	38	42	0.132	$0.612 * 10^{-1}$	0.146	0.132	$0.589 * 10^{-1}$	0.145
1/40	1/42	1/44	1/46	1854	41	43	0.129	$0.574 * 10^{-1}$	0.141	0.129	$0.584 * 10^{-1}$	0.142
1/42	1/44	1/46	1/48	2030	42	46	0.126	$0.560 * 10^{-1}$	0.138	0.126	$0.539 * 10^{-1}$	0.137
1/44	1/46	1/48	1/50	2214	45	47	0.124	$0.527 * 10^{-1}$	0.134	0.124	$0.536 * 10^{-1}$	0.135

Table B.3: Dimensions and mesh sizes for mortar BEM experiment 2

Mortar BEM experiment 3 (Results in Figure 5.7)

max h			min h	Dimension			Part 1 of	Part 2 of	Mortar	Part 1 of	Part 2 of	Mortar
h_1	h_2	h_3	h_4	X_h	M_k I	M_k II	Error I	Error I	BEM I	Error II	Error II	BEM II
1/8	1/10	1/12	1/14	126	9	11	0.267	0.221	0.347	0.267	0.222	0.347
1/12	1/16	1/20	1/24	344	15	21	0.209	0.194	0.285	0.209	0.184	0.279
1/16	1/22	1/28	1/34	670	20	28	0.177	0.168	0.244	0.177	0.170	0.245
1/20	1/28	1/36	1/44	1104	26	38	0.157	0.150	0.217	0.157	0.129	0.203
1/24	1/34	1/44	1/54	1646	31	45	0.142	0.137	0.198	0.142	0.138	0.198
1/28	1/40	1/52	1/64	2296	37	55	0.131	0.127	0.183	0.131	0.106	0.169

Table B.4: Dimensions and mesh sizes for mortar BEM experiment 3

Mortar BEM experiment 4 (Results in Figure 5.10)

max h		min h	Dimension			Part 1 of	Part 2 of	Mortar	Part 1 of	Part 2 of	Mortar
h_1	h_2	h_3	X_h	M_k I	M_k II	Error I	Error I	BEM I	Error II	Error II	BEM II
1/2	1/4	1/4	10	3	2	0.505	0.632	0.809	0.505	0.632	0.809
1/3	1/6	1/6	24	3	2	0.410	0.460	0.616	0.410	0.460	0.616
1/4	1/8	1/8	44	6	4	0.352	0.404	0.536	0.349	0.388	0.522
1/5	1/10	1/10	70	6	4	0.311	0.355	0.472	0.310	0.347	0.465
1/6	1/12	1/12	102	9	6	0.283	0.312	0.421	0.281	0.316	0.423
1/7	1/14	1/14	140	9	6	0.260	0.295	0.393	0.259	0.293	0.391
1/8	1/16	1/16	184	12	8	0.242	0.263	0.358	0.241	0.274	0.365
1/9	1/18	1/18	234	12	8	0.227	0.258	0.344	0.227	0.258	0.344
1/10	1/20	1/20	290	15	10	0.215	0.234	0.318	0.214	0.245	0.326
1/11	1/22	1/22	352	15	10	0.205	0.233	0.310	0.204	0.233	0.310
1/12	1/24	1/24	420	18	12	0.196	0.213	0.290	0.195	0.224	0.297
1/13	1/26	1/26	494	18	12	0.188	0.214	0.284	0.187	0.215	0.285
1/14	1/28	1/28	574	21	14	0.181	0.198	0.268	0.180	0.207	0.275
1/15	1/30	1/30	660	21	14	0.174	0.199	0.264	0.174	0.200	0.265
1/16	1/32	1/32	752	24	16	0.169	0.185	0.250	0.168	0.194	0.257
1/17	1/34	1/34	850	24	16	0.163	0.187	0.248	0.163	0.188	0.249
1/18	1/36	1/36	954	27	18	0.159	0.174	0.236	0.158	0.183	0.242
1/19	1/38	1/38	1064	27	18	0.154	0.177	0.235	0.154	0.177	0.235
1/20	1/40	1/40	1180	30	20	0.150	0.165	0.223	0.150	0.173	0.229
1/21	1/42	1/42	1302	30	20	0.147	0.168	0.223	0.146	0.169	0.223
1/22	1/44	1/44	1430	33	22	0.143	0.158	0.213	0.143	0.165	0.219
1/23	1/46	1/46	1564	33	22	0.140	0.161	0.213	0.140	0.161	0.213
1/24	1/48	1/48	1704	36	24	0.137	0.151	0.204	0.137	0.158	0.209
1/25	1/50	1/50	1850	36	24	0.134	0.154	0.204	0.134	0.155	0.205
1/26	1/52	1/52	2002	39	26	0.132	0.145	0.196	0.131	0.152	0.201
1/27	1/54	1/54	2160	39	26	0.129	0.148	0.196	0.129	0.149	0.197

Table B.5: Dimensions and mesh sizes for mortar BEM experiment 4

Mortar BEM experiment 5 (results in Figure 5.11)

max h		min h	Dimension			Part 1 of	Part 2 of	Mortar	Part 1 of	Part 2 of	Mortar
h_1	h_2	h_3	X_h	M_k	M_k II	Error I	Error I	BEM I	Error II	Error II	BEM II
1/4	1/4	1/6	25	3	3	0.397	0.337	0.521	0.397	0.337	0.521
1/5	1/6	1/8	45	4	4	0.339	0.293	0.448	0.339	0.294	0.449
1/6	1/8	1/10	71	6	5	0.301	0.270	0.405	0.301	0.273	0.407
1/7	1/10	1/12	103	7	6	0.274	0.261	0.378	0.274	0.261	0.379
1/8	1/12	1/14	141	9	7	0.253	0.246	0.353	0.253	0.247	0.354
1/9	1/14	1/16	185	10	8	0.236	0.238	0.335	0.236	0.238	0.335
1/10	1/16	1/18	235	12	9	0.223	0.226	0.317	0.222	0.227	0.318
1/11	1/18	1/20	291	13	10	0.211	0.219	0.304	0.211	0.219	0.304
1/12	1/20	1/22	353	15	11	0.201	0.209	0.290	0.201	0.211	0.291
1/13	1/22	1/24	421	16	12	0.192	0.204	0.280	0.192	0.204	0.280
1/14	1/24	1/26	495	18	13	0.185	0.196	0.269	0.185	0.197	0.270
1/15	1/26	1/28	575	19	14	0.178	0.192	0.261	0.178	0.191	0.261
1/16	1/28	1/30	661	21	15	0.172	0.185	0.252	0.172	0.186	0.253
1/17	1/30	1/32	753	22	16	0.166	0.181	0.246	0.166	0.181	0.246
1/18	1/32	1/34	851	24	17	0.161	0.175	0.238	0.161	0.176	0.239
1/19	1/34	1/36	955	25	18	0.157	0.172	0.233	0.157	0.172	0.233
1/20	1/36	1/38	1065	27	19	0.153	0.166	0.226	0.153	0.168	0.227
1/21	1/38	1/40	1181	28	20	0.149	0.164	0.221	0.149	0.164	0.221
1/22	1/40	1/42	1303	30	21	0.145	0.159	0.215	0.145	0.160	0.216
1/23	1/42	1/44	1431	31	22	0.142	0.157	0.212	0.142	0.157	0.212
1/24	1/44	1/46	1565	33	23	0.139	0.152	0.206	0.139	0.154	0.207
1/25	1/46	1/48	1705	34	24	0.136	0.151	0.203	0.136	0.151	0.203
1/26	1/48	1/50	1851	36	25	0.133	0.147	0.198	0.133	0.148	0.199
1/27	1/50	1/52	2003	37	26	0.131	0.146	0.196	0.130	0.146	0.195
1/28	1/52	1/54	2161	39	27	0.128	0.141	0.191	0.128	0.143	0.192

Table B.6: Dimensions and mesh sizes for mortar BEM experiment 5

Mortar BEM experiment 6 (Results in Figure 5.12)

max h	min h		Dimension			Part 1 of	Part 2 of	Mortar	Part 1 of	Part 2 of	Mortar
h_3	h_1	h_2	X_h	M_k I	M_k II	Error I	Error I	BEM I	Error II	Error II	BEM II
1/2	0.1250	0.1667	27	4	3	0.468	0.575	0.741	0.458	0.635	0.783
1/3	0.0625	0.0833	80	7	4	0.382	0.278	0.472	0.367	0.466	0.593
1/4	0.0417	0.0556	161	11	7	0.320	0.215	0.385	0.310	0.397	0.504
1/5	0.0313	0.0417	270	14	8	0.281	0.182	0.335	0.274	0.354	0.448
1/6	0.0250	0.0333	407	18	11	0.254	0.164	0.302	0.248	0.321	0.406
1/7	0.0208	0.0278	572	21	12	0.233	0.150	0.277	0.228	0.298	0.375
1/8	0.0179	0.0238	765	25	15	0.216	0.139	0.257	0.213	0.278	0.350
1/9	0.0156	0.0208	986	28	16	0.203	0.131	0.241	0.200	0.263	0.330
1/10	0.0139	0.0185	1235	32	19	0.192	0.123	0.228	0.189	0.249	0.312
1/11	0.0125	0.0167	1512	35	20	0.182	0.118	0.217	0.180	0.237	0.298
1/12	0.0114	0.0152	1817	39	23	0.174	0.112	0.207	0.172	0.227	0.285
1/13	0.0104	0.0139	2150	42	24	0.166	0.108	0.199	0.165	0.218	0.273

Table B.7: Dimensions and mesh sizes for mortar BEM experiment 6

Mortar BEM experiment 7 (Results in Figure 5.15)

max h	min h	Dimension X_h	Dimension M_k I	Dimension M_k II	Part 1 of Error I	Part 2 of Error I	Mortar BEM I	Part 1 of Error II	Part 2 of Error II	Mortar BEM II
7/20	1/4	16	4	4	0.449	0.581	0.734	0.449	0.581	0.734
7/30	1/6	36	4	4	0.356	0.499	0.613	0.356	0.499	0.613
7/40	1/8	64	8	8	0.311	0.301	0.433	0.311	0.301	0.433
7/50	1/10	100	8	8	0.275	0.327	0.427	0.271	0.319	0.419
7/60	1/12	144	12	12	0.250	0.238	0.345	0.250	0.238	0.345
1/10	1/14	196	12	12	0.229	0.270	0.354	0.230	0.256	0.344
7/80	1/16	256	16	16	0.215	0.200	0.294	0.215	0.200	0.294
7/90	1/18	324	16	16	0.201	0.233	0.308	0.202	0.215	0.295
7/100	1/20	400	20	20	0.191	0.178	0.261	0.191	0.178	0.261
7/110	1/22	484	20	20	0.182	0.208	0.276	0.182	0.191	0.264
7/120	1/24	576	24	24	0.174	0.162	0.238	0.174	0.162	0.238
7/130	1/26	676	24	24	0.167	0.189	0.252	0.167	0.173	0.241
1/20	1/28	784	28	28	0.161	0.150	0.220	0.161	0.150	0.220
7/150	1/30	900	28	28	0.155	0.175	0.234	0.155	0.159	0.223
7/160	1/32	1024	32	32	0.150	0.140	0.205	0.150	0.140	0.205
7/170	1/34	1156	32	32	0.145	0.163	0.218	0.146	0.148	0.208
7/180	1/36	1296	36	36	0.142	0.132	0.194	0.142	0.132	0.194
7/190	1/38	1444	36	36	0.137	0.153	0.206	0.138	0.139	0.196
7/200	1/40	1600	40	40	0.134	0.125	0.183	0.134	0.125	0.183
1/30	1/42	1764	40	40	0.131	0.145	0.195	0.131	0.132	0.186
7/220	1/44	1936	44	44	0.128	0.119	0.175	0.128	0.119	0.175
7/230	1/46	2116	44	44	0.125	0.138	0.186	0.125	0.125	0.177
7/240	1/48	2304	48	48	0.122	0.114	0.167	0.122	0.114	0.167

Table B.8: Dimensions and mesh sizes for mortar BEM experiment 7

Mortar BEM experiment 8 (Results in Figure 5.16)

min h			max h	Dimension			Part 1 of	Part 2 of	Mortar	Part 1 of	Part 2 of	Mortar
h_1	h_2	h_3	h_4	X_h	M_k I	M_k II	Error I	Error I	BEM I	Error II	Error II	BEM II
1/10	7/40	1/6	7/20	54	7	5	0.368	0.453	0.583	0.364	0.575	0.680
1/12	7/50	1/8	7/30	86	9	7	0.312	0.357	0.474	0.310	0.412	0.516
1/14	7/60	1/10	7/40	126	11	9	0.273	0.326	0.425	0.275	0.298	0.405
1/16	1/10	1/12	7/50	174	13	11	0.249	0.260	0.360	0.248	0.289	0.381
1/18	7/80	1/14	7/60	230	15	13	0.228	0.261	0.346	0.229	0.237	0.330
1/20	7/90	1/16	1/10	294	17	15	0.213	0.213	0.302	0.213	0.243	0.323
1/22	7/100	1/18	7/80	366	19	17	0.200	0.227	0.303	0.201	0.202	0.284
1/24	7/110	1/20	7/90	446	21	19	0.190	0.187	0.266	0.190	0.210	0.283
1/26	7/120	1/22	7/100	534	23	21	0.180	0.205	0.273	0.181	0.179	0.254
1/28	7/130	1/24	7/110	630	25	23	0.173	0.168	0.241	0.173	0.187	0.255
1/30	1/20	1/26	7/120	734	27	25	0.166	0.187	0.250	0.166	0.163	0.232
1/32	7/150	1/28	7/130	846	29	27	0.160	0.154	0.222	0.160	0.170	0.233
1/34	7/160	1/30	1/20	966	31	29	0.154	0.174	0.232	0.154	0.150	0.216
1/36	7/170	1/32	7/150	1094	33	31	0.149	0.144	0.207	0.149	0.157	0.217
1/38	7/180	1/34	7/160	1230	35	33	0.145	0.163	0.218	0.145	0.141	0.202
1/40	7/190	1/36	7/170	1374	37	35	0.141	0.135	0.195	0.141	0.147	0.203
1/42	7/200	1/38	7/180	1526	39	37	0.137	0.154	0.206	0.137	0.133	0.191
1/44	1/30	1/40	7/190	1686	41	39	0.133	0.128	0.185	0.133	0.138	0.192
1/46	7/220	1/42	7/200	1854	43	41	0.130	0.146	0.195	0.130	0.126	0.181
1/48	7/230	1/44	1/30	2030	45	43	0.127	0.122	0.176	0.127	0.131	0.183
1/50	7/240	1/46	7/220	2214	47	45	0.124	0.139	0.187	0.124	0.120	0.173

Table B.9: Dimensions and mesh sizes for mortar BEM experiment 8

Mortar BEM experiment 9 (Results in Figure 5.17)

min h			max h	Dimension			Part 1 of	Part 2 of	Mortar	Part 1 of	Part 2 of	Mortar
h_1	h_2	h_3	h_4	X_h	M_k I	M_k II	Error I	Error I	BEM I	Error II	Error II	BEM II
1/10	7/40	1/6	7/20	54	7	5	0.368	0.453	0.583	0.364	0.575	0.680
1/18	1/10	1/10	7/30	164	12	8	0.288	0.346	0.450	0.285	0.409	0.498
1/26	7/100	1/14	7/40	334	19	13	0.244	0.286	0.376	0.244	0.299	0.386
1/34	7/130	1/18	7/50	564	24	16	0.215	0.249	0.329	0.214	0.294	0.364
1/42	7/160	1/22	7/60	854	31	21	0.195	0.224	0.297	0.195	0.234	0.305
1/50	7/190	1/26	1/10	1204	36	24	0.179	0.206	0.273	0.178	0.243	0.301
1/58	7/220	1/30	7/80	1614	43	29	0.167	0.192	0.254	0.167	0.201	0.261
1/66	7/250	1/34	7/90	2084	48	32	0.157	0.180	0.239	0.156	0.210	0.261

Table B.10: Dimensions and mesh sizes for mortar BEM experiment 9

Bibliography

[1] I. Babuška. The finite element method with Lagrangian multipliers. *Numer. Math.*, 1972.

[2] I. Babuška and G. N. Gatica. On the mixed finite element method with Lagrange multipliers. *Numer. Methods Partial Differential Equation*, 19:192–210, 2003.

[3] F. Ben Belgacem. The mortar finite element method with Lagrange multiplier. *Numer. Math.*, 84:173–197, 1999.

[4] F. Ben Belgacem and Y. Maday. The mortar finite element method for three dimensional finite elements. *M^2AN Math. Model. Numer. Anal.*, 31:289–302, 1997.

[5] C. Bernardi, Y. Maday, and A. T. Patera. Domain decomposition by the mortar element method. In H. G. Karper and M. Garbey, editors, *Asymptotic and Numerical methods for partial differential equations with critical parameters*, pages 269–286. Kluwer Academic Publishers, Netherlands, 1993.

[6] C. Bernardi, Y. Maday, and A. T. Patera. A new nonconforming approach to domain decomposition: the mortar element method. In H. Brezis and J. L. Lions, editors, *Nonlinear Partial Differential Equations and their Applications*, pages 13–51. Pitman, New York, 1994.

[7] A. Bespalov and N. Heuer. The p-version of the boundary element method for a three-dimensional crack problem. *Numer. Methods Partial Differential Eq.*, 19:243–258, 2003.

[8] A. Bespalov and N. Heuer. The hp-version of the boundary element method with quasi-uniform meshes in three dimensions. *ESAIM Math. Model. Numer. Anal.*, 42(5):821–849, 2008.

[9] D. Braess. *Finite Elements. Theory, fast solvers, and applications in solid mechanics.* Cambridge University Press, Cambridge, 3rd edition, 2007.

[10] D. Braess and W. Dahmen. Stability estimates of the mortar finite element method for 3-dimensional problems. *East-West J. Numer. Math.*, 6:249–264, 1998.

[11] D. Braess, W. Dahmen, and C. Wieners. A multigrid algorithm for the mortar finite element method. *SIAM J. Numer. Anal.*, 37:48–69, 1999.

[12] D. Braess, M. Dryja, and W. Hackbusch. A multigrid method for nonconforming fe-discretisations with application to nonmatching grids. *Computing*, 63:1–25, 199.

[13] S. C. Brenner. Poincaré-Friedrichs inequalities for piecewise H^1 functions. *SIAM J. Numer. Anal.*, 41:306–324, 2003.

[14] S. C. Brenner and L. R. Scott. *The Mathematical Theory of Finite Element Methods*. Springer, New York, 2nd edition, 2002.

[15] A. Buffa, M. Costabel, and D. Sheen. On traces for $H(curl, \Omega)$ in Lipschitz domains. *J. Math. Anal. Appl*, 276:845–867, 2002.

[16] M. Cessenat. *Mathematical methods in electromagnetism*, volume 41 of *Advances in Mathematical Applied Science*. World Scientific, Singapore, 1996.

[17] A. Chernov, M. Maischak, and E. P. Stephan. *hp*-mortar boundary element method for two-body contact problems with friction. *Math. Methods Appl. Sci.*, 31:2029–2054, 2008.

[18] P. G. Ciarlet. *The finite element for elliptic problems*. North-Holland, Amsterdam, 1978.

[19] M. Costabel. Boundary integral operators on Lipschitz domains: Elementary results. *SIAM J. Math. Anal.*, 19:613–626, 1988.

[20] W. Dahmen, B. Faermann, I. G. Graham, W. Hackbusch, and S. A. Sauter. Inverse inequalities on non-quasi-uniform meshes and application to the mortar element method. *Math. Comp*, 73:1107–1138, 2004.

[21] M. R. Dorr. The approximation theory for the *p*-version of the finite element method. *SIAM J. Numer. Anal.*, 21:1180–1207, 1984.

[22] K. Eriksson, D. Estep, P. Hansbro, and C. Johnson. *Computational Differential Equations*. Cambridge University Press, Cambridge, 1996.

[23] V.J. Ervin, N. Heuer, and E.P. Stephan. On the *h-p* version of the boundary element method for Symm's integral equation on polygons. *Comput. Methods Appl. Mech. Engrg.*, 110:25–38, 1993.

[24] G. I. Eskin. *Boundary value problems for elliptic pseuddifferential equations*, volume 52 of *Translations of Mathematical Monographs*. American Mathematical Society, Providence, RI, 1981.

[25] G. Gatica, M. Healey, and N. Heuer. The boundary element method with Lagrangian multipliers. *Numer. Methods Partial Differential Eq.*, 25(6):1303–1341, 2009.

[26] P. Grisvard. *Elliptic Problems in Nonsmooth Domains*. Pitman Publishing Inc., Boston, 1985.

[27] H. Han. The boundary integro-differential equations of three-dimensional Neumann problem in linear elasticity. *Numer. Math.*, 68:269–281, 1994.

[28] M. Healey and N. Heuer. Mortar boundary elements. arxiv:0901.4960, 2009.

[29] N. Heuer. Additive Schwarz method for the p-version of the boundary element method for the single layer potential on a plane screen. *Numer. Math.*, 88:485–511, 2001.

[30] N. Heuer and FJ. Sayas. Crouzeix-Raviart boundary elements. *Numer. Math.*, 112(3):381–401, 2009.

[31] G. C. Hsiao and W. L. Wendland. A finite element method for some integral equations of the first kind. *J. Math. Anal. Appl.*, 58:449–481, 1977.

[32] G. C. Hsiao and W. L. Wendland. *Boundary Integral Equations*. Springer, Berlin, 2008.

[33] G. C. Hsiao and W. L. Wendland. The *hp*-version of the boundary element method with quasi-uniform meshes in three dimensions. *ESAIM Math. Model. Numer. Anal.*, 42:821–849, 2008.

[34] C. Johnson. *Numerical solution of partial differential equations by the finite element method*. Cambridge University Press, Cambridge, 1987.

[35] C. Kim, R. D. Lazarov, J. E. Pasciak, and P. S. Vassilevski. Multiplier spaces for the finite element method in three dimensions. *SIAM J. Numer. Anal.*, 39:519–538, 2001.

[36] A. Klawonn and O. B. Widlund. A domain decomposition method with Lagrange multipliers andd inexact solvers for linear elasticity. *SIAM J. Sci. Comput.*, 22:1199–1219, 2000.

[37] V.D. Kupradze. *Three-dimensional problems of the mathematical theory of elasticity and thermoelasticity*. North-Holland, Amsterdam, 1979.

[38] J. L. Lions and E. Magenes. *Non-Homogeneous Boundary Value Problems and Applications I.* Springer-Verlag, New York, 1972.

[39] M. Maischak. The analytical computation of the Galerkin elements for the Laplace, Lame, and Helmholtz equation in 3D-BEM. Report, Institute fur Angewandte Mathematik, University of Hannover, Germany, 2000.

[40] A.-W. Maue. Zur formulierung eines allgemeinen beugungsproblems durch eine integralgleichung. *Zeitschrift fur Physik*, 126:601–618, 1949.

[41] W. McLean. *Strongly Elliptic Systems and Boundary Integral Equations.* Cambridge University Press, Cambridge, 2000.

[42] S. E. Mikhailov. About traces, extensions and co-normal derivative operators on Lipschitz domains. In C. Constanda and S. Potapenko, editors, *Integral methods in science and engineering: techniques and applications*, pages 151–162. Birkhäuser, Boston, 2007.

[43] J.-C. Nédélec. Integral equations with nonintegrable kernels. *Integral Equations Operator Theory*, 5:562–572, 1982.

[44] J.-C. Nédélec and J. Planchard. Une méthode variationnelle d'éléments finis pour la résolution numérique d'un probléme exteriieur dans R^3. *RAIRO*, 7:105–129, 1973.

[45] A. Patel, A. K. Pani, and N. Nataraj. Mortar element methods for parabolic problems. *Numer. Methods Partial Differential Eq.*, 24:1460–1484, 2008.

[46] A. Quateroni and A. Valli. *Domain Decomposition Methods for Partial Differential Equations.* Oxford University Press, Oxford, 1999.

[47] P. A. Raviart and J. M. Thomas. Primal hybrid finite element methods for 2nd order elliptic equations. *Math. Comp.*, 31:391–413, 1977.

[48] J. E. Roberts and J. M. Thomas. Mixed and hybrid methods (in finite elements problems). In P. G. Ciarlet and J. L. Lions, editors, *Handbook of numerical analysis*, volume 2, pages 523, 525–639. North-Holland, Amsterdam, 1991.

[49] F.J. Sayas. Infimum-supremum. *Boletin SEMA*, 41, 2007.

[50] P. Seshaiyer and M. Suri. Uniform *hp* convergence results for the mortar finite element method. *Math. Comp.*, 69:521–546, 2000.

[51] O. Steinbach. *Numerical Approximation Methods for Elliptic Boundary Value Problems.* Springer Science+Business Media, LLC, New York, 2008.

[52] E. P. Stephan. A boundary integral equation method for three-dimensional crack problems in elasticity. *Math. Meth. in the Appl. Sci.*, 8:609–623, 1986.

[53] E. P. Stephan. Boundary integral equations for screen problems in R^3. *Integral Equations Operator Theory*, 10:257–263, 1987.

[54] A. Toselli and O. Widlund. *Domain Decomposition Methods - algorithms and theory*. Springer-Verlag, Berlin, 2005.

[55] T. von Petersdorff and E. P. Stephan. Decompositions in edge and corner singularities for the solution of the Dirichlet problem of the Laplacian in a polyhedron. *Math. Nachr.*, 149:71–104, 1990.

[56] T. von Petersdorff and E. P. Stephan. Regularity of mixed boundary value problems in R^3 and boundary element methods on graded meshes. *Math. Methods Appl. Sci.*, 12:229–249, 1990.

[57] B. Wohlmuth. Hierarchical a posteriori error estimators for mortar finite element methods with Lagrange multipliers. *SIAM J. Numer. Anal.*, 36:1636–1658, 1999.

[58] B. I. Wohlmuth. A mortar finite element method using dual spaces for the Lagrangian multiplier. *SIAM J. Numer. Anal.*, 38:989–1012, 2000.

Index